

# Advances

## in Clinical and Experimental Medicine

MONTHLY ISSN 1899-5276 (PRINT) ISSN 2451-2680 (ONLINE)

[advances.umw.edu.pl](http://advances.umw.edu.pl)

2024, Vol. 33, No. 6 (June)

Impact Factor (IF) – 2.1  
Ministry of Science and Higher Education – 70 pts  
Index Copernicus (ICV) – 161.11 pts



WROCLAW  
MEDICAL UNIVERSITY

Advances  
in Clinical and Experimental  
Medicine



# Advances in Clinical and Experimental Medicine

ISSN 1899-5276 (PRINT)

ISSN 2451-2680 (ONLINE)

advances.umw.edu.pl

**MONTHLY 2024**  
**Vol. 33, No. 6**  
**(June)**

Advances in Clinical and Experimental Medicine (*Adv Clin Exp Med*) publishes high-quality original articles, research-in-progress, research letters and systematic reviews and meta-analyses of recognized scientists that deal with all clinical and experimental medicine.

## Editorial Office

ul. Marcinkowskiego 2–6  
50-368 Wrocław, Poland  
Tel.: +48 71 784 12 05  
E-mail: redakcja@umw.edu.pl

## Editor-in-Chief

Prof. Donata Kurpas

## Deputy Editor

Prof. Wojciech Kosmala

## Managing Editor

Marek Misiak, MA

## Statistical Editors

Wojciech Bombała, MSc

Łucja Janek, MSc

Anna Kopszak, MSc

Dr. Krzysztof Kujawa

Jakub Wronowicz, MSc

## Manuscript editing

Marek Misiak, MA

Paulina Piątkowska, MA

## Publisher

Wrocław Medical University  
Wybrzeże L. Pasteura 1  
50-367 Wrocław, Poland

Online edition is the original version  
of the journal

## Scientific Committee

Prof. Sandra Maria Barbalho

Prof. Antonio Cano

Prof. Chong Chen

Prof. Breno Diniz

Prof. Erwan Donal

Prof. Chris Fox

Prof. Yuko Hakamata

Prof. Carol Holland

Prof. Sabine Bährer-Kohler

Prof. Markku Kurkinen

Prof. Christos Lionis

Prof. Raimundo Mateos

Prof. Zbigniew W. Raś

Prof. Jerzy W. Rozenblit

Prof. Silvina Santana

Prof. Sajee Sattayut

Prof. James Sharman

Prof. Jamil Shibli

Prof. Michał J. Toborek

Prof. László Vécsei

Prof. Cristiana Vitale

Prof. Hao Zhang

## Section Editors

### Basic Sciences

Prof. Iwona Bil-Lula

Prof. Bartosz Kempisty

Dr. Wiesława Kranc

Dr. Anna Lebedeva

### Clinical Anatomy, Legal Medicine, Innovative Technologies

Prof. Rafael Boscolo-Berto

### Dentistry

Prof. Marzena Dominiak

Prof. Tomasz Gedrange

Prof. Jamil Shibli

### Laser Dentistry

Assoc. Prof. Kinga Grzech-Leśniak

### Dermatology

Prof. Jacek Szepietowski

### Emergency Medicine, Innovative Technologies

Prof. Jacek Smereka

### Gynecology and Obstetrics

Prof. Olimpia Sipak-Szmigiel

### Histology and Embryology

Dr. Mateusz Olbromski

### Internal Medicine

#### Angiology

Dr. Angelika Chachaj

#### Cardiology

Prof. Wojciech Kosmala

Dr. Daniel Morris

#### Endocrinology

Prof. Marek Bolanowski

#### Gastroenterology

Assoc. Prof. Katarzyna Neubauer

### Hematology

Prof. Andrzej Deptała  
Prof. Dariusz Wołowicz

### Nephrology and Transplantology

Assoc. Prof. Dorota Kamińska  
Prof. Krzysztof Letachowicz

### Pulmonology

Prof. Anna Brzecka

### Microbiology

Prof. Marzenna Bartoszewicz  
Assoc. Prof. Adam Junka

### Molecular Biology

Dr. Monika Bielecka

Prof. Jolanta Saczko

### Neurology

Assoc. Prof. Magdalena Koszewicz  
Assoc. Prof. Anna Pokryszko-Dragan

Dr. Masaru Tanaka

### Neuroscience

Dr. Simone Battaglia  
Dr. Francesco Di Gregorio

### Oncology

Prof. Andrzej Deptała  
Prof. Adam Maciejczyk

### Gynecological Oncology

Dr. Marcin Jędryka

### Ophthalmology

Dr. Małgorzata Gajdzis

### Orthopedics

Prof. Paweł Reichert

### Otolaryngology

Assoc. Prof. Tomasz Zatoński

### Pediatrics

### Pediatrics, Metabolic Pediatrics, Clinical Genetics, Neonatology, Rare Disorders

Prof. Robert Śmigiel

### Pediatric Nephrology

Prof. Katarzyna Kiliś-Pstrusińska

### Pediatric Oncology and Hematology

Assoc. Prof. Marek Ussowicz

### Pharmaceutical Sciences

Assoc. Prof. Marta Kepińska  
Prof. Adam Matkowski

### Pharmacoeconomics, Rheumatology

Dr. Sylwia Szafraniec-Buryło

### Psychiatry

Dr. Melike Küçükkarapınar  
Prof. Jerzy Leszek  
Assoc. Prof. Bartłomiej Stańczykiewicz

### Public Health

Prof. Monika Sawhney  
Prof. Izabella Uchmanowicz

### Qualitative Studies, Quality of Care

Prof. Ludmiła Marcinowicz

### Radiology

Prof. Marek Szaśniadek

### Rehabilitation

Dr. Elżbieta Rajkowska-Labon

### Surgery

Assoc. Prof. Mariusz Chabowski  
Assoc. Prof. Mirosław Kozłowski  
Prof. Renata Taboła

### Telemedicine, Geriatrics, Multimorbidity

Assoc. Prof. Maria Magdalena  
Bujnowska-Fedak

---

## Editorial Policy

Advances in Clinical and Experimental Medicine (Adv Clin Exp Med) is an independent multidisciplinary forum for exchange of scientific and clinical information, publishing original research and news encompassing all aspects of medicine, including molecular biology, biochemistry, genetics, biotechnology and other areas. During the review process, the Editorial Board conforms to the "Uniform Requirements for Manuscripts Submitted to Biomedical Journals: Writing and Editing for Biomedical Publication" approved by the International Committee of Medical Journal Editors ([www.ICMJE.org](http://www.ICMJE.org)). The journal publishes (in English only) original papers and reviews. Short works considered original, novel and significant are given priority. Experimental studies must include a statement that the experimental protocol and informed consent procedure were in compliance with the Helsinki Convention and were approved by an ethics committee.

For all subscription-related queries please contact our Editorial Office: [redakcja@umw.edu.pl](mailto:redakcja@umw.edu.pl)

For more information visit the journal's website: [advances.umw.edu.pl](http://advances.umw.edu.pl)

Pursuant to the ordinance of the Rector of Wrocław Medical University No. 37/XVI R/2024, from March 1, 2024, authors are required to pay a fee for each manuscript accepted for publication in the journal Advances in Clinical and Experimental Medicine. The fee amounts to 1600 EUR for all types of papers.

Advances in Clinical and Experimental Medicine has received financial support from the resources of Ministry of Science and Higher Education within the "Social Responsibility of Science – Support for Academic Publishing" project based on agreement No. RCN/SP/0584/2021.



Ministry of Education and Science  
Republic of Poland

Czasopismo Advances in Clinical and Experimental Medicine korzysta ze wsparcia finansowego ze środków Ministerstwa Edukacji i Nauki w ramach programu „Społeczna Odpowiedzialność Nauki – Rozwój Czasopism Naukowych” na podstawie umowy nr RCN/SP/0584/2021.



Ministerstwo  
Edukacji i Nauki

Indexed in: MEDLINE, Science Citation Index Expanded, Journal Citation Reports/Science Edition, Scopus, EMBASE/Excerpta Medica, Ulrich's™ International Periodicals Directory, Index Copernicus

Typographic design: Piotr Gil, Monika Kołęda

DTP: Wydawnictwo UMW

Cover: Monika Kołęda

Printing and binding: PRINT PROFIT Sp. z o.o., Koźmin 27, 59-900 Zgorzelec



## Contents

### Meta-analysis

- 553 Wenping Yan, Fenju Sun, Meng Xu, Qi Zhang  
**A meta-analysis of the impact of the problem-based method of learning combined with mind mapping on nursing instruction**

### Original papers

- 563 Bing Peng, Yanlin Zhang, Liqing Cheng, Yuping Zhang, Xiaotian Lei, Weiling Leng, Jing Wang, Songwei Wu, Xiaoqun Wu, Yanling Zheng  
**Improving insulin self-injection accuracy in patients with diabetes mellitus through a nursing project**
- 573 Jianping Wang, Jian Zhang, Jie Gao, Mengmeng Zhao, Zhenkai Ma  
**Neoadjuvant camrelizumab and chemotherapy in patients with resectable esophageal squamous cell carcinoma: A prospective, single-arm, open-label study**
- 583 Miłosz Miedziaszczyk, Andrzej Oko, Anna Wolc, Aldona Woźniak, Ilona Idasiak-Piechocka  
**Assessment of serum concentration and urinary excretion of tumor necrosis factor receptor 1 and 2 and their potential as markers of immunoglobulin A nephropathy activity**
- 593 Maksymilian Hanarz, Aleksander Siniarski, Renata Gołębiowska-Wiatrak, Jadwiga Nessler, Krzysztof Piotr Malinowski, Grzegorz Gajos  
**Gender-related and PUFA-related differences in lipoprotein-associated phospholipase A2 levels in patients with type 2 diabetes and atherosclerotic cardiovascular disease**
- 601 Marzena Dominiak, Anna Leszczyszyn, Izabela Łaczmarska, Monika Machoy, Hanna Gerber, Joseph Choukroun, Tomasz Gedrange, Sylwia Hnitecka  
**Relationship in development of malocclusions to polymorphisms of selected vitamin D receptors**
- 609 Jingwei Cheng, Jaewoo Lee, Yangqing Liu, Yanfang Wang, Mingtao Duan, Zhen Zeng  
**Effects of myostatin gene knockout on white fat browning and related gene expression in type 2 diabetic mice**
- 619 Yanting Dong, Xiaohui Zhou, Nan Zhang  
**CCN1 inhibition affects the function of endothelial progenitor cells under high-glucose condition**
- 633 Zhijin Lu, Tao Tang, Juan Huang, Yongqiang Shi  
**Nerolidol inhibited U-251 human glioblastoma cell proliferation and triggered apoptosis via the upregulation of the p38 MAPK signaling pathway**
- 641 Yu Zhang, Yurong Zhang, Siyu He, Weixing Wang  
**Lysyl oxidase-mediated elastin upregulation promotes the proliferation and migration of human retinal endothelial cells**

### Research letters

- 653 Steven Parker, Kinga Grzech-Leśniak, Mark Cronshaw, Jacek Matys, Aldo Brugnera Jr, Samir Nammour  
**Full operating parameter recording as an essential component of the reproducibility of laser-tissue interaction and treatments**



# A meta-analysis of the impact of the problem-based method of learning combined with mind mapping on nursing instruction

Wenping Yan<sup>A</sup>, Fenju Sun<sup>B</sup>, Meng Xu<sup>C</sup>, Qi Zhang<sup>D,F</sup>

Department of Anesthesia and Surgery, Northwest Women and Children's Hospital (Maternal and Child Health Hospital of Shaanxi Province), Xi'an, China

A – research concept and design; B – collection and/or assembly of data; C – data analysis and interpretation; D – writing the article; E – critical revision of the article; F – final approval of the article

Advances in Clinical and Experimental Medicine, ISSN 1899–5276 (print), ISSN 2451–2680 (online)

*Adv Clin Exp Med.* 2024;33(6):553–561

## Address for correspondence

Qi Zhang  
E-mail: Zhang80191991@outlook.com

## Funding sources

None declared

## Conflict of interest

None declared

Received on March 17, 2023

Reviewed on May 24, 2023

Accepted on July 27, 2023

Published online on October 13, 2023

## Abstract

**Background.** Nowadays, there are a variety of viewpoints on problem-based learning (PBL) and mind mapping teaching outcomes in nursing education, but there are not many thorough assessments that are pertinent.

**Objectives.** We performed a meta-analysis to evaluate the effect of the PBL method combined with mind mapping on nursing instruction.

**Materials and methods.** A systematic literature search up to July 2022 was performed, and 1765 related studies were evaluated. The chosen studies comprised 1473 nursing teaching participants as the trial's baseline, with 770 of them using the PBL model with mind mapping and 703 enrolled as controls. Odds ratio (OR) and mean difference (MD) with 95% confidence intervals (95% CIs) were calculated to assess the effect of the PBL method combined with mind mapping on nursing instructions using dichotomous and continuous methods with a random or fixed effect model. The study protocol was registered in PROSPERO (registration No. CRD 42022432130).

**Results.** The PBL model with mind mapping reached a significantly higher results of nursing knowledge test (MD: 7.29, 95% CI: 6.88–7.71,  $p < 0.001$ ) and pediatric practice test (MD: 9.89, 95% CI: 9.04–10.74,  $p < 0.001$ ), as well as higher students' ability of independent learning (OR: 3.49, 95% CI: 2.11–5.76,  $p < 0.001$ ) compared to the controls in nursing teaching.

**Conclusions.** The PBL model with mind mapping resulted in a significantly higher results of nursing knowledge test, pediatric practice test and students' ability of independent learning compared to controls in nursing teaching.

**Key words:** nursing teaching adult, problem-based learning teaching model joint with mind mapping, pediatric practice test, nursing knowledge test, meta-analysis

## Cite as

Yan W, Sun F, Xu M, Zhang Q. A meta-analysis of the impact of the problem-based method of learning combined with mind mapping on nursing instruction. *Adv Clin Exp Med.* 2024;33(6):553–561. doi:10.17219/acem/170097

## DOI

10.17219/acem/170097

## Copyright

Copyright by Author(s)

This is an article distributed under the terms of the Creative Commons Attribution 3.0 Unported (CC BY 3.0) (<https://creativecommons.org/licenses/by/3.0/>)

## Introduction

Nursing education is crucial for enhancing the student's quality of learning, improving their clinical practice abilities and applying information in addition to providing theoretical knowledge.<sup>1</sup> As a result of the paradigm shift in medical education, the problem-based method of learning has been successful in many medical education courses both in China and overseas.<sup>2</sup> The problem-based learning (PBL) approach can strengthen critical thinking skills in students through interactive collaboration with their peers to analyze and solve complex problems via independent information processing. In medical education, the transition into clinical clerkship after years of pre-clinical studies is frustrating and anxiety-provoking. Therefore, PBL can play a pivotal role in familiarization with various topics, including the structure of effective medical teams, electronic health record utilization and inpatient admission regulation. Moreover, patient-centered scenarios can be represented using the PBL model. Recently, web-based applications have been incorporated alongside PBL to provide realistic exposure to practical clinical activities, including inpatient and outpatient care.<sup>3</sup>

However, in several studies, the basic implementation of the problem-based method of learning has proven ineffective for assisting students to acquire the necessary knowledge in a systematic manner. Additionally, the model performs poorly for some students in basic specialized courses and is more challenging for individuals with low learning capacities, which can result in learning fatigue and less-than-expected learning outcomes.<sup>3-5</sup> The medical education has evolved in recent years due to the popularity and dissemination of mind mapping technique. Mind mapping is helpful in systemic education because it connects the relatively scattered knowledge acquired through problem-based methods using logic and memory, making abstract problems concrete and making difficult problems easier.<sup>6,7</sup> Students can create visual images to represent their ideas in a meaningful way. Studies have reported that mind mapping application in medical and health-related science education significantly enhanced long-term memorization of factual information, and both mind mapping and PBL approaches encourage the adoption of deeper learning levels in medical students.

Mind maps can be used in the classroom to somewhat counteract the limitations of the problem-based method of learning, and both instructional approaches have complementary benefits that can support student learning.<sup>8-20</sup> The PBL integration with mind mapping had a positive impact on student understanding and overall cognition. In addition, Ravindranath et al. revealed that mind map integration in the PBL model helped students to better summarize discussions and improved the PBL-based learning process.<sup>19</sup>

There are now a variety of viewpoints on the PBL method and mind mapping teaching outcomes. However, in China, there are not many thorough assessments of employing these 2 educational methodologies in nursing training that are pertinent. We have performed a meta-analysis of studies on the PBL and mind mapping in order to examine the impact of the combined usage of these 2 methods on nursing education in China.

## Objectives

The aim of the study was to determine the impact of the problem-based method of learning and mind mapping on nurse training.

## Materials and methods

The design of this meta-analysis was based on the Preferred Reporting Items for Systematic Reviews and Meta-Analyses (PRISMA) guidelines. No ethical approval from the institutional board was required because this study is a meta-analysis of previously published data without individual patient data.<sup>21,22</sup>

## Eligibility criteria

The primary aim of the included studies centered on evaluating the impact of the problem-based educational model with mind mapping on nursing education and analyzing the PBL teaching approach in combination with mind mapping compared to controls.<sup>21,22</sup>

## Information sources

The principal objectives of the present study were to investigate the influence of the PBL model of teaching on nursing education, as well as the effect of the problem-based approach and mind mapping as a teaching technique. The study protocol was registered in PROSPERO (registration No. CRD 42022432130). Studies including human participants and publications in any language were reviewed. The inclusion rate was unaffected by the size of the trial. Review articles, comments and studies that did not provide a method for quantifying data were omitted from the list of publications. The course of the study is depicted in Fig. 1. The specified inclusion criteria for research studies were as follows: 1) research studies designed as prospective, observational, controlled trial, or retrospective studies; 2) the intended subjects consisted of nursing subjects; 3) the intervention regimen relied on both the PBL educational model and mind mapping technique; and 4) the studies aimed to compare the PBL educational model in combination with mind mapping to controls.

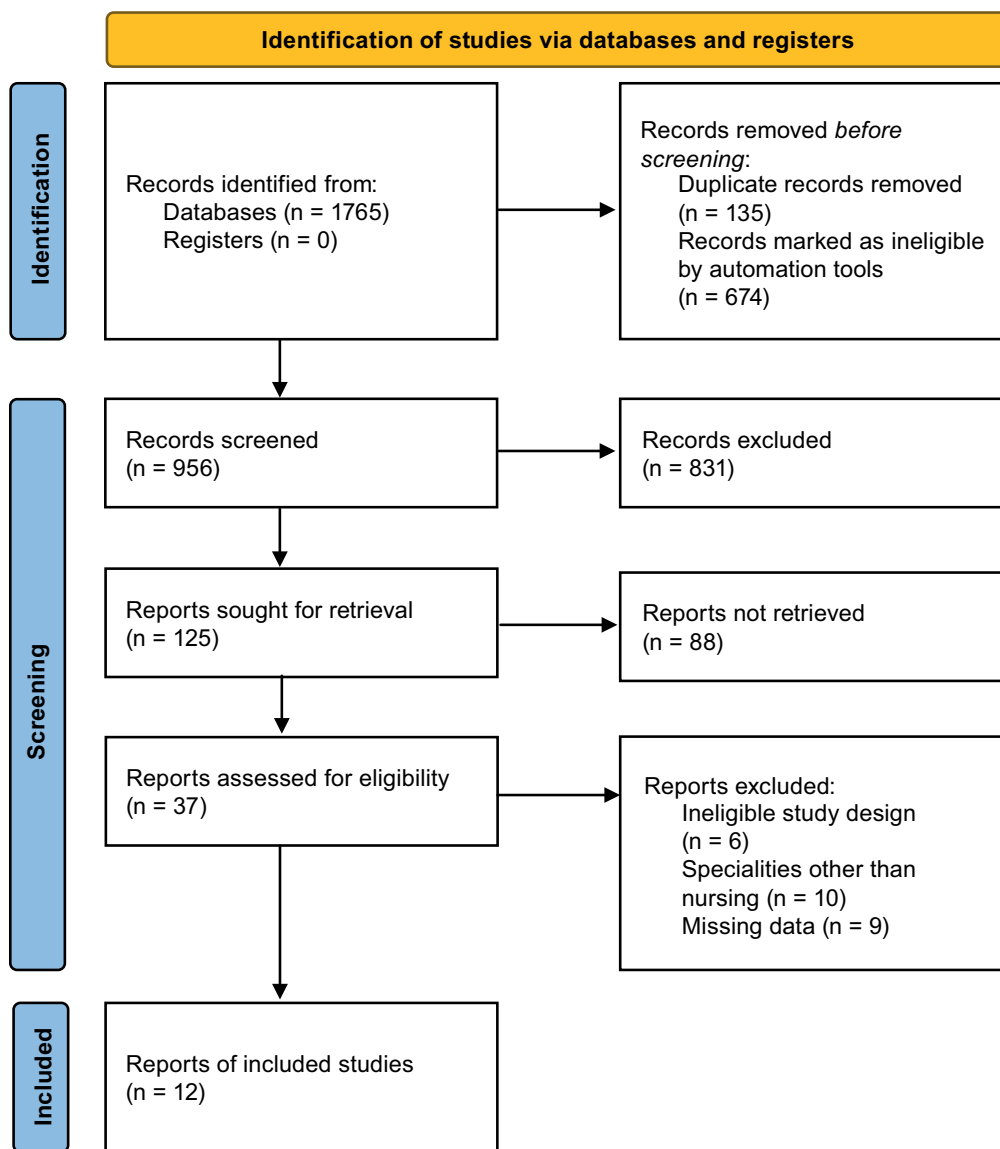


Fig. 1. Flowchart of the study process

Studies that did not assess the impact of the problem-based method of learning combined with mind mapping in nursing subjects, research on nursing instruction without the PBL approach combined with mind mapping in comparison to controls, and research on nursing instruction without the problem-based method of learning combined with mind mapping were excluded from the analysis.

### Search strategy

According to the PICOS concept, we developed a protocol for search strategy and characterized it as follows: nursing subjects were denoted by the letter P (“population”), the problem-based method of learning combined with mind mapping was the “intervention” or “exposure”, whereas the “comparison” or “control” was the “problem-based method of learning combined with mind mapping.” The results of practical tests, nursing knowledge tests and autonomous learning survey were the “outcomes”. There were no constraints on the “study design” of the investigation.<sup>22</sup>

We conducted a comprehensive search of the OVID, Embase, PubMed, Cochrane Library, and Google Scholar databases (Table 1) through March 2023 using a combination of keywords and correlated terms regarding nursing teaching of adults, PBL combined with mind mapping, practice test results, nursing knowledge test, and self-learning capabilities. To avoid articles that did not demonstrate a relationship between the PBL method combined with mind mapping and controls in nursing teaching individuals, all enrolled papers were merged into a single EndNote file (EndNote; Clarivate, London, UK), duplicates were removed, and the titles and abstracts were reviewed.

### Selection process

According to the PRISMA guidelines, 2 authors (MX and QZ) screened the retrieved publications and independently evaluated their eligibility for inclusion in the meta-analysis.

Table 1. Search strategy for each database

Database	Search strategy
PubMed	#1 "problem-based learning teaching model joint with mind mapping" [MeSH Terms] OR "PBL" [All Fields] OR "nursing teaching" [All Fields] OR "practice test" [All Fields] OR "nursing knowledge test" [All Fields] #2 "students' ability of independent learning" [MeSH Terms] OR "problem-based learning model joint with mind mapping" [All Fields] OR "practice test" [All Fields] OR "nursing knowledge test" [All Fields] #3 #1 AND #2
Embase	#1 "problem-based learning model joint with mind mapping"/exp OR "PBL"/exp OR "nursing teaching"/exp OR "practice test"/exp OR "nursing knowledge test" #2 "autonomous learning"/exp OR "practice test"/exp OR "nursing knowledge test" #3 #1 AND #2
Cochrane Library	#1 (problem-based learning model joint with mind mapping): ti,ab,kw OR (PBL): ti,ab,kw OR (nursing teaching): ti,ab,kw OR (practice test): ti,ab,kw (word variations have been searched) #2 (nursing knowledge test): ti,ab,kw OR (autonomous learning): ti,ab,kw OR (practice test): ti,ab,kw OR (nursing knowledge test): ti,ab,kw (word variations have been searched) #3 #1 AND #2
Google Scholar	#1 "problem-based learning model joint with mind mapping" OR "nursing teaching" OR "practice test" OR "nursing knowledge test" #2 "autonomous learning" OR "problem-based learning model joint with mind mapping" OR "PBL" OR "pediatric practice test" OR "nursing knowledge test" #3 #1 AND #2
OVID	#1 "problem-based learning model joint with mind mapping" OR "nursing teaching" [All Fields] OR "practice test" [All Fields] OR "nursing knowledge test" [All Fields] #2 "autonomous learning" OR "PBL" OR "problem-based learning model joint with mind mapping" [All Fields] OR "practice test" [All Fields] OR "nursing knowledge test" [All Fields] #3 #1 AND #2

MeSH – medical subject headings; ti,ab,kw – terms in either title or abstract or keyword fields; exp – exploded indexing term.

## Data collection process

The criteria for data collection included the surname of the primary author, the study period, the publication year, the country or region, the population type, the interventional measures, and the outcomes measures (e.g., nursing knowledge tests, practice tests and autonomous learning abilities). Quantitative and qualitative assessment techniques, the information source, the evaluation of the results, and statistical analysis were also analyzed.<sup>23</sup>

## Data items

When single research evaluating the impact of the problem-based approach of learning coupled with mind mapping and compared to controls in nursing teaching yielded contradictory results, we gathered the data independently.

## Risk of bias assessment

Two authors (WY and FS) separately reviewed the methodology of the chosen publications to determine the potential for bias in each research study. The methodological quality was assessed using the Risk of Bias tool from the Cochrane Handbook for Systematic Reviews of Interventions (version 5.1.0).<sup>24</sup> Each study was classified into one of the 3 categories used to describe the risk of bias (ROB). A low ROB was identified as a study that satisfied all quality criteria. A study was classified as having a moderate ROB if one or more requirements were not met

or were not included. If all of the quality criteria were not satisfied or were partially met, the research was deemed to have a high ROB. Inconsistencies or disagreements were solved by the re-evaluation of the original text and referring to the corresponding author (QZ).

## Effect measurements

Sensitivity analyses were performed and limited to research that reported and evaluated the effect of the problem-based technique of learning and mind mapping in comparison to a control group. Using sensitivity and subclass analyses, the PBL method of learning was compared to mind mapping and controls.

## Synthesis methods

The present meta-analysis calculated the odds ratio (OR) for the student's ability to self-learn and the mean difference (MD) between knowledge and practice test scores with a 95% confidence interval (95% CI). We computed the  $I^2$  index, which has a range of 0–100%. Values at 0%, 25%, 50%, and 75% exhibited absence, minimal, moderate, and significant heterogeneity, respectively.<sup>25</sup> To ensure the use of the proper model, we assessed the eligible studies in terms of their similarities and discrepancies, including the effect size and the main population characteristics. Since all studies included undergraduate nursing students, were designed as randomized controlled trials (RCTs), and shared the PBL with mind mapping as intervention, the fixed-effect model was applied in all analyses.

**Table 2.** Characteristics of the studies selected for the meta-analysis

Study	Country	Study design	Total number of participants	PBL and mind mapping (participants, n)	Control intervention (participants, n)	Outcomes of interest
Linyan and Liyun, 2018 <sup>8</sup>	Taiwan	RCT	48	24	PBL/24	knowledge test; practice test; autonomous learning survey
Linna, 2019 <sup>9</sup>	Taiwan	RCT	50	25	conventional lectures/25	knowledge test; practice test
Ya, 2019 <sup>10</sup>	China	RCT	60	30	PBL/30	knowledge test; practice test; autonomous learning survey
Jing et al., 2019 <sup>11</sup>	China	RCT	508	285	conventional lectures/223	knowledge test
Ying, 2020 <sup>12</sup>	China	RCT	210	105	conventional lectures/105	knowledge test; practice test
Yizhu et al., 2020 <sup>13</sup>	Taiwan	RCT	70	35	conventional lectures/35	knowledge test; practice test; autonomous learning survey
Yi et al., 2020 <sup>14</sup>	China	RCT	40	20	conventional lectures/20	knowledge test; practice test
Zhou et al., 2021 <sup>15</sup>	China	RCT	102	51	conventional lectures/51	knowledge test
Zheng et al., 2021 <sup>16</sup>	China	RCT	186	93	conventional lectures/93	autonomous learning survey
Mengmeng, 2021 <sup>17</sup>	China	RCT	48	24	PBL/24	knowledge test; practice test
Xiaoxin, 2021 <sup>18</sup>	China	RCT	80	40	conventional lectures/40	knowledge test; practice test
Kan et al., 2022 <sup>20</sup>	China	RCT	71	38	conventional lectures/33	knowledge test; autonomous learning survey
Total			1473	770	703	–

RCT – randomized controlled trial; PBL – problem-based learning.

We assessed the eligible studies for subclass analysis. The value of  $p = 0.05$  indicated statistical significance for subcategory differences.

## Reporting bias assessment

Egger's regression test for the evaluation of quantitative publication bias and funnel plots displaying the logarithm of ORs compared to their standard errors were used to subjectively and quantitatively measure the publication bias (the publication bias was considered present for  $p < 0.05$ ).<sup>25</sup>

## Certainty assessment

All  $p$ -values were calculated using two-tailed tests. Reviewer Manager v. 5.3 (The Nordic Cochrane Centre, The Cochrane Collaboration, Copenhagen, Denmark) was used to produce the graphs and to conduct statistical analyses.

## Results

### Baseline characteristics of the analyzed studies

Twelve articles published between 2018 and 2022 satisfied the inclusion criteria and were chosen from a total

of 1765 relevant research studies for the meta-analysis.<sup>8–18,20</sup> Table 2 displays the results described in these research articles. A total of 1473 nursing students participated in the baseline trials presented in the chosen studies, with 770 employing the problem-based technique of learning coupled with mind mapping and 703 serving as controls. There were 40–508 people present when the trial first began. Eleven studies presented data organized by the results of nursing knowledge tests, 8 studies data organized by practice tests, and 5 studies data organized by the students' capacity for autonomous learning.

### Nursing knowledge test results

The use of the PBL method in conjunction with mind mapping (Fig. 2) resulted in significantly higher scores on the nursing knowledge test (MD: 7.29; 95% CI: 6.88–7.71,  $p < 0.001$ ). The heterogeneity level ( $I^2$  index) between the studies was high ( $p = 0.002$ ,  $I^2 = 63%$ ).

### Practice test results

The practice test outcomes showed significantly higher results ( $p < 0.001$ ) for the PBL modality in combination with mind mapping, as illustrated in Fig. 3, with a MD of 9.89 (95% CI: 9.04–10.74,  $p < 0.001$ ) and a high level of heterogeneity ( $p < 0.001$ ,  $I^2 = 76%$ ).



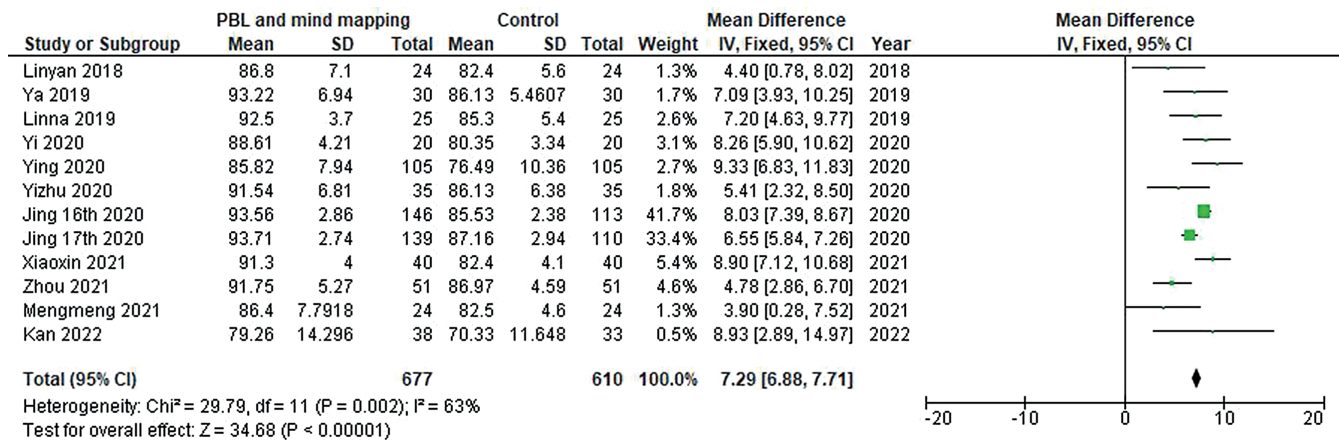


Fig. 2. Forest plot evaluating the effect of the problem-based learning (PBL) method combined with mind mapping compared to controls on the nursing knowledge test outcomes in nursing subjects

SD – standard deviation; 95% CI – 95% confidence interval; df – degrees of freedom.

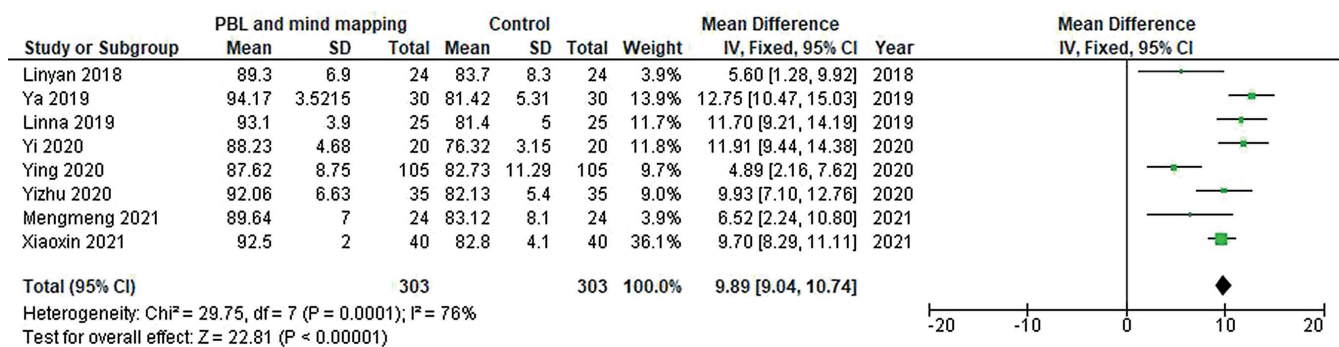


Fig. 3. Forest plot evaluating the effect of the problem-based learning (PBL) method combined with mind mapping compared to controls on the practice test outcomes in nursing subjects

SD – standard deviation; 95% CI – 95% confidence interval; df – degrees of freedom.

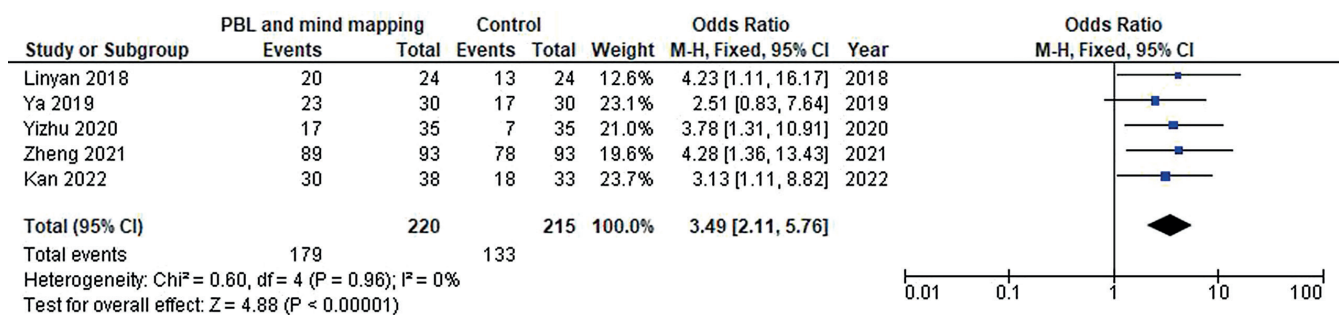


Fig. 4. Forest plot evaluating the effect of the problem-based learning (PBL) method combined with mind mapping compared to controls on the nursing subjects' ability of independent learning

SD – standard deviation; 95% CI – 95% confidence interval; df – degrees of freedom.

## Autonomous learning abilities

The combination of the PBL modality with mind mapping showed a significant improvement in the nursing students' capacity for independent learning among a total of 179 subjects, compared to 133 subjects in the control groups (Fig. 4). The pooled OR was 3.49 (95% CI: 2.11–5.76,  $p < 0.001$ ) and there was no heterogeneity between the studies ( $I^2 = 0\%$ ,  $p = 0.96$ ).

Due to a lack of data on gender, age and ethnicity, it was not possible to use stratified models to assess the impact of these variables on comparison results. A visual examination of the funnel plot showed general symmetrical distribution (Fig. 5). The quantitative evaluations utilizing Egger's regression test were nonsignificant for the knowledge test, practice test and autonomous learning ( $p = 0.87$ , 0.65 and 0.79, respectively), suggesting no publication bias. However, most of the included RCTs were found to have



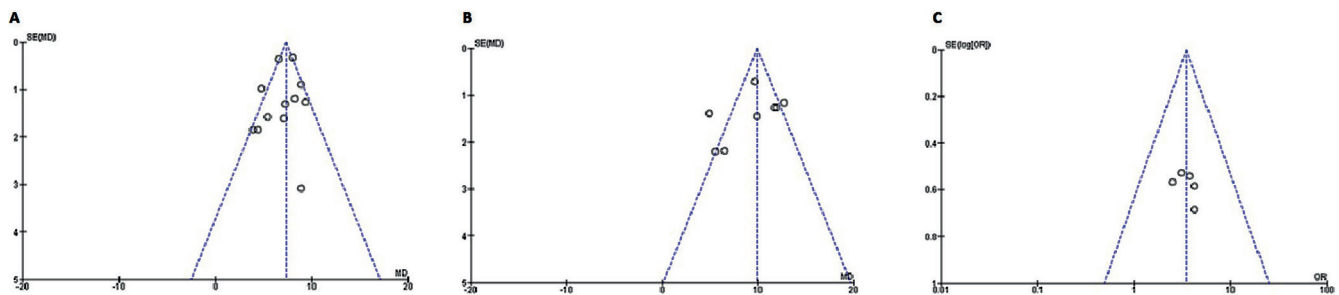


Fig. 5. Funnel plots of publication bias between studies. A. Nursing knowledge test outcomes; B. Practice test outcomes; C. The students' ability of independent learning

SE – standard error; MD – mean difference; OR – odds ratio.

low methodological quality, no bias in selective reporting and minimal outcome data.

## Discussion

The studies evaluated in this meta-analysis included 1473 nursing student participants, with 770 of them using the problem-based method of learning paired with mind mapping and 703 enrolled as controls.<sup>8–19</sup> When compared to the controls, the PBL approach with mind mapping reached significantly higher scores in the nursing knowledge test, the practice test and the student's capacity for independent learning measurements. However, analyzing the results requires caution due to the small sample size (8 out of 12 studies in the meta-analysis) and the sparse study population in several comparisons.

One of the required courses in today's medical schools is nursing.<sup>1,26</sup> The problem-based method of learning combined with mind mapping is an essential tactic for implementing cutting-edge teaching concepts, deepening teaching reform and improving teaching quality.<sup>8–19</sup> Our results, which are consistent with those of several studies conducted both in China and abroad, suggest that the problem-based method of learning combined with mind mapping aids nursing students in understanding theoretical material while also boosting practical abilities and enjoyment of self-learning. A substantial number of notable primary articles served as the foundation for this meta-analysis.<sup>2,27</sup>

Few studies met the inclusion requirements. Some papers omitted the descriptions of the random allocation technique, allocation concealment or blinding. Due to the significant likelihood of bias and the generally poor quality of papers, the results were not very strong. The study's general conclusions were unaffected by a sensitivity analysis. To collect pertinent research data more thoroughly, improve the standard of the study and provide reliable and accurate results, RCTs should be performed in accordance with methodological principles going forward. Furthermore, there is a limited amount of published research on the simultaneous use of both teaching modes

in undergraduate nursing education. Smaller control and intervention groups were utilized in the majority of RCTs included in this study. We believe that these problems could be solved over time and with more research.

This meta-analysis investigated the impact of the PBL approach and mind mapping on teaching methodologies.<sup>28–34</sup> Clarifying potential links and contrasting the effects of the PBL teaching method with mind mapping compared to controls on the outcomes under consideration still require more research, for which larger, more homogeneous samples are needed. This point was made in a prior study that used a related meta-analysis technique and discovered similar beneficial results for the problem-based method of learning paired with mind mapping.<sup>35</sup> High evidence RCTs with robust findings are necessary to assess these factors. Since our meta-analysis was unable to determine whether differences in gender, ethnicity and age are related to the outcomes, it is crucial to evaluate these factors in the subsequent studies. In conclusion, as compared to the controls, the problem-based method of learning with mind mapping techniques reached considerably higher nursing knowledge exam results, practice test results and improved student's ability to learn independently.<sup>35–40</sup>

## Limitations

There is a possibility of selection bias because several papers were excluded from the meta-analysis. However, the excluded publications did not adhere to the standards for inclusion in our meta-analysis. For 8 out of the 12 selected studies, sample sizes were under 100. Also, we were unable to investigate whether confounding factors such as age, gender or ethnicity had an impact on the results. The study's objective was to contrast the results of the control group with the PBL strategy using mind maps for nursing education. Owing to the inclusion of erroneous or missing data from previous research, bias may have been exacerbated. Additionally, the nutritional status of the participants and their age and gender were possible sources of bias. Regrettably, some unreported studies and data gaps can skew the effect being investigated.

## Conclusions

The combination of the PBL approach with mind mapping compared to controls in nurse training had significantly increased learning outcomes, as shown in the scores of nursing knowledge tests, practice tests and the student's capacity for independent learning. Thus, the combination of these 2 modalities, PBL and mind mapping, is suitable for nursing education and promotes better learning abilities. Due to the small sample size of 8 out of the 12 studies in the meta-analysis and the dearth of studies in several comparisons, careful interpretation of the results is required. Further studies with higher quality and larger sample sizes are warranted to explore more suitable teaching modalities in nursing to improve educational quality.

### ORCID iDs

Wenping Yan  <https://orcid.org/0009-0007-7615-6473>

Fenju Sun  <https://orcid.org/0009-0004-6645-853X>

Meng Xu  <https://orcid.org/0009-0002-2028-0401>

Qi Zhang  <https://orcid.org/0000-0001-6461-5934>

### References

- Oermann MH. Nursing education research: A new era. *Nurse Educ*. 2020;45(3):115–115. doi:10.1097/NNE.0000000000000830
- Gao X, Luo S, Mu D, Xiong Y, Guanlian L, Wan C. Effects of problem-based learning in paediatric education in China: A meta-analysis. *J Evid Based Med*. 2016;9(3):136–143. doi:10.1111/jebm.12190
- Fadial T, Bhandari S. 395TF interactive problem-based learning: Does the use of a novel web application improve medical student preparedness for clinical clerkships? *Ann Emerg Med*. 2020;76(4):S150–S151. doi:10.1016/j.annemergmed.2020.09.411
- Noordegraaf-Eelens L, Kloeg J, Noordzij G. PBL and sustainable education: Addressing the problem of isolation. *Adv Health Sci Educ Theory Pract*. 2019;24(5):971–979. doi:10.1007/s10459-019-09927-z
- Neville A, Norman G, White R, McMaster at 50: Lessons learned from five decades of PBL. *Adv Health Sci Educ Theory Pract*. 2019;24(5):853–863. doi:10.1007/s10459-019-09908-2
- Oliveira B, Fonseca M, Rendas A, Carreiro-Martins P, Neuparth N. A scoping review comparing different mapping approaches pointing to the need for standardizing concept maps in medical education: A preliminary analysis. *KM&EL*. 2023;15(3):392–419. doi:10.34105/j.kmel.2023.15.023
- Daley BJ, Torre DM. Concept maps in medical education: An analytical literature review. *Med Educ*. 2010;44(5):440–448. doi:10.1111/j.1365-2923.2010.03628.x
- Linyan Y. Experience of case teaching in the teaching of respiratory diseases. *China Cont Med Edu*. 2018;12(14):24–46. [https://oversea.cnki.net/KCMS/detail/detail.aspx?dbcode=CJFD&dbname=CJFDLAST2018&filename=JXUY201812013&uniplatform=OVERSEA&v=\\_wLDLkT4QtPAwoCSzwJvCake66bMZPWZRHRJgggyhbNOcVb5YfiAPoaSKR\\_ybGMk](https://oversea.cnki.net/KCMS/detail/detail.aspx?dbcode=CJFD&dbname=CJFDLAST2018&filename=JXUY201812013&uniplatform=OVERSEA&v=_wLDLkT4QtPAwoCSzwJvCake66bMZPWZRHRJgggyhbNOcVb5YfiAPoaSKR_ybGMk). Accessed August 12, 2022.
- Linna C. Research on the application of mind mapping combined with PBL teaching method in medical nursing teaching. *Teach Learn Nurs*. 2019;14(4):181–182. doi:10.1016/S1557-3087(19)30205-7
- Yun SY, Choi JY. A comparative study on learning outcomes according to the Integration Sequences of S-PBL in Nursing Students: Randomized crossover design. *J Korean Acad Nurs*. 2019;49(1):92–103. doi:10.4040/jkan.2019.49.1.92
- Jing B, Qin Q, Sun D. Application of mind mapping in emergency nursing teaching for nursing students in high vocational colleges. In: *Proceedings of the 2019 3rd International Conference on Education, Economics and Management Research (ICEEMR 2019)*. Singapore: Atlantis Press; 2019. doi:10.2991/assehr.k.191221.108
- Ying L, Lin-Feng M, Juan-Juan W. Application of PBL combined with mind mapping in clinical nursing teaching of urology [in Chinese]. *Educ Teach Forum*. 2020;26:319–320. <https://oversea.cnki.net/KCMS/detail/detail.aspx?dbcode=CJFD&dbname=CJFDLAST2020&filename=JYJU202026160&uniplatform=OVERSEA&v=mvIVmf-aT18bKLn4O-2HhvMS9akPD8456a0HzEkndzL-RCoLKHtete8Xn0xz43igg>. Accessed October 15, 2022.
- Zhu Y, Liu Y, Guo L, et al. Testing two student nurse stress instruments in Chinese nursing students: A comparative study using exploratory factor analysis. *Biomed Res Int*. 2020;2020:6987198. doi:10.1155/2020/6987198
- Yi L, Mingyan J, Jianguo F, et al. Application of problem-based learning combined with team-based learning methods in clinical probation teaching of bone tumor [in Chinese]. *West Chin Med J*. 2020;10(24):1235–1238. [https://oversea.cnki.net/KCMS/detail/detail.aspx?dbcode=CJFD&dbname=CJFDLAST2020&filename=HXYY202-010016&uniplatform=OVERSEA&v=GwHhKrlJARnbeixHlka-WaFyKBHazeO1C9Is7p0liafc\\_TUr02VT9V\\_f78TYqQC](https://oversea.cnki.net/KCMS/detail/detail.aspx?dbcode=CJFD&dbname=CJFDLAST2020&filename=HXYY202-010016&uniplatform=OVERSEA&v=GwHhKrlJARnbeixHlka-WaFyKBHazeO1C9Is7p0liafc_TUr02VT9V_f78TYqQC)
- Zhou F, Guan Y, Hu H, Deng Y, Wei S. Teaching practice and exploration of cloud class combined with mind map design in biochemistry course in colleges and universities of traditional Chinese medicine in the internet era. *J Phys Conf Ser*. 2021;1852(4):042056. doi:10.1088/1742-6596/1852/4/042056
- Zheng S, Zhang M, Zhao C, et al. The effect of PBL combined with comparative nursing rounds on the teaching of nursing for traumatology. *Am J Transl Res*. 2021;13(4):3618–3625. PMID:34017543.
- Mengmeng L, Qingfeng L, Jingyi L, Xian J. Application of PBL combined with CBL in clinical practice teaching of dermatology [in Chinese]. *Chin Cont Med Edu*. 2022;8:56–59. [https://oversea.cnki.net/KCMS/detail/detail.aspx?dbcode=CJFD&dbname=CJFDLAST2022&filename=JXUY202208016&uniplatform=OVERSEA&v=plBY\\_w2Zx24kz6Kykegplk1haTVLQvGsmtkyC4W7oHOD1\\_fvQw2BfX\\_jn5wuc](https://oversea.cnki.net/KCMS/detail/detail.aspx?dbcode=CJFD&dbname=CJFDLAST2022&filename=JXUY202208016&uniplatform=OVERSEA&v=plBY_w2Zx24kz6Kykegplk1haTVLQvGsmtkyC4W7oHOD1_fvQw2BfX_jn5wuc). Accessed November 14, 2022.
- Xiaoxin S, Xu H, Mengzhi L. Application analysis of PBL combined with mind mapping in clinical nursing teaching of Urology Department. *Special Health Issue*. 2021;30:256–257. [http://www.cnki.net/KCMS/detail/detail.aspx?dbcode=CJFD&dbname=CJFDLAST2020&filename=JYJU202026160&uniplatform=OVERSEA&v=mvIVmf-aT18bKLn4O2HhvMS9akPD8456a0HzEkndzL9gnn\\_RN1LYqgzvNo9bK5Df](http://www.cnki.net/KCMS/detail/detail.aspx?dbcode=CJFD&dbname=CJFDLAST2020&filename=JYJU202026160&uniplatform=OVERSEA&v=mvIVmf-aT18bKLn4O2HhvMS9akPD8456a0HzEkndzL9gnn_RN1LYqgzvNo9bK5Df). Accessed September 5, 2022.
- Ravindranath S, Abrew W, Nadarajah V. Student's perception of mind mapping in problem-based learning. *J Contemp Med Edu*. 2016;2(2):61. doi:10.5455/jcme.20160620013341
- Kan C, He Y, Ren H, Liu X, Sun L. Analysis of the effect of professional teaching staff construction in the training of low-level nurses in operating room. *Nurs Commun*. 2022;6:e2022011. doi:10.53388/IN2022011
- Higgins JPT, Thompson S, JJ Deeks, Altman D. Measuring inconsistency in meta-analyses. *BMJ*. 2003;327(7414):557–560. doi:10.1136/bmj.327.7414.557
- Liberati A, Altman DG, Tetzlaff J, et al. The PRISMA statement for reporting systematic reviews and meta-analyses of studies that evaluate health care interventions: Explanation and elaboration. *J Clin Epidemiol*. 2009;62(10):e1–e34. doi:10.1016/j.jclinepi.2009.06.006
- Gupta S, Rout G, Patel AH, et al. Efficacy of generic oral directly acting agents in patients with hepatitis C virus infection. *J Viral Hepat*. 2018;25(7):771–778. doi:10.1111/jvh.12870
- Higgins JPT, Altman DG, Gotzsche PC, et al. The Cochrane Collaboration's tool for assessing risk of bias in randomised trials. *BMJ*. 2011;343:d5928. doi:10.1136/bmj.d5928
- Higgins JPT, Thomas J, Chandler J, Cumpston M, Li T, Page MJ, Welch VA, eds. *Cochrane Handbook for Systematic Reviews of Interventions*. 2<sup>nd</sup> ed. Chichester, UK: John Wiley & Sons; 2019. doi:10.1002/9781119536604
- Sheikhbahaei S, Trahan TJ, Xiao J, et al. FDG-PET/CT and MRI for evaluation of pathologic response to neoadjuvant chemotherapy in patients with breast cancer: A meta-analysis of diagnostic accuracy studies. *Oncologist*. 2016;21(8):931–939. doi:10.1634/theoncologist.2015-0353
- Muraraneza C, Mtshali GN. Planning reform to competency based curricula in undergraduate nursing and midwifery education: A qualitative study. *Nurse Educ Today*. 2021;106:105066. doi:10.1016/j.nedt.2021.105066

28. Niu Y, Liu T, Li K, et al. Effectiveness of simulation debriefing methods in nursing education: A systematic review and meta-analysis. *Nurse Educ Today*. 2021;107:105113. doi:10.1016/j.nedt.2021.105113
29. Elgendy MO, Hassan AH, Saeed H, Abdelrahim ME, Eldin RS. Asthmatic children and MDI verbal inhalation technique counseling. *Pulm Pharmacol Ther*. 2020;61:101900. doi:10.1016/j.pupt.2020.101900
30. Osama H, Abdullah A, Gamal B, et al. Effect of honey and royal jelly against cisplatin-induced nephrotoxicity in patients with cancer. *J Am Coll Nutr*. 2017;36(5):342–346. doi:10.1080/07315724.2017.1292157
31. Sayed AM, Khalaf AM, Abdelrahim MEA, Elgendy MO. Repurposing of some anti-infective drugs for COVID-19 treatment: A surveillance study supported by an in silico investigation. *Int J Clin Pract*. 2021;75(4):e13877. doi:10.1111/ijcp.13877
32. Madney YM, Laz NI, Elberry AA, Rabea H, Abdelrahim MEA. The influence of changing interfaces on aerosol delivery within high flow oxygen setting in adults: An in-vitro study. *J Drug Deliv Sci Technol*. 2020;55:101365. doi:10.1016/j.jddst.2019.101365
33. Hassan A, Rabea H, Hussein RRS, et al. In-vitro characterization of the aerosolized dose during non-invasive automatic continuous positive airway pressure ventilation. *Pulm Ther*. 2016;2(1):115–126. doi:10.1007/s41030-015-0010-y
34. Harb HS, Laz NI, Rabea H, Abdelrahim MEA. First-time handling of different inhalers by chronic obstructive lung disease patients. *Exp Lung Res*. 2020;46(7):258–269. doi:10.1080/01902148.2020.1789903
35. Romanko L. *The Role of Concept Mapping in the Development of Critical Thinking Skills in Student and Novice Nurses: A Quantitative Meta-Analysis*. Vancouver, Canada: University of British Columbia; 2016. doi:10.14288/1.0228162
36. Osama H, Rabea HM, Abdelrahman MA. The impact of mindfulness-based stress reduction on psychological health among patients with chronic diseases during COVID-19 outbreak lockdown. *Beni Suef Univ J Basic Appl Sci*. 2023;12(1):50. doi:10.1186/s43088-023-00389-2
37. Waltz CF, Jenkins LS, Han N. The use and effectiveness of active learning methods in nursing and health professions education: A literature review. *Nurs Educ Perspect*. 2014;35(6):392–400. doi:10.5480/13-1168
38. Daley BJ, Morgan S, Black SB. Concept maps in nursing education: A historical literature review and research directions. *J Nurs Educ*. 2016;55(11):631–639. doi:10.3928/01484834-20161011-05
39. Gao X, Wang L, Deng J, Wan C, Mu D. The effect of the problem based learning teaching model combined with mind mapping on nursing teaching: A meta-analysis. *Nurse Educ Today*. 2022;111:105306. doi:10.1016/j.nedt.2022.105306
40. Yue M, Zhang M, Zhang C, Jin C. The effectiveness of concept mapping on development of critical thinking in nursing education: A systematic review and meta-analysis. *Nurse Educ Today*. 2017;52:87–94. doi:10.1016/j.nedt.2017.02.018



# Improving insulin self-injection accuracy in patients with diabetes mellitus through a nursing project

\*Bing Peng<sup>1,A,B</sup>, \*Yanlin Zhang<sup>1,A,D</sup>, Liqing Cheng<sup>1,A,D</sup>, Yuping Zhang<sup>1,A</sup>, Xiaotian Lei<sup>1,A,B</sup>, Weiling Leng<sup>1,A</sup>, Jing Wang<sup>1,A,D</sup>, Songwei Wu<sup>1,A,D</sup>, Xiaoqun Wu<sup>2,A,C,F</sup>, Yanling Zheng<sup>1,A,C,F</sup>

<sup>1</sup> Department of Endocrinology, The First Affiliated Hospital of Army Medical University, Chongqing, China

<sup>2</sup> Department of Nursing, Chongqing Changshou District People's Hospital, China

A – research concept and design; B – collection and/or assembly of data; C – data analysis and interpretation; D – writing the article; E – critical revision of the article; F – final approval of the article

Advances in Clinical and Experimental Medicine, ISSN 1899–5276 (print), ISSN 2451–2680 (online)

Adv Clin Exp Med. 2024;33(6):563–572

## Address for correspondence

Yanling Zheng  
E-mail: 13996232425@139.com

## Funding sources

None declared

## Conflict of interest

None declared

## Acknowledgements

We would like to thank the First Affiliated Hospital of Army Medical University for help with reviewing the manuscript. We also thank Dr. Yu Lian and Dr. Yan Shi for their advice.

\*Bing Peng and Yanlin Zhang contributed equally to this work.

Received on November 24, 2022

Reviewed on March 31, 2023

Accepted on August 1, 2023

Published online on September 25, 2023

## Abstract

**Background.** Non-standardized insulin injection has an impact on the efficacy of glucose control.

**Objectives.** The aim of the study was to explore the effectiveness of a nursing project in improving the insulin self-injection accuracy of diabetes mellitus patients.

**Materials and methods.** A total of 200 type 2 diabetes patients who received insulin therapy with an insulin pen were recruited at the First Affiliated Hospital of Army Medical University (Chongqing, China). Patients were randomly assigned to a control (n = 100) or intervention (n = 100) group. Conventional health education was conducted in the control group, while a nursing project and conventional health education were undertaken in the intervention group. The following parameters were analyzed between the 2 groups: standardized insulin pen use at admission and discharge, glycosylated hemoglobin (HbA1c), time in range (TIR), and adipose hyperplasia incidence rate 6 months after discharge.

**Results.** Concerning standardized insulin self-injection, the intervention group was superior to the control group, and the difference between the 2 groups was statistically significant ( $p < 0.05$ ). The HbA1c levels ( $p = 0.000$ ), TIR ( $p = 0.005$ ) and adipose hyperplasia incidence rate 6 months after discharge ( $p = 0.000$ ) all improved in the intervention group compared to the control group.

**Conclusions.** The application of the nursing project effectively improved the efficacy of glucose control in diabetes mellitus patients.

**Key words:** diabetes mellitus, insulin injection, nursing project, blood glucose management

## Cite as

Peng B, Zhang Y, Cheng L, et al. Improving insulin self-injection accuracy in patients with diabetes mellitus through a nursing project.

Adv Clin Exp Med. 2024;33(6):563–572.

doi:10.17219/acem/170224

## DOI

10.17219/acem/170224

## Copyright

Copyright by Author(s)

This is an article distributed under the terms of the Creative Commons Attribution 3.0 Unported (CC BY 3.0) (<https://creativecommons.org/licenses/by/3.0/>)

## Background

Diabetes mellitus is a serious public health issue worldwide.<sup>1–3</sup> Based on the International Diabetes Federation (IDF) Diabetes Atlas (10<sup>th</sup> edition),<sup>4</sup> nearly 537 million people between 20 and 79 years of age have diabetes mellitus globally, accounting for 10.5% of the adult population. Furthermore, the global population of diabetes mellitus patients is estimated to increase to 643 million (11.3%) and 783 million (12.2%) by 2030 and 2045, respectively.

According to domestic and foreign guidelines, novel hypoglycemic drugs have been most frequently recommended in recent years. However, insulin is still critical for diabetes mellitus management<sup>5–8</sup> and is the primary drug used for the lifelong treatment of type 1 diabetes patients and some type 2 diabetes patients.<sup>9–12</sup> The drug is widely applied in anti-diabetic treatment, but its glucose control effect is unsatisfactory. Studies have shown that the insulin utilization rate by diabetes patients is 50%, but the standard rate of blood glucose reduction is <35%.<sup>13</sup>

The efficacy of insulin injection therapy is affected by the dosage form, the injection device and the technique used.<sup>14,15</sup> When treating hypoglycemic patients using an insulin pen, most clinicians focus on dose adjustment and ignore the standardization and improvement of injection techniques.<sup>16</sup> Although standardized treatment with an insulin pen plays a critical role in treatment,<sup>17</sup> improper injection directly affects glucose control and poses an enormous risk to clinical treatment and patient self-management. As revealed by surveys, many problems occur during insulin treatment, such as inadequate disinfection, using the wrong injection mode, repeated injections at the same site, improper model of pen selection, repeated use of needles, improper drug loading and unloading, errors in injection time, and inappropriate drug storage. These issues can lead to large fluctuations in blood glucose and increase hypoglycemic risk, local skin infection, subcutaneous adipose hyperplasia, and other skin complications.<sup>17,18–22</sup> Furthermore, they gravely influence the effective management of blood glucose and place a substantial economic burden on patients and society.<sup>22,23</sup>

A nursing project is a scientific approach used to improve nursing quality, defined as organizationally analyzing specific issues in nursing work with limited resources and timing, elucidating their root causes, proposing systematic solutions, and achieving specific goals to improve nursing quality and benefit patients. The project procedure follows a sequence of subject determination, status survey, goal setting, cause analysis, countermeasure development, countermeasure implementation, and effectiveness evaluation.

In this study, glycosylated hemoglobin (HbA1c) and time in range (TIR) were used to evaluate the effectiveness of the nursing project. The HbA1c is the gold standard for the clinical evaluation of blood glucose control and reflects the blood glucose level 2–3 months before enrollment, though it does not detect hyperglycemic and hypoglycemic

events.<sup>24,25</sup> In recent years, this drawback has been offset by the emergence and development of continuous glucose monitoring (CGM) techniques that make the general blood glucose profile available.<sup>26,27</sup> Time in range is a new concept for improving glucose fluctuation monitoring described in the Chinese Guidelines for Prevention and Treatment of Type 2 Diabetes (2020 edition),<sup>5</sup> and is the core indicator of the CGM technique. The application of TIR is a novel study design in the nursing field.

## Objectives

The aim of the study was to explore the effectiveness of a nursing project in improving the insulin self-injection accuracy of patients with diabetes mellitus. We analyzed a comprehensive nursing intervention and therapeutic efficacy in patients with this disease who were treated with an insulin pen in the Department of Endocrinology of the First Affiliated Hospital of Army Medical University between January 2020 and March 2021.

## Materials and methods

### Study design

A prospective, single-center, randomized, controlled, open trial was conducted in Chongqing in China. Patients with diabetes mellitus recruited from the Department of Endocrinology of the First Affiliated Hospital of Army Medical University between January 2020 and March 2021 were the participants in the study.

The Ethics Committee of the First Affiliated Hospital of Army Medical University approved the study (approval No. KY2020085), which was registered with the Chinese Clinical Trial Registry (registration No. ChiCTR2100052472). The study complied with the ethical principles of the Helsinki Declaration. All participants gave written informed consent.

### Participants

A total of 200 diabetes mellitus patients admitted to the Department of Endocrinology in our hospital between January 2020 and March 2021 were recruited as study participants. The inclusion criteria were as follows: 1) patients diagnosed with type 2 diabetes mellitus according to the World Health Organization Diagnostic Criteria for Diabetes Mellitus (1999); 2) patients who received premixed insulin therapy using 32G 4-mm insulin pen needles (BD Biosciences, San Jose, USA)<sup>16</sup>; 3) patients who had complete cognition and showed good self-care, and who were capable of cooperating with the study and independently finishing the study questionnaire; 4) patients who continued receiving the same treatment after



discharge; and 5) patients who understood and agreed to participate in this study and gave written informed consent. The exclusion criteria were: 1) patients with severe hepatic and renal impairment or serious complications; 2) patients with mental diseases or self-care and cognitive impairments; and 3) patients with a surgical history at the injection site (e.g., surgical scar) or skin diseases (e.g., dermatitis or psoriasis).

Participants were randomly divided into 2 groups using a random number generator and sealed envelope, blinded to investigators, including statisticians. A nursing project and conventional health education were performed in the intervention group, while conventional health education was conducted in the control group. Based on our experience, the mean TIR was estimated at 56% in the control group and at 65% in the intervention group.

The sample size in both groups was determined using IBM SPSS v. 23.0 statistical software (IBM Corp., Armonk, USA), with  $\alpha = 0.0$  and  $\beta = 0.10$ , i.e.,  $n_1 = n_2 = 85$ . As estimated with a hypothesized lost-to-follow-up rate of 10%, the sample size would be  $n_1 = n_2 = 85 \div 0.9 = 94$ . Therefore, 100 patients were included in each group.

## Materials

The following materials were used: FreeStyle Optium Neo H glucometer (Abbott Diabetes Care Ltd., Alameda, USA); blood glucose test strips employing the glucose dehydrogenase method (#4500184071; Abbott Diabetes Care Ltd.); FreeStyle Libre H Flash Continuous Glucose Monitoring System (Abbott Diabetes Care Ltd.); D-100 Hemoglobin Testing System and corollary high-performance liquid chromatography (HPLC) reagents (Bio-Rad Laboratories Inc., Hercules, USA).

## Methods

Conventional health education for the control group on day 1 after admission involved primary care nurses carrying out an evaluation and scoring single items concerning the standardization of patients' insulin self-injections, according to the Segmentation Scoring Form for Standardized Insulin Pen Use (developed in reference to the Indian Forum for Injection Technique; see Supplementary Table 1).<sup>19,28</sup> The nurses found weak links and incorrect operations, then immediately corrected these problems and provided guidance. In addition, they fully implemented health education on standard insulin pen injections and distributed an operational workflow chart and alternating chart of the injection site. Every Wednesday, the primary care nurses encouraged patients and their families to concentrate on watching a standardized insulin injection video and on-site operation demonstration. In this way, patients were educated with theoretical diabetes mellitus knowledge and guided to do an operational exercise within the education tool for the "Standard Injection Week for

Chinese Patients with Diabetes Mellitus" (hereafter referred to as the "model"). On the last day before discharge, the primary care nurses guided patients to complete their self-injection of insulin. On the day of discharge, the primary care nurses finished patient assessments with on-site scoring of the standardization of each patient's insulin self-injection, according to the Segmentation Scoring Form for Standardized Insulin Pen Use. Subsequently, they optimized the education plan according to assessment results.

After discharge, the patients made a follow-up visit to a specialist nursing clinic for diabetes mellitus once per month, consecutively, for 6 months, and continued using the health education leaflet, operation workflow chart and alternating chart of the injection site distributed during hospitalization.

## Nursing project and conventional health education for the interventional group

### Establishment of the nursing project team

The nursing project team consisted of a leader, 2 diabetes specialist nurses and 12 primary care nurses.

### Preliminary analysis of the nursing project

We retrospectively analyzed the comprehension of an insulin injection technique using an insulin pen by patients with diabetes mellitus in 2019. The team members discussed, analyzed and summarized the following 10 items: insulin type, disinfection mode, standardized needle use, injection time, indwelling time, injection site, insulin pen installation, pre-injection exhaustion, premixed insulin vial-shaking, and insulin storage.<sup>14,19</sup> Then, they conclusively characterized issues under 4 headings: patient, nurse, method, and environment (Fig. 1).<sup>14</sup> Improvement measures of the nursing project are shown in Supplementary Table 2.

### Summary after discharge

The primary care nurses finished admission and discharge statistical analyses and compared and evaluated patients' injections. Six months after discharge, they conducted analyses, comparisons and evaluations of HbA1c, adipose hyperplasia incidence rate, and the 14-day TIR in the 2 groups.

### Indicator evaluation

#### Comprehension of insulin injection

The standardized insulin injection was comprehensively evaluated by segmentation scoring according to the Segmentation Scoring Form for Standardized Insulin Pen Use (Supplementary Table 1). Statistical analyses were performed before and after the nursing project intervention.

**Table 1.** Baseline characteristics of the trial participants across groups (control/intervention)

Variable		Control (n = 100)	Intervention (n = 100)	Test statistic (U) for the Mann–Whitney U test (intergroup)	p-value for the Mann– Whitney U test (intergroup)
Age	min	33.00	35.00	0.77	0.440
	Q1	54.00	52.00		
	median	61.00	59.00		
	mean	60.24	59.33		
	Q3	67.00	67.50		
	max	79.00	79.00		
	SD	9.82	10.23		
BMI	min	18.70	14.90	1.08	0.279
	Q1	23.20	22.15		
	median	24.75	24.50		
	mean	24.85	24.17		
	Q3	26.60	26.35		
	max	34.00	32.90		
	SD	2.95	3.36		
Cognitive ability score	min	24.00	24.00	0.80	0.422
	Q1	26.00	26.00		
	median	27.00	27.00		
	mean	27.22	27.02		
	Q3	28.00	28.00		
	max	30.00	30.00		
	SD	1.57	1.93		
Fasting blood glucose	min	4.10	3.90	0.06	0.952
	Q1	7.65	7.90		
	median	10.65	11.90		
	mean	11.81	11.55		
	Q3	15.10	13.90		
	max	27.80	36.80		
	SD	5.23	4.91		
Glycosylated hemoglobin	min	5.30	5.80	0.75	0.455
	Q1	7.85	8.40		
	median	9.70	10.10		
	mean	9.83	10.08		
	Q3	11.50	11.25		
	max	15.00	16.70		
	SD	2.33	2.19		
Course of diabetes mellitus score	min	1.00	1.00	0.60	0.546
	Q1	6.00	6.00		
	median	10.00	11.00		
	mean	10.70	11.62		
	Q3	15.50	15.00		
	max	30.00	43.00		
	SD	6.31	7.60		

Q1 – 1<sup>st</sup> quartile; Q3 – 3<sup>rd</sup> quartile; min – minimum; max – maximum; SD – standard deviation; BMI – body mass index. The p-value was considered not significant for  $p > 0.05$ .



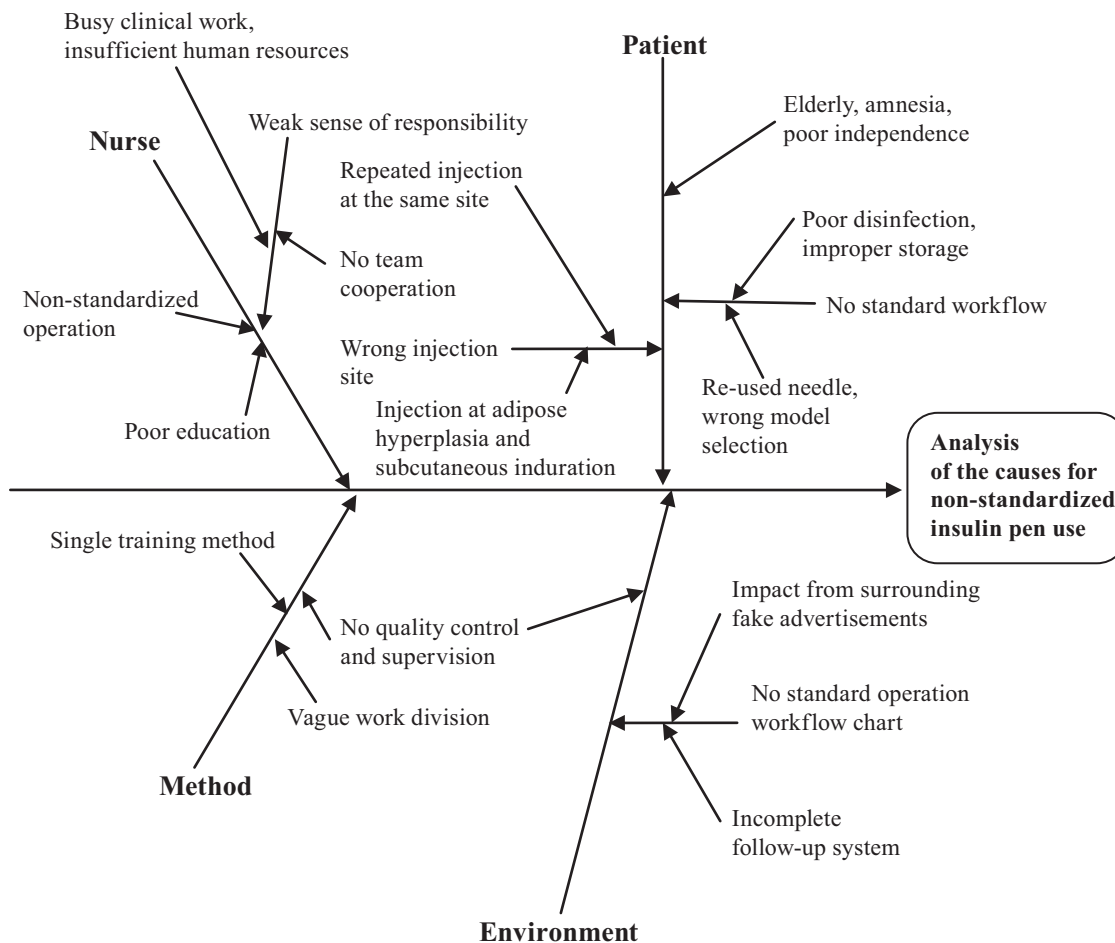


Fig. 1. Fishbone diagram analysis

Table 2. Comparison of insulin injection scores at admission and discharge from the hospital across groups (control/intervention)

Variable	Control (n = 100)			Intervention (n = 100)			Test statistic (U) for the Mann–Whitney test (intergroup)	p-value for the Mann–Whitney U test (intergroup)
	median	IQR	95% CI	median	IQR	95% CI		
Insulin installation scores (at admission)	2.0	0.0	–0.12–0.12	2.0	0.0	–0.12–0.12	0.16	0.872
Insulin installation scores (at discharge)	4.0	1.0	0.25–1.75	10.0	2.0	1.04–2.96	12.12	<0.001
Pre-injection exhaustion scores (at admission)	0.0	2.0	2.00–2.00	0.0	2.0	2.00–2.00	0.00	1.000
Pre-injection exhaustion scores (at discharge)	2.0	5.0	4.22–5.78	10.0	0.0	–1.65–1.65	12.09	<0.001
Standardized needle use scores (at admission)	0.0	4.0	3.58–4.42	0.0	4.0	3.75–4.25	0.11	0.910
Standardized needle use scores (at discharge)	4.0	0.0	–1.84–1.84	10.0	1.0	–0.87–2.87	12.46	<0.001
Injection time scores (at admission)	5.0	0.0	0.00–0.00	5.0	0.0	0.00–0.00	0.27	0.789
Injection time scores (at discharge)	5.0	0.0	0.00–0.00	10.0	0.0	–0.51–0.51	10.59	<0.001
Premixed insulin vial-shaking scores (at admission)	5.0	0.0	–1.45–1.45	5.0	0.0	–2.69–2.69	0.55	0.586
Premixed insulin vial-shaking scores (at discharge)	5.0	5.0	0.63–9.37	10.0	0.0	0.00–0.00	9.18	<0.001

p < 0.001 based on the Mann–Whitney U test; 95% CI – 95% confidence interval; IQR – interquartile range.

### Blood glucose control criteria

In accordance with the Chinese Guidelines for the Prevention and Treatment of Type 2 Diabetes (2020 edition)<sup>5</sup> and the interpretation of the International Consensus on Time in Range,<sup>29,30</sup> the analysis showed HbA1c  $\leq$  6.5%. Blood glucose within the 24-hour TIR was 3.9–10.0 mmol/L for 70% of the time.

### Adipose hyperplasia grading

Adipose hyperplasia grading was calculated based on the guidelines outlined in the study by Conwell et al.<sup>28</sup>

### Statistical analyses

The research utilized biomedical and demographic data (age and gender) of trial participants to understand the effects of the intervention across treatment and control groups. The descriptive statistics (mean, median, min, max, 1<sup>st</sup> quartile (Q1), 3<sup>rd</sup> quartile (Q3), and standard deviation (SD)) were used to analyze the distribution of baseline characteristics, including age, body mass index (BMI), cognitive ability score, fasting blood glucose, HbA1c, and diabetes mellitus. Percentage values were utilized for the categorical variable (gender).

The normality of discrete and continuous variables, such as insulin installation scores, pre-injection exhaustion scores, injection time scores, standardized use of insulin needle scores, premixed insulin vial-shaking scores, HbA1c, and TIR, were assessed using graphical methods (histograms, density plots, box plots, and quantile-quantile (Q-Q) plots). The outliers revealed in box plots were examined for typos and human errors. No outliers were removed as they were free from human error.

After assessing the data distribution of continuous/discrete variables (HbA1c, discharge scores of insulin TIR, injection time scores, standardized use of insulin needle scores, and other related indicators) using histograms with density plots and Q-Q plots, these variables were found to be non-normally distributed. The non-normally distributed data were compared between 2 groups (control and intervention) using a Mann–Whitney U test at a 5% significance level. The median value, interquartile range (IQR) and 95% confidence intervals (95% CIs) for the IQR were estimated and presented with U test statistics and p-values. The  $\chi^2$  test assessed the differences in categorical variable proportions across groups (control and intervention).

All statistical analyses employed IBM SPSS v. 23.0 (IBM Corp.) and Stata v. 13.0 (StataCorp LLC, College Station, USA) software.

## Results

The medical professional recruited 210 participants who satisfied the inclusion criteria. Ten participants who refused to participate in the research were excluded, and

the remaining 200 individuals were randomly assigned to a control or an intervention group. Figure 2 shows the study participation flowchart. Due to an epidemic, all patients undertook their daily activities locally and showed good compliance. There was no loss at follow-up.

The proportions of males who participated and were followed up during the trial across control and intervention groups were 62% and 63%, respectively. Around 38% of females were included in the control group, while there were 37% of females in the intervention group (Fig. 3).

The baseline profile of the 200 trial participants (100 per group) is shown in Table 1. The mean age of the participants in the intervention group was 59.33 years (Q1: 52.00, Q3: 67.50), which was relatively lower than the mean age in the control group (60.24 years, Q1: 54.00, Q3: 67.00).

The mean BMI of the intervention group was 24.17 kg/m<sup>2</sup> (Q1: 22.15, Q3: 26.35). In the control group, the mean cognitive ability score was 27.22 (Q1: 26.00, Q3: 28.00), and it was 0.20 points higher than that in the intervention group. Mean fasting glucose levels in the control group (11.81, Q1: 7.65, Q3: 15.10) were higher by 0.26 points than those in the intervention group (11.55, Q1: 7.90, Q3: 13.90). Meanwhile, HbA1c levels among control participants (9.83, Q1: 7.85, Q3: 11.50) were 0.25 points lower than those in the intervention group (10.08, Q1: 8.40, Q3: 11.25). Finally, the mean course of diabetes mellitus score was 0.92 points lower

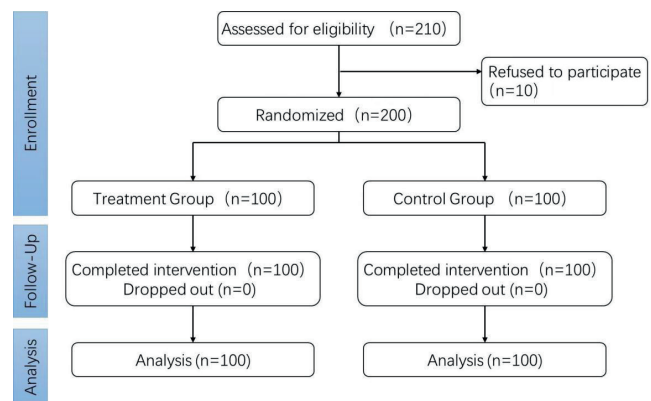


Fig. 2. Study participation flowchart

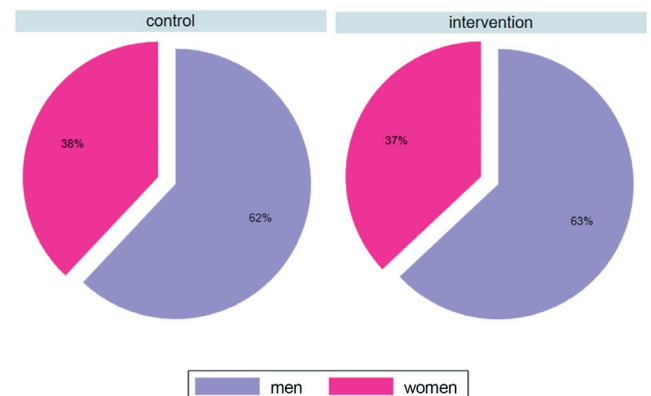


Fig. 3. Gender of study participants by group (control & intervention)

in the control group (10.70, Q1: 6, Q3: 15.50) compared to the intervention group (11.62, Q1: 6.00, Q3: 15.00).

No statistically significant differences ( $p > 0.05$ ) were found with regards to age, BMI, fasting blood glucose, HbA1c, course of diabetes mellitus, or insulin injection frequency between the 2 groups at a 5% significance level.

Table 2 shows the improved effectiveness of insulin pen injections between admission and discharge in the intervention and control groups. The median scores of insulin installation at discharge were significantly higher ( $U = 12.12, p < 0.001$ ) in the intervention group (median/IQR: 10.0/2.0, 95% CI: 1.04–2.96) compared to the control group (median/IQR: 4.0/1.0, 95% CI: 0.25–1.75). Similarly, median scores of pre-injection exhaustion were significantly higher ( $U = 12.09, p < 0.001$ ) in the intervention group (median/IQR: 10.0/0.0, 95% CI: –1.65–1.65) than in the control group (median/IQR: 2.0/5.0, 95% CI: 4.22–5.78). The median score for standardized needle use at discharge was also higher in the intervention group (median/IQR: 10.0/1.0, 95% CI: –0.87–2.87) compared to the control group (median/IQR: 4.0/0.0, 95% CI: –1.84–1.84).

Scores of injection time at discharge revealed a significant increase ( $U = 10.59, p < 0.001$ ) in the intervention group (median/IQR: 10.0/0.0, 95% CI: –0.51–0.51) compared to the control group (median/IQR: 5.0/0.0, 95% CI: 0.00–0.00). Meanwhile, median scores of premixed insulin vial-shaking were lower at discharge in the control group (median/IQR: 5.0/5.0, 95% CI: 0.63–9.37) than in the intervention group (median/IQR: 10.0/0.0, 95% CI: 0.00–0.00).

Table 3 outlines changes between the 2 groups in HbA1c levels on admission and after discharge and TIR at discharge. After 6 months of the nursing project intervention, a statistically significant decrease in the HbA1c level ( $U = 2.97, p = 0.003$ ) was observed in the intervention group (median/

IQR: 7.0/2.1, 95% CI: 1.47–2.70) in comparison to the control group (median/IQR: 7.7/2.5, 95% CI: 2.10–3.24). Similarly, a significant increase was observed in TIR after discharge ( $U = 2.72, p = 0.007$ ) in the intervention group (median/IQR: 69.5/30.0, 95% CI: 24.42–35.58) compared to the control group (median/IQR: 59.5/32.0, 95% CI: 23.39–40.61).

The  $\chi^2$  analysis demonstrated a statistically significant difference in adipose hyperplasia incidence rate after insulin application between the 2 groups ( $\chi^2 = 26.4, p = 0.048$ ). Improvements in the intervention group compared to the control group were as follows: 13.0% for mild, 6.0% for moderate and 2% for severe adipose hyperplasia. The nursing project effectively improved the therapeutic efficacy of insulin injections in diabetes mellitus patients (Table 4).

## Discussion

Diabetes mellitus patients who require insulin injection have a low standard-reaching rate for glucose control, with non-drug factors being a major concern.<sup>16</sup> In this study, we explored the effectiveness of a nursing project for improving patient insulin self-injection. The main difference between the 2 groups was that the intervention group underwent 6 health education courses implementing the latest course design of comprehensive and intensive lectures. Most diabetes mellitus patients are elderly with poor memory and have great difficulty rapidly accepting and storing knowledge, so such a course design is helpful for them. The improvements in insulin pen injections (installation) were significantly superior in the intervention group compared to the control group ( $p < 0.001$ ). Thus, the nursing project successfully standardized the injection technique in a short period of time and is therefore worthy of implementation.

**Table 3.** Comparison of HbA1c level in participants at admission (pre) and discharge (post) across groups (control/intervention)

Variable	Control (n = 100)		Intervention (n = 100)		Test statistic (U) for the Mann–Whitney test (intergroup)	p-value for the Mann–Whitney U test (intergroup)
	median (IQR)	95% CI	median (IQR)	95% CI		
HbA1c (at admission)	9.7 (3.7)	2.87–4.30	10.1 (2.9)	2.05–3.84	0.75	0.455
HbA1c (at discharge)	7.7 (2.5)	2.10–3.24	7.0 (2.1)	1.47–2.70	2.97	0.003
TIR (after discharge)	59.5 (32.0)	23.39–40.61	69.5 (30.0)	24.42–35.58	2.72	0.007

HbA1c – glycosylated hemoglobin; TIR – time in range; 95% CI – 95% confidence interval; IQR – interquartile range.

**Table 4.** Effectiveness of insulin self-injection on adipose hyperplasia

Risk levels		Control group (n = 100)	Intervention group (n = 100)	$\chi^2$ statistic	p-value (intergroup)
		Adipose hyperplasia, n (%)	mild		
	moderate	13 (13.0)	6 (6.0)		
	severe	8 (8.0)	2 (2.0)		

\*p-value was calculated using the  $\chi^2$  test.

The HbA1c and time in range, the latest study method used in the nursing field and an important indicator for the clinical evaluation of the efficacy of glucose control, were used as primary and secondary endpoints, respectively, to evaluate the effectiveness of the nursing project in this study. We found a statistically significant difference in TIR ( $p = 0.007$ ) and HbA1c ( $p = 0.003$ ) between the 2 groups at 6 months, indicating an obvious improvement in the intervention group. Time in range reached 65% of the expected target in the intervention group, and it reached the recommended level (70%) after long-term intervention.<sup>31</sup> These findings are similar to the results of a previous study.<sup>16</sup>

Comprehensive non-drug interventions work more slowly than drug interventions. However, most hypoglycemic drugs have serious side effects and may be used as adjuvant therapy to reduce the daily insulin dose, as shown in a previous study.<sup>16</sup> Standardized insulin pen use effectively reduced variations in insulin absorption<sup>32,33</sup> and stably controlled blood glucose so that it approached or reached the target level, confirming the efficacy of the nursing project and improving patient satisfaction with treatment. In this study, we explored the relationship between TIR and standardized insulin injection but did not elucidate influential factors and their effects, which will be the direction of subsequent nursing research.

Similar to a previous study,<sup>22</sup> patients using premixed insulin were selected at enrollment since a lack of standardized vial-shaking of premixed insulin may lead to an increased proportion of short-acting insulin and thus increase the risk of hypoglycemia, affecting the glucose control effect.<sup>5</sup> In our study, patients were unfamiliar with the vial-shaking skills required for premixing insulin, though the nursing project achieved a limited improvement by reinforcement. This observation is largely related to patients not giving sufficient importance to a standardized injection technique, a lack of formal pre-hospital training, and a lack of references to guidelines, as well as the intervention time of the nursing project. A 7-day nursing intervention during hospitalization failed to induce a successful switch from a conventional injection technique to a post-intervention standardized injection technique in patients, highlighting that the intervention time of the nursing project needs to be prolonged.

In contrast to previous investigations,<sup>14,19</sup> this study demonstrated that the injection time was associated with pre-injection hunger in patients. Newly admitted patients showed excessive hunger due to medical examination requirements. Patients often self-injected insulin and then ate several snacks before the provision of staple foods. Some patients, especially those requiring 3 injections, missed regular meals because of the demand for a medical examination. As a result, insulin injections could not be determined as being pre-breakfast or pre-lunch. For the fasting examination, some patients underwent a fasting state of 10 h or longer due to a long waiting period for

various reasons and probably presented with hypoglycemic symptoms. The evaluation and intervention of these patients are critical and will be investigated by a subgroup study in our subsequent nursing project plan.

Adipose hyperplasia is an insulin injection-related complication that manifests as skin swelling or subcutaneous induration, but its pathogenesis is unknown. It is perhaps associated with the overall time of insulin treatment, a lack of change in the injection site and repeated needle use.<sup>34</sup> The overall time for insulin treatment is uncontrollable and is a blind spot in our study, thus it will be the subject of future research. The lack of change in the injection site and repeated needle use can be improved by the nursing project to decrease the adipose hyperplasia incidence rate and reduce insulin dose and treatment costs.<sup>16,19</sup> In the present study, 4 conventional injection sites (abdomen, upper arm, thigh, and buttocks) were selected, and a 32G 4-mm insulin pen needle was used in all enrolled patients. Buttock injections were difficult for patients, and they required assistance from their families or doctors/nurses to change injection sites in order to reduce the occurrence of adipose hyperplasia. Studies have suggested that the skin thickness of the Asian population is 1.7–2.8 mm on average.<sup>35,36</sup> A 4-mm needle is sufficiently long to penetrate the skin by vertical insertion and short enough to effectively reduce the risk of injection into the muscle layer<sup>37</sup> while reducing and preventing the occurrence of hypoglycemia. Previous studies have demonstrated the safety of the 4-mm needle in all populations.<sup>16</sup> Therefore, other needle models were excluded at patient enrollment.

From a technical perspective, conventional health education and a nursing project alongside conventional health education were conducted in the control and intervention groups, respectively. As shown by the study results, the incidence rate of adipose hyperplasia 6 months after discharge was lower in the intervention group than in the control group ( $p = 0.048$ ), highlighting the efficacy of the nursing project. However, such improvement was insignificant due to the short intervention time of only 6 months. The occurrence of adipose hyperplasia is a long process; thus, good comparability requires standardized insulin injections over the long term.

## Limitations

The study was limited by the small sample size and not employing ultrasonic diagnosis of skin and subcutaneous tissues in patients with adipose hyperplasia. Future research will focus on the following aspects: 1) the nursing of patients with concomitant diseases and diabetes complications, such as diabetes with Alzheimer's disease or Parkinsonian syndromes, and impaired vision caused by diabetic optic neuropathy, as well as how these affect standardized insulin injections; and 2) the relationship between the TIR and chronic diabetes complications.



## Conclusions

In conclusion, the application of a nursing project had a positive role in providing knowledge on insulin, using standardized injections and patient self-management, and effectively improved therapeutic efficacy, reducing the occurrence of adipose hyperplasia. Therefore, a nursing project intervention has the potential for clinical application and is worthy of implementation. Another type of intervention, telenursing, is also feasible for standardizing the insulin injection technique.

## Supplementary data

The supplementary materials are available at <https://doi.org/10.5281/zenodo.8137362>. The package contains the following files:

Supplementary Table 1. Segmentation scoring form for standardized insulin pen use.

Supplementary Table 2. Improvement measures of nursing project.


Supplementary Fig. 1. Distribution of data of baseline characteristics of the trial participants across groups.

Supplementary Fig. 2. Distribution of data of glycosylated hemoglobin before and after treatment across groups.

Supplementary Fig. 3. Distribution of data of insulin type scores across groups.

## ORCID iDs

Bing Peng  <https://orcid.org/0009-0002-4591-4327>

Yanlin Zhang  <https://orcid.org/0009-0002-5316-8301>

Liqing Cheng  <https://orcid.org/0009-0009-7218-4498>

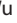
Yuping Zhang  <https://orcid.org/0009-0005-0272-7355>

Xiaotian Lei  <https://orcid.org/0000-0002-9615-7381>

Weiling Leng  <https://orcid.org/0000-0001-9375-9726>

Jing Wang  <https://orcid.org/0009-0008-8191-8062>

Songwei Wu  <https://orcid.org/0009-0005-6410-2203>

Xiaoqun Wu  <https://orcid.org/0009-0007-7864-9183>

Yanling Zheng  <https://orcid.org/0009-0002-3151-5843>

## References

- Mezquita-Raya P, Darbà J, Ascanio M, Ramírez De Arellano A. Cost-effectiveness analysis of insulin degludec compared with insulin glargine u100 for the management of type 1 and type 2 diabetes mellitus: From the Spanish National Health System perspective. *Expert Rev Pharmacoecon Outcomes Res.* 2017;17(6):587–595. doi:10.1080/14737167.2017.1345628
- Saeedi P, Petersohn I, Salpea P, et al. Global and regional diabetes prevalence estimates for 2019 and projections for 2030 and 2045: Results from the International Diabetes Federation Diabetes Atlas, 9<sup>th</sup> edition. *Diabetes Res Clin Pract.* 2019;157:107843. doi:10.1016/j.diabres.2019.107843
- Jin X, Zhu DD, Chen BZ, Ashfaq M, Guo XD. Insulin delivery systems combined with microneedle technology. *Adv Drug Deliv Rev.* 2018;127:119–137. doi:10.1016/j.addr.2018.03.011
- Sun H, Saeedi P, Karuranga S, et al. IDF Diabetes Atlas: Global, regional and country-level diabetes prevalence estimates for 2021 and projections for 2045. *Diabetes Res Clin Pract.* 2022;183:109119. doi:10.1016/j.diabres.2021.109119
- Shi G, Zhu N, Qiu L, et al. Impact of the 2020 China Diabetes Society Guideline on the prevalence of diabetes mellitus and eligibility for antidiabetic treatment in China. *Int J Gen Med.* 2021;14:6639–6645. doi:10.2147/IJGM.S331948
- Gupta R, Ghosh A, Singh AK, Misra A. Clinical considerations for patients with diabetes in times of COVID-19 epidemic. *Diabetes Metab Syndr.* 2020;14(3):211–212. doi:10.1016/j.dsx.2020.03.002
- Hirsch IB, Juneja R, Beals JM, Antalis CJ, Wright EE. The evolution of insulin and how it informs therapy and treatment choices. *Endocr Rev.* 2020;41(5):733–755. doi:10.1210/edrv/bnaa015
- Zhang Y, Yu J, Kahkoska AR, Wang J, Buse JB, Gu Z. Advances in transdermal insulin delivery. *Adv Drug Deliv Rev.* 2019;139:51–70. doi:10.1016/j.addr.2018.12.006
- Chinese Elderly Type 2 Diabetes Prevention and Treatment of Clinical Guidelines Writing Group, Geriatric Endocrinology and Metabolism Branch of Chinese Geriatric Society, Geriatric Endocrinology and Metabolism Branch of Chinese Geriatric Health Care Society, Geriatric Professional Committee of Beijing Medical Award Foundation, National Clinical Medical Research Center for Geriatric Diseases (PLA General Hospital). Clinical guidelines for prevention and treatment of type 2 diabetes mellitus in the elderly in China (2022 edition) [in Chinese]. *Zhonghua Nei Ke Za Zhi.* 2022;61(1):12–50. doi:10.3760/cma.j.cn112138-20211027-00751
- Garber AJ, Handelsman Y, Grunberger G, et al. Consensus Statement by the American Association of Clinical Endocrinologists and American College of Endocrinology on the Comprehensive Type 2 Diabetes Management Algorithm: 2020 Executive Summary. *Endocr Pract.* 2020;26(1):107–139. doi:10.4158/CS-2019-0472
- American Diabetes Association. Classification and diagnosis of diabetes: Standards of Medical Care in Diabetes (2020). *Diabetes Care.* 2020;43(Suppl 1):S14–S31. doi:10.2337/dc20-S002
- Davies MJ, D'Alessio DA, Fradkin J, et al. Management of hyperglycemia in type 2 diabetes, 2018: A Consensus Report by the American Diabetes Association (ADA) and the European Association for the Study of Diabetes (EASD). *Diabetes Care.* 2018;41(12):2669–2701. doi:10.2337/dci18-0033
- Tosun B, Cinar FI, Topcu Z, et al. Do patients with diabetes use the insulin pen properly? *Afr Health Sci.* 2019;19(1):1628. doi:10.4314/ahs.v19i1.38
- Gorska-Ciebiada M, Masierek M, Ciebiada M. Improved insulin injection technique, treatment satisfaction and glycemic control: Results from a large cohort education study. *J Clin Transl Endocrinol.* 2020;19:100217. doi:10.1016/j.jcte.2020.100217
- Zhang LJ, Guan H, Han TT, et al. Current status and its influencing factors of injection technique among patients with self-injection of insulin [in Chinese]. *Chinese Nursing Management.* 2017;480–485. [http://en.cnki.com.cn/Article\\_en/CJFDTOTAL-GLHL201704013.htm](http://en.cnki.com.cn/Article_en/CJFDTOTAL-GLHL201704013.htm). Accessed April 1, 2017.
- Grassi G, Scuntero P, Trepiccioni R, Marubbi F, Strauss K. Optimizing insulin injection technique and its effect on blood glucose control. *J Clin Transl Endocrinol.* 2014;1(4):145–150. doi:10.1016/j.jcte.2014.07.006
- Gradel AKJ, Porsgaard T, Lykkesfeldt J, et al. Factors affecting the absorption of subcutaneously administered insulin: Effect on variability. *J Diabetes Res.* 2018;2018:1205121. doi:10.1155/2018/1205121
- Kalra S, Hirsch LJ, Frid A, Deeb A, Strauss KW. Pediatric insulin injection technique: A multi-country survey and clinical practice implications. *Diabetes Ther.* 2018;9(6):2291–2302. doi:10.1007/s13300-018-0514-1
- Patil M, Sahoo J, Kamalanathan S, et al. Assessment of insulin injection techniques among diabetes patients in a tertiary care centre. *Diabetes Metab Syndr.* 2017;11(Suppl 1):S53–S56. doi:10.1016/j.dsx.2016.09.010
- Pozzuoli GM, Laudato M, Barone M, Crisci F, Pozzuoli B. Errors in insulin treatment management and risk of lipohypertrophy. *Acta Diabetol.* 2018;55(1):67–73. doi:10.1007/s00592-017-1066-y
- Gentile S, Guarino G, Strollo F. How to treat improper insulin injection-related lipohypertrophy: A 3-year follow-up of a monster case and an update on treatment. *Diabetes Res Clin Pract.* 2021;171:108534. doi:10.1016/j.diabres.2020.108534
- Ji L, Sun Z, Li Q, et al. Lipohypertrophy in China: Prevalence, risk factors, insulin consumption, and clinical impact. *Diabetes Technol Ther.* 2017;19(1):61–67. doi:10.1089/dia.2016.0334
- Ji L, Chandran A, Inocencio TJ, et al. The association between insurance coverage for insulin pen needles and healthcare resource utilization among insulin-dependent patients with diabetes in China. *BMC Health Serv Res.* 2018;18(1):300. doi:10.1186/s12913-018-3095-9

24. Bergenstal RM, Gal RL, Beck RW. Racial differences in the relationship of glucose concentrations and hemoglobin A<sub>1c</sub> levels. *Ann Intern Med*. 2018;168(3):232. doi:10.7326/L17-0589
25. Dai DJ, Lu JY, Zhang L, et al. The appropriate cut-off point of time in range (TIR) for evaluating glucose control in type 2 diabetes mellitus. *Chinese Journal of Diabetes*. 2019;139–140. [https://xueshu.baidu.com/usercenter/paper/show?paperid=1p5p08w0767x0680tk650xh026164101&site=xueshu\\_se](https://xueshu.baidu.com/usercenter/paper/show?paperid=1p5p08w0767x0680tk650xh026164101&site=xueshu_se). Accessed October 1, 2020.
26. Conwell LS, Pope E, Artiles AM, Mohanta A, Daneman A, Daneman D. Dermatological complications of continuous subcutaneous insulin infusion in children and adolescents. *J Pediatr*. 2008;152(5):622–628. doi:10.1016/j.jpeds.2007.10.006
27. Karges B, Schwandt A, Heidtmann B, et al. Association of insulin pump therapy vs. insulin injection therapy with severe hypoglycemia, ketoacidosis, and glycemic control among children, adolescents, and young adults with type 1 diabetes. *JAMA*. 2017;318(14):1358. doi:10.1001/jama.2017.13994
28. Tandon N, Kalra S, Balhara YP, et al. Forum for Injection Technique (FIT), India: The Indian recommendations 2.0, for best practice in Insulin Injection Technique, 2015. *Indian J Endocr Metab*. 2015;19(3):317. doi:10.4103/2230-8210.152762
29. Blanco M, Hernández MT, Strauss KW, Amaya M. Prevalence and risk factors of lipohypertrophy in insulin-injecting patients with diabetes. *Diabetes Metab*. 2013;39(5):445–453. doi:10.1016/j.diabet.2013.05.006
30. Vaag A, Handberg A, Lauritzen M, Henriksen JE, Pedersen KD, Beck-Nielsen H. Variation in absorption of NPH insulin due to intramuscular injection. *Diabetes Care*. 1990;13(1):74–76. doi:10.2337/diacare.13.1.74
31. Li H, Li YB. Interpretation of International Consensus on Time in Range. *Chinese Journal of Diabetes*. 2019;825–827. <https://rs.yiigle.com/CN2021/1173390.htm>. Accessed December 1, 2019.
32. Engwerda EEC, Tack CJ, De Galan BE. Pharmacokinetic and pharmacodynamic variability of insulin when administered by jet injection. *J Diabetes Sci Technol*. 2017;11(5):947–952. doi:10.1177/1932296817699638
33. Ji LN, Guo XH, Huang J, et al. Chinese Technical Guidelines for Injection of Diabetic Drugs (2016) [in Chinese]. *Chinese Journal of Diabetes*. 2017;79–105. <https://rs.yiigle.com/CN115791201702/945763.htm>. Accessed September 1, 2017.
34. Vardar B, Kızılcı S. Incidence of lipohypertrophy in diabetic patients and a study of influencing factors. *Diabetes Res Clin Pract*. 2007;77(2):231–236. doi:10.1016/j.diabres.2006.12.023
35. Sim KH, Hwang MS, Kim SY, Lee HM, Chang JY, Lee MK. The appropriateness of the length of insulin needles based on determination of skin and subcutaneous fat thickness in the abdomen and upper arm in patients with type 2 diabetes. *Diabetes Metab J*. 2014;38(2):120. doi:10.4093/dmj.2014.38.2.120
36. Catambing I, Villa M. Ultrasonographic measurement of skin and subcutaneous thickness at insulin injection sites among adult Filipinos with diabetes. *J ASEAN Fed Endocr Soc*. 2014;29(1):24–32. Accessed May 31, 2014.
37. Gibney MA, Arce CH, Byron KJ, Hirsch LJ. Skin and subcutaneous adipose layer thickness in adults with diabetes at sites used for insulin injections: Implications for needle length recommendations. *Curr Med Res Opin*. 2010;26(6):1519–1530. doi:10.1185/03007995.2010.481203

# Neoadjuvant camrelizumab and chemotherapy in patients with resectable esophageal squamous cell carcinoma: A prospective, single-arm, open-label study

Jianping Wang<sup>A,B,E</sup>, Jian Zhang<sup>C</sup>, Jie Gao<sup>D</sup>, Mengmeng Zhao<sup>B</sup>, Zhenkai Ma<sup>A,E,F</sup>

Department of Thoracic Surgery, People's Hospital of Yangzhong, China

A – research concept and design; B – collection and/or assembly of data; C – data analysis and interpretation; D – writing the article; E – critical revision of the article; F – final approval of the article

Advances in Clinical and Experimental Medicine, ISSN 1899–5276 (print), ISSN 2451–2680 (online)

*Adv Clin Exp Med.* 2024;33(6):573–581

## Address for correspondence

Zhenkai Ma  
E-mail: yzmzk@163.com

## Funding sources

None declared

## Conflict of interest

None declared

Received on April 3, 2023

Reviewed on July 9, 2023

Accepted on August 2, 2023

Published online on September 7, 2023

## Cite as

Wang J, Zhang J, Gao J, Zhao M, Ma Z. Neoadjuvant camrelizumab and chemotherapy in patients with resectable esophageal squamous cell carcinoma: A prospective, single-arm, open-label study. *Adv Clin Exp Med.* 2024;33(6):573–581. doi:10.17219/acem/170265

## DOI

10.17219/acem/170265

## Copyright

Copyright by Author(s)

This is an article distributed under the terms of the Creative Commons Attribution 3.0 Unported (CC BY 3.0) (<https://creativecommons.org/licenses/by/3.0/>)

## Abstract

**Background.** Esophageal cancer (EC) is a major cause of cancer-related deaths worldwide, bringing tremendous pressure to the healthcare system and patients. Esophageal squamous cell carcinoma (ESCC) is the main subtype of EC in the Chinese population.

**Objectives.** This study aimed to extend the neoadjuvant therapy cycle to 4 cycles and evaluate the efficacy and safety of neoadjuvant camrelizumab combined with chemotherapy for the treatment of resectable ESCC.

**Materials and methods.** The enrolled patients received neoadjuvant camrelizumab (200 mg, day 1), nab-paclitaxel (260 mg/m<sup>2</sup>, day 1) and carboplatin (area under curve; 5 mg/mL/min) every 21 days for 4 cycles, and surgery was performed within 4–6 weeks after the first day of the 4<sup>th</sup> treatment cycle. The primary endpoint of the study was the pathological complete response (pCR) rate.

**Results.** From December 15, 2021, to October 1, 2022, a total of 35 patients were enrolled in the study. All patients completed the full 4-cycle treatment and were deemed fit for surgical intervention. Thirty-four (97.1%) patients achieved R0 resection, 18 (51.4%) showed a pCR rate, and 27 (77.1%) achieved a major pathological response (MPR). Tumor degradation was observed in 30 out of 35 patients (85.7%). Multivariate logistic regression analyses further confirmed that age (odds ratio (OR) = 6.710, 95% confidence interval (95% CI): 3.512–44.403) and programmed death-ligand 1 (PD-L1) (OR = 2.855, 95% CI: 1.181–3.079) were independent predictors of pCR. The most prevalent adverse event (AE) was leukopenia, which was experienced by 23 out of 35 patients (65.7%). Grade 3 or higher AEs included leukopenia in 2 cases (5.7%) and neutropenia in 12 cases (34.3%). No delays in surgery were observed.

**Conclusions.** As demonstrated in this study, the 4 cycles of camrelizumab combined with nab-paclitaxel and carboplatin, which exhibited a relatively high pCR rate and acceptable safety, suggest a strong rationale for its further evaluation in resectable ESCC.

**Key words:** esophageal squamous cell carcinoma (ESCC), neoadjuvant therapy, anti-programmed death-1 (PD-1), camrelizumab

## Background

Esophageal cancer (EC) is a major cause of cancer-related deaths worldwide, bringing tremendous pressure to the healthcare system and patients.<sup>1–3</sup> Esophageal cancer primarily consists of 2 different epidemiological and pathological diseases, namely esophageal squamous cell carcinoma (ESCC) and esophageal adenocarcinoma.<sup>4</sup> Esophageal squamous cell carcinoma is the main subtype of EC in the Chinese population.<sup>5,6</sup> Surgery remains the primary treatment for resectable ESCC, but up to 50% of patients fail to achieve R0 resection, resulting in early postoperative recurrence.<sup>7</sup> Neoadjuvant chemoradiotherapy followed by surgery is a widely used standard treatment for patients with resectable EC.<sup>8,9</sup> In a study of preoperative chemoradiotherapy (carboplatin, paclitaxel and radiotherapy), known as Chemoradiotherapy for EC followed by Surgery Study (CROSS), there was an overall improvement in survival lasting at least 10 years in patients with locally advanced resectable EC.<sup>10,11</sup> However, the long-term clinical outcomes of neoadjuvant chemoradiotherapy remain unsatisfactory because death still occurs in more than half of patients.<sup>10</sup> Moreover, the perioperative toxicities caused by chemoradiation reduce its attractiveness to patients.<sup>12</sup> Therefore, clinicians and ESCC patients urgently need a neoadjuvant regimen that is more effective and less toxic.

Preclinical studies have shown that the combination of programmed cell death 1 (PD-1) inhibitors and chemotherapy can further strengthen the host immune response and prevent cancer cell escape.<sup>13</sup> In previous studies, the majority of neoadjuvant PD-1 antibody-combined therapy involved 2 cycles, while 4 cycles of neoadjuvant PD-1 antibody-combined therapy are rarely used.<sup>14</sup> Lv et al. reported that 3–4 cycles of neoadjuvant sintilimab, an immune checkpoint inhibitor targeting PD-1, plus chemotherapy in resectable locally advanced ESCC have a higher pathological complete response (pCR) rate than only 2 cycles of neoadjuvant sintilimab plus chemotherapy (47.9% compared to 12.5%;  $p = 0.0003$ ).<sup>15</sup> This suggests that extending the neoadjuvant therapy cycle may increase the pCR rate, which is associated with prolonged overall survival (OS).<sup>16,17</sup> Camrelizumab, a product developed in China, is a novel IgG4-kappa anti-PD-1 inhibitor that has been administered in the treatment of many types of malignancies.<sup>18</sup> Two cycles of neoadjuvant camrelizumab combined with chemotherapy have been shown to be effective and tolerable in newly diagnosed resectable ESCC, achieving pCR in 25% of patients.<sup>19</sup> Thus, although using 2 cycles of neoadjuvant therapy has been successful, 75% of patients still do not achieve pCR. Therefore, the extension of the camrelizumab-combined therapy cycle in patients with resectable locally advanced ESCC is worth exploring.

## Objectives

This study aimed to extend the neoadjuvant therapy cycle to 4 cycles and evaluate the efficacy and safety of neoadjuvant camrelizumab combined with chemotherapy for the treatment of resectable ESCC, hoping to develop a more effective regimen to enhance the clinical outcomes of ESCC patients.

## Materials and methods

### Study design and participants

In this prospective, single-arm study, we compared the efficacy and safety in a group of ESCC patients receiving 4 cycles of neoadjuvant camrelizumab-combined therapy with a group of historical controls who received only 2 cycles of neoadjuvant camrelizumab-combined therapy. The flowchart for the study is presented in Fig. 1. The study was conducted from December 15, 2021, to October 1, 2022, at the People's Hospital of Yangzhong (China). The inclusion criteria were as follows: 1) histologically confirmed resectable (stage II or III) ESCC; 2) male or female patients; 3) aged 18–75 years; 4) with an Eastern Cooperative Oncology Group (ECOG) score of 0 or 1. The exclusion criteria were as follows: 1) severe disease within the previous 5 years; 2) prior history of anti-PD-1 or anti-programmed death-ligand 1 (anti-PD-L1) treatment; 3) prior history of interstitial lung disease or active non-infectious pneumonia; 4) treatment with corticosteroids or other immunosuppressants in the preceding 2 weeks. The expression of the PD-L1 biomarker was not considered in the enrolled patients.

All patients provided written informed consent before enrollment, and the study was approved by the ethics committee of the People's Hospital of Yangzhong (approval No. 2021142). All patients enrolled in this experiment were Chinese.

### Procedures

All patients underwent clinical evaluation, including upper gastrointestinal endoscopy with diagnostic biopsy, computed tomography (CT) of the chest, ultrasonography of the major organs, routine electrocardiogram, echocardiography, pulmonary function test, and radionuclide bone scintigraphy. Before undergoing surgical resection, patients were treated with 4 cycles of the following drugs intravenously: camrelizumab (200 mg on day 1 every 3 weeks), nab-paclitaxel (260 mg/m<sup>2</sup> on day 1 every 3 weeks) and carboplatin (area under the curve of 5 mg/mL/min on day 1 every 3 weeks).

After the completion of neoadjuvant therapy, a reassessment was conducted to exclude patients with surgical contraindications. The reassessment included the same



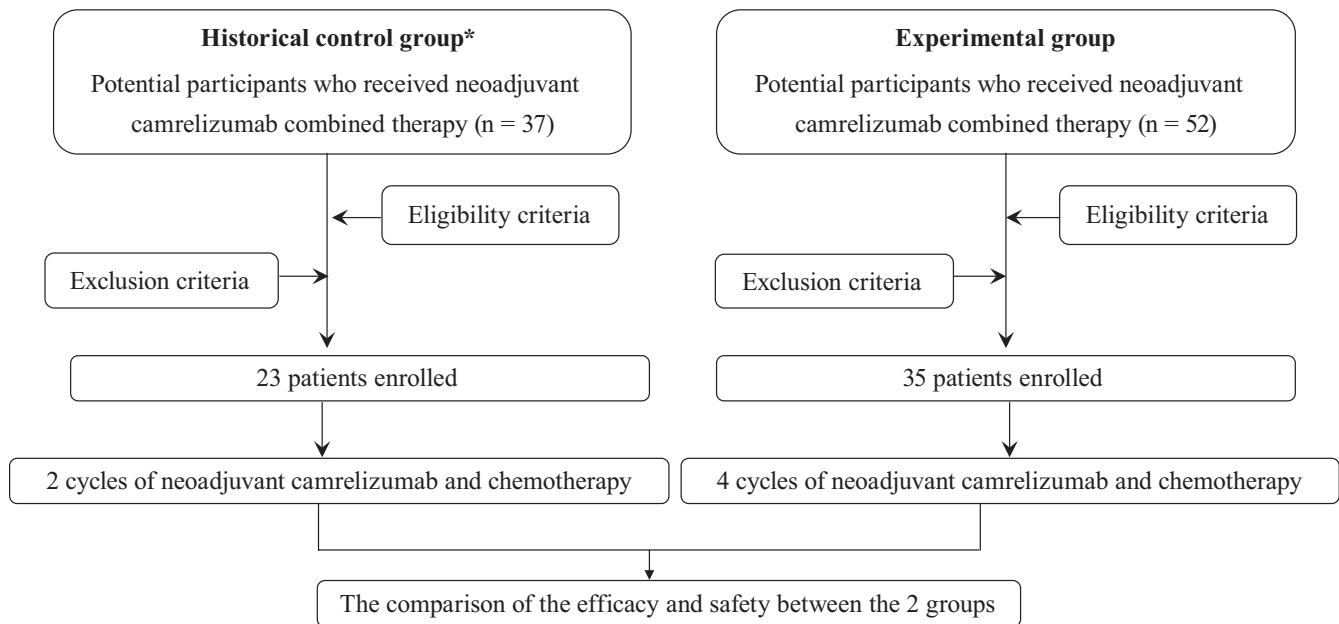


Fig. 1. Study flowchart based on the study by Yang et al.<sup>17</sup>

tests as the pretreatment staging. Surgery was scheduled to be performed within 4–6 weeks after the 1<sup>st</sup> day of the 4<sup>th</sup> treatment cycle. McKeown or Ivor Lewis esophagectomy was performed according to standard institutional procedures, including double-field lymphadenectomy and total mediastinal lymphadenectomy.

## Outcomes

The primary endpoint of this study was pCR, defined as no residual tumor cells. The secondary endpoints included major pathological response (MPR), defined as <10% residual tumor cells, R0 resection rate, objective response rate (ORR), disease control rate (DCR), disease-free survival (DFS, calculated from the date of enrollment), overall survival (OS), and safety. According to the Response Evaluation Criteria in Solid Tumors (RECIST) v. 1.1, the target lesion of EC was defined as lymph nodes with a small diameter ( $\geq 15$  mm); the primary esophageal lesion was not considered the target lesion. Tumor response was evaluated every 2 cycles. Toxicity profiles were evaluated using the National Cancer Institute Common Terminology Criteria for Adverse Events (NCI-CTCAE) (v. 5.0).

## Statistical analyses

According to a previous study,<sup>17</sup> the pCR rate of 2 cycles of neoadjuvant therapy was 25%, while 50% was the expected rate in our study. The sample size ensuring a higher pCR rate was calculated using PASS 15 software (NCSS LCC, Kaysville, USA). A total of 30 eligible subjects would be required to detect a difference between 25% and 50% pCR rate with a power of 80%. Considering a 15% patient loss, at least 35 cases would need to be enrolled. Categorical

variables, including gender, smoking status, tumor location, ECOG performance status, alcohol consumption, clinical tumor stage, clinical nodal stage, clinical TNM stage, histologic grade, and PD-L1, were presented as frequency count (percentage), and numerical variables were presented as median (interquartile range (IQR)) or mean  $\pm$  standard deviation ( $M \pm SD$ ). Survival probability was evaluated using the Kaplan–Meier method. Multivariate logistic regression analysis was performed to explore the independent predictors of pCR. The goodness of fit was assessed using Nagelkerke  $R^2$ . Multicollinearity was checked using the variance inflation factor (VIF); the VIF values of all independent predictors were less than 2. All reported p-values were bilateral, with  $p < 0.05$  considered statistically significant.

## Results

### Baseline

From December 15, 2021, to October 1, 2022, a total of 52 patients from the People's Hospital of Yangzhong were screened as eligible for the experimental group. Thirty-five patients were enrolled after providing informed consent (Fig. 1). As seen in Table 1, 19 patients (54.3%) in the experimental group were under 65 years old, and 16 (45.7%) patients were over 65 years old. Among all the patients, 71.4% were male (25 patients) and 28.6% were female (10 patients). Most of the patients (54.3%) were former or current smokers. The tumors were located in the upper segment (11.4%), middle segment (45.7%) and lower segment (42.9%) of the esophagus. Before treatment, T3 (62.9%) was the predominant clinical tumor

**Table 1.** Baseline characteristics of the patients

Characteristic		Experimental group (n = 35)	Historical control group* (n = 23)
Age, n (%) [years]	≤65	19 (54.3)	N/A
	>65	16 (45.7)	N/A
Gender, n (%)	male	25 (71.4)	22 (95.7)
	female	10 (28.6)	1 (4.3)
ECOG performance status, n (%)	0	27 (77.1)	21 (91.3)
	1	8 (22.9)	2 (8.7)
Smoking status, n (%)	never	16 (45.7)	7 (30.4)
	former or current	19 (54.3)	16 (69.6)
Alcohol consumption, n (%)	never	14 (40.0)	11 (47.8)
	former or current	21 (60.0)	12 (52.2)
Tumor location, n (%)	upper segment	4 (11.4)	1 (4.3)
	middle segment	16 (45.7)	9 (39.1)
	lower segment	15 (42.9)	13 (56.5)
Clinical tumor stage, n (%)	T1	7 (20.0)	N/A
	T2	4 (11.4)	N/A
	T3	22 (62.9)	N/A
	T4	2 (5.7)	N/A
Clinical nodal stage, n (%)	N0	6 (17.1)	N/A
	N1	23 (65.7)	N/A
	N2	6 (17.1)	N/A
Clinical TNM stage, n (%)	II	13 (37.1)	8 (34.8)
	III	22 (62.9)	15 (65.2)
Histologic grade, n (%)	well differentiated	6 (17.1)	N/A
	moderately differentiated	8 (22.9)	N/A
	poorly differentiated	21 (60.0)	N/A
PD-L1, CPS, n (%)	<1	17 (48.6)	7 (30.4)
	≥1	18 (51.4)	12 (52.2)

ECOG – Eastern Cooperative Oncology Group; TNM – tumor node metastasis; PD-L1 – programmed death-ligand 1; CPS – combined positive score; N/A – not applicable; \* based on the results obtained by Yang et al.<sup>17</sup>

stage, while N1 (65.7%) was the most common clinical nodal stage. Thirteen patients (37.1%) had stage II tumors and 22 patients (62.9%) had stage III tumors. Twenty-seven patients (77.1%) had an ECOG performance score of 0 and 8 patients (22.9%) had a score of 1. The PD-L1 expression was evaluated in the biopsy samples. The results showed that 18 samples (51.4%) were PD-L1-positive (combined positive score (CPS) ≥ 1) and 17 samples (48.6%) were PD-L1-negative (CPS < 1). Tumors were determined to be well differentiated in 6 patients (17.1%), moderately differentiated in 8 patients (22.9%) and poorly differentiated in 21 patients (60.0%). Overall, there were slightly more female patients in the experimental group than in the historical control group, and there were also more patients with an ECOG performance score of 1 in the experimental group. The baseline characteristics of the 35 patients in the experimental group and the 23 patients in the historical control group are summarized in Table 1.

## Tumor response

Following a course of 4 cycles of neoadjuvant immunotherapy in combination with chemotherapy, 28 patients with target lesions were evaluable for response in the experimental group. Two patients (7.1%) achieved complete response, 25 patients (89.3%) showed partial response, 1 patient (3.6%) remained stable, and no patients had progressive disease, resulting in an ORR of 96.4% and a DCR of 100.0% (Table 2 and Fig. 2). In the historical control group, the ORR and DCR were 90.5% and 100.0%, respectively. The details of these outcomes are presented in Table 2.

## Surgical and pathological outcomes

In the experimental group, 35 patients underwent surgery, with 34 (97.1%) achieving R0 resection, 18 (51.4%) showing pCR and 27 (77.1%) achieving MPR (Table 3).

**Table 2.** Tumor response

Variable		Experimental group (n = 28)	Historical control group* (n = 21)
Best overall response, n (%)	complete response	2 (7.1)	1 (4.8)
	partial response	25 (89.3)	18 (85.7)
	stable disease	1 (3.6)	2 (9.5)
Progressive disease		0	0
Objective response rate, n (%)		27 (96.4)	19 (90.5)
Disease control rate, n (%)		28 (100.0)	21 (100.0)

\* based on the results obtained by Yang et al.<sup>17</sup>

**Table 3.** Surgical and pathological outcomes

Characteristics		Experimental group (n = 35)	Historical control group* (n = 20)
Successful R0 resection, n (%)		34 (97.1)	20 (100)
Pathological response, n (%)	pCR	18 (51.4)	5 (25.0)
	MPR	27 (77.1)	10 (50.0)
Downstaging of TNM stage, n (%)	yes	30 (85.7)	13 (65.0)
	no	5 (14.3)	7 (35.0)
Blood loss (mL), median (IQR)		100.0 (65.0–185.0)	N/A
Cumulative operative time (min), M ±SD		265.9 ±46.7	292.5 ±53.1
Postoperative hospital stay [days], median (IQR)		21.0 (20.0–25.0)	N/A
Surgical complications, n (%)	anastomotic leakage	1 (2.9)	2 (10.0)
	pulmonary infection	2 (5.7)	1 (5.0)
	incisional hernia	1 (2.9)	N/A
	postoperative bleeding	1 (2.9)	1 (5.0)
	postoperative hoarseness	1 (2.9)	1 (5.0)

pCR – pathological complete response; MPR – major pathological response; M ±SD – mean ± standard deviation; TNM – tumor node metastasis; IQR – interquartile range; N/A – not applicable; \* based on the results obtained by Yang et al.<sup>17</sup>

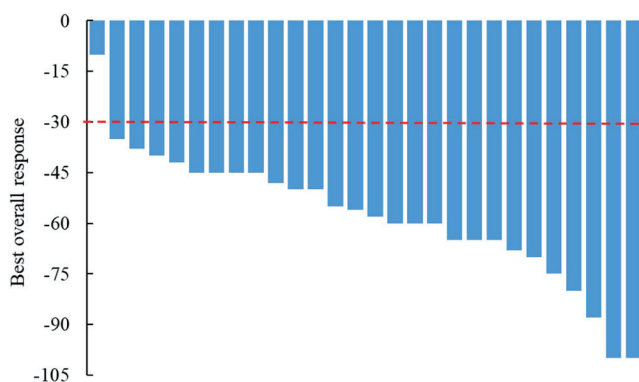


**Fig. 2.** Bar plot of the best overall response in the population (n = 28) according to RECIST1.1. Each bar represents 1 patient

Tumor degradation was observed in 30 out of 35 patients (85.7%). The median intraoperative blood loss was 100.0 mL (IQR: 65.0–185.0 mL), and the average operative time was 265.9 ±46.7 min. The median hospital stay after surgery was 21.0 days (IQR: 20.0–25.0). Table 3 summarizes the postoperative complications, which included 1 case each of anastomotic leakage, incisional hernia, heavy bleeding, and hoarseness, and 2 cases of pulmonary infection (5.7%). No serious complications, such as respiratory

failure, heart failure, deep vein thrombosis, or acute respiratory distress syndrome, were reported. The proportions of patients achieving pCR, MPR and downstaging of the tumor node metastasis (TNM) stage were higher in the experimental group than in the historical control group, and the pCR rate improved by 26.4%. The incidence of surgical complications was low in both groups. The details are listed in Table 3.

### Exploratory analysis

To further clarify the relationship between the baseline characteristics and pCR in patients with resectable ESCC, the Box–Tidwell test was conducted. Its results revealed a linear relationship between all continuous independent variables and the dependent variable logit conversion value (all  $p > 0.05$ ) (Supplementary Table 1). Next, we performed a multivariate logistic regression analysis and confirmed that age (OR = 6.710, 95% CI: 3.512–44.403) and PD-L1 CPS (OR = 2.855, 95% CI: 1.181–3.079) were independent predictors of pCR (Table 4), indicating that the drug was more effective for patients aged <65 years and with a higher expression of PD-L1 (Nagelkerke  $R^2 = 0.676$ ,  $p = 0.010$ ).

**Table 4.** Multivariate analyses for pathological complete response (PCR) in patients with resectable esophageal squamous cell carcinoma in the experimental group

Variable	OR (95% CI)	p-value	
Age [years]	>65	reference	
	≤65	6.710 (3.512, 44.403)	0.016
Gender	male	reference	
	female	1.510 (0.022, 15.010)	0.842
ECOG performance status	0	reference	
	1	0.315 (0.008, 6.843)	0.475
Smoking status	never	reference	
	former or current	0.163 (0.002, 4.553)	0.322
Alcohol consumption	never	reference	
	former or current	1.373 (0.091, 26.837)	0.819
Tumor location	upper segment	reference	
	middle segment	6.798 (0.075, 18.282)	0.430
	lower segment	1.924 (0.020, 3.485)	0.780
Histologic grade	well differentiated	reference	
	moderately differentiated	0.070 (0.002, 2.910)	0.221
	poorly differentiated	1.464 (0.047, 49.315)	0.821
Clinical TNM stage	II	reference	
	III	0.120 (0.003, 1.772)	0.170
PD-L1 CPS	<1	reference	
	≥1	2.855 (1.181, 3.079)	0.036

ECOG – Eastern Cooperative Oncology Group; TNM – tumor node metastasis; PD-L1 – programmed death-ligand 1; CPS – combined positive score; OR – odds ratio; 95% CI – 95% confidence interval.

## Safety and follow-up

A summary of adverse events (AEs) is presented in Table 5. In the experimental group, the most prevalent AE was leukopenia, which was experienced by 23 out of 35 patients (65.7%). Other common AEs among patients included asthenia (62.9%), alopecia (60.0%), neutropenia (60.0%), rash (60.0%), and anemia (54.3%). The grade 3 or higher AEs included leukopenia in 2 cases (5.7%) and neutropenia in 12 cases (34.3%). One patient experienced a massive esophageal hemorrhage 3 weeks before surgery but was successfully treated and underwent successful surgery. Other AEs observed during neoadjuvant therapy included an increase in alanine aminotransferase (ALT), which occurred in 14 cases (40.0%), reactive cutaneous capillary endothelial proliferation (RCCEP), which occurred in 14 cases (40.0%), and increased aspartate aminotransferase, which occurred in 12 cases (34.3%). None of these caused any treatment suspensions, dose reductions or surgical delays, and the patients remained generally stable until the last follow-up. In the historical control group, alopecia was the most common AE, followed by asthenia, leukopenia, neutropenia, and rash, with hyperthyroidism being the least common. In addition, the 12-month DFS was 71.2%, and the 12-month OS rate was 94.4% in the experimental group (Fig. 3,4).

## Discussion

This study prospectively evaluated the efficacy and safety of surgery after neoadjuvant camrelizumab combined with chemotherapy for the treatment of resectable ESCC. The study extended the neoadjuvant treatment regimen to 4 cycles, hoping to develop a more effective regimen to enhance the clinical outcomes in ESCC patients.

In the preoperative setting, chemotherapy combined with radiotherapy is the current standard neoadjuvant regimen, and it is being used as a combination partner of immunotherapy in many ongoing trials.<sup>20,21</sup> However, due to the toxic effects of radiotherapy, a less harmful regimen is being sought.<sup>22</sup> Thus, we were interested in exploring the response of ESCC to immunotherapy combined with chemotherapy. Indeed, in our study, neoadjuvant chemotherapy in conjunction with camrelizumab achieved a pCR rate of 51.4%, which was significantly higher than that of previously reported neoadjuvant immunotherapy combined with chemotherapy (22.2%, 25% and 46.2%),<sup>7,17,23</sup> improving the pCR rate by 29.2%, 26.4% and 5.2%, respectively. The reason for this may be that the patients in the previous studies received only 2 or 3 cycles of neoadjuvant therapy, while our patients were treated with 4 cycles. In addition, 30 out of 35 surgical patients (85.7%) had degraded TNM staging after

Table 5. Adverse events

Adverse event, n (%)	Experimental group (n = 35)		Historical control group* (n = 23)	
	any grade	grade ≥3	any grade	grade ≥3
Leukopenia	23 (65.7)	2 (5.7)	14 (60.9)	2 (8.7)
Asthenia	22 (62.9)	0	15 (65.2)	0
Alopecia	21 (60.0)	0	19 (82.6)	0
Neutropenia	21 (60.0)	12 (34.3)	14 (60.9)	9 (39.1)
Rash	21 (60.0)	0	14 (60.9)	0
Anemia	19 (54.3)	0	13 (56.5)	0
Alanine aminotransferase increased	14 (40.0)	0	10 (43.5)	0
RCCEP	14 (40.0)	0	9 (39.1)	0
Aspartate aminotransferase increased	12 (34.3)	0	8 (34.8)	0
Hyperbilirubinemia	11 (31.4)	0	8 (34.8)	0
Thrombocytopenia	10 (28.6)	0	7 (30.4)	0
Decreased appetite	10 (28.6)	0	8 (34.8)	0
Vomiting	7 (20.0)	0	5 (21.7)	0
Oral mucositis	6 (17.1)	0	4 (17.4)	0
Diarrhea	5 (14.3)	0	3 (13.0)	0
Nausea	4 (11.4)	0	3 (13.0)	0
Constipation	4 (11.4)	0	3 (13.0)	0
Edema	3 (8.6)	0	2 (8.7)	0
Fever	3 (8.6)	0	2 (8.7)	0
Hyperthyroidism	1 (2.9)	0	1 (4.3)	0

RCCEP – reactive cutaneous capillary endothelial proliferation; \* based on the results obtained by Yang et al.<sup>17</sup>

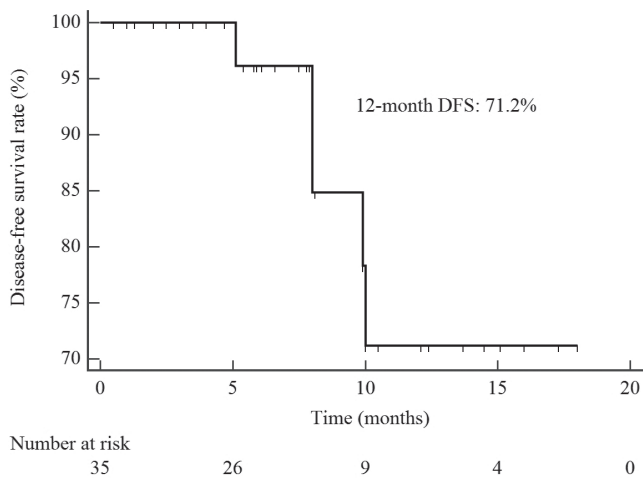


Fig. 3. Disease-free survival (DFS) curve of all patients who received surgery (n = 35)

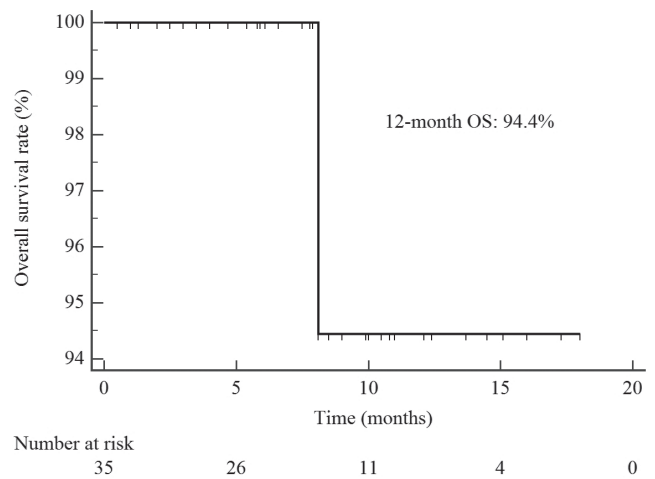


Fig. 4. Overall survival (OS) curve of all patients who received surgery (n = 35)

treatment, which is higher than that reported in the previous literature (65%).<sup>17</sup>

The findings of several important studies, including CROSS, NEOCRTEC5010 and the CheckMate 577 trial, have made neoadjuvant chemoradiotherapy combined with surgery a commonly accepted treatment option for resectable ESCC in Western countries.<sup>8,10,24</sup> The usage of neoadjuvant chemoradiotherapy is limited due to the added toxicity from chemotherapy and radiotherapy.<sup>25,26</sup> Reducing the dose to mitigate toxicity may reduce patient adherence,

and neoadjuvant chemoradiotherapy can also lead to complications during surgery, such as tissue adhesion and swelling, and increase the risk of perioperative issues, such as radiation pneumonitis-induced respiratory failure, which may offset the intended survival benefits from neoadjuvant chemoradiotherapy.<sup>27,28</sup> Our study results indicate that leukopenia was the most frequently occurring AE, affecting 23 out of 35 patients. Other common AEs included asthenia, alopecia, neutropenia, rash, and anemia. We also identified grade 3 or higher AEs, including leukopenia in 2 cases



and neutropenia in 12 cases. Regarding postoperative complications, our study found a 2.9% incidence of anastomotic leakage, which is lower than what was previously reported in the CROSS study (22%). It should be noted that the study reports successful treatment and surgery of 1 patient who experienced massive esophageal hemorrhage 3 weeks prior to surgery. We detected increased levels of alanine aminotransferase in 14 cases, RCCEP in 14 cases and increased levels of aspartate aminotransferase in 12 cases, but none of these resulted in treatment suspensions, dose reductions or surgical delays.

Previous research has shown that several clinical biomarkers, including neutrophil-to-lymphocyte ratio (NLR), platelet-to-lymphocyte ratio (PLR) and lymphocyte-to-monocyte ratio (LMR), have moderate predictive value for prognosis. However, their potential for predicting the efficacy of immunotherapy remains rarely reported.<sup>29,30</sup> In recent years, the importance of PD-L1 expression level has been a popular topic in immunotherapy. However, earlier clinical trial results indicate that immunotherapy combined with chemotherapy is beneficial in the entire population, including those with negative PD-L1 expression, which led to PD-L1 detection being non-essential.<sup>31,32</sup> Interestingly, our exploratory analysis showed that patients with higher PD-L1 expression were more likely to benefit from neoadjuvant therapies; thus, the PD-L1 expression seems to be a predictive factor for pCR after neoadjuvant immunotherapy. In addition, patients aged >65 years achieved a lower pCR, which may be attributed to the physiologic decline in the functions of major organs in older patients.<sup>33</sup> The guiding value of age and PD-L1 expression level in immunotherapy should be recognized and is worthy of further exploration in future large sample studies.

## Limitations

There are 2 limitations to this study. First, the sample size was small, implying that a larger cohort is necessary to further validate these findings. Second, owing to the short duration of follow-up, median DFS and OS were not reported, but follow-up is still in progress.

## Conclusions

In conclusion, the results of this study suggest that the extension of the treatment cycle to 4 cycles of neoadjuvant camrelizumab combined with chemotherapy may offer a promising treatment option for patients with resectable ESCC. Further large-sample studies are needed to confirm these results.

## Data availability statement

The data from this study are available from the corresponding author upon reasonable request.

## Supplementary data

The supplementary materials are available at <https://doi.org/10.5281/zenodo.8199073>. The package contains the following files:

Supplementary Table 1. The results of Box–Tidwell test.

## ORCID iDs

Jianping Wang  <https://orcid.org/0009-0002-8914-5961>

Jian Zhang  <https://orcid.org/0009-0003-8740-8702>

Jie Gao  <https://orcid.org/0009-0000-5062-3626>

Mengmeng Zhao  <https://orcid.org/0009-0003-5772-0041>

Zhenkai Ma  <https://orcid.org/0009-0003-3503-7532>

## References

- Enzinger PC, Mayer RJ. Esophageal cancer. *N Engl J Med*. 2003;349(23):2241–2252. doi:10.1056/NEJMra035010
- Abnet CC, Arnold M, Wei WQ. Epidemiology of esophageal squamous cell carcinoma. *Gastroenterology*. 2018;154(2):360–373. doi:10.1053/j.gastro.2017.08.023
- Siegel RL, Miller KD, Fuchs HE, Jemal A. Cancer statistics, 2022. *CA Cancer J Clin*. 2022;72(1):7–33. doi:10.3322/caac.21708
- Smyth EC, Lagergren J, Fitzgerald RC, et al. Oesophageal cancer. *Nat Rev Dis Primers*. 2017;3(1):17048. doi:10.1038/nrdp.2017.48
- Morgan E, Soerjomataram I, Runggay H, et al. The global landscape of esophageal squamous cell carcinoma and esophageal adenocarcinoma incidence and mortality in 2020 and projections to 2040: New estimates from GLOBOCAN 2020. *Gastroenterology*. 2022;163(3):649–658.e2. doi:10.1053/j.gastro.2022.05.054
- Chen W, Zheng R, Baade PD, et al. Cancer statistics in China, 2015. *CA Cancer J Clin*. 2016;66(2):115–132. doi:10.3322/caac.21338
- Zhang Z, Ye J, Li H, et al. Neoadjuvant sintilimab and chemotherapy in patients with resectable esophageal squamous cell carcinoma: A prospective, single-arm, phase 2 trial. *Front Immunol*. 2022;13:1031171. doi:10.3389/fimmu.2022.1031171
- Kelly RJ, Ajani JA, Kuzdzal J, et al. Adjuvant nivolumab in resected esophageal or gastroesophageal junction cancer. *N Engl J Med*. 2021;384(13):1191–1203. doi:10.1056/NEJMoa2032125
- Wang H, Tang H, Fang Y, et al. Morbidity and mortality of patients who underwent minimally invasive esophagectomy after neoadjuvant chemoradiotherapy vs. neoadjuvant chemotherapy for locally advanced esophageal squamous cell carcinoma: A randomized clinical trial. *JAMA Surg*. 2021;156(5):444. doi:10.1001/jamasurg.2021.0133
- Eyck BM, Van Lanschot JJB, Hulshof MCCM, et al. Ten-year outcome of neoadjuvant chemoradiotherapy plus surgery for esophageal cancer: The randomized controlled CROSS trial. *J Clin Oncol*. 2021;39(18):1995–2004. doi:10.1200/JCO.20.03614
- Raza F, Zafar H, Zhang S, et al. Recent advances in cell membrane-derived biomimetic nanotechnology for cancer immunotherapy. *Adv Healthcare Mater*. 2021;10(6):2002081. doi:10.1002/adhm.202002081
- Wang W, Yi Y, Jia Y, et al. Neoadjuvant chemotherapy with liposomal paclitaxel plus platinum for locally advanced esophageal squamous cell cancer: Results from a retrospective study. *Thorac Cancer*. 2022;13(6):824–831. doi:10.1111/1759-7714.14328
- Yi M, Zheng X, Niu M, Zhu S, Ge H, Wu K. Combination strategies with PD-1/PD-L1 blockade: Current advances and future directions. *Mol Cancer*. 2022;21(1):28. doi:10.1186/s12943-021-01489-2
- He W, Wang C, Li C, et al. The efficacy and safety of neoadjuvant immunotherapy in resectable locally advanced esophageal squamous cell carcinoma: A systematic review and meta-analysis. *Front Immunol*. 2023;14:1118902. doi:10.3389/fimmu.2023.1118902
- Lv H, Tian Y, Li J, et al. Neoadjuvant sintilimab plus chemotherapy in resectable locally advanced esophageal squamous cell carcinoma. *Front Oncol*. 2022;12:864533. doi:10.3389/fonc.2022.864533
- Markham A, Keam SJ. Camrelizumab: First global approval. *Drugs*. 2019;79(12):1355–1361. doi:10.1007/s40265-019-01167-0
- Yang W, Xing X, Yeung SCJ, et al. Neoadjuvant programmed cell death 1 blockade combined with chemotherapy for resectable esophageal squamous cell carcinoma. *J Immunother Cancer*. 2022;10(1):e003497. doi:10.1136/jitc-2021-003497

16. Cortazar P, Zhang L, Untch M, et al. Pathological complete response and long-term clinical benefit in breast cancer: The CTNeoBC pooled analysis. *Lancet*. 2014;384(9938):164–172. doi:10.1016/S0140-6736(13)62422-8
17. Spring LM, Fell G, Arfe A, et al. Pathologic complete response after neoadjuvant chemotherapy and impact on breast cancer recurrence and survival: A comprehensive meta-analysis. *Clin Cancer Res*. 2020;26(12):2838–2848. doi:10.1158/1078-0432.CCR-19-3492
20. Chan KKW, Saluja R, Delos Santos K, et al. Neoadjuvant treatments for locally advanced, resectable esophageal cancer: A network meta-analysis. *Int J Cancer*. 2018;143(2):430–437. doi:10.1002/ijc.31312
21. Markar SR, Noordman BJ, Mackenzie H, et al. Multimodality treatment for esophageal adenocarcinoma: Multi-center propensity-score matched study. *Ann Oncol*. 2017;28(3):519–527. doi:10.1093/annonc/mdw560
22. Huang J, Xu J, Chen Y, et al. Camrelizumab versus investigator's choice of chemotherapy as second-line therapy for advanced or metastatic oesophageal squamous cell carcinoma (ESCOR): A multicentre, randomised, open-label, phase 3 study. *Lancet Oncol*. 2020;21(6):832–842. doi:10.1016/S1470-2045(20)30110-8
23. Duan H, Shao C, Pan M, et al. Neoadjuvant pembrolizumab and chemotherapy in resectable esophageal cancer: An open-label, single-arm study (PEN-ICE). *Front Immunol*. 2022;13:849984. doi:10.3389/fimmu.2022.849984
24. Yang H, Liu H, Chen Y, et al. Neoadjuvant Chemoradiotherapy Followed by Surgery Versus Surgery Alone for Locally Advanced Squamous Cell Carcinoma of the Esophagus (NEOCRTEC5010): A phase III multicenter, randomized, open-label clinical trial. *J Clin Oncol*. 2018;36(27):2796–2803. doi:10.1200/JCO.2018.79.1483
25. Kauppila JH, Mattsson F, Brusselsaers N, Lagergren J. Prognosis of oesophageal adenocarcinoma and squamous cell carcinoma following surgery and no surgery in a nationwide Swedish cohort study. *BMJ Open*. 2018;8(5):e021495. doi:10.1136/bmjopen-2018-021495
26. Kulangara K, Zhang N, Corigliano E, et al. Clinical utility of the combined positive score for programmed death ligand-1 expression and the approval of pembrolizumab for treatment of gastric cancer. *Arch Pathol Lab Med*. 2019;143(3):330–337. doi:10.5858/arpa.2018-0043-OA
27. Mariette C, Dahan L, Mornex F, et al. Surgery alone versus chemoradiotherapy followed by surgery for stage I and II esophageal cancer: Final analysis of randomized controlled phase III trial FFCD 9901. *J Clin Oncol*. 2014;32(23):2416–2422. doi:10.1200/JCO.2013.53.6532
28. Lantuejoul S, Sound-Tsao M, Cooper WA, et al. PD-L1 testing for lung cancer in 2019: Perspective from the IASLC Pathology Committee. *J Thorac Oncol*. 2020;15(4):499–519. doi:10.1016/j.jtho.2019.12.107
29. Lubbers M, Van Det MJ, Kreuger MJ, et al. Totally minimally invasive esophagectomy after neoadjuvant chemoradiotherapy: Long-term oncologic outcomes. *J Surg Oncol*. 2018;117(4):651–658. doi:10.1002/jso.24935
30. Warner S, Chang YH, Paripati H, et al. Outcomes of minimally invasive esophagectomy in esophageal cancer after neoadjuvant chemoradiotherapy. *Ann Thorac Surg*. 2014;97(2):439–445. doi:10.1016/j.athoracsur.2013.09.042
31. Castoro C, Scarpa M, Cagol M, et al. Nodal metastasis from locally advanced esophageal cancer: How neoadjuvant therapy modifies their frequency and distribution. *Ann Surg Oncol*. 2011;18(13):3743–3754. doi:10.1245/s10434-011-1753-9
32. Shen D, Chen Q, Wu J, Li J, Tao K, Jiang Y. The safety and efficacy of neoadjuvant PD-1 inhibitor with chemotherapy for locally advanced esophageal squamous cell carcinoma. *J Gastrointest Oncol*. 2021;12(1):1–10. doi:10.21037/jgo-20-599
33. Frasci G. Chemotherapy of lung cancer in the elderly. *Crit Rev Oncol Hematol*. 2002;41(3):349–361. doi:10.1016/S1040-8428(01)00145-7





# Assessment of serum concentration and urinary excretion of tumor necrosis factor receptor 1 and 2 and their potential as markers of immunoglobulin A nephropathy activity

Miłosz Miedziaszczyk<sup>1,A–D,F</sup>, Andrzej Oko<sup>1,E,F</sup>, Anna Wolc<sup>2,3,C,F</sup>, Aldona Woźniak<sup>4,B</sup>, Ilona Idasiak-Piechocka<sup>1,B,C,E,F</sup>

<sup>1</sup> Department of Nephrology, Transplantology and Internal Medicine, Poznan University of Medical Sciences, Poland

<sup>2</sup> Department of Animal Science, Iowa State University, Ames, USA

<sup>3</sup> Hy-Line International, Dallas Center, USA

<sup>4</sup> Department of Clinical Pathology, Poznan University of Medical Sciences, Poland

A – research concept and design; B – collection and/or assembly of data; C – data analysis and interpretation;

D – writing the article; E – critical revision of the article; F – final approval of the article

Advances in Clinical and Experimental Medicine, ISSN 1899–5276 (print), ISSN 2451–2680 (online)

*Adv Clin Exp Med.* 2024;33(6):583–591

## Address for correspondence

Miłosz Miedziaszczyk

E-mail: m.miedziaszczyk@wp.pl

## Funding sources

None declared

## Conflict of interest

None declared

Received on August 23, 2022

Reviewed on May 21, 2023

Accepted on August 13, 2023

Published online on November 14, 2023

## Cite as

Miedziaszczyk M, Oko A, Wolc A, Woźniak A, Idasiak-Piechocka I. Assessment of serum concentration and urinary excretion of tumor necrosis factor receptor I and II and their potential as markers of immunoglobulin A nephropathy activity. *Adv Clin Exp Med.* 2024;33(6):583–591. doi:10.17219/acem/171000

## DOI

10.17219/acem/171000

## Copyright

Copyright by Author(s)

This is an article distributed under the terms of the Creative Commons Attribution 3.0 Unported (CC BY 3.0) (<https://creativecommons.org/licenses/by/3.0/>)

## Abstract

**Background.** Tumor necrosis factor receptor 1 (TNFR1) and 2 (TNFR2) can be cleaved from the cell surface and circulate alone or in combination with tumor necrosis factor alpha (TNF- $\alpha$ ). These soluble receptors may play a key role in regulating the inflammatory response.

**Objectives.** The study aimed to evaluate the role of TNFRs in regulating the inflammatory response in immunoglobulin A nephropathy (IgAN).

**Materials and methods.** The study included 26 patients with newly diagnosed and biopsy-confirmed IgAN and 20 healthy controls. Study material included blood and fresh urine collected the morning before kidney biopsy and therapy. The serum concentrations of TNFR1 (STNFR1) and TNFR2 (STNFR2) and urinary excretion of TNFR1 (UTNFR1) and TNFR2 (UTNFR2) were determined with immunoassay. Subsequently, the data were evaluated statistically.

**Results.** The STNFR1 and STNFR2 levels were higher in IgAN patients than in healthy subjects (4747.87 pg/mL and 2817.62 pg/mL compared to 2755.68 pg/mL (95% CI: from –2948.41 to –1035.97;  $p = 0.001$ ) and 1437.83 pg/mL (95% CI: from –1958.50 to –419.60;  $p = 0.001$ ). The power of the test was 98.5% for STNFR1 and 96% for STNFR2. Urinary concentrations only increased for TNFR1 (3551.29 compared to 2338.95 pg/mg of creatinine (Cr) (95% CI: from –2247.03 to –177.66;  $p = 0.023$ ). The STNFR1 marker was characterized by a sensitivity of 73.08% and a specificity of 90.00% ( $p < 0.001$ ).

**Conclusions.** Our results suggest that TNFR1 and TNFR2 are good markers of TNF- $\alpha$  pathway activation in IgAN patients.

**Key words:** tumor necrosis factor  $\alpha$ , tumor necrosis factor receptor I (TNFR1), tumor necrosis factor receptor II (TNFR2), marker of IgA nephropathy

## Background

Tumor necrosis factor alpha (TNF- $\alpha$ ) is a pleiotropic cytokine that plays a vital role in inflammatory processes and stimulates the production of cytokines such as interleukin (IL)-1 $\beta$ , IL-6 and IL-8. It also affects the secretion of adhesion molecules at endothelial cell junctions, as well as chemokines such as monocyte chemoattractant protein-1 (MCP-1), macrophage inflammatory protein-2 (MIP-2), regulated upon activation, normal T cell expressed and presumably secreted (RANTES), and macrophage inflammatory protein-1 alpha (MIP-1 $\alpha$ ).<sup>1–3</sup> Furthermore, TNF- $\alpha$  has immunoregulatory properties and can induce several anti-inflammatory and regulatory cytokines.<sup>4</sup> It is mainly produced by macrophages, dendritic cells and T lymphocytes,<sup>5</sup> and is a transmembrane protein (TMP) that can be cleaved<sup>1</sup> by disintegrin and metalloprotease 17 protein (ADAM-17), and released into the circulation as a functional soluble protein.<sup>6</sup> The TNF- $\alpha$  is usually undetectable in healthy kidneys.<sup>4</sup> It binds on the cell surface to 2 transmembrane receptors, tumor necrosis factor receptor 1 (TNFR1) (also known as CD120A or p55) and tumor necrosis factor receptor 2 (TNFR2) (also known as CD120B or P75),<sup>1</sup> which are differently expressed on cells and tissues.

The TNFRs demonstrate various biological effects, including survival, differentiation, proliferation, migration, inflammation, and cell death. The TNFR1 mainly plays a pro-inflammatory role, whereas TNFR2 may be involved in immunoregulation.<sup>5</sup> Both receptors can be cleaved from the cell surface and circulate alone or in combination with TNF- $\alpha$ .<sup>1</sup> The soluble TNFRs can participate in the regulation of inflammatory responses by binding and neutralizing free TNF- $\alpha$ .<sup>4</sup> The TNFR1 can be detected in almost all cell types, while TNFR2 is found in oligodendrocytes, astrocytes, T cells, myocytes, thymocytes, the endothelium, and human mesenchymal stem cells. In the human kidney, TNFR1 is expressed in the normal glomerular endothelium, where it is mainly localized to the Golgi apparatus,<sup>6</sup> whereas TNFR2 is not usually expressed.<sup>4</sup>

Several studies have associated the expression of TNF- $\alpha$  or TNFRs with various kidney diseases.<sup>1</sup> In inflammatory and autoimmune kidney diseases, TNF- $\alpha$  plays a role in the cascade leading to kidney damage, and its expression is associated with damage.<sup>2</sup> Moreover, increased TNFR levels are associated with the progression of various types of glomerulonephritis (GN).<sup>1,7</sup> Monoclonal antibodies can inhibit TNF- $\alpha$  receptor binding.<sup>1</sup> Simultaneous or specific blocking of TNFR1 and TNFR2 may reveal different receptor functions, which, in turn, may prove useful in developing a specific therapeutic strategy targeting TNFR.<sup>2</sup>

## Objectives

Immunoglobulin A nephropathy (IgAN) accounts for the highest percentage of GN. Considering the relatively high incidence rate, the foundation of our study was

to search for new markers of the disease, and the primary concept was to ensure fast and non-invasive diagnosis of patients with IgAN. The research aimed to assess concentrations of serum TNFR1 (STNFR1), STNFR2, urinary TNFR1 (UTNFR1), and UTNFR2 to determine their potential relationship with clinical markers of IgAN activity.

## Materials and methods

### Study design, setting and participants

Over a period of 2 years, the study comprised 26 Caucasian patients (15 women and 11 men) with a mean age of  $40 \pm 15$  years who presented with newly diagnosed biopsy-confirmed IgAN. The study was conducted in the Department of Nephrology, Transplantology, and Internal Medicine of Poznan University of Medical Sciences. The Bioethics Committee at Poznan University of Medical Sciences reviewed and approved the study (No. 444/11). The control group consisted of 20 healthy individuals, matched for gender and age. All kidney tissue samples were obtained by percutaneous renal biopsy. A standard examination of cortical tissue under light microscopy and immunofluorescence was performed. In all patients, blood and fresh urine were collected in the morning before kidney biopsy and treatment. Urine samples were centrifuged at 1000 g for 5 min, and supernatants were stored at  $-70^{\circ}\text{C}$  until tested. The serum concentrations of TNF- $\alpha$ , TNFR1 and TNFR2, and urinary excretion of TNFR1 and TNFR2 were determined using the Quantkine Human soluble TNFR1 and soluble TNFR2 immunoassay (Cat. No. DRT 100; R&D Systems, Minneapolis, USA). The assay measured soluble TNFRs and TNF-associated soluble TNFRs. The TNFR concentrations were expressed in picograms per milliliter and TNFR excretion was expressed in picograms per milligram of creatinine (Cr).

### Variables

We examined renal histological findings using the mesangial hypercellularity, endocapillary hypercellularity, segmental glomerulosclerosis, and tubular atrophy/interstitial fibrosis (MEST) Oxford classification. However, we only analyzed segmental glomerulosclerosis and tubular atrophy/interstitial fibrosis because mesangial hypercellularity ( $M1 > 0.5$ ) was present in all patients except for one. The severity of tubular atrophy/interstitial fibrosis was classified as T0 (0–25%;  $n = 14$ ), T1 (26–50%;  $n = 6$ ) or T2 (>50%;  $n = 6$ ). Segmental glomerulosclerosis was classified as S0 (absent;  $n = 7$ ) or S1 (present;  $n = 19$ ). Unfortunately, we could not assess endocapillary hypercellularity based on pathomorphological descriptions. The estimated glomerular filtration rate (eGFR) was calculated using the Cockcroft–Gault formula. The mean ( $\pm$  standard deviation;  $M \pm SD$ ) eGFR was  $97.05 \pm 24.12$  mL/min/1.73 m<sup>2</sup>. Normal renal function

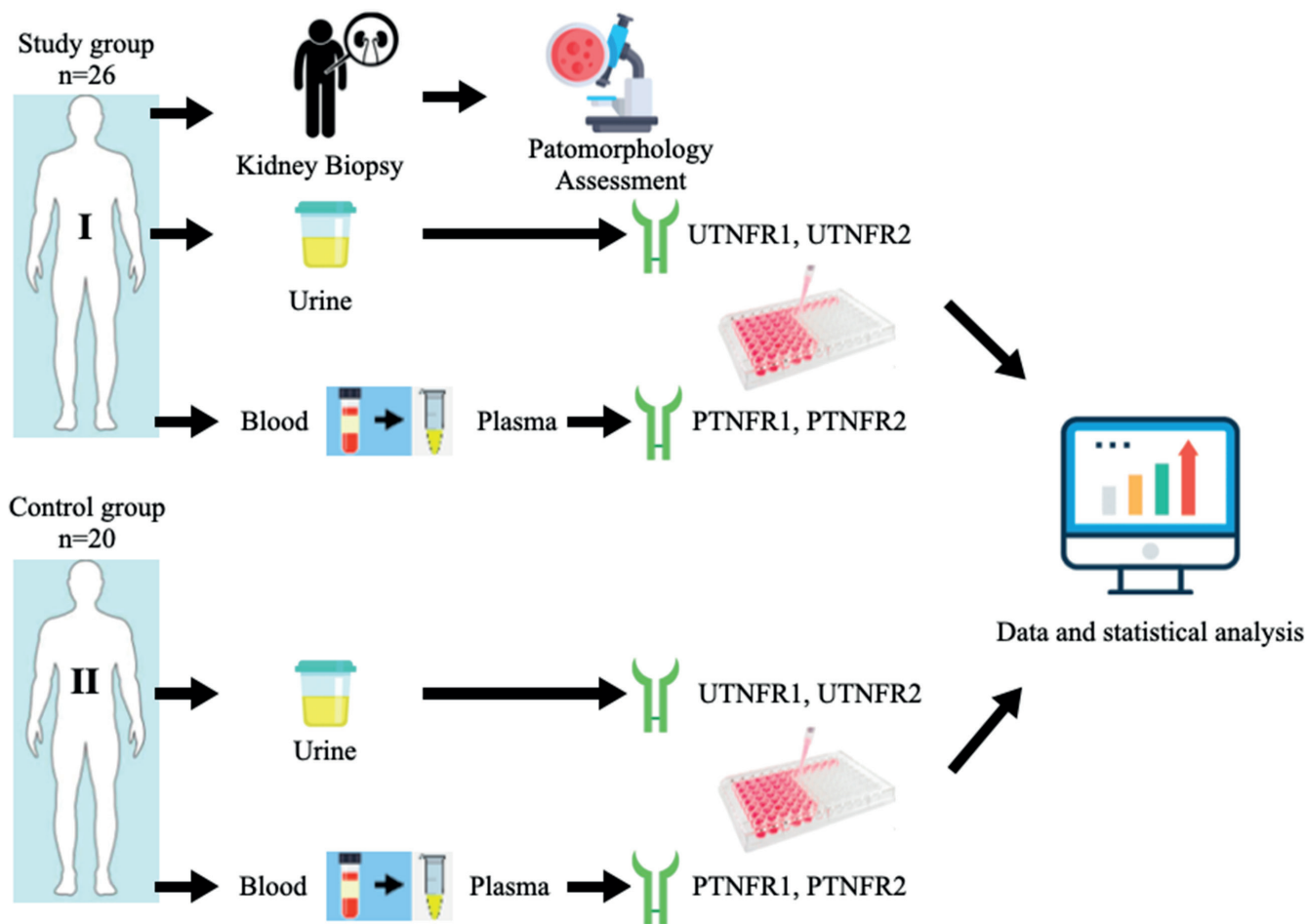


Fig. 1. Materials and methods

was defined as an eGFR  $\geq 90$  mL/min/1.73 m<sup>2</sup>. The values mentioned above are normal for most IgAN patients. Stage I chronic kidney disease (CKD) was found in 17 subjects, 7 presented stage II, and 2 patients had stage III CKD. Urinary protein excretion (UPE) was measured from 24-hour urine collection, and microscopic analysis of the urine sediment was performed. Eight patients developed nephrotic syndrome, and hypertension (blood pressure  $\geq 140/90$  mm Hg) was reported in 6 participants. The characteristics of the research group are presented in Table 1. All patients were treated with an angiotensin-converting enzyme inhibitor (ACEI) and/or an angiotensin II type 1 (AT1) receptor antagonist. Other antihypertensive drugs were also administered to achieve the recommended target blood pressure  $<130/80$  mm Hg or  $<125/75$  mm Hg when urinary protein excretion was  $>1.0$  g/24 h. Fourteen patients were treated with glucocorticoids (GCs), and 2 received GCs and mycophenolate mofetil. The stages of the study are illustrated in Fig. 1.

### Bias

The potential effects of non-renal sources on UTNFR1 were reduced by only including subjects without comorbid diseases. As such, patients with symptoms of acute and

chronic inflammatory diseases other than GN were excluded from the study. Patients were coded appropriately, and the researcher studying the parameters did not know which group patients were assigned to, though the physician was not blinded.

### Study size

The size of the study and control groups was estimated based on a similar study in the available scientific literature.<sup>4</sup>

### Statistical analyses

Data are presented as  $M \pm SD$  and 95% confidence intervals (95% CIs). The correlations between the 2 interval variables were calculated using Pearson’s correlation. The Shapiro–Wilk test verified whether the TNFR concentration values followed a normal distribution. The equality of variances was tested using the Fisher–Snedecor test.

Student’s t-test compared differences between unpaired variables with a normal distribution and equal variances, and Welch’s test compared data with unequal variances. The Mann–Whitney U test assessed differences between unpaired variables with non-normal distribution.

**Table 1.** Characteristics of the study group

Characteristic		Value	p-value (Shapiro–Wilk test)
Gender (men/women), n		11/15	–
Age [years]		Q1: 27 Q2: 33.5 Q3: 49	0.003
Urinary protein excretion [g/24 h]	patients with nephrotic syndrome (n = 8)	Q1: 4.88 Q2: 8.24 Q3: 12.25	0.017
	patients with non-nephrotic syndrome (n = 18)	1.22 ± 0.90	0.115
eGFR [mL/min/1.73 m <sup>2</sup> ]	patients with eGFR ≥ 90 (n = 17)	109.45 ± 18.38	0.057
	patients with eGFR < 90 (n = 9)	73.63 ± 14.06	0.240
BP values (systolic/diastolic)	patients with arterial hypertension (n = 6)	142.5 ± 6.45/90 ± 7.91	0.918/0.505
	normotensive patients (n = 20)	Q1: 115/72.5 Q2: 120/80 Q3: 125/82.5	0.442/0.040

eGFR – estimated glomerular filtration rate; BP – blood pressure. The values are given as number of patients (n) or mean ± standard deviation (M ± SD).

**Table 2.** Statistical parameters for the assessment of differences in serum concentrations of TNFR1 (STNFR1) and TNFR2 (STNFR2) and urinary excretion of TNFR1 (UTNFR1) and TNFR2 (UTNFR2)

Statistical parameters	STNFR1	STNFR2	UTNFR1	UTNFR2
Shapiro–Wilk test	p = 0.337	<b>p = 0.039</b>	p = 0.888	p = 0.072
F test of variance homogeneity	p = 0.675	<b>p = 0.001</b>	p = 0.169	p = 0.095
95% CI	<b>from –2948.41 to –1035.97</b>	<b>from –1958.50 to –419.60</b>	from –2247.03 to –177.66	from –1424.21 to 154.19
t-test for independent groups	<b>p = 0.001</b>	<b>p = 0.001*</b>	<b>p = 0.023</b>	p = 0.112
df	44	–	44	44
Power of the test (1-β)×100%	<b>98.5%</b>	<b>96%</b>	67%	<50%

95% CI – 95% confidence interval; df – degrees of freedom; \*Mann–Whitney U test. Values in bold are statistically significant.

A receiver operating characteristic (ROC) curve determined classifier quality, sensitivity and specificity, and the analysis established the optimal cutoff point. All statistical analyses employed MedCalc, v. 20.006 (MedCalc Software Ltd., Ostend, Belgium).

## Results

No significant differences were found between serum TNF-α levels of IgAN patients (25.64 pg/mL) and healthy control (26.99 pg/mL) (95% CI: –3.7–5.1; p = 0.627). However, STNFR1 and STNFR2 concentrations were significantly higher in IgAN patients than in healthy participants (4747.87 pg/mL and 2817.62 pg/mL compared to 2755.68 (95% CI: –2948.41––1035.97; p = 0.001) and 1437.83 pg/mL (95% CI: from –1958.50 to –419.60; p = 0.001)). The power of the test was 98.5% for STNFR1 and 96% for STNFR2. The UTNFR1 excretions were considerably higher in IgAN patients compared to healthy subjects (3551.29 pg/mg of Cr compared to 2338.95 pg/mg of Cr (95% CI: from –2247.03 to –177.66; p = 0.023)). The power of the test in this case was 67%. The results are presented in Fig. 2 and Table 2.

Positive correlations were observed between STNFR2 levels in IgAN patients and serum Cr (r = 0.4359, p = 0.026) and urinary protein excretion (r = 0.4639, p = 0.017). Meanwhile, a negative correlation was shown between STNFR2 concentration and serum albumin (r = –0.6392, p = 0.001). The results are illustrated in Fig. 3.

The marker quality was assessed using the ROC analysis, and their sensitivity and specificity were described accordingly. The STNFR1 showed a sensitivity of 73.08% and a specificity of 90.00% (p < 0.001) (Fig. 4), with the optimal cutoff point established at 3381 pg/mL. The other results of the analysis are presented in Table 3.

In patients with nephrotic syndrome, STNFR2 level was significantly higher compared to patients with non-nephrotic proteinuria (3904.55 pg/mL compared to 2334.53 pg/mL; 95% CI: 261.15–2878.88; p = 0.021), although no significant differences were detected between these 2 groups for STNFR1 (4521.44 pg/mL compared to 4848.50 pg/mL; 95% CI: from –1815.30 to 1635.00; p = 0.567), UTNFR1 (3102.55 pg/mg of Cr compared to 3750.73 pg/mg of Cr; 95% CI: from –2353.61 to 1057.24; p = 0.441) or UTNFR2 (2268.14 pg/mg of Cr compared to 2713.76 pg/mg of Cr; 95% CI: –1774.57–883.32; p = 0.496).

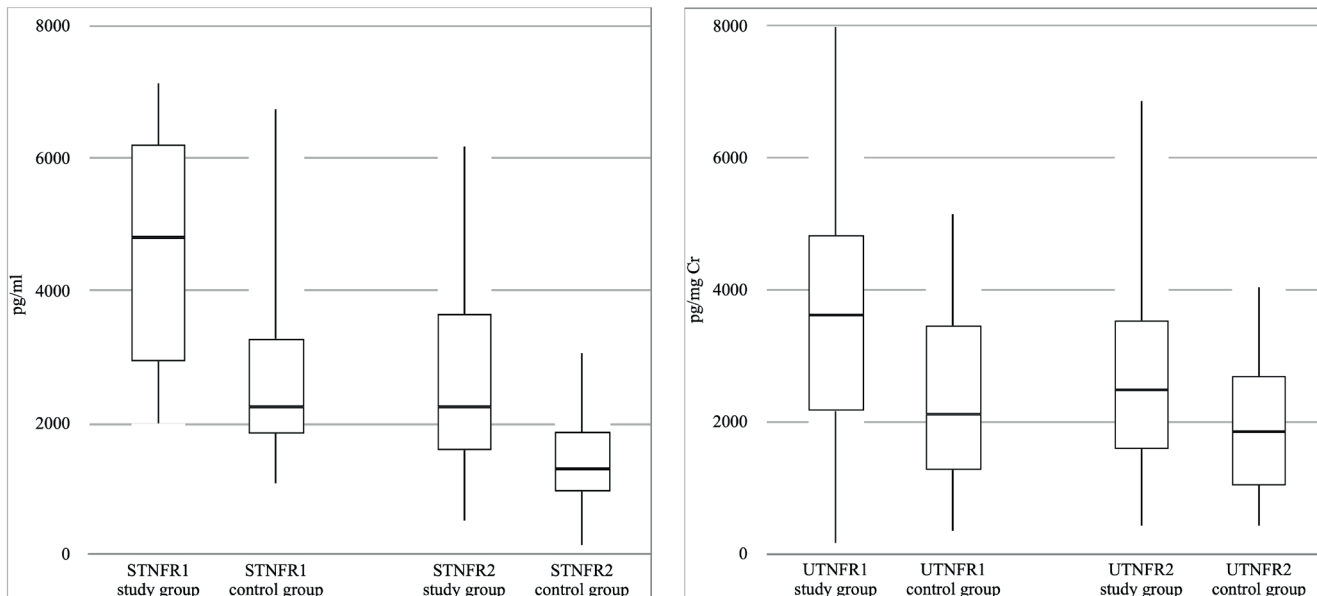


Fig. 2. Comparison of mean serum tumor necrosis factor receptor 1 (STNFR1), STNFR2, urinary TNFR1 (UTNFR1), and UTNFR2 levels in immunoglobulin A nephropathy (IgAN) patients and healthy controls

Table 3. Receiver operating characteristic (ROC) curve

Variable	Sensitivity	Specificity	Values	Youden's J statistic	AUC	Standard error	p-value
STNFR1	73.08	90.00	3381 pg/mL	0.6308	0.813	0.0685	<b>&lt;0.001</b>
STNFR2	76.92	70.00	1561.4 pg/mL	0.4692	0.783	0.0683	<b>&lt;0.001</b>
UTNFR1	69.23	70.00	2407.1 pg/mg Cr	0.3923	0.698	0.0786	<b>0.012</b>
UTNFR2	50.00	75.00	2474.7 pg/mg Cr	0.2500	0.631	0.0831	0.116

STNFR1 – serum concentrations of tumor necrosis factor receptor 1 (TNFR1); STNFR2 – serum concentrations of TNFR2; UTNFR1 – urinary excretion of TNFR1; UTNFR2 – urinary excretion of TNFR2; Cr – serum creatinine; AUC – area under the ROC curve. Values in bold are statistically significant.

The patients with an eGFR < 90 mL/min/1.73 m<sup>2</sup> had significantly higher STNFR2 values than patients with an eGFR ≥ 90 mL/min/1.73 m<sup>2</sup> (3809.51 pg/mL compared to 2292.49 pg/mL; 95% CI: 245.93–2788.10; p = 0.021). No significant differences were observed in STNFR1 (5016.70 pg/mL compared to 4605.54 pg/mL; 95% CI: –1019.07–1841.39; p = 0.559), UTNFR1 (3904.10 pg/mg of Cr compared to 3364.51 pg/mg of Cr; 95% CI: from –1120.50 to 2199.68; p = 0.509) or UTNFR2 (3170.61 pg/mg of Cr compared to 2262.19 pg/mg of Cr; 95% CI: from –336.13 to 2152.97; p = 0.145).

Comparisons of patients with arterial hypertension (blood pressure ≥140/90 mm Hg) to patients without hypertension revealed no significant differences in levels of STNFR1 (4606.78 pg/mL compared to 4790.19 pg/mL; 95% CI: from –1808.33 to 1441.51; p = 0.818), STNFR2 (2417.53 pg/mL compared to 2937.64 pg/mL; 95% CI: from –2111.57 to 1071.35; p = 0.506), UTNFR1 (4071.82 pg/mg of Cr compared to 3395.14 pg/mg of Cr; 95% CI: from –2466.10 to 3819.46; p = 0.617), and UTNFR2 (3719.53 pg/mg of Cr compared to 2233.78 pg/mg of Cr; 95% CI: from –757.48 to 3728.99; p = 0.156).

There were no differences between patients for mean STNFR1, STNFR2, UTNFR1, or UTNFR2 values based

on segmental glomerulosclerosis or tubular atrophy/interstitial fibrosis severity (Table 4).

## Discussion

Immunoglobulin A nephropathy is a form of glomerulopathy known more specifically as GN and represents the most common primary GN in many countries. The disease can be classified into histological and clinical types, though the pathogenetic mechanisms are not entirely known. However, mesangial pathogenic polymeric IgA1 (galactose-deficient IgA1; Gd-IgA1) deposition, mesangial cell proliferation, increased extracellular matrix synthesis, and glomerular infiltration of macrophages, monocytes and T lymphocytes are frequently observed. The unique localization is due to the presence of IgA1 (CD71) receptors on mesangial cells.<sup>8,9</sup> Immunoglobulin A initiates an immune reaction and combines with the resulting antibodies to form immune complexes that accumulate as deposits in the mesangium, which leads to cellular and mesangial matrix proliferation.

Clinically, the first manifestation of IgAN is an episode of hematuria, which predominantly occurs following



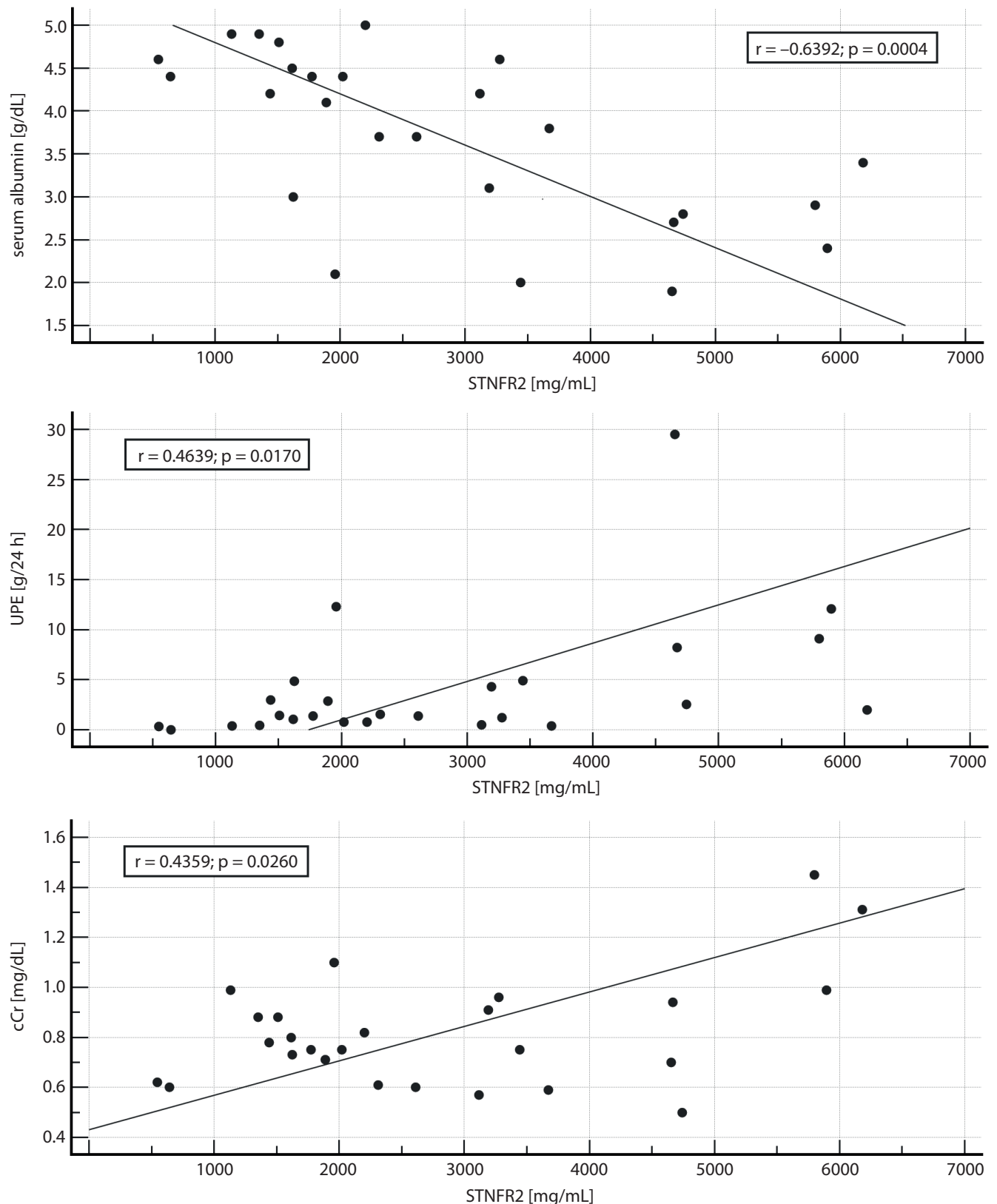


Fig. 3. The correlation (Pearson's correlation) between serum tumor necrosis factor receptor 2 (STNFR2), serum creatinine (Cr), urinary protein excretion (UPE), and serum albumin in patients with primary immunoglobulin A nephropathy (IgAN)

a non-specific upper respiratory tract infection and resolves spontaneously after several days. The picture may vary in the pathomorphological examination. Therefore, an additional immunofluorescence test should be

performed.<sup>8</sup> Evidence suggests that cytokines play a crucial role in IgAN pathogenesis and progression, with TNF- $\alpha$  having a notable involvement. Indeed, TNF- $\alpha$  expression is preferentially increased in the glomeruli in various



**Table 4.** The relationship between histopathological kidney examination and tumor necrosis factor receptor (TNFR) concentrations

Statistical parameter	STNFR1	STNFR2	UTNFR1	UTNFR2
Shapiro–Wilk test	p = 0.253	p = 0.077	p = 0.941	p = 0.607
F test of variance homogeneity	p = 0.967	p = 0.832	p = 0.729	p = 0.290
S0	5585.38	2859.64	3732.90	1819.00
S1	4570.11	2931.96	4153.06	3123.11
p-value of t-test for independent groups	p = 0.246	p = 0.931	p = 0.655	p = 0.103
df	19	19	19	19
Shapiro–Wilk test	p = 0.140	p = 0.078	p = 0.732	p = 0.390
F test of variance homogeneity	p = 0.669	p = 0.556	p = 0.094	p = 0.350
T0	4962.58	2602.55	4493.71	3073.48
T1	4669.53	2637.65	4444.70	2793.60
p-value of t-test for independent groups	p = 0.766	p = 0.969	p = 0.959	p = 0.768
df	14	14	14	14
Shapiro–Wilk test	<b>p = 0.037</b>	<b>p = 0.042</b>	p = 0.494	p = 0.333
F test of variance homogeneity	p = 0.664	p = 0.739	p = 0.822	p = 0.872
T0	4962.58	2602.55	4493.71	3073.48
T2	4563.92	3885.66	2682.02	2201.70
p-value of t-test for independent groups	p = 0.646*	p = 0.104*	p = 0.080	p = 0.348
df	–	–	15	15

UTNFR1 – urinary excretion of TNFR1; UTNFR2 – urinary excretion of TNFR2; STNFR 1 – serum concentration of TNFR1; STNFR 2 – serum concentration of TNFR2; df – degrees of freedom; \*Mann–Whitney U test. Values in bold are statistically significant.

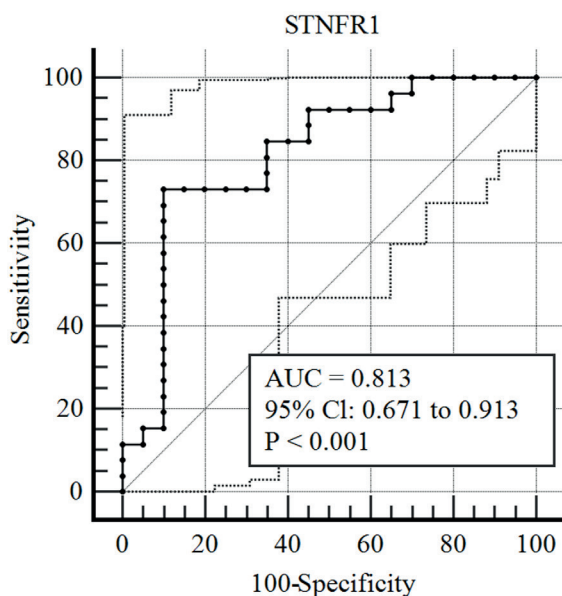


**Fig. 4.** Receiver operating characteristic (ROC) curve chart (black dotted line) and its 95% CI (95% confidence intervals) for serum tumor necrosis factor receptor 1 (STNFR1)

AUC – area under the ROC curve.

forms of GN,<sup>4,10,11</sup> and correlates with increased serum and urinary excretion of the cytokine.<sup>4</sup> These observations indicate that damaged kidneys constitute the source of increased production and excretion of TNF- $\alpha$  and TNFRs in primary GN patients. Moreover, TNFR1 and TNFR2 are involved in the caspase activation pathways after binding to TNF- $\alpha$  and cause epithelial cell proliferation

in the proximal tubule and renal interstitial damage. Interestingly, both receptors can also be cleaved from the cell surface, circulate alone or in combination with TNF- $\alpha$ , and may participate in inflammatory response regulation.

There is a strong correlation between tubulointerstitial tissue damage severity and subsequent renal function deterioration in IgAN and diabetic nephropathy (DN).<sup>12</sup> Chan et al. demonstrated that after IgA deposition, TNF- $\alpha$  released from mesangial cells activates proximal tubular epithelial cells (PTEC), leading to further inflammatory changes in the renal interstitium.<sup>12</sup> In contrast, Lai et al. found that IgA-conditioned medium prepared by culturing human mesangial cells (IgA-HMC medium) with IgA from IgAN patients significantly increased gene expression and TNF- $\alpha$  synthesis by podocytes. These, in turn, may play a role in interstitial damage development in IgAN by enhancing tubular epithelial cell activation and increasing TNF- $\alpha$  synthesis in mesangial cell inflammatory lesion cultures. However, TNF- $\alpha$  from mesangial cells and podocytes increases TNFR expression.<sup>9</sup> This mechanism leads to increased TNFR excretion from mesangial cell and podocyte membranes, which may account for the increased serum and urine TNFR levels observed in our IgAN patients.

Several studies have found that levels of the molecules associated with circulating TNF pathway markers, such as TNF- $\alpha$  and TNFRs, are significantly higher in CKD patients and that these levels correlate closely with changes in eGFR.<sup>4,13–15</sup> Moreover, the results of the Joslin Kidney Study demonstrated that increased levels of circulating

TNFR1 and TNFR2 were very strong predictors of DN progression to end-stage renal disease (ESRD).<sup>16,17</sup> However, little is known about the clinical and histological association of circulating TNFRs, or the urinary excretion of TNFRs, in IgAN patients.

Our previous study showed that UTNFR1 excretion was significantly higher in patients with various types of chronic GN, including approx. 35% of IgAN patients, compared to healthy controls.<sup>4</sup> Although Sonoda et al. did not find differences in UTNFR levels between IgAN patients and healthy controls, they observed that STNFR levels were considerably higher in IgAN patients.<sup>14</sup> It should be emphasized that STNFR measurements were not performed in our previous study. The present study confirmed that TNFR1 and TNFR2 serum levels were significantly higher in patients with IgAN than in healthy subjects. However, urinary excretion was only significantly higher for TNFR1. These results indicate that STNFR1, STNFR2 and UTNFR1 levels may constitute a marker of the TNF- $\alpha$  pathway activation in the kidneys, which contributes to the deterioration of renal function. Moreover, TNF- $\alpha$  pathway activation directly increases glomerular vasoconstriction and albumin permeability, while kidney exposure to TNF- $\alpha$  increases TNFR messenger ribonucleic acid (mRNA) expression in the renal interstitial tubule, causing cell death.

Zwiech et al. observed a significant increase in STNFR1, STNFR2, UTNFR1, and UTNFR2 in their study group (patients with IgAN).<sup>15</sup> In our previous paper, UTNFR excretion correlated negatively with eGFR in IgAN patients.<sup>4</sup> Sonoda et al. also emphasized the negative correlation between serum and urinary excretion of TNFRs with eGFR in IgAN patients, although the correlation between STNFRs and eGFR was stronger than the correlation between UTNFRs and eGFR.<sup>14</sup> In the present study, a negative correlation was also observed between serum and urinary excretion of TNFRs and eGFR in IgAN patients. However, the correlation between UTNFRs and eGFR was stronger than between STNFRs and eGFR (STNFR1 ( $r = -0.1060$ ,  $p = 0.606$ ), STNFR2 ( $r = -0.0899$ ,  $p = 0.663$ ), UTNFR1 ( $r = -0.1547$ ,  $p = 0.451$ ), UTNFR2 ( $r = -0.3466$ ,  $p = 0.083$ )). These data suggest that increased STNFR and UTNFR levels confirm the activation of the renal TNF- $\alpha$  pathway in IgAN patients.

There was no significant correlation between UTNFRs and STNFRs. Conversely, experimental studies have demonstrated that the induction of immune damage to the kidneys (anti-glomerular basement membrane antibody-induced experimental nephritis) results in higher STNFR1 and UTNFR1 values.<sup>18</sup>

Each TNFR plays a separate role in inflammation, apoptosis and necrosis. However, the current study found a strong correlation between urinary excretion of TNFR1 and TNFR2 (Pearson's correlation coefficient,  $r = 0.8218$ ,  $p < 0.001$ ), but no correlation was observed between serum TNFR1 and TNFR2 (Pearson's correlation coefficient,

$r = 0.1146$ ,  $p = 0.577$ ). Another vital issue is the source of TNFRs in serum and urine. The TNFR levels were compared in patients who presented with severe tubulointerstitial fibrosis on histopathology, with the group showing either no or mild tubulointerstitial fibrosis. However, no significant differences were noted for STNFR concentrations and UTNFR excretion. In addition, TNFR levels were compared in patients with and without nephrotic syndrome, and no relevant results were obtained.

A significant positive correlation was found between STNFR2, serum Cr ( $r = 0.4359$ ,  $p = 0.026$ ) and UPE ( $r = 0.4407$ ,  $p = 0.027$ ). Nevertheless, a negative correlation was observed between the STNFR2 concentrations and serum albumin ( $r = -0.6392$ ,  $p = 0.001$ ). Urinary protein excretion is considered an indicator of the severity of glomerular barrier damage, and a critical factor contributing to tubulointerstitial tissue damage and accelerated fibrotic processes, which lead to a rapid deterioration in kidney function.

In the available scientific literature, no study has assessed the applicability of TNFR concentrations in serum and urine as potential markers of IgAN. The marker quality was evaluated using ROC analysis, and sensitivity and specificity of TNFR concentrations were described. The potential marker, STNFR1, characterized by a sensitivity of 73.08% and a specificity of 90%, was statistically significant ( $p < 0.001$ ). The optimal cutoff point for TNFR1 was determined to be 3381 pg/mL. Given that the power of the test for differences in STNFR1 concentrations between the control and the study groups was 98.5%, we can conclude that STNFR1 may prove to be a good marker of IgAN activity.

## Limitations

The study was limited due to a lack of immunohistochemical tests, meaning that evaluating TNFR expression in kidney biopsy samples was not possible. Therefore, increased TNFR expression in renal tissue could not be directly determined. The causal relationship between TNFRs and renal tubulointerstitial fibrosis remains unclear due to the cross-sectional design. The 2<sup>nd</sup> limitation was the low number of patients and the lack of a follow-up study estimating the correlation of initial STNFR and UTNFR concentrations with disease course and progression.

The study aimed to assess TNFR concentrations in serum and urine. However, these parameters were not examined in other types of GN due to difficulties in obtaining a sufficiently large study group. Nonetheless, IgAN is the most common type of GN, and disease incidence is lower for other types of primary GN. As such, time is needed to gather enough patients to compare our results with other GN types. Future studies should account for this aspect and explore it further to obtain information on which types of GN have elevated levels of the markers studied.

## Conclusions


The results presented above indicate that significantly increased STNFR1, STNFR2 and UTNFR1 concentration levels may be considered good markers of renal TNF- $\alpha$  pathway activation in patients with newly diagnosed IgAN. The assessment of STNFR2 concentration may represent an effective instrument for estimating IgAN activity, and should be considered in clinical practice. Finally, further studies should focus on the correlations between histopathological changes and the applicability of TNFR2 as a non-invasive marker of IgAN prognosis.

### ORCID iDs

Miłosz Miedziaszczyk  <https://orcid.org/0000-0002-9773-1461>

Andrzej Oko  <https://orcid.org/0000-0002-3394-7140>

Anna Wolc  <https://orcid.org/0000-0003-1190-5713>

Ilona Idasiak-Piechocka  <https://orcid.org/0000-0002-2291-1484>

### References

- McAdoo SP, Pusey CD. Is there a role for TNF $\alpha$  blockade in ANCA-associated vasculitis and glomerulonephritis? *Nephrol Dial Transplant*. 2017;32(Suppl 1):i80–i88. doi:10.1093/ndt/gfw361
- Merkle M, Ribeiro A, Wörnle M. TLR3-dependent regulation of cytokines in human mesangial cells: A novel role for IP-10 and TNF- $\alpha$  in hepatitis C-associated glomerulonephritis. *Am J Physiol Renal Physiol*. 2011;301(1):F57–F69. doi:10.1152/ajprenal.00083.2011
- Upadhyay A, Larson MG, Guo CY, et al. Inflammation, kidney function and albuminuria in the Framingham Offspring cohort. *Nephrol Dial Transplant*. 2011;26(3):920–926. doi:10.1093/ndt/gfq471
- Idasiak-Piechocka I, Oko A, Pawliczak E, Kaczmarek E, Czekalski S. Urinary excretion of soluble tumour necrosis factor receptor 1 as a marker of increased risk of progressive kidney function deterioration in patients with primary chronic glomerulonephritis. *Nephrol Dial Transplant*. 2010;25(12):3948–3956. doi:10.1093/ndt/gfq310
- Huang YS, Fu SH, Lu KC, et al. Inhibition of tumor necrosis factor signaling attenuates renal immune cell infiltration in experimental membranous nephropathy. *Oncotarget*. 2017;8(67):111631–111641. doi:10.18632/oncotarget.22881
- Speeckaert MM, Speeckaert R, Laute M, Vanholder R, Delanghe JR. Tumor necrosis factor receptors: Biology and therapeutic potential in kidney diseases. *Am J Nephrol*. 2012;36(3):261–270. doi:10.1159/000342333
- Wu T, Xie C, Wang HW, et al. Elevated urinary VCAM-1, P-selectin, soluble TNF receptor-1, and CXC chemokine ligand 16 in multiple murine lupus strains and human lupus nephritis. *J Immunol*. 2007;179(10):7166–7175. doi:10.4049/jimmunol.179.10.7166
- Shu KH, Lee SH, Cheng CH, Wu MJ, Lian JD. Impact of interleukin-1 receptor antagonist and tumor necrosis factor- $\alpha$  gene polymorphism on IgA nephropathy. *Kidney Int*. 2000;58(2):783–789. doi:10.1046/j.1523-1755.2000.00227.x
- Lai KN, Leung JCK, Chan LYY, et al. Activation of podocytes by mesangial-derived TNF- $\alpha$ : Glomerulo-podocytic communication in IgA nephropathy. *Am J Physiol Renal Physiol*. 2008;294(4):F945–F955. doi:10.1152/ajprenal.00423.2007
- Navarro JF, Mora C, Gomez M, Muros M, Lopez-Aguilar C, Garcia J. Influence of renal involvement on peripheral blood mononuclear cell expression behaviour of tumour necrosis factor- and interleukin-6 in type 2 diabetic patients. *Nephrol Dial Transplant*. 2007;23(3):919–926. doi:10.1093/ndt/gfm674
- Navarro JF, Mora C, Muros M, Garcia J. Urinary tumour necrosis factor-excretion independently correlates with clinical markers of glomerular and tubulointerstitial injury in type 2 diabetic patients. *Nephrol Dial Transplant*. 2006;21(12):3428–3434. doi:10.1093/ndt/gfl469
- Chan LYY, Leung JCK, Tsang AWL, Tang SCW, Neng Lai K. Activation of tubular epithelial cells by mesangial-derived TNF- $\alpha$ : Glomerulo-tubular communication in IgA nephropathy. *Kidney Int*. 2005;67(2):602–612. doi:10.1111/j.1523-1755.2005.67116.x
- Kacprzyk F. Serum concentration and urinary excretion of soluble receptors for tumor necrosis factor in patients with primary glomerulonephritis [in Polish]. *Pol Merkur Lek*. 2003;15(88):383–386; discussion 386–387. PMID:14974372.
- Sonoda Y, Gohda T, Suzuki Y, et al. Circulating TNF receptors 1 and 2 are associated with the severity of renal interstitial fibrosis in IgA nephropathy. *PLoS One*. 2015;10(4):e0122212. doi:10.1371/journal.pone.0122212
- Zwiech R, Kacprzyk F, Szuflet A, Nowicki M. Prognostic values of serum concentration and urinary excretion of interleukin-1 receptor antagonist and tumor necrosis factor receptors type I and II in patients with IgA nephropathy [in Polish]. *Pol Arch Med Wewn*. 2005;113(4):326–333. PMID:16209246.
- Gohda T, Niewczas MA, Ficociello LH, et al. Circulating TNF receptors 1 and 2 predict stage 3 CKD in type 1 diabetes. *J Am Soc Nephrol*. 2012;23(3):516–524. doi:10.1681/ASN.2011060628
- Niewczas MA, Gohda T, Skupien J, et al. Circulating TNF receptors 1 and 2 predict ESRD in type 2 diabetes. *J Am Soc Nephrol*. 2012;23(3):507–515. doi:10.1681/ASN.2011060627
- Wu T, Xie C, Bhaskarabhatla M, et al. Excreted urinary mediators in an animal model of experimental immune nephritis with potential pathogenic significance. *Arthritis Rheum*. 2007;56(3):949–959. doi:10.1002/art.22556



# Gender-related and PUFA-related differences in lipoprotein-associated phospholipase A2 levels in patients with type 2 diabetes and atherosclerotic cardiovascular disease

Maksymilian Hanarz<sup>1,D,E</sup>, Aleksander Siniarski<sup>2,3,A–F</sup>, Renata Gołębiowska-Wiatrak<sup>3,B</sup>,  
Jadwiga Nessler<sup>2,3,F</sup>, Krzysztof Piotr Malinowski<sup>4,C</sup>, Grzegorz Gajos<sup>2,3,A,B,E,F</sup>

<sup>1</sup> Jagiellonian University Medical College, Kraków, Poland

<sup>2</sup> Department of Coronary Artery Disease and Heart Failure, Institute of Cardiology, Faculty of Medicine, Jagiellonian University Medical College, Kraków, Poland

<sup>3</sup> St. John Paul II Hospital, Kraków, Poland

<sup>4</sup> Department of Bioinformatics and Telemedicine, Faculty of Medicine, Jagiellonian University Medical College, Kraków, Poland

A – research concept and design; B – collection and/or assembly of data; C – data analysis and interpretation;

D – writing the article; E – critical revision of the article; F – final approval of the article

Advances in Clinical and Experimental Medicine, ISSN 1899–5276 (print), ISSN 2451–2680 (online)

*Adv Clin Exp Med.* 2024;33(6):593–600

## Address for correspondence

Aleksander Siniarski

E-mail: aleksandersiniarski@gmail.com

## Funding sources

None declared

## Conflict of interest

None declared

## Acknowledgements

The publication was supported by a grant from Jagiellonian University Medical College (Uniwersytet Jagielloński Collegium Medicum N41/DBS/000711) awarded to Grzegorz Gajos.

Received on April 3, 2023

Reviewed on July 14, 2023

Accepted on August 13, 2023

Published online on September 25, 2023

## Cite as

Hanarz M, Siniarski A, Gołębiowska-Wiatrak R, Nessler J, Malinowski KP, Gajos G. Gender-related and PUFA-related differences in lipoprotein-associated phospholipase a2 levels in patients with type 2 diabetes and atherosclerotic cardiovascular disease. *Adv Clin Exp Med.* 2024;33(6):593–600. doi:10.17219/acem/171002

## DOI

10.17219/acem/171002

## Copyright

Copyright by Author(s)

This is an article distributed under the terms of the Creative Commons Attribution 3.0 Unported (CC BY 3.0) (<https://creativecommons.org/licenses/by/3.0/>)

## Abstract

**Background.** Lipoprotein-associated phospholipase A2 (Lp-PLA2) may play an important role in the development of atherosclerotic cardiovascular disease (ASCVD). Increased plasma levels of Lp-PLA2 may predict future cardiovascular (CV) events in type 2 diabetes (T2D). The potential beneficial effects of polyunsaturated fatty acids (PUFA) on ASCVD have been widely investigated. However, the impact of different PUFA concentrations on Lp-PLA2 remains uncertain.

**Objectives.** We sought to determine the intergender differences in a population of patients with both T2D and ASCVD regarding Lp-PLA2 mass and the association between Lp-PLA2 mass and plasma levels of PUFA.

**Materials and methods.** In this cross-sectional study, we measured the Lp-PLA2 mass, PUFA concentrations and inflammatory markers in 74 patients (49 males and 25 females) with T2D and ASCVD.

**Results.** In this very high-risk population, males had, on average, 33.6% higher levels of Lp-PLA2 than females. The Lp-PLA2 mass was positively associated with interleukin 6 (IL-6) ( $r = 0.27$ ,  $p = 0.019$ ), creatinine ( $r = 0.29$ ,  $p = 0.03$ ) and triglyceride levels ( $r = 0.41$ ,  $p = 0.002$ ). Additionally, male gender and higher levels of triglycerides, leptin, oxidized low-density lipoprotein (oxLDL), and intercellular adhesion molecule 1 (ICAM-1) were independent predictors for an increased Lp-PLA2. Moreover, arachidonic acid (AA) negatively correlated with Lp-PLA2 ( $r = -0.26$ ,  $p = 0.024$ ), which was especially apparent in the female subgroup.

**Conclusions.** In the population of patients with ASCVD and T2D, males present with higher plasma levels of Lp-PLA2 than females. Additionally, higher plasma levels of AA were associated with lower Lp-PLA2 levels. Our findings support the utilization of Lp-PLA2 as a novel biomarker in ASCVD risk assessment in a very high CV risk population.

**Key words:** coronary artery disease, Lp-PLA2, PUFA, type 2 diabetes mellitus, gender differences



## Background

Atherosclerotic cardiovascular disease (ASCVD) is a leading cause of death in both Europe and the USA.<sup>1,2</sup> Despite notable progress in the prevention and treatment of coronary artery disease (CAD), there is still a very high prevalence of new adverse cardiovascular (CV) events in this population.<sup>3</sup>

The development of ASCVD and its progression have been largely associated with vascular inflammation.<sup>4</sup> Increased levels of inflammatory biomarkers such as interleukin-6 (IL-6), high-sensitivity C-reactive protein (hsCRP) and the macrophage-derived lipoprotein-associated phospholipase A2 (Lp-PLA2) enzyme can be used to assess the residual CV risk.<sup>5–7</sup> The main function of Lp-PLA2 is to hydrolyze the proinflammatory mediators in order to reduce their bioactivity. However, this simultaneously increases their proatherogenic properties.<sup>6,8</sup> It is well established that type 2 diabetes (T2D) is an important ASCVD risk factor that is highly associated with ongoing inflammation and increased levels of Lp-PLA2.<sup>9</sup> Moreover, the collaborative data of 32 prospective studies demonstrated that Lp-PLA2 is associated with proatherogenic lipids, underlining the significance of the activity and mass of this phospholipase on the progression of ASCVD.<sup>10</sup> The Lp-PLA2 is a promising biomarker that can be included in the risk assessment of patients with ASCVD<sup>11,12</sup> or used as a potential target for ASCVD treatment.<sup>13,14</sup>

It has been observed that males had higher levels of Lp-PLA2, but the relationship between Lp-PLA2 and gender is not yet evident, especially in the very high CV risk population of patients with both ASCVD and T2D.<sup>9,14,15</sup>

We have previously observed that the supplementation of polyunsaturated omega-3 fatty acids (n-3 PUFA) is beneficial in patients with ASCVD and results in the Lp-PLA2 mass reduction,<sup>16,17</sup> but there is not enough evidence to determine which polyunsaturated fatty acids (PUFA) influence Lp-PLA2 to the greatest extent. However, there is a lack of a clear answer to whether the concentration of PUFA in patients at baseline can predict the levels of Lp-PLA2. If that would be the case, PUFA could be a useful tool to predict outcomes in a very high CV risk group and their response to the therapies such as PUFA supplementation.

## Objectives

This study primarily aimed to provide additional knowledge about Lp-PLA2 in patients with both ASCVD and T2D. The secondary aim of this study was to determine the influence of different PUFA plasma concentrations on the Lp-PLA2 mass.

## Materials and methods

### Study design and subjects

This prospective, cross-sectional study consecutively recruited patients with both T2D (diagnosed in accordance with the 2018 American Diabetes Association guidelines), optimally treated for over 6 months before the enrollment, and ASCVD. The diagnosis of ASCVD was defined as CAD, established with an invasive coronary angiography (50% lumen narrowing in the proximal left main coronary artery or left anterior descending artery, or 70% lumen narrowing in any other segment of the coronary artery). The exclusion criteria included type 1 diabetes, not optimally treated T2D (glycated hemoglobin A1c (HbA1c) >9%), current infection, acute coronary syndrome (3 months prior to enrollment), PUFA supplementation 6 months before the examination, chronic anticoagulant therapy, bleeding, platelet count lower than  $100 \times 10^9/L$ , serum creatinine levels higher than  $177 \mu\text{mol/L}$  or  $2 \text{ mg/dL}$ , increased alanine transaminase (ALT, 1.5 times above the upper-reference limit), chronic treatment with steroids or non-steroidal anti-inflammatory drugs (not including acetylsalicylic acid), malignant neoplastic disease, a life expectancy of less than 12 months, abuse of alcohol or drugs, and pregnancy.

Patients were screened and eventually enrolled in 2 major tertiary-reference cardiology centers in southern Poland. We initially enrolled 126 patients who met the inclusion criteria. Forty-three patients were excluded due to the exclusion criteria, and 9 patients refused to participate in the study. Eventually, 74 patients were included in the final analysis and were subsequently divided into 2 groups based on their gender.

Obesity was diagnosed based on a body mass index (BMI)  $\geq 30 \text{ kg/m}^2$ . Arterial hypertension was defined as a blood pressure  $\geq 140 \text{ mm Hg}$  and/or  $\geq 90 \text{ mm Hg}$  (systolic and diastolic, respectively) – measured during 2 separate ambulatory visits. Current smoking was defined as smoking at least 1 cigarette per day.

This study was performed in compliance with the Good Clinical Practice (GCP) International Conference on Harmonization and was approved by the local ethics committee (Jagiellonian University Medical College, approval No. KBET/190/B/2012). All study participants provided written informed consent. This study complied with the Declaration of Helsinki.

### Sample collection and routine laboratory tests

Fasting blood (25 mL) was drawn from an antecubital vein and immediately stored in tubes containing 3.2% trisodium citrate. Samples were processed up to 60 min after blood collection. Serum total cholesterol (TC), low-density lipoprotein cholesterol (LDL-C), high-density lipoprotein cholesterol (HDL-C), triglyceride (TG), glucose, HbA1c,



and thyroid stimulating hormone (TSH) levels were determined using the biochemical analyzer cobas® 6000 (Roche Diagnostics, Basel, Switzerland). Creatinine was assayed by a routine laboratory technique, and estimated glomerular filtration rate (eGFR) was evaluated based on the Modification of Diet in Renal Disease (MDRD) formula. Complete blood count (CBC), including red blood cells, white blood cells, hemoglobin, hematocrit, red blood cell distribution width, platelet distribution width, and platelet count, was analyzed using standard laboratory evaluation (Sysmex XT-2000i; Sysmex Corp., Tokyo, Japan).

## PUFA measurements

The PUFA measurements were assayed as described before.<sup>18</sup> Briefly, samples were stored at  $-70^{\circ}\text{C}$  until the biochemical measurement of the serum fatty acids of the phospholipid fraction was performed. The analytical procedure comprised several steps: 1) extraction of total lipids in serum; 2) lipid fraction separation using Sep-Pak NH<sub>2</sub> columns (Waters Corporation, Milford, USA); and 3) methylation and separation of the phospholipids fraction from fatty acid by gas chromatography (Agilent Technologies, Wilmington, USA). The method was calibrated using the calibration mixture (Sigma-Aldrich, Steinheim, Germany). The fatty acids of the plasma phospholipid fraction were demonstrated in  $\mu\text{mol/L}$ .

## Lp-PLA2 assessment

The Lp-PLA2 mass was measured with a colorimetric activity method using a rate reaction enzyme assay, with 1-myristoyl-2-(4-nitrophenylsuccinyl) phosphatidylcholine as the substrate. The assay precision ranged between 1.5% and 1.8%.

## Bias and confounder

The study participants were all diagnosed with T2D and ASCVD, 2 conditions that have been linked to elevated levels of Lp-PLA2. As such, these conditions may exert an influence on the obtained measurements. Furthermore, the average age of the population under investigation was 65 years, which might have played a role in the expression of Lp-PLA2 or other relevant parameters. To minimize any potential sources of bias, laboratory measurements and statistical analyses were conducted by experienced personnel and were subject to double-checking protocols.

## Other biomarkers

The levels of IL-6 and tumor necrosis factor alpha (TNF- $\alpha$ ) were evaluated using an enzyme-linked immunosorbent assay (ELISA) (R&D Systems, Minneapolis, USA). Oxidized LDL (oxLDL) and myeloperoxidase were assessed

with the use of an ELISA (Mercodia AB, Uppsala, Sweden). The hsCRP levels were measured using latex nephelometry (Dade Behring, Marburg, Germany).

## Statistical analyses

Continuous variables were expressed as mean and standard deviation ( $M \pm SD$ ) or median (interquartile range (IQR)). Categorical variables were presented as numbers (percentages). The normality distribution was determined with the Shapiro–Wilk test. Student’s t-test or the Mann–Whitney U test was used to calculate the intergroup differences for continuous variables. The  $\chi^2$  test was used to evaluate the differences in categorical variables between the study groups (with or without a Yates’s continuity correction or Fisher’s exact test). To assess the association between 2 continuous variables, Pearson or Spearman rank correlation coefficients were calculated (with a normal or non-normal distribution, respectively).

Both univariable and multivariable linear regression analyses were calculated to demonstrate the relationship between the Lp-PLA2 value and tested variables. We have built the optimal multivariable model from preselected variables (potential predictors) such as gender, systolic blood pressure, LDL-C, HbA1c, TG, body fat percentage, and visceral fat percentage, among others. Multicollinearity was assessed using variance inflation factors (VIFs). Hat values were used to investigate leveraging observations. The best model was obtained using stepwise (backward/forward) regression with Bayesian information criterion (BIC) as a target. The  $R^2$  was used to evaluate the goodness-of-fit for the final model. Validation was performed using the bootstrap method with 1000 replications.

The sample size was calculated based on our previous research, and it was powered to have a 90% chance of detecting a 15% difference in fibrin clot properties between the analyzed groups using a p-value of 0.05.<sup>19</sup> To deliver that level of statistical power, at least 23 patients in each group were required.

All statistical tests were two-sided. A value of  $p < 0.05$  was considered statistically significant.

All statistical analyses were calculated using Statistica v. 12.0 PL (StatSoft Polska, Kraków, Poland) and R 4.1.1 software (R Foundation for Statistical Computing, Vienna, Austria).

## Results

### Demographics and clinical description

The final analysis included 74 patients (49 (66.22%) males and 25 (33.78%) females) with both ASCVD and T2D (Table 1). The ages ranged from 47 to 85 years, and the female population was, on average, older than the male population (Table 1).

**Table 1.** Baseline characteristics of the study population (n = 74)

Variable		All (n = 74)	Males (n = 49)	Females (n = 25)	p-value
	Age	65.6 ± 6.8	64.43 ± 5.98	67.84 ± 7.93	0.04
Risk factors	hypertension, n (%)	72 (97.3)	48 (98)	24 (96)	0.62
	hyperlipidemia, n (%)	50 (67.6)	32 (65.3)	18 (72)	0.56
	metabolic syndrome, n (%)	74 (100)	49 (100)	25 (100)	1.00
	obesity, n (%)	49 (66.2)	37 (75.5)	12 (48)	0.018
	waist circumference [cm]	106.5 ± 9.4	109.43 ± 9.11	100.78 ± 7.13	0.0002
	BMI [kg/m <sup>2</sup> ]	31.2 ± 3.6	31.66 ± 3.19	30.34 ± 4.10	0.13
	visceral fat, %	16 ± 4.67	18.16 ± 3.79	11.81 ± 3.10	<0.001
	body fat, %	32.25 (28.40–41.58)	30.6 (25.8–33.2)	41.8 (35.1–47.4)	<0.001
	current smoking, n (%)	28 (37.8)	18 (37)	10 (40)	0.78
Medical history	type 2 diabetes duration [years]	10 (6–15)	10 (6–12)	10 (6–20)	0.31
	peripheral artery disease, n (%)	26 (35.1)	19 (38.8)	7 (28)	0.36
	coronary artery disease, n (%)	74 (100)	49 (100)	25 (100)	1.00
	previous MI, n (%)	28 (37.8)	19 (38.8)	9 (36)	0.82
	NSTEMI, n (%)	15 (20.3)	10 (20.4)	5 (20)	0.79
	STEMI, n (%)	15 (20.3)	11 (22.5)	4 (16)	0.73
Baseline laboratory investigations	HbA1c, %	7.24 ± 0.94	7.23 ± 1.04	7.2 ± 0.7	0.36
	eGFR [mL/min/1.73 m <sup>2</sup> ]	77.9 ± 14	77.88 ± 13.68	77.86 ± 14.88	0.97
	TC [mmol/L]	3.86 ± 0.91	3.85 ± 0.98	3.9 ± 0.8	0.89
	LDL-C [mmol/L]	1.91 (1.53–2.64)	1.89 (1.47–2.84)	2.07 (1.53–2.59)	0.61
	HDL-C [mmol/L]	1.24 ± 0.38	1.17 ± 0.36	1.4 ± 0.4	0.049
	TG [mmol/L]	1.35 (1.12–1.92)	1.46 (1.19–1.99)	1.18 (0.95–1.88)	0.08
	AST [U/L]	19 (16–23)	18 (16–23)	19 (16–23)	0.71
	ALT [U/L]	22 (14–28)	24 (14–31)	21 (12–25)	0.31
	INR	0.98 (0.95–1.02)	0.98 (0.96–1)	0.96 (0.92–1.03)	0.29
aPTT [s]	25.6 (23.55–27.3)	25.75 (23.95–27.6)	25.35 (22.8–27.3)	0.28	

BMI – body mass index; MI – myocardial infarction; NSTEMI – non-ST-elevation myocardial infarction; STEMI – ST-elevation myocardial infarction; HbA1c – glycated hemoglobin A1c; eGFR – estimated glomerular filtration rate; TC – total cholesterol; LDL-C – low-density lipoprotein cholesterol; HDL-C – high-density lipoprotein cholesterol; TG – triglycerides; AST – aspartate aminotransferase; ALT – alanine transaminase; INR – international normalized ratio; aPTT – activated partial thromboplastin time. Data are presented as mean ± standard deviation (M ± SD), median (interquartile range (IQR)), or number (percentage).

All subjects had a very high CV risk (e.g., T2D, obesity, hypertension, hyperlipidemia, and CAD), including 30 (40.6%) patients with a history of previous myocardial infarction (MI). There was no statistically significant difference between genders regarding risk factors and medical history, except for higher values in waist circumference in the male population. However, waist circumference did not correlate with Lp-PLA2 and was not an independent risk factor for increased Lp-PLA2 mass. However, despite a higher percentage of body fat (%) in the women subgroup, they had a lower concentration of Lp-PLA2. In contrast, male patients had higher values of visceral fat (%). Finally, in both analyzed groups, visceral fat ( $r = -0.17$ ,  $p = 0.36$  in males and  $r = -0.1$ ,  $p = 0.72$  in females) and body fat ( $r = -0.18$ ,  $p = 0.24$  in males and  $r = -0.02$ ,  $p = 0.94$  in females) were not associated with Lp-PLA2 mass.

In general, the female population had higher levels of HDL-C and lower levels of TG than the male population.

Moreover, treatment regimens were not significantly different between genders (Supplementary Table 1). Despite the significant difference in age between males and females, there were no significant associations between Lp-PLA2 concentration and age in both males ( $r = 0.19$ ,  $p = 0.19$ ) and females ( $r = 0.30$ ,  $p = 0.14$ ).

### Lp-PLA2 and inflammatory biomarkers

Based on our research, males had, on average, higher levels of Lp-PLA2 in the plasma than females (Table 2, Fig. 1). Male gender positively correlated with the levels of Lp-PLA2 ( $r = 0.31$ ,  $p = 0.006$ ), and Lp-PLA2 was positively associated with IL-6 ( $r = 0.27$ ,  $p = 0.019$ ), creatinine level ( $r = 0.29$ ,  $p = 0.03$ ) and TG ( $r = 0.41$ ,  $p = 0.002$ ).

Interestingly, no differences were observed in the majority of analyzed inflammatory biomarkers (myeloperoxidase, IL-6, oxLDL, TNF- $\alpha$ , and hsCRP) between both genders, except for Lp-PLA2 (Table 2).

**Table 2.** Inflammatory status of the study population

Variable	Females (n = 25)	Males (n = 49)	p-value
oxLDL [mU/L]	62.50 (31.40–120.60)	55.50 (35.40–179.90)	0.76
Myeloperoxidase [ng/mL]	30.05 (16.28–54.42)	31.11 (21.58–44.44)	0.88
Lp-PLA2 [ng/mL]	109.40 (78.69–137.85)	146.21 (110.31–181.13)	0.006
TNF-α [pg/mL]	1.51 (1.31–1.85)	1.48 (1.28–1.71)	0.81
IL-6 [pg/mL]	1.93 (1.62–2.50)	2.01 (1.55–3.01)	0.82
hsCRP [mg/L]	1.64 (0.84–2.31)	1.54 (0.71–3.29)	0.99

oxLDL – oxidized low-density lipoprotein; Lp-PLA2 – lipoprotein-associated phospholipase A2; TNF-α – tumor necrosis factor alpha; IL-6 – interleukin 6; hsCRP – high-sensitivity C-reactive protein. Data are presented as median (interquartile range (IQR)).

**Table 3.** Independent predictors of lipoprotein-associated phospholipase A2 (Lp-PLA2) – a multivariable linear regression model

Variable	β	95% CI	Standard error	t value	p-value
Female gender	–33.84	–63.58; –4.10	14.86	–2.28	0.026
Body fat (%)	–1.15	–2.78; 0.48	0.81	–1.42	0.16
TG	29.13	12.27; 45.99	8.43	3.46	0.001
oxLDL	0.03	–0.02; 0.08	0.02	1.28	0.20

TG – triglycerides; oxLDL – oxidized low-density lipoprotein; ICAM-1 – intercellular adhesion molecule-1; β – coefficient; 95% CI – 95% confidence interval.

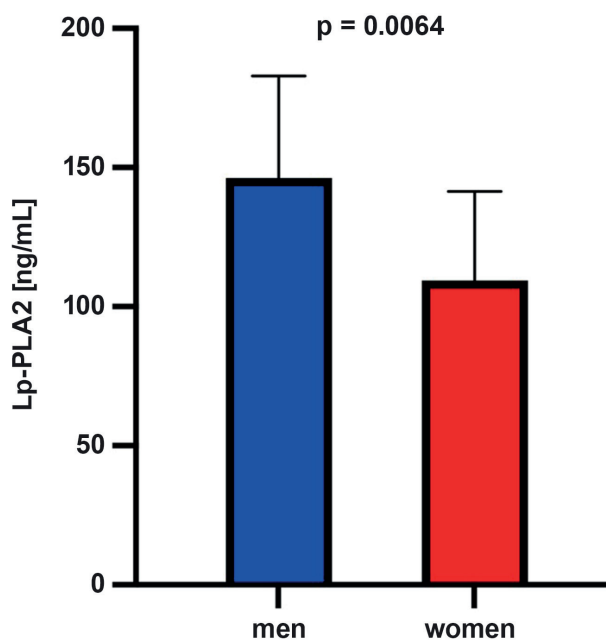


**Fig. 1.** Lipoprotein-associated phospholipase A2 (Lp-PLA2) concentration between men and women with both atherosclerotic cardiovascular disease (ASCVD) and type 2 diabetes (T2D). The horizontal line represents the mean, and the upper and lower bars represent the standard deviation from the mean

Finally, the presented multivariate model showed that female gender (decreasing Lp-PLA2 mass) and TG (increasing Lp-PLA2 mass) were independent predictors of Lp-PLA2 concentration (Table 3).

### PUFA and Lp-PLA2

The PUFA concentrations did not differ between genders except for arachidic acid with linoleic acid (C20+C18:3(n-6))

concentration, which was higher in the female group (Supplementary Table 2). In the female population, there was a negative correlation between arachidonic acid (AA) and Lp-PLA2 mass ( $r = -0.53$ ,  $p = 0.007$ ). In contrast, the male subgroup did not show a significant correlation between AA and Lp-PLA2 mass. The correlations between PUFA plasma concentrations and the Lp-PLA2 mass are presented in Table 4.

### Discussion

The main objective of this study was to determine the intergender differences in Lp-PLA2 levels in a very high CV risk population. We have demonstrated that the plasma mass levels of Lp-PLA2 were significantly higher in males compared to females in patients with both ASCVD and T2D. To the best of our knowledge, our study is the first to describe gender-related differences in plasma Lp-PLA2 levels in the analyzed patient population.

The collaborative data from 32 prospective studies showed that in both patients with stable ASCVD and without ASCVD, males had a higher Lp-PLA2 mass than females.<sup>10</sup> However, the population of patients with T2D represented a small percentage of the analyzed population, and Lp-PLA2 activity and mass have been independent predictors of adverse CV events in T2D; therefore, they may be important markers in such populations.<sup>15</sup> Our research showed similar findings. In the population of patients with T2D and ASCVD, males, on average, had higher levels of Lp-PLA2 than females. In support of our findings, it has been reported that in patients with vascular diseases such as cerebral stroke, males had higher levels of Lp-PLA2 than females.<sup>14</sup>

**Table 4.** Correlation between lipoprotein-associated phospholipase A2 (Lp-PLA2) plasma levels and fatty acid concentration in plasma

Variable	All (n = 74)	Females (n = 25)	Males (n = 49)
C12	r = -0.21, p = 0.079	r = 0.13, p = 0.54	r = 0.18, p = 0.22
C14	r = 0.02, p = 0.84	r = -0.24, p = 0.25	r = 0.16, p = 0.29
C16	r = 0.08, p = 0.52	r = -0.21, p = 0.32	r = -0.05, p = 0.72
C16:1	r = 0.03, p = 0.78	r = -0.29, p = 0.17	r = 0.14, p = 0.35
C18	r = -0.1, p = 0.4	r = -0.23, p = 0.26	r = -0.26, p = 0.07
C18:1	r = -0.06, p = 0.64	r = -0.14, p = 0.51	r = -0.02, p = 0.87
C18:2(n-6)	r = 0.11, p = 0.34	r = -0.004, p = 0.98	r = 0.17, p = 0.25
C18:3(n-3)	r = 0.08, p = 0.48	r = 0.2, p = 0.33	r = 0.16, p = 0.28
C20+C18:3(n-6)	r = -0.09, p = 0.46	r = -0.14, p = 0.51	r = 0.04, p = 0.78
C20:2(n-6)	r = 0.08, p = 0.51	r = 0.17, p = 0.43	r = 0.06, p = 0.7
C20:4 (AA)	r = -0.26, p = 0.024	r = -0.53, p = 0.007	r = -0.16, p = 0.27
C20:5(n-3)	r = -0.004, p = 0.98	r = -0.2, p = 0.33	r = 0.02, p = 0.87
C24	r = -0.08, p = 0.53	r = -0.34, p = 0.1	r = -0.03, p = 0.86
C22:6(n-3)	r = -0.02, p = 0.85	r = -0.06, p = 0.79	r = -0.08, p = 0.57

C12 – lauric acid; C14 – myristic acid; C16 – palmitic acid; C16:1 – palmitoleic acid; C18 – stearic acid; C18:1 – oleic acid; C18:2(n-6) – linoleic acid; C18:3(n-3) – alpha-linolenic acid; C20+C18:3(n-6) – arachidic acid with linoleic acid; C20:2(n-6) – eicosadienoic acid; C20:4 (AA) – arachidonic acid; C20:5(n-3) – eicosapentaenoic acid; C24 – lignoceric acid; C22:6(n-3) – docosahexaenoic acid. Data are presented as Pearson's correlation coefficient with a p-value.

Contrary to those findings, Lu et al. reported that in a young population of patients after acute myocardial infarction (AMI), female gender was associated with higher levels of Lp-PLA2.<sup>20</sup> This association could be explained by the fact that the analyzed female patients had higher inflammatory markers after AMI compared to males, which could translate to elevated levels of Lp-PLA2.<sup>20</sup>

A higher detected Lp-PLA2 mass was demonstrated to correlate with higher rates of adverse CV events.<sup>21</sup> It was also shown that statins lower Lp-PLA2 levels by reducing the macrophage content in atherosclerotic lesions.<sup>22</sup> Nevertheless, we reported that males had higher levels of Lp-PLA2 mass despite a similar proportion of statin therapy between both genders.

The association between T2D and chronic low-grade inflammation is a well-known fact, and it was shown that biomarkers such as interleukin-1 $\beta$ , vascular endothelial growth factor (VEGF) and Lp-PLA2 might play an important role in the occurrence of diabetic complications.<sup>23,24</sup>

In a study by Siddiqui et al., it was reported that patients with poorly controlled T2D and high Lp-PLA2 activity had higher rates of major adverse cardiac events (MACE). This study investigated the association of Lp-PLA2 with metabolic control (HbA1c) in a diabetic population and its impact on MACE.

The Lp-PLA2 was reported to be related to endothelial damage, characterized by the weakening of the anticoagulant and anti-inflammatory functions of the endothelium,<sup>25</sup> thereby making Lp-PLA2 a possible marker reflecting the extent of ASCVD.<sup>26</sup> We have also observed that Lp-PLA2 is closely related to other markers of vascular inflammation, such as oxLDL, which is consistent with previous research.<sup>27</sup>

Interestingly, we demonstrated that Lp-PLA2 was the only analyzed inflammatory biomarker that varied between both genders in the researched population. The gender-related difference in Lp-PLA2 levels is particularly significant because Lp-PLA2 has been implicated as a potential biomarker for ASCVD. Therefore, the higher levels of Lp-PLA2 in men could be a contributing factor to the increased risk of adverse events.

Those results support the concept of Lp-PLA2 plasma levels as a useful marker of ASCVD,<sup>28</sup> especially in the population with a very high CV risk.

We have demonstrated that females, despite a significantly higher body fat percentage, were characterized by substantially lower concentrations of Lp-PLA2 when compared to males. Interestingly, those differences were not associated with significant correlations between visceral or body fat percentage and Lp-PLA2 mass in both analyzed groups. Therefore, despite the higher body fat percentage, females appear to be associated with a lower level of visceral fat when compared to males, which may potentially be reflected in lower concentrations of Lp-PLA2 in women, but further research on a larger scale is needed in this regard.

In our study, males had higher values of waist circumference than females, which partly explained high Lp-PLA2 plasma levels in male patients. It was previously reported that adipose tissue can be an active source of Lp-PLA2.<sup>29,30</sup> However, we observed no correlation between these 2 variables, and waist circumference was not an independent risk factor for an increased Lp-PLA2 mass.

It is also important to mention that IL-6 and hsCRP are often present in obese patients,<sup>31</sup> but in our research, they were not independent risk factors for an increased



Lp-PLA2 mass. The Lp-PLA2 concentration may affect the development of ASCVD in men far beyond the issue of excessive body weight, abnormal abdominal circumference and the inflammatory state associated with obesity.

The beneficial effect of PUFA on ASCVD prevention is well established.<sup>17</sup> It was also shown that the administration of PUFAs reduced the levels of Lp-PLA2 in ASCVD patients.<sup>16,17</sup> However, in our current study, out of all measured PUFAs, only the AA concentration was associated with lower Lp-PLA2 levels. This association was especially strong in the female subpopulation. A study by Steffen et al. and a study by Fragopoulou et al. demonstrated that AA levels negatively correlated with Lp-PLA2 mass when adjusted for covariates such as inflammation.<sup>32–34</sup>

In contrast to those findings, AA is well characterized for being inflammatory, but it also generates lipoxins – powerful non-classic eicosanoids that silence inflammatory signaling pathways<sup>33</sup> and suppress an inducer of Lp-PLA2 expression.<sup>34</sup>

To date, there have been few studies that examined AA in the context of Lp-PLA2. However, based on our data and presented scientific papers, we could argue that a higher concentration of AA affects the inflammatory cascade in such a way that it may lower levels of Lp-PLA2, making AA an important tool in the treatment of patients at very high CV risk. However, further research is needed to fully examine the influence of AA on Lp-PLA2.

## Limitations

We have several limitations to acknowledge. The cross-sectional nature of the study did not allow our research to infer causality. Moreover, there was no follow-up, and the sample size was limited. A larger observational study, including follow-up, would be beneficial to confirm our hypothesis. Third, the smaller number of female patients could have had an impact on the observed differences between measured parameters. Fourth, the treatment with statins and  $\beta$ -blockers, both of which can influence the levels of Lp-PLA2, were common in both analyzed subgroups. Additionally, it was suggested that the association between the Lp-PLA2 mass and atherosclerosis development in T2D patients may be weaker in subclinical ASCVD,<sup>35</sup> but the association between T2D and its activity in more advanced atherosclerotic lesions remains strong.<sup>36</sup> Further, the dietary pattern can differ between males and females, and its possible association with PUFA concentrations was not assessed. We are aware of the potential impact of dietary habits on Lp-PLA2 activity, but the goal of the present study was not to evaluate the influence of dietary patterns on Lp-PLA2 levels. Instead, our focus was to investigate the differences between genders and their associations with measured serum levels of monounsaturated fatty acids, and n-3 and n-6 PUFAs.

Another limitation of our study is that it relied solely on Lp-PLA2 mass, which may lead to the underdiagnosis

of CV risk caused by increased LDL-C levels. Therefore, additional measurements of Lp-PLA2 activity may be used to mitigate the influence of LDL-C levels on Lp-PLA2 as a biomarker. Nevertheless, Lp-PLA2 mass measurements should be interpreted in conjunction with other laboratory tests, such as LDL-C, for better risk stratification.

The LDL-C levels may lead to the underdiagnosis of CV risk. However, assessing Lp-PLA2 activity can be beneficial in preventing this situation and enhancing risk assessment.

## Conclusions

In conclusion, we demonstrated that in the population of patients with both ASCVD and T2D, males had higher plasma levels of Lp-PLA2 than females, thus making it a potential biomarker for the assessment of gender-related CV risk stratification. This study provides further evidence that AA plasma concentrations are negatively associated with Lp-PLA2 blood levels.

## Supplementary data

The supplementary materials are available at <https://doi.org/10.5281/zenodo.8169154>. The package contains the following files:

Supplementary Table 1. Comparison of baseline characteristics of males compared to females in the studied population.

Supplementary Table 2. The gender differences in concentration of fatty acids in plasma.

## ORCID iDs

Aleksander Siniarski  <https://orcid.org/0000-0002-7493-3626>  
 Renata Gołębiewska-Wiatrak  <https://orcid.org/0000-0003-3884-7269>  
 Jadwiga Nessler  <https://orcid.org/0000-0002-5076-5816>  
 Krzysztof Piotr Malinowski  <https://orcid.org/0000-0003-2189-0498>  
 Grzegorz Gajos  <https://orcid.org/0000-0002-7361-3559>

## References

1. Townsend N, Kazakiewicz D, Lucy Wright F, et al. Epidemiology of cardiovascular disease in Europe. *Nat Rev Cardiol*. 2022;19(2):133–143. doi:10.1038/s41569-021-00607-3
2. Ahmad FB, Cisewski JA, Miniño A, Anderson RN. Provisional mortality data : United States, 2020. *MMWR Morb Mortal Wkly Rep*. 2021;70(14):519–522. doi:10.15585/mmwr.mm7014e1
3. De Bacquer D, De Smedt D, Kotseva K, et al; On behalf of the EUROASPIRE Investigators. Incidence of cardiovascular events in patients with stabilized coronary heart disease: The EUROASPIRE IV follow-up study. *Eur J Epidemiol*. 2019;34(3):247–258. doi:10.1007/s10654-018-0454-0
4. Christodoulidis G, Vittorio TJ, Fudim M, Lerakis S, Kosmas CE. Inflammation in coronary artery disease. *Cardiol Rev*. 2014;22(6):279–288. doi:10.1097/CRD.000000000000006
5. Anderson JL. Lipoprotein-associated phospholipase A2: An independent predictor of coronary artery disease events in primary and secondary prevention. *Am J Cardiol*. 2008;101(12A):S23–S33. doi:10.1016/j.amjcard.2008.04.015
6. Silva IT, Mello AP, Damasceno NR. Antioxidant and inflammatory aspects of lipoprotein-associated phospholipase A2 (Lp-PLA2): A review. *Lipids Health Dis*. 2011;10(1):170. doi:10.1186/1476-511X-10-170

7. Kaptoge S, Seshasai SRK, Gao P, et al. Inflammatory cytokines and risk of coronary heart disease: New prospective study and updated meta-analysis. *Eur Heart J*. 2014;35(9):578–589. doi:10.1093/eurheartj/ehz367
8. Tsimikas S, Tsimionis LD, Tselepis AD. New insights into the role of lipoprotein(a)-associated lipoprotein-associated phospholipase A<sub>2</sub> in atherosclerosis and cardiovascular disease. *Arterioscler Thromb Vasc Biol*. 2007;27(10):2094–2099. doi:10.1161/01.ATV.0000280571.28102.d4
9. Mayer O, Seidlerová J, Filipovský J, et al. Unexpected inverse relationship between impaired glucose metabolism and lipoprotein-associated phospholipase A<sub>2</sub> activity in patients with stable vascular disease. *Eur J Intern Med*. 2014;25(6):556–560. doi:10.1016/j.ejim.2014.05.010
10. Thompson A, Gao P, Orfei L, et al. Lipoprotein-associated phospholipase A<sub>2</sub> and risk of coronary disease, stroke, and mortality: Collaborative analysis of 32 prospective studies. *Lancet*. 2010;375(9725):1536–1544. doi:10.1016/S0140-6736(10)60319-4
11. Packard CJ. Lipoprotein-associated phospholipase A<sub>2</sub> as a biomarker of coronary heart disease and a therapeutic target. *Curr Opin Cardiol*. 2009;24(4):358–363. doi:10.1097/HCO.0b013e32832bcb22
12. Li J, Zhou Z, Niu X, Li H. Lipoprotein-associated phospholipase A<sub>2</sub> in cardiac disease: A potential early biomarker of unstable coronary artery disease. *Clin Lab*. 2020;66(5). doi:10.7754/Clin.Lab.2019.190719
13. O'Donoghue M, Morrow DA, Sabatine MS, et al. Lipoprotein-associated phospholipase A<sub>2</sub> and its association with cardiovascular outcomes in patients with acute coronary syndromes in the PROVE IT-TIMI 22 (PRavastatin Or atorVastatin Evaluation and Infection Therapy–Thrombolysis In Myocardial Infarction) trial. *Circulation*. 2006;113(14):1745–1752. doi:10.1161/CIRCULATIONAHA.105.612630
14. Alkuraishy HM, Al-Gareeb AI, Waheed HJ. Lipoprotein-associated phospholipase A<sub>2</sub> is linked with poor cardio-metabolic profile in patients with ischemic stroke: A study of effects of statins. *J Neurosci Rural Pract*. 2018;09(04):496–503. doi:10.4103/jnrp.jnrp\_97\_18
15. Hatoum IJ, Hu FB, Nelson JJ, Rimm EB. Lipoprotein-associated phospholipase A<sub>2</sub> activity and incident coronary heart disease among men and women with type 2 diabetes. *Diabetes*. 2010;59(5):1239–1243. doi:10.2337/db09-0730
16. Gajos G, Rostoff P, Undas A, Piwowarska W. Effects of polyunsaturated omega-3 fatty acids on responsiveness to dual antiplatelet therapy in patients undergoing percutaneous coronary intervention. *J Am Coll Cardiol*. 2010;55(16):1671–1678. doi:10.1016/j.jacc.2009.11.080
17. Gajos G, Zalewski J, Mostowik M, Konduracka E, Nessler J, Undas A. Polyunsaturated omega-3 fatty acids reduce lipoprotein-associated phospholipase A<sub>2</sub> in patients with stable angina. *Nutr Metab Cardiovasc Dis*. 2014;24(4):434–439. doi:10.1016/j.numecd.2013.09.011
18. Poreba M, Mostowik M, Siniarski A, et al. Treatment with high-dose n-3 PUFAs has no effect on platelet function, coagulation, metabolic status or inflammation in patients with atherosclerosis and type 2 diabetes. *Cardiovasc Diabetol*. 2017;16(1):50. doi:10.1186/s12933-017-0523-9
19. Gajos G, Zalewski J, Rostoff P, Nessler J, Piwowarska W, Undas A. Reduced thrombin formation and altered fibrin clot properties induced by polyunsaturated omega-3 fatty acids on top of dual antiplatelet therapy in patients undergoing percutaneous coronary intervention (OMEGA-PCI Clot). *Arterioscler Thromb Vasc Biol*. 2011;31(7):1696–1702. doi:10.1161/ATVBAHA.111.228593
20. Lu Y, Zhou S, Dreyer RP, et al. Sex differences in inflammatory markers and health status among young adults with acute myocardial infarction: Results from the VIRGO (Variation in Recovery: Role of Gender on Outcomes of Young Acute Myocardial Infarction Patients) study. *Circ Cardiovasc Qual Outcomes*. 2017;10(2):e003470. doi:10.1161/CIRCOUTCOMES.116.003470
21. Maiolino G. Lipoprotein-associated phospholipase A<sub>2</sub> prognostic role in atherosclerotic complications. *World J Cardiol*. 2015;7(10):609. doi:10.4330/wjc.v7.i10.609
22. Cai A, Li G, Chen J, Li X, Li L, Zhou Y. Increased serum level of Lp-PLA<sub>2</sub> is independently associated with the severity of coronary artery diseases: A cross-sectional study of Chinese population. *BMC Cardiovasc Disord*. 2015;15(1):14. doi:10.1186/s12872-015-0001-9
23. Papatheodorou K, Banach M, Bekiari E, Rizzo M, Edmonds M. Complications of diabetes 2017. *J Diabetes Res*. 2018;2018:3086167. doi:10.1155/2018/3086167
24. Ju HB, Zhang FX, Wang S, et al. Effects of fenofibrate on inflammatory cytokines in diabetic retinopathy patients. *Medicine (Baltimore)*. 2017;96(31):e7671. doi:10.1097/MD.00000000000007671
25. Siddiqui MK, Smith G, St Jean P, et al. Diabetes status modifies the long-term effect of lipoprotein-associated phospholipase A<sub>2</sub> on major coronary events. *Diabetologia*. 2022;65(1):101–112. doi:10.1007/s00125-021-05574-5
26. Lavi S, McConnell JP, Rihal CS, et al. Local production of lipoprotein-associated phospholipase A<sub>2</sub> and lysophosphatidylcholine in the coronary circulation: Association with early coronary atherosclerosis and endothelial dysfunction in humans. *Circulation*. 2007;115(21):2715–2721. doi:10.1161/CIRCULATIONAHA.106.671420
27. Ikonomidis I, Kadoglou NNP, Tritakis V, et al. Association of Lp-PLA<sub>2</sub> with digital reactive hyperemia, coronary flow reserve, carotid atherosclerosis and arterial stiffness in coronary artery disease. *Atherosclerosis*. 2014;234(1):34–41. doi:10.1016/j.atherosclerosis.2014.02.004
28. Kim M, Yoo HJ, Kim M, et al. Associations among oxidative stress, Lp-PLA<sub>2</sub> activity and arterial stiffness according to blood pressure status at a 3.5-year follow-up in subjects with prehypertension. *Atherosclerosis*. 2017;257:179–185. doi:10.1016/j.atherosclerosis.2017.01.006
29. Charniot JC, Khani-Bittar R, Albertini JP, et al. Interpretation of lipoprotein-associated phospholipase A<sub>2</sub> levels is influenced by cardiac disease, comorbidities, extension of atherosclerosis and treatments. *Int J Cardiol*. 2013;168(1):132–138. doi:10.1016/j.ijcard.2012.09.054
30. Battineni G, Sagaro GG, Chintalapudi N, Amenta F, Tomassoni D, Tayebati SK. Impact of obesity-induced inflammation on cardiovascular diseases (CVD). *Int J Mol Sci*. 2021;22(9):4798. doi:10.3390/ijms22094798
31. Jackisch L, Kumsaiyai W, Moore JD, et al. Differential expression of Lp-PLA<sub>2</sub> in obesity and type 2 diabetes and the influence of lipids. *Diabetologia*. 2018;61(5):1155–1166. doi:10.1007/s00125-018-4558-6
32. Rao SR. Inflammatory markers and bariatric surgery: A meta-analysis. *Inflamm Res*. 2012;61(8):789–807. doi:10.1007/s00011-012-0473-3
33. Steffen BT, Steffen LM, Liang S, Tracy R, Jenny NS, Tsai MY. n-3 and n-6 fatty acids are independently associated with lipoprotein-associated phospholipase A<sub>2</sub> in the Multi-Ethnic Study of Atherosclerosis. *Br J Nutr*. 2013;110(9):1664–1671. doi:10.1017/S0007114513000949
34. Fragopoulou E, Detopoulou P, Alepoudea E, Nomikos T, Kalogeropoulos N, Antonopoulou S. Associations between red blood cells fatty acids, desaturases indices and metabolism of platelet activating factor in healthy volunteers. *Prostaglandins Leukot Essent Fatty Acids*. 2021;164:102234. doi:10.1016/j.plefa.2020.102234
35. Cicero AFG, Nascetti S, López-Sabater MC, et al. Changes in LDL fatty acid composition as a response to olive oil treatment are inversely related to lipid oxidative damage: The EUROLIVE Study. *J Am Coll Nutr*. 2008;27(2):314–320. doi:10.1080/07315724.2008.10719705
36. Lin XH, Xu MT, Tang JY, et al. Effect of intensive insulin treatment on plasma levels of lipoprotein-associated phospholipase A<sub>2</sub> and secretory phospholipase A<sub>2</sub> in patients with newly diagnosed type 2 diabetes. *Lipids Health Dis*. 2016;15(1):203. doi:10.1186/s12944-016-0368-3



# Relationship in development of malocclusions to polymorphisms of selected vitamin D receptors

Marzena Dominiak<sup>1,A–F</sup>, Anna Leszczyszyn<sup>1,A–E</sup>, Izabela Łacmańska<sup>2,A–D</sup>, Monika Machoy<sup>3,A–C</sup>, Hanna Gerber<sup>4,C–E</sup>, Joseph Choukroun<sup>5,C–E</sup>, Tomasz Gedrange<sup>6,C–E</sup>, Sylwia Hnitecka<sup>4,C–E</sup>

<sup>1</sup> Department of Dental Surgery, Wrocław Medical University, Poland

<sup>2</sup> Department of Genetics, Wrocław Medical University, Poland

<sup>3</sup> Department of Orthodontics, Pomeranian Medical University, Szczecin, Poland

<sup>4</sup> Department of Maxillofacial Surgery, Wrocław Medical University, Poland

<sup>5</sup> Private Pain Clinic, Nice, France

<sup>6</sup> Department of Orthodontics, Technische Universität Dresden, Germany

A – research concept and design; B – collection and/or assembly of data; C – data analysis and interpretation; D – writing the article; E – critical revision of the article; F – final approval of the article

Advances in Clinical and Experimental Medicine, ISSN 1899–5276 (print), ISSN 2451–2680 (online)

Adv Clin Exp Med. 2024;33(6):601–608

## Address for correspondence

Sylwia Hnitecka

E-mail: sylwia.hnitecka@gmail.com

## Funding sources

None declared

## Conflict of interest

None declared

Received on December 11, 2022

Reviewed on July 15, 2023

Accepted on July 24, 2023

Published online on February 14, 2024

## Cite as

Dominiak M, Leszczyszyn A, Łacmańska I, et al. Relationship in development of malocclusions to polymorphisms of selected vitamin D receptors. *Adv Clin Exp Med.* 2024;33(6):601–608. doi:10.17219/acem/169977

## DOI

10.17219/acem/169977

## Copyright

Copyright by Author(s)

This is an article distributed under the terms of the Creative Commons Attribution 3.0 Unported (CC BY 3.0) (<https://creativecommons.org/licenses/by/3.0/>)

## Abstract

**Background.** The development of malocclusion is related to various factor, many of which are still not fully explained. The steroid hormone, 1,25-dihydroxyvitamin D<sub>3</sub>, has pleiotropic effects. It plays a key role in skeletal metabolism and the control of cell repair by attaching to the nuclear vitamin D steroid receptor (VDR). This vitamin affects bone turnover through the processes of bone tissue formation and resorption via its action on cells of the osteoblastic and osteoclastic lineage, exerts a modulating effect on the immune system, and is involved in the regulation of cell proliferation and differentiation. The role of vitamin D<sub>3</sub> (VD<sub>3</sub>) and its receptor polymorphisms is a rarely studied topic in dentistry. Due to the proven influence on bone turnover processes and immune responses, the main research topic is its relation to periodontal diseases, but so far, its role in the formation and development of malocclusions has not been assessed.

**Objectives.** This study aimed to assess the association of selected VDR polymorphisms: *Cdx2* (*rs11658820*), *TaqI* (*rs7975232*), *BsmI* (*rs1544410*), *Apal* (*rs7975232*), and *FokI* (*rs2228570*) with the development of malocclusions.

**Materials and methods.** A prospective observational study was performed. The examination consisted of a medical interview, intra- and extraoral orthodontic diagnosis, alginate impression, cone beam computed tomography (CBCT), and venous blood sample to obtain genomic DNA and assess VDR polymorphisms.

**Results.** The *rs11658820* polymorphism causes an almost 4-fold increase in the probability of the presence of a malocclusion. GT and TT genotypes of *rs7975232* are also associated with a similar risk – almost 6 and almost 5 times higher, respectively. In turn, the effect of the *rs2228570*-AG and GG genotype polymorphisms on the occurrence of transversal anomalies was demonstrated (odds ratio (OR) = 8.46 and OR = 6.92, respectively).

**Conclusions.** The association of individual polymorphisms with specific malocclusions should be carefully assessed, especially since some trends have been indicated.

**Key words:** vitamin D, orthodontics, VDR, malocclusion

## Background

The development of skeletal and maxillary defects is related to various general prenatal, postnatal and local factors. Many etiological factors of occlusal anomalies are still not fully explained. Proffit et al. distinguished 3 categories of malocclusion etiologies: specific, environmental and genetic.<sup>1,2</sup> General factors include endocrine disorders (which can cause, among others, gigantism or acromegaly) or systemic diseases such as rickets.<sup>3,4</sup> The environmental factors include dysfunctions of, e.g., swallowing, posture, breathing, chewing, and speech, and parafunctions, such as sucking lips, cheeks, fingers, and the presence of caries causing premature loss of deciduous teeth.<sup>5</sup> Malocclusion can be divided into 3 planes.<sup>6</sup> There are 3 groups of malocclusions: vertical (e.g., deep bite, open bite), horizontal (i.e., prognathism, retrognathia) and transverse (buccal, cross-bite, lingual crossbite – often associated with a deficiency in the growth of one of the arches, maxilla or mandible).

Vitamins have an enormous influence on facial development.<sup>7–11</sup> Vitamin D (VD) is produced by the skin after sun exposure or provided in the diet. Calcitriol becomes an active fat-soluble hormone. It exerts pleiotropic effects on the body, having significant functional and regulatory effects. Its autocrine and paracrine activities complete the endocrine activity, which controls the absorption of calcium and phosphorus through the direct stimulation of the vitamin D receptor (VDR) in tissues. Acting as a neuro-mediator, it influences the production of antioxidants and regulates the cell's growth. Vitamin D3 (VD3) plays a key role in skeletal metabolism (mostly bone turnover) by attaching to nuclear steroid receptors (Fig. 1).<sup>12–15</sup> Expression and nuclear activation of the VDR are necessary for the effects of VD. Several genetic variations have been identified in the VDR. The *VDR* gene is located on chromosome 12 (12q12–q14). It consists of 9 exons encoding a protein with 427 amino acids. This receptor belongs to the nuclear receptor superfamily of ligand-activated transcription factors. It induces genomic regulation of downstream targets involved in numerous biological activities, i.e., calcium and

phosphate homeostasis in bone metabolism. Vitamin D receptor participates in the actions of VD, establishing a heterodimer with the retinoid x receptor (RXR). The RXR-VDR complex translocates into the nucleus and binds the VD response element (VDRE) in the promoter regions of VD target genes.<sup>16</sup> The genes that code for the enzymes, receptors and transporters that participate in VD metabolism are highly polymorphic. Due to this, the presence of single nucleotide polymorphisms (SNPs) in specific genes influences VD serum levels and their activity.<sup>17</sup>

More studies focusing on the importance of *VDR* polymorphisms prove their connection with various diseases, such as osteoporosis, colorectal cancer risk, gastrointestinal diseases, and regulation of host–bacterial interactions.<sup>13,14,18–20</sup> The role of VD3 and *VDR* polymorphisms is a rarely studied topic in dentistry. Due to the proven influence on bone turnover processes and immune responses, the main research topic is its relation to periodontal diseases. Unfortunately, its role is not fully explained.<sup>21,22</sup> So far, its possible influence on the formation and development of malocclusions has not been assessed.

## Objectives

This study aimed to prospectively assess the impact of *VDR* polymorphisms which are most often analyzed, recorded and known in the literature, and which have been associated with various effects on many diseases – *Cdx2* (*rs11658820*), *TaqI* (*rs7975232*), *BsmI* (*rs1544410*), *ApaI* (*rs7975232*), and *FokI* (*rs2228570*) – on the development of malocclusion.

## Materials and methods

### Study group

A prospective observational study was carried out in a randomly selected group of 113 patients in a private dental practice in Wrocław between 2017 and 2018. The analysis included patients of both sexes, Caucasians above 18 years of age, who came for dental check-ups. The exclusion criteria were age of the patients (<18 years) and lack of consent to participate in at least 1 component of the study. Also, patients with severe diseases that can have a significant impact on skeletal dysmorphisms (such as fibrous dysplasia and cherubism) and those that can change the occlusions, such as trauma to the craniofacial skeleton or maxillofacial surgeries, were excluded.

### Research components

The examination consisted of 4 parts: 1) a medical interview; 2) an assessment of the oral cavity in the orthodontic aspect with an alginate impression for the diagnostic

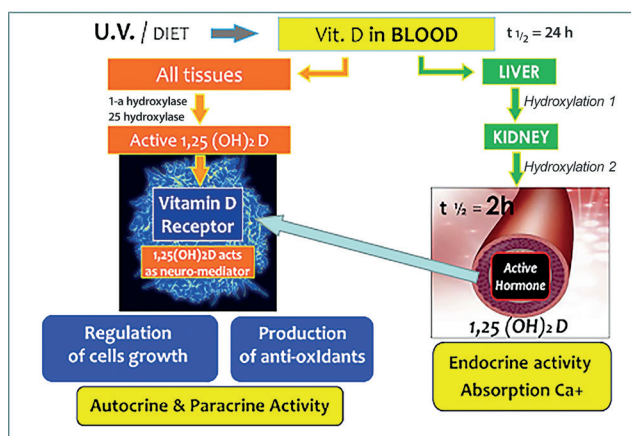


Fig. 1. Vitamin D (VD) hydroxylation and vitamin D receptor (VDR) activity

model; 3) radiographic images; and 4) a venous blood sample to obtain genomic deoxyribonucleic acid (DNA) and assess *VDR* polymorphisms. The medical interview included: demographic data (age, sex), habits (smoking, alcohol consumption) and comorbidities. A detailed examination of the oral cavity assessed:

- canine class and Angle's class<sup>1</sup> on both sides; if the first molar or canine was missing, the class on this side was not assessed;
- vertical and horizontal bite [mm];
- crowding on the 3-point scale in the maxilla and the mandible:
  - 1<sup>st</sup> degree (no space for half of the incisor),
  - 2<sup>nd</sup> degree (no space for 1.5 incisors),
  - 3<sup>rd</sup> degree (no space for 2 or more incisors),
  - the 2<sup>nd</sup> and 3<sup>rd</sup> degree (indications for extraction treatment);
- malocclusion (in the sagittal, horizontal, and orbital planes).

Each patient underwent an alginate impression to prepare a diagnostic model for analysis, an intraoral photograph showing the upper and lower incisors, and volumetric tomography of the maxillary and mandibular regions using Carestream® (Carestream Health, New York, USA). The models were analyzed using the Pont,<sup>23</sup> Korkhaus<sup>24</sup> and Popovich<sup>25</sup> indices.

## Laboratory analysis

Laboratory tests of peripheral blood collected from the antecubital fossa were carried out. The following polymorphisms were analyzed: *Cdx2* (*rs11568820*), *TaqI* (*rs731236*), *ApaI* (*rs7975232*), *BsmI* (*rs1544410*), and *FokI* (*rs2228570*). *BsmI* and *ApaI* stemmed from substitution in intron 8. *TaqI*

resulted from a substitution of cytosine (C) with thymine (T) in exon 9. These SNPs are situated near the 3'-UTR, which is a 3'-3'-Untranslated Region. They are believed to alter the stability of the mRNA of *VDR*. *Cdx2* in exon 1 influences *VDR* transcriptional activity (G allele decreases relative to the A allele). *FokI* in exon 2 is the start codon for the *VDR* gene and involves a change of ATG to ACG.<sup>26</sup>

Genomic DNA from peripheral lymphocytes was isolated from the 200 µL of whole blood using Prepito DNA Blood D250 Kit and chemagic™. Prepito® instruments (PerkinElmer, Waltham, USA) were used strictly according to the producer's protocol.

The primer sequences for polymerase chain reaction (PCR) were previously described by Lins et al.<sup>27</sup> (Table 1). Polymerase chain reaction was performed using Taq polymerase (5 U/µL), 0.5 µL, provided with ×10 buffer with 15 mM MgCl<sub>2</sub>, 2 µL (Qiagen, Hilden, Germany); dNTPs (2 mM each, Fermentas, Burlington, Canada), 2 µL; all primers (10 mM; Generi Biotech, Hradec Králové, Czech Republic), 1 µL of each; extracted DNA, 2 µL; and H<sub>2</sub>O for a final volume of 20 µL. The cycle parameters were as follows: initial denaturation at 95°C for 5 min, 35 cycles of 95°C for 30 s, 58°C for 30 s, 72°C for 30 s, followed by a final extension at 72°C for 10 min in a T-100 thermocycler (Bio-Rad, Hercules, USA) (Fig. 2). The products were evaluated using a 2.5% agarose gel. Conditions of polymerase chain reaction (PCR) were previously described by Laczmanski et al.<sup>18–20</sup>

*Cdx2*, *ApaI*, *BsmI*, *FokI*, and *TaqI* *VDR* gene polymorphisms were genotyped using SNaPshot reaction according to the producer's protocol (SNaPshot Multiplex Kit; Applied Biosystems, Waltham, USA).

Obtained products were separated using an ABI 310 Genetic Analyzer with GeneScan Analysis v. 3.1.2 software (Applied Biosystems/Thermo Fisher Scientific, Waltham,

**Table 1.** Polymerase chain reaction (PCR) primers designed to amplify fragments harboring the 5 vitamin D receptor (*VDR*) single nucleotide polymorphism (SNP) according to Lins et al.<sup>27</sup>

Single nucleotide polymorphism	PCR primer forward/reverse/ SNaPshot probe sequences	Polymorphism	Size of product [bp]
PCR primer forward/reverse			
<i>ApaI</i> ( <i>rs7975232</i> ) <i>TaqI</i> ( <i>rs731236</i> )	F 5'CTGCCGTTGAGTGCTGTGT	–	242
	R 5'TCGGCTAGCTTCTGGATCAT		
<i>BsmI</i> ( <i>rs1544410</i> )	F 5'CCTCACTGCCCTTAGCTCTG	–	209
	R 5'CCATCTCTCAGGCTCCAAAG		
<i>FokI</i> ( <i>rs2228570</i> )	F 5'GGCCTGCTTGCTTTCTTAC	–	147
	R 5'TCACCTGAAGAAGCCTTTGC		
<i>Cdx2</i> ( <i>rs11568820</i> )	F 5'CATTGTAGAACATCTTTGTATCAGGA	–	224
	R 5'GACAAAAAGGATCAGGGATGA		
SNaPshot probe sequences			
<i>rs7975232</i>	(T) <sub>12</sub> GTGGTGGGATTGAGCAGTGAGG	G/T	34
<i>rs1544410</i>	(T) <sub>21</sub> CAGAGCCTGAGTATTGGGAATG	C/T	43
<i>rs2228570</i>	(T) <sub>31</sub> GCTGGCCGCCATTGCCTCC	A/G	50
<i>rs731236</i>	(T) <sub>9</sub> GCGGTCCTGGATGGCCTC	A/G	27

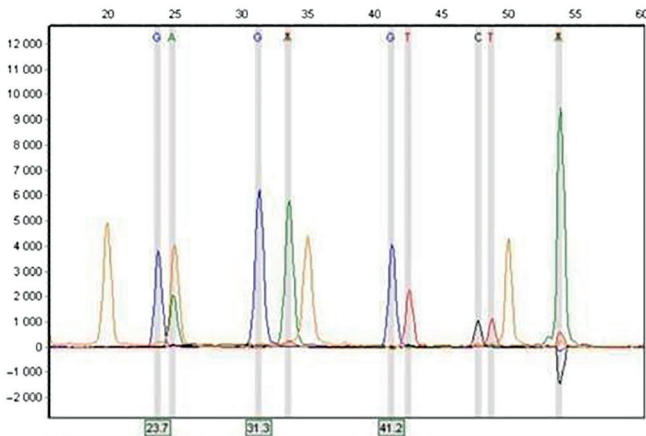


Fig. 2. Capillary electrophoresis

USA), Matrix Standard Set DS-02 for dye set E5 and the GeneScan™ 120 LIZ™ dye Size Standard (Applied Biosystems/Thermo Fisher Scientific) for 15 min. The results were analyzed using GeneMarker v. 1.85 software (SoftGenetics LLC, State College, USA).

## Statistical analyses

The statistical analysis was carried out using Statistica v. 13.3 software (TIBCO Software Inc., Palo Alto, USA). Allele frequencies were assessed by gene counting, and the distribution of the polymorphic variants was tested against the Hardy–Weinberg equilibrium (HWE). The HWE was analyzed using the  $\chi^2$  test. As the data include only 2 options (yes/no), the results are presented in multiway tables (contingency) in the form of cardinality (n) and a structure index (%). The  $\chi^2$  tests of independence were used to assess the significance of the relationship between the occurrence of malocclusions and variants of genotypes, and in the case of 4-field tables (2×2), when the numbers expected in one of the cells were lower than 5, Fisher's exact test was used.

We intend to recruit 113 participants. The sample size calculation was based on the study report by Mozaffari-Khosravi et al.<sup>28</sup> and Föcker et al.,<sup>29</sup> where VD differences and influence were measured. Score points were used as input for the sample size calculation, which yielded a final sample size of 81 participants (t-test,  $\alpha = 0.05$ ; powered at 80% to detect a true difference). Attrition was assumed to be 20%, demanding the recruitment of 100 participants. Tests for deviations from the HWE were separately performed using  $\chi^2$  distribution for each SNP. Bonferroni correction to multiple testing was done.

The study was conducted according to the guidelines of the Declaration of Helsinki, and the Bioethics Committee's approval was obtained (approval No. KB-442/2017 by the Bioethics Committee of Wrocław Medical University). We used the STrengthening the Reporting of OBservational studies in Epidemiology (STROBE) cross-sectional checklist when writing our study.

## Results

The analysis included 113 patients (52 men and 61 women) aged 18–62 years (mean  $36.5 \pm 11.8$  years), who voluntarily completed their medical interview, participated in a clinical trial and donated a blood sample for laboratory tests.

The profile of the examined people can be described as generally healthy people, with a relatively high quality of life. Accompanying systemic diseases in examined group was only 13.2% (autoimmune – 13.2%, gastrointestinal – 8.8%, cardiovascular – 4.4%, metabolic – 0.9%).

The Hardy–Weinberg law of frequencies of *rs11568820*, *rs731236*, *rs7975232*, *rs1544410*, and *rs2228570* polymorphism genotypes in the population was checked. The distribution of genotypes of all these 5 polymorphisms did not deviate from equilibrium.

## Malocclusion anomalies

For most of the patients, Angle's and canine 1<sup>st</sup> class anomalies were diagnosed (right side 49.1%, left side 46.5%, right side 66.7%, left side 67.5%, respectively). Concerning the teeth's position, the teeth were crowded in the mandible (n = 47, 41.6%) and the maxilla (n = 32, 28.3%). The reduction of the upper arch (n = 43, 38.1%) and changes in overbite (n = 29, 25.7%) were relatively frequent. Other irregularities were diagnosed less frequently. The frequency of occurrence of particular defects (in detail) in the studied population is presented in Table 2.

### *Cdx2* (*rs11568820*)

Patients with the T allele present were over 4 times more likely to develop a narrower upper arch than those without this allele (OR = 4.4). Also, patients with a T allele present were over 16 times more likely to develop shortened upper arches (OR = 16.3) (Table 3).

### *FokI* (*rs2228570*)

At the significance level of  $\alpha = 0.05$ , there is no basis to reject the null hypothesis that the *FokI* genotype contributes to the occurrence of a widened lower arch. However, a  $p = 0.0842$  may indicate a certain tendency of dependence on the influence of the polymorphic form of AA on the more frequent occurrence of a widened lower arch (Table 4).

### *BsmI* (*rs1544410*)

At the significance level of  $\alpha = 0.05$ , there is no basis to reject the null hypothesis that the *BsmI* genotype affects the occurrence of widened lower arches. However, a  $p = 0.0738$  may indicate a tendency for the influence of the polymorphic form of CC on the more frequent occurrence of this malocclusion. At the significance level of  $\alpha = 0.05$ , there is no basis to reject the null hypothesis that the *BsmI* genotype affects the occurrence degrees of freedom (df) widened upper

**Table 2.** The frequency of occurrence of particular defects (detailed) in the studied population

Type of malocclusion anomalies		Presence of a defect	
		yes n (%)	no n (%)
Upper arch	narrowed	31 (27.4)	82 (72.6)
	widened	3 (2.65)	110 (97.35)
	shortened	3 (2.65)	110 (97.35)
	spaced	15 (13.3)	98 (86.7)
Lower arch	narrowed	14 (12.4)	99 (87.6)
	widened	6 (5.3)	107 (94.7)
	shortened	2 (1.8)	111 (98.2)
	spaced	6 (5.3)	107 (94.7)
Crowding	maxilla	32 (28.3)	81 (71.7)
	mandible	47 (41.6)	66 (58.4)
Distocclusions	class II	10 (8.8)	103 (91.2)
	retrognathia	16 (14.15)	97 (85.85)
Tête-à-tête	–	8 (7.1)	(92.9)
Mesioclusionion	class III	4 (3.5)	(96.5)
	prognathism	5 (4.4)	(95.6)
Vertical malocclusions	anterior open bite	3 (2.65)	(97.35)
	lateral open bite	1 (0.9)	(99.1)
	deep bite	22 (19.5)	(80.5)
Transverse malocclusions	buccal crossbite	18 (15.9)	(84.1)
	lingual crossbite	2 (1.8)	(98.2)

n – number of people.

**Table 3.** Malocclusion depending on the variants of the *Cdx2* (*rs11568820*) genotype. Test result (p) and the odds ratio (OR); df = 1

Genotype	Upper arch-narrowed		Pearson's $\chi^2$ test	p-value	OR (95% CI)	Upper arch-shortened		Pearson's $\chi^2$ test	p-value	OR (95% CI)
	no	yes				no	yes			
CC	76 (76.8%)	23 (23.2%)	7.085	0.0078	1.00 (ref.)	98 (99.0%)	1 (1.0%)	8.364	0.0038	1.00 (ref.)
TC	6 (42.9%)	8 (57.1%)			4.4 (1.38–14.01)	12 (85.7%)	12 (14.3%)			16.3 (1.38–193.9)

95% CI – 95% confidence interval

**Table 4.** Malocclusion depending on the variants of the *FokI* (*rs2228570*) genotype. Test result (p); degrees of freedom (df) = 2

Genotype	Lower arch-widened		Pearson's $\chi^2$ test	p-value
	no	yes		
GG	31 (96.88%)	1 (3.13%)	4.948	0.0842
AG	49 (98.00%)	1 (2.00%)		
AA	27 (87.10%)	4 (12.90%)		

arches. However,  $p = 0.0816$  may indicate a certain tendency. The fact that in the study group, the CC genotype does not occur in people with a widened upper arch is probably significant. The fact is that people with a widened upper arch are poorly represented (only 3) (Table 5).

No statistically significant correlations were found between the occurrence of other malocclusions and the previously described polymorphisms.

**Table 5.** Malocclusion depending on the variants of the *BsmI* (*rs1544410*) genotype. Test result (p); degrees of freedom (df) = 2

Genotype	Lower arch-spaced		Pearson's $\chi^2$ test	p-value	Lower arch-widened		Pearson's $\chi^2$ test	p-value
	no	yes			no	yes		
TT	20 (100.00%)	0 (0.00%)	5.212	0.0738	18 (90.00%)	2 (10.00%)	5.011	0.0816
CT	43 (97.73%)	1 (2.27%)			43 (97.73%)	1 (2.27%)		
CC	37 (88.10%)	5 (11.90%)			42 (100.00%)	0 (0.00%)		



### *TaqI* (rs731236) and *Apal* (rs7975232)

At the significance level of  $\alpha = 0.05$ , there was no significant difference in the genotype distribution or the allele frequencies of *VDR TaqI* and *Apal* (rs7975232) between patients with analyzed dental anomalies and controls.

## Discussion

Based on the analysis of articles available in the PubMed database, it was determined that this is the first study to investigate the association between the *VDR* polymorphisms *Cdx2* (rs11658820), *TaqI* (rs7975232), *BsmI* (rs1544410), *Apal* (rs7975232) and *FokI* (rs2228570), and the occurrence of dental malocclusion. For this reason, it is not possible to compare the results obtained with other similar analyses. The commonly known factors that influence the development of dental malocclusions may not be considered modifiable. By understanding the negative impact of parafunctions, one can try to prevent them, thus reducing the risk of occlusal anomalies.

In our previous analysis, we wanted to determine whether VD deficiency could promote the development of dental malocclusion. We studied a group of 113 patients. Vitamin D3 deficiency was found in about ¾ of the study participants. This study showed that VD3 deficiency could be one of the significant factors affecting the development of the jaw. The patients had a higher risk of a narrowed (OR = 4.4) and shortened arch (OR = 16.3). Thus, there was a correlation between the deficiency of this hormone and the underdevelopment of the maxilla. The analysis showed that patients largely do not supplement this hormone, and if they do, it is in a dosage that is too low.<sup>29</sup> In another publication, the relationship between a low level of VD and the narrowing of the upper dental arch, crowding and crossbite was demonstrated. It can be concluded that there is a connection between this hormone deficiency and the underdevelopment of the upper jaw.<sup>30</sup>

The rs11658820 polymorphism is located upstream in the 5' UTR of the gene and significantly alters the transcriptional activity of the promoter region of *VDR*. The rs2228570 polymorphism is located in promoter region 5' of exon 2 and causes the synthesis of a longer protein, which is not so effective as a transcriptional activator of *VDR*. The rs1544410 polymorphism is located in the last intron. The rs7975232 polymorphism is also located in the last intron and affects stability of mRNA and translational activity of *VDR* while rs731236 polymorphism (located in exon 9) leads to silent codon generation.<sup>31</sup>

*VDR* polymorphisms are mostly investigated with their effects on systemic diseases such as multiple sclerosis,<sup>32</sup> allergic diseases<sup>33</sup> and malignancies.<sup>20,34,35</sup> With regard to bone metabolism and related diseases, the main search is for associations with the risk of developing osteoporosis

and low bone mineral density. A recent meta-analysis showed that *VDR BsmI* genotype is associated with increased risk of postmenopausal osteoporosis in Caucasians but not in Asians. Thus, the authors demonstrated the differences arising from race in the populations studied. Recently, the study of VD and its receptor has been gaining importance, including in the craniofacial field. Yildiz et al.<sup>36</sup> investigated the possible association between the *VDR-BsmI* variant and susceptibility to temporomandibular joint disorders (dislocation with reduction (DDR) and VD) in a group of 114 Turkish patients. Vitamin D levels were significantly different between patients and controls. They found that VD levels were significantly lower in the DDR patients. Interestingly, their study showed that *VDR* genotype distributions were different in the 2 groups regarding the *BsmI* variant. There was a statistically significant difference between the 2 studied groups regarding genotype distribution and allele frequency, people with bb genotypes, and B alleles. They concluded that the *VDR BsmI* BB genotype was increased in the controls compared to DDR patients, and homozygous individuals with BB genotypes had a 2.03-fold higher protective role against developing DDR.<sup>36</sup>

Dental research pays attention to the importance of the *VDR* gene in various types of cancer (including head and neck cancers). It is believed that polymorphisms in *VDR* gene may influence both prognosis and the risk and incidence of cancer.<sup>37</sup> Studies by Małodoba-Mazur et al.<sup>38</sup> indicated a genetic link between the occurrence of oral cancer and rs2238135 in the *VDR* gene<sup>38,39</sup> compared with healthy patients. The *VDR* Tt genotype has been shown to be significantly more common for patients with oral squamous cell carcinoma (OSCC) than in those with other genotypes. Women, in particular, were at increased risk of this malignancy. Studies indicate that the *VDR TaqI* polymorphism may be related to the susceptibility of OSCC. Moreover, genetic polymorphisms in the *VDRs* and genes involved in VD metabolism, such as *CYP24B1* and *CYP27B1*, may influence susceptibility to OSCC. Zeljic et al.<sup>40</sup> showed that the polymorphism of the *CYP24A1* gene might influence the susceptibility to the development of oral cancers, and the polymorphism of the *FokI VDR* gene may be considered a prognostic factor, as it has been shown to be associated with mortality.<sup>40</sup>

Analyses were also conducted regarding the relationship between *VDR* and the risk of caries. The results were inconclusive, although not excluding the existence of such an impact.<sup>41,42</sup> Available research is often conducted on periodontitis, whose etiology is known to be multifactorial, with a significant genetic role. This disease results in the progressive loss of alveolar bone, inevitably leading to the loss of support for the teeth and, consequently, tooth loss. Susceptibility to this pathology is analyzed in various aspects, including *VDR* polymorphisms. Although the meta-analysis by Wan et al. did not show the association of the *Apal* polymorphism with the development



of periodontal disease in either Caucasian or Asian patients, the authors found a link between this disease entity and the *FokI* and *BsmI* polymorphisms in both ethnic groups. Additionally, *FokI* has been associated with susceptibility to aggressive periodontitis in the Chinese population. *TaqI*, on the other hand, has an impact on periodontal disease in the Caucasian population.<sup>22</sup>

Our prospective study similarly showed a significant effect of *Cdx2* and the possible tendency of *FokI* and *BsmI* on jaw development. Our results show an association between VD and jaw growth, especially maxillary underdevelopment. Therefore, conclusions can be drawn that the reduction in VD leads to a reduced size of the jaw.

Recently, other aspects of the hormone in question have also been indicated. Vitamin D also plays an important role in the healing and osseointegration of implants. It was found that the first period after implant surgery crucially depends on the role of this hormone in the induction of anti-inflammatory cytokines and a reduction in the level of proinflammatory cytokines, thus reducing the body's response to surgical intervention. Moreover, it affects the processes of activation and differentiation of osteoblasts and osteoclasts, increasing osteoid mineralization. These mechanisms are also important in the later period – after loading the implant with a prosthetic crown.<sup>43</sup> Another study found that adequate levels of 25-hydroxycholecalciferol on the day of surgery and VD deficiency treatment significantly increase bone levels at the implant site in the process of radiologically assessed osseointegration.<sup>44</sup>









## Limitations

This was the first in a series of prospective studies to initially determine whether there were relationships between the development of malocclusions and specific *VDR* polymorphisms. Due to the complexity of the planned study definition, including not only clinical evaluation but also laboratory tests, a relatively small group of patients was included in the analysis, but one that allows for a meaningful statistical evaluation. Further similar studies are planned with the participation of a much larger number of people and among different patient groups focused especially on the analysis of those relationships for which certain tendencies have been demonstrated.

## Conclusions

For some of the analyzed SNPs, real trends and an increased risk of development of anomalies and malocclusion were shown. The limitation of this study is the relatively small number of samples. The analysis of a larger population may identify other significant relations. Due to the demonstration of racial differences, it is worth considering conducting such studies among representatives of the Caucasian race and various other ethnic groups.

## ORCID iDs

Marzena Dominiak  <https://orcid.org/0000-0001-8943-0549>  
 Anna Leszczyszyn  <https://orcid.org/0000-0001-7853-2814>  
 Izabela Łaczmajska  <https://orcid.org/0000-0003-2458-5755>  
 Monika Machoy  <https://orcid.org/0000-0001-5787-222X>  
 Hanna Gerber  <https://orcid.org/0000-0002-0954-3955>  
 Joseph Choukroun  <https://orcid.org/0000-0002-4466-5149>  
 Tomasz Gedrange  <https://orcid.org/0000-0002-3551-6467>  
 Sylwia Hnitecka  <https://orcid.org/0000-0002-1171-9817>

## References

- Rapeepattana S, Thearmontree A, Suntornlohanakul S. Etiology of malocclusion and dominant orthodontic problems in mixed dentition: A cross-sectional study in a group of Thai children aged 8–9 years. *J Int Soc Prevent Community Dent.* 2019;9(4):383. doi:10.4103/jispcd.JISPCD\_120\_19
- Proffit WR. *Contemporary Orthodontics.* 6<sup>th</sup> ed. Philadelphia, USA: Elsevier; 2018. ISBN:978-0-323-54387-3.
- Fanghänel J, Gedrange T. On the development, morphology and function of the temporomandibular joint in the light of the orofacial system. *Ann Anat.* 2007;189(4):314–319. doi:10.1016/j.aanat.2007.02.024
- Weingärtner J, Maile S, Fanghänel J, Proff P, Gedrange T. Growth-related changes of parameters of the methylation cycle and jejunal aminopeptidase M in the rat. *Exp Toxicol Pathol.* 2008;59(5):291–295. doi:10.1016/j.etp.2007.09.004
- Øgaard B, Larsson E, Lindsten R. The effect of sucking habits, cohort, sex, intercanine arch widths, and breast or bottle feeding on posterior crossbite in Norwegian and Swedish 3-year-old children. *Am J Orthod Dentofacial Orthop.* 1994;106(2):161–166. doi:10.1016/S0889-5406(94)70034-6
- Fanghänel J, Gedrange T, Proff P. The face-physiognomic expressiveness and human identity. *Ann Anat.* 2006;188(3):261–266. doi:10.1016/j.aanat.2005.11.013
- Krawiec M, Dominiak M. The role of vitamin D in the human body with a special emphasis on dental issues: Literature review. *Dent Med Probl.* 2018;55(4):419–424. doi:10.17219/dmp/99051
- Krawiec M, Dominiak M. Prospective evaluation of vitamin D levels in dental treated patients: A screening study. *Dent Med Probl.* 2021; 58(3):321–326. doi:10.17219/dmp/134911
- Weingärtner J, Lotz K, Fanghänel J, Gedrange T, Bienengraber V, Proff P. Induction and prevention of cleft lip, alveolus and palate and neural tube defects with special consideration of B vitamins and the methylation cycle. *J Orofac Orthop.* 2007;68(4):266–277. doi:10.1007/s00056-007-0701-6
- Weingärtner J, Maile S, Proff P, et al. Secondary palatal closure in rats in association with relative maternofetal levels of folic acid, vitamin B12, and homocysteine. *Ann Anat.* 2007;189(3):229–233. doi:10.1016/j.aanat.2006.10.006
- Weingartner J, Proff P, Fanghanel J, et al. Different bone sensitivity to malformations induced by procarbazine in fetal rats. *J Physiol Pharmacol.* 2008;59(Suppl 5):17–25. PMID:19075321.
- Suh KT, Eun IS, Lee JS. Polymorphism in vitamin D receptor is associated with bone mineral density in patients with adolescent idiopathic scoliosis. *Eur Spine J.* 2010;19(9):1545–1550. doi:10.1007/s00586-010-1385-y
- El Jilani MM, Mohamed AA, Zeglam HB, et al. Association between vitamin D receptor gene polymorphisms and chronic periodontitis among Libyans. *Libyan J Med.* 2015;10(1):26771. doi:10.3402/ljm.v10.26771
- Imani D, Razi B, Motallebnezhad M, Rezaei R. Association between vitamin D receptor (VDR) polymorphisms and the risk of multiple sclerosis (MS): An updated meta-analysis. *BMC Neurol.* 2019;19(1):339. doi:10.1186/s12883-019-1577-y
- Ho YP, Lin YC, Yang YH, et al. Association of vitamin D receptor gene polymorphisms and periodontitis in a Taiwanese Han population. *J Dent Sci.* 2017;12(4):360–367. doi:10.1016/j.jds.2017.07.001
- Gasperini B, Visconti VV, Ciccacci C, et al. Role of the vitamin D receptor (VDR) in the pathogenesis of osteoporosis: A genetic, epigenetic and molecular pilot study. *Genes.* 2023;14(3):542. doi:10.3390/genes14030542
- Rojo-Tolosa S, Márquez-Pete N, Gálvez-Navas JM, et al. Single nucleotide polymorphisms in the vitamin D metabolic pathway and their relationship with high blood pressure risk. *Int J Mol Sci.* 2023; 24(6):5974. doi:10.3390/ijms24065974

18. Laczmanska I, Laczmanski L, Bebenek M, et al. Vitamin D receptor gene polymorphisms in relation to the risk of colorectal cancer in the Polish population. *Tumor Biol.* 2014;35(12):12397–12401. doi:10.1007/s13277-014-2554-0
19. Laczmanski L, Milewicz A, Puzianowska-Kuznicka M, et al. Interrelation between genotypes of the vitamin D receptor gene and serum sex hormone concentrations in the Polish elderly population: The PolSenior study. *Exp Gerontol.* 2014;57:188–190. doi:10.1016/j.exger.2014.06.007
20. Laczmanski L, Lwow F, Mossakowska M, et al. Association between vitamin D concentration and levels of sex hormones in an elderly Polish population with different genotypes of VDR polymorphisms (rs10735810, rs1544410, rs7975232, rs731236). *Gene.* 2015;559(1):73–76. doi:10.1016/j.gene.2015.01.022
21. Murthykumar K, Arjunker R, Jayaseelan VP. Association of vitamin D receptor gene polymorphism (rs10735810) and chronic periodontitis. *J Invest Clin Dent.* 2019;10(4):e12440. doi:10.1111/jicd.12440
22. Wan QS, Li L, Yang SK, Liu ZL, Song N. Role of vitamin D receptor gene polymorphisms on the susceptibility to periodontitis: A meta-analysis of a controversial issue. *Genet Test Mol Biomarkers.* 2019;23(9):618–633. doi:10.1089/gtmb.2019.0021
23. Joondeph DR, Riedel RA, Moore AW. Pont's index: A clinical evaluation. *Angle Orthod.* 1970;40(2):112–118. doi:10.1043/0003-3219(1970)040<0112:PIACE>2.0.CO;2
24. Korkhaus G. Present orthodontic thought in Germany. *Am J Orthod.* 1960;46(4):270–287. doi:10.1016/0002-9416(60)90195-0
25. Popovich F, Thompson GW. Craniofacial templates for orthodontic case analysis. *Am J Orthod.* 1977;71(4):406–420. doi:10.1016/0002-9416(77)90244-5
26. Nakhl S, Sleilaty G, Chouery E, Salem N, Chahine R, Farès N. Fokl vitamin D receptor gene polymorphism and serum 25-hydroxyvitamin D in patients with cardiovascular risk. *Arch Med Sci Atheroscler Dis.* 2019;4(1):298–303. doi:10.5114/amsad.2019.91437
27. Lins TCL, Nogueira LR, Lima RM, Gentil P, Oliveira RJ, Pereira RW. A multiplex single-base extension protocol for genotyping Cdx2, Fokl, BsmI, Apal, and TaqI polymorphisms of the vitamin D receptor gene. *Genet Mol Res.* 2007;6(2):316–324. PMID:17573662.
28. Mozaffari-Khosravi H, Nabizade L, Yassini-Ardakani SM, Hadinedoushan H, Barzegar K. The effect of 2 different single injections of high dose of vitamin D on improving the depression in depressed patients with vitamin D deficiency: A randomized clinical trial. *J Clin Psychopharmacol.* 2013;33(3):378–385. doi:10.1097/JCP.0b013e31828f619a
29. Föcker M, Antel J, Grasmann C, et al. Effect of an vitamin D deficiency on depressive symptoms in child and adolescent psychiatric patients. A randomized controlled trial: Study protocol. *BMC Psychiatry.* 2018;18(1):57. doi:10.1186/s12888-018-1637-7
30. Leszczyszyn A, Hnitecka S, Dominiak M. Could vitamin D3 deficiency influence malocclusion development? *Nutrients.* 2021;13(6):2122. doi:10.3390/nu13062122
31. Yesil S, Tanyildiz HG, Tekgunduz SA, et al. Vitamin D receptor polymorphisms in immune thrombocytopenic purpura. *Pediatrics International.* 2017;59(6):682–685. doi:10.1111/ped.13273
32. Liao JL, Qin Q, Zhou YS, et al. Vitamin D receptor Bsm I polymorphism and osteoporosis risk in postmenopausal women: A meta-analysis from 42 studies. *Genes Nutr.* 2020;15(1):20. doi:10.1186/s12263-020-00679-9
33. Gnagnarella P, Raimondi S, Aristarco V, et al. Vitamin D receptor polymorphisms and cancer. In: Reichrath J, ed. *Sunlight, Vitamin D and Skin Cancer.* Vol. 1268. Advances in Experimental Medicine and Biology. Cham, Switzerland: Springer International Publishing; 2020:53–114. doi:10.1007/978-3-030-46227-7\_4
34. Zhang L, Zhang S, He C, Wang X. VDR gene polymorphisms and allergic diseases: Evidence from a meta-analysis. *Immunol Invest.* 2020;49(1-2):166–177. doi:10.1080/08820139.2019.1674325
35. Shaikh F, Baig S, Jamal Q. Do VDR gene polymorphisms contribute to breast cancer? *Asian Pac J Cancer Prev.* 2016;17(2):479–483. doi:10.7314/APJCP.2016.17.2.479
36. Yildiz S, Tümer MK, Yigit S, Nursal AF, Rustemoglu A, Balel Y. Relation of vitamin D and BsmI variant with temporomandibular diseases in the Turkish population. *Br J Oral Maxillofac Surg.* 2021;59(5):555–560. doi:10.1016/j.bjoms.2020.08.101
37. Fathi N, Ahmadian E, Shahi S, et al. Role of vitamin D and vitamin D receptor (VDR) in oral cancer. *Biomed Pharmacother.* 2019;109:391–401. doi:10.1016/j.biopha.2018.10.102
38. Małodobra-Mazur M, Paduch A, Lebioda A, et al. VDR gene single nucleotide polymorphisms and their association with risk of oral cavity carcinoma. *Acta Biochim Pol.* 2012;59(4):627–630. PMID:23189278.
39. Khammissa RAG, Fourie J, Motswaledi MH, Ballyram R, Lemmer J, Feller L. The biological activities of vitamin D and its receptor in relation to calcium and bone homeostasis, cancer, immune and cardiovascular systems, skin biology, and oral health. *Biomed Res Int.* 2018;2018:9276380. doi:10.1155/2018/9276380
40. Zeljic K, Jovanovic I, Jovanovic J, Magic Z, Stankovic A, Supic G. MicroRNA meta-signature of oral cancer: Evidence from a meta-analysis. *Ups J Med Sci.* 2018;123(1):43–49. doi:10.1080/03009734.2018.1439551
41. Cogulu D, Onay H, Ozdemir Y, Aslan GI, Ozkinay F, Eronat C. The role of vitamin D receptor polymorphisms on dental caries. *J Clin Pediatr Dent.* 2016;40(3):211–214. doi:10.17796/1053-4628-40.3.211
42. Barbosa MCF, Lima DC, Reis CLB, et al. Vitamin D receptor FokI and BgII genetic polymorphisms, dental caries, and gingivitis. *Int J Paediatr Dent.* 2020;30(5):642–649. doi:10.1111/ipd.12631
43. Trybek G, Aniko-Włodarczyk M, Kwiatek J, et al. The effect of vitamin D3 on the osteointegration of dental implant. *Baltic J Health Phys Act.* 2018;15(7):25–33. doi:10.29359/BJHPA.10.4.02
44. Kwiatek J, Jaroń A, Trybek G. Impact of the 25-hydroxycholecalciferol concentration and vitamin D deficiency treatment on changes in the bone level at the implant site during the process of osseointegration: A prospective, randomized, controlled clinical trial. *J Clin Med.* 2021;10(3):526. doi:10.3390/jcm10030526

# Effects of myostatin gene knockout on white fat browning and related gene expression in type 2 diabetic mice

Jingwei Cheng<sup>1,2,A</sup>, Jaewoo Lee<sup>3,B</sup>, Yangqing Liu<sup>4,D</sup>, Yanfang Wang<sup>5,F</sup>, Mingtao Duan<sup>2,C</sup>, Zhen Zeng<sup>6,E</sup>

<sup>1</sup> School of Physical Education, Henan University, Kaifeng, China

<sup>2</sup> School of Sports Science, Kyonggi University, Suwon, South Korea

<sup>3</sup> Graduate School, Kyonggi University, Suwon, South Korea

<sup>4</sup> Department of Editing, Henan Provincial People's Hospital, Zhengzhou University People's Hospital, China

<sup>5</sup> Department of Endocrinology, Henan Provincial People's Hospital, Zhengzhou University People's Hospital, China

<sup>6</sup> Graduate School, Kyonggi University, Suwon, South Korea

A – research concept and design; B – collection and/or assembly of data; C – data analysis and interpretation; D – writing the article; E – critical revision of the article; F – final approval of the article

Advances in Clinical and Experimental Medicine, ISSN 1899–5276 (print), ISSN 2451–2680 (online)

Adv Clin Exp Med. 2024;33(6):609–617

## Address for correspondence

Yanfang Wang

E-mail: 1028476711@qq.com

## Funding sources

None declared

## Conflict of interest

None declared

## Acknowledgements

We would like to thank Editage ([www.editage.co.kr](http://www.editage.co.kr)) for English-language editing.

Received on April 21, 2022

Reviewed on May 7, 2023

Accepted on August 16, 2023

Published online on October 13, 2023

## Cite as

Cheng J, Lee J, Liu Y, Wang Y, Duan M, Zeng Z. Effects of myostatin gene knockout on white fat browning and related gene expression in type 2 diabetic mice. *Adv Clin Exp Med*. 2024;33(6):609–617. doi:10.17219/acem/171300

## DOI

10.17219/acem/171300

## Copyright

Copyright by Author(s)

This is an article distributed under the terms of the Creative Commons Attribution 3.0 Unported (CC BY 3.0) (<https://creativecommons.org/licenses/by/3.0/>)

## Abstract

**Background.** Myostatin (Mstn) plays an important role in adipocyte growth, differentiation and metabolism, leading to the development of obesity.

**Objectives.** We aimed to explore the effect of Mstn on white fat browning in a mouse model of type 2 diabetes mellitus (T2DM).

**Materials and methods.** Twelve wild-type (WT), 12 heterozygous (Mstn(+/-)) and 12 homozygous (Mstn(-/-)) male mice were randomly divided into 6 groups: WT, Mstn(+/-), Mstn(-/-), WT+DM, Mstn(+/-)+DM, and Mstn(-/-)+DM. The first 3 groups were fed normal chow, while the last 3 were fed high-fat diet and administered streptozotocin to generate T2DM. Subsequently, body mass, length, and white and brown fat masses were measured, after which Lee's index, white–brown ratio and fat index were calculated. The serum free fatty acid (FFA) levels were detected using enzyme-linked immunosorbent assay (ELISA). Hematoxylin and eosin (H&E) staining was used to analyze white and brown fat cell morphology. The relative expression levels of peroxisome proliferator-activated receptor-gamma (PPAR $\gamma$ ), peroxisome proliferator-activated receptor-gamma coactivator-1 alpha (PGC-1 $\alpha$ ), uncoupling protein 1 (UCP1), and cluster of differentiation 137 (CD137) protein were determined with western blotting.

**Results.** The Mstn(-/-) group displayed higher levels of PPAR $\gamma$ , PGC-1 $\alpha$  and CD137 proteins in white and brown fat compared to the WT and Mstn(+/-) groups, while the expression level of UCP1 protein in the Mstn(-/-) group was higher than in the WT group. The expression levels of PPAR $\gamma$ , PGC-1 $\alpha$ , UCP1, and CD137 proteins in the WT+DM group were lower than in the WT group. Moreover, PPAR $\gamma$ , PGC-1 $\alpha$ , UCP1, and CD137 proteins were more highly expressed in the Mstn(-/-)+DM group compared to the WT+DM and Mstn(+/-)+DM groups.

**Conclusions.** The *Mstn* gene inhibition antagonizes obesity phenotypes, such as white fat accumulation and lipid metabolism derangement caused by T2DM, thus promoting white fat browning.

**Key words:** diabetes mellitus type 2, obesity, mice, myostatin, brown adipose tissue

## Background

Skeletal muscle, brown fat and white fat significantly contribute to maintaining the body's energy balance, consuming energy through muscle fiber contraction, as well as non-shivering thermogenesis and energy storage, respectively. However, white fat can be converted into brown fat under certain conditions to ameliorate obesity. In type 2 diabetes mellitus (T2DM), energy metabolism is unbalanced, skeletal muscle decreases, white fat increases, and sarcopenic obesity arises. Therefore, increasing skeletal muscle and promoting the browning of white fat is beneficial to treating obesity, T2DM and other metabolic diseases. Skeletal muscle can secrete various myokines, which act as cross-talk messengers between skeletal muscle and fat.<sup>1</sup> Myostatin (*Mstn*), which negatively regulates muscle growth and development, is an important myokine secreted by skeletal muscle.<sup>2</sup> After *Mstn* knockout, mice fed high-fat or regular diet showed decreased fat mass and increased muscle mass,<sup>3</sup> suggesting that *Mstn* can regulate lipid metabolism in T2DM. However, whether *Mstn* can promote the browning of white fat in T2DM remains unclear.

## Objectives

We aimed to observe the expression of a gene associated with white fat browning in diabetic *Mstn* knockout mice and explore the effect of *Mstn* on white fat browning in T2DM mice.

## Materials and methods

### Animals

All animal experiments followed the Animal Research: Reporting of In Vivo Experiments (ARRIVE) guidelines and were performed in accordance with the UK Animal (Scientific Procedures) Act 1986, the relevant guidelines, the EU Directive 2010/63/EU for animal testing, or the management and use guidelines of the National Institute of Health (NIH).

Saiye Biotechnology Co. Ltd. (Guangzhou, China) provided the following 6-week-old male C57BL/6N mice: 12 homozygous *Mstn* knockout (*Mstn*(-/-)) mice, 12 heterozygous *Mstn* knockout (*Mstn*(+/-)) mice and 12 wild-type (WT) mice. Mice were acclimatized for 1 week at an indoor temperature of 22–24°C, 40–60% humidity, and 12-h day and night cycles and were provided with sufficient food and water before the beginning of the study.

### Grouping and modeling

The 12 WT, 12 heterozygous (*Mstn*(+/-)) and 12 homozygous (*Mstn*(-/-)) mice were randomly divided into 2 large groups (control and T2DM groups), which were then divided

into 6 smaller groups (6 animals per group), as follows: WT group, *Mstn*(+/-) group, *Mstn*(-/-) group, WT+DM group, *Mstn*(+/-)+DM group, and *Mstn*(-/-)+DM group. The first 3 groups were fed normal chow, while the remaining 3 groups were fed high-fat diet and a small dose of streptozotocin to generate T2DM models. The WT+DM, *Mstn*(+/-)+DM and *Mstn*(-/-)+DM groups were fed high-fat diet for 6 weeks and injected intraperitoneally with 2% streptozotocin (Sigma-Aldrich, St. Louis, USA) (prepared with sodium citrate buffer) at 50 mg/kg without fasting. Then, 72 h after the streptozotocin injection, and followed by 6-hour fasting, tail vein blood was collected and fasting blood glucose was measured. The criteria for a successful induction of T2DM in the mice were as follows: mice with fasting blood glucose  $\geq 16.7$  mmol/L and the occurrence of polydipsia, polyphagia, polyuria, and weight loss. The WT, *Mstn*(+/-) and *Mstn*(-/-) groups were injected intraperitoneally with equal doses of citrate buffer as the control.

### Measurement of body mass and length

The body mass and length (from the nasal tip to the anus) for each group were measured before and after diabetes induction. Lee's index was calculated and used to assess the degree of obesity in mice, as follows (Equation 1):

$$\text{Lee's index} = \frac{\text{body mass [g]}^{1/3} \times 1000}{\text{body length [cm]}} \quad (1)$$

### Detection of blood lipids

After 6 h of fasting, 0.2 mL of mouse tail vein blood was collected and centrifuged at 3000 rpm for 5 min. The serum was collected to detect the triacylglycerol (TG), total cholesterol (TC), low-density lipoprotein cholesterol (LDL-C), and high-density lipoprotein cholesterol (HDL-C) levels using an automatic biochemical analyzer (AU400; Beckman Coulter, Brea, USA). The serum free fatty acid (FFA) level was detected with the use of an FFA enzyme-linked immunosorbent assay (ELISA) kit (Cloud-Clone, Houston, USA) and a microplate reader (ELx808; BioTeK, Winooski, USA).

### Measurement of white and brown fat mass

The mice were sacrificed by cervical dislocation, after which white adipose (groin, epididymis and mesenteric) and brown adipose (scapula) tissues were quickly dissected and weighed. The white–brown ratio and fat index were calculated as follows (Equation 2 and Equation 3):

$$\text{white–brown ratio} = \frac{\text{white fat mass [g]}}{\text{brown fat mass [g]}} \quad (2)$$

$$\text{fat index} = \frac{(\text{white fat mass} + \text{brown fat mass}) \text{ [g]}}{\text{body mass [g]}} \quad (3)$$



Half of the white adipose tissue in the groin and half of the brown adipose tissue in the scapula were stored in liquid nitrogen, while the other halves were preserved in 4% neutral buffered formalin and embedded in paraffin by a tissue-dehydrating machine (JT-12S; Junjie, Shenzhen, China).

## Hematoxylin and eosin staining and the analysis of adipose tissue

Instruments and reagents for hematoxylin and eosin (H&E) staining and the analysis of adipose tissue are detailed in the Supplementary Materials. Images of adipose tissue sections were viewed under an optical microscope (E100; Nikon Corp., Tokyo, Japan), and the adipose tissue morphology was analyzed using ImageJ software (National Institutes of Health, Bethesda, USA).

## Detection of white fat browning-related gene expression

Western blotting was used to measure the expression levels of the following proteins: peroxisome proliferator-activated receptor gamma (PPAR $\gamma$ ), peroxisome proliferator-activated receptor-gamma coactivator-1 alpha (PGC-1 $\alpha$ ), uncoupling protein 1 (UCP-1), and cluster of differentiation 137 (CD137). Briefly, 50 mg of adipose tissue was treated with protein lysis solution to completely lyse the tissue, which was then centrifuged at 12,000 rpm for 10 min, and the supernatant was collected (Supplementary Materials).

## Detection of Mstn expression in the gastrocnemius muscle and serum

After the mice were sacrificed, the left gastrocnemius muscle was dissected. Western blotting was used to detect the expression level of Mstn in the gastrocnemius using the same procedure as above. The serum Mstn level was detected using Mstn ELISA kit (Cloud-Clone), according to the manufacturer's instructions.

## Statistical analyses

The IBM SPSS v. 22.0 (IBM Corp., Armonk, USA) and GraphPad Prism v. 8.0 (GraphPad Software, San Diego, USA) were utilized to analyze the experimental data and present the results, respectively. A bootstrapped one-way analysis of variance (ANOVA) was used for comparisons among the 6 groups, followed by Tukey's post hoc test. Representative results are shown as mean  $\pm$  standard deviation ( $M \pm SD$ ), and  $p < 0.05$  was considered statistically significant.

# Results

## Indicators of growth and obesity

Lee's index and the white–brown ratio were significantly lower in the Mstn(–/–) group than in the WT and Mstn(+/-) groups ( $p < 0.05$ ). There was no significant difference in the fat index between the Mstn(–/–) group and the WT or Mstn(+/-) groups ( $p > 0.05$ ). Lee's index was lower in the WT+DM group than in the WT group, while the white–brown ratio and fat index were higher in the WT+DM group than in the WT group ( $p < 0.05$ ). The Mstn(–/–)+DM group displayed lower Lee's index and white–brown ratio compared to the WT+DM and Mstn(+/-)+DM groups ( $p < 0.05$ ). The fat index was lower in the Mstn(–/–)+DM group than in the WT+DM group ( $p < 0.05$ ), but it was not significantly different compared with that in the Mstn(+/-)+DM group ( $p > 0.05$ ) (Supplementary Table 1 and Fig. 1).

## Lipid metabolism indicators

The serum TG and TC levels were both lower in the Mstn(–/–) group than in the WT and Mstn(+/-) groups (both  $p < 0.05$ ). Moreover, the LDL-C, HDL-C and FFA levels in the Mstn(–/–) group were not significantly different compared with those in the WT and Mstn(+/-) groups ( $p > 0.05$ ). The TG, TC, LDL-C, and FFA levels were higher in the WT+DM group than in the WT group, while the HDL-C level was lower in the WT+DM group than in the WT group ( $p < 0.05$ ). The TC level was lower in the Mstn(–/–)+DM group than in the WT+DM and Mstn(+/-)+DM groups, while the HDL-C level was higher in the Mstn(–/–)+DM group compared to the WT+DM and Mstn(+/-)+DM groups ( $p < 0.05$ ). The serum TG, LDL-C and FFA levels were lower in the Mstn(–/–)+DM group than in the WT+DM group ( $p < 0.05$ ) and showed no significant difference compared with those in the Mstn(+/-)+DM group ( $p > 0.05$ ) (Supplementary Table 2 and Fig. 2).

## Morphology of white adipocytes

White adipocytes in the WT group displayed a full shape and uniform size. Interestingly, when compared with the WT group, the number of white adipocytes in the Mstn(–/–) group was significantly increased, while the volume was significantly reduced, and they showed an irregular shape. The performance of the Mstn(+/-) group was between that of the WT and Mstn(–/–) groups. Compared with the WT group, the volume of white adipocytes in the WT+DM group was significantly greater, with variable sizes and fused cells. The number of white adipocytes in the Mstn(–/–)+DM group was significantly increased, whereas the size of their white adipocytes was significantly reduced compared to the WT+DM group. As expected, the results for the Mstn(+/-)+DM group were between that of the WT+DM and Mstn(–/–)+DM groups (Fig. 3A).

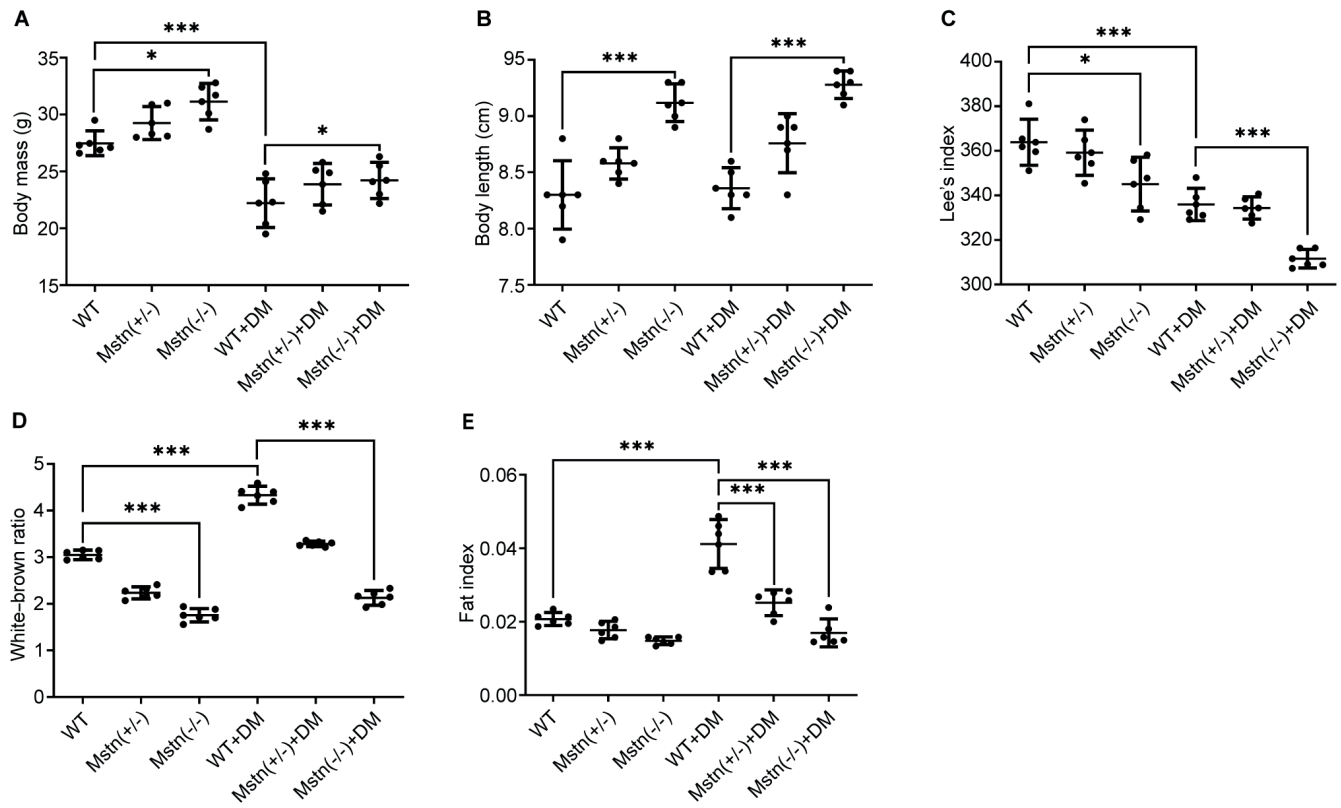


Fig. 1. Indicators of growth and obesity. Body mass (A), body length (B), Lee's index (C), white-brown ratio (D), and fat index (E). Means and 95% confidence intervals (95% CIs) are presented. Bootstrap one-way analysis of variance (ANOVA) was used for comparisons between the 6 groups

\* $p < 0.05$ ; \*\*\* $p < 0.001$ ; DM – diabetes mellitus; WT – wild-type; Mstn – myostatin.

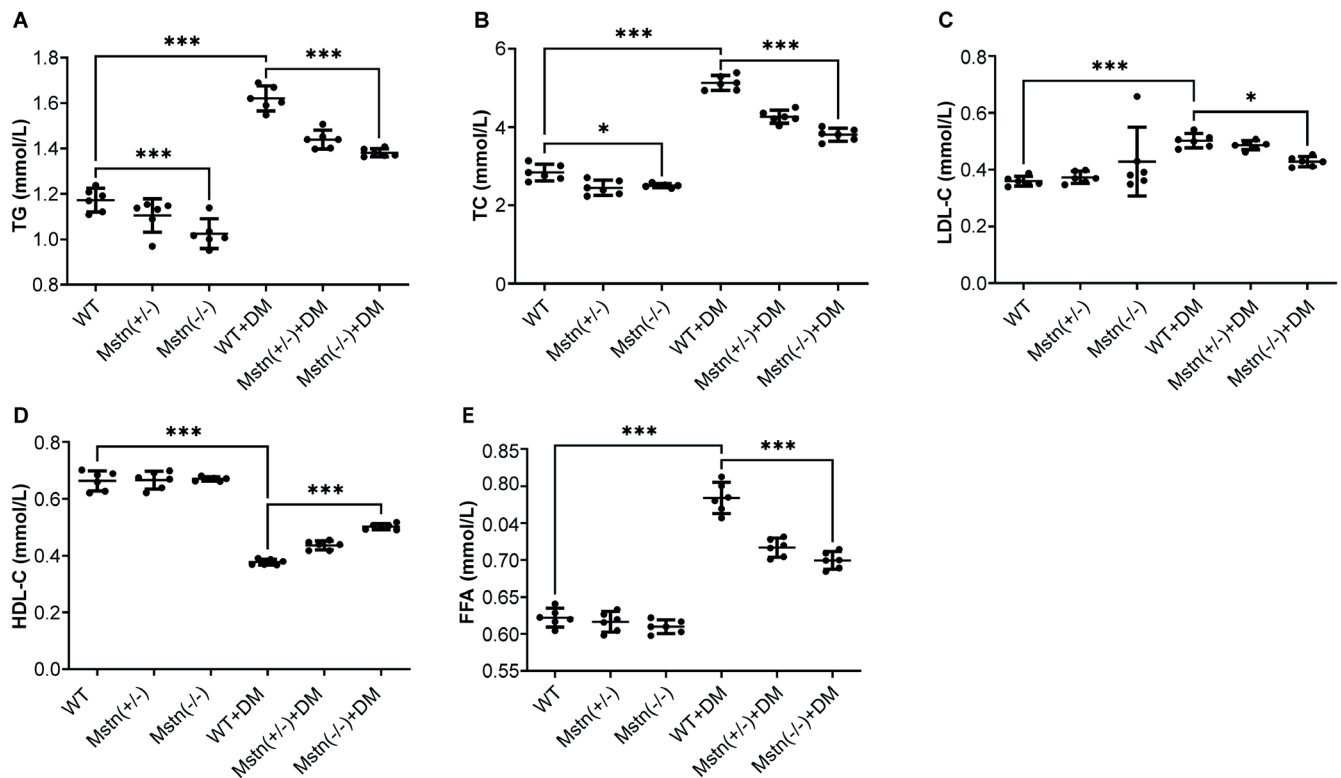


Fig. 2. Lipid metabolism indicators. Triacylglycerol (TG) (A), total cholesterol (TC) (B), low-density lipoprotein cholesterol (LDL-C) (C), high-density lipoprotein cholesterol (HDL-C) (D), and free fatty acid (FFA) (E). Means and 95% confidence intervals (95% CIs) are presented. Bootstrap one-way analysis of variance (ANOVA) was used for comparisons between the 6 groups

\* $p < 0.05$ ; \*\*\* $p < 0.001$ ; DM – diabetes mellitus; WT – wild-type; Mstn – myostatin.



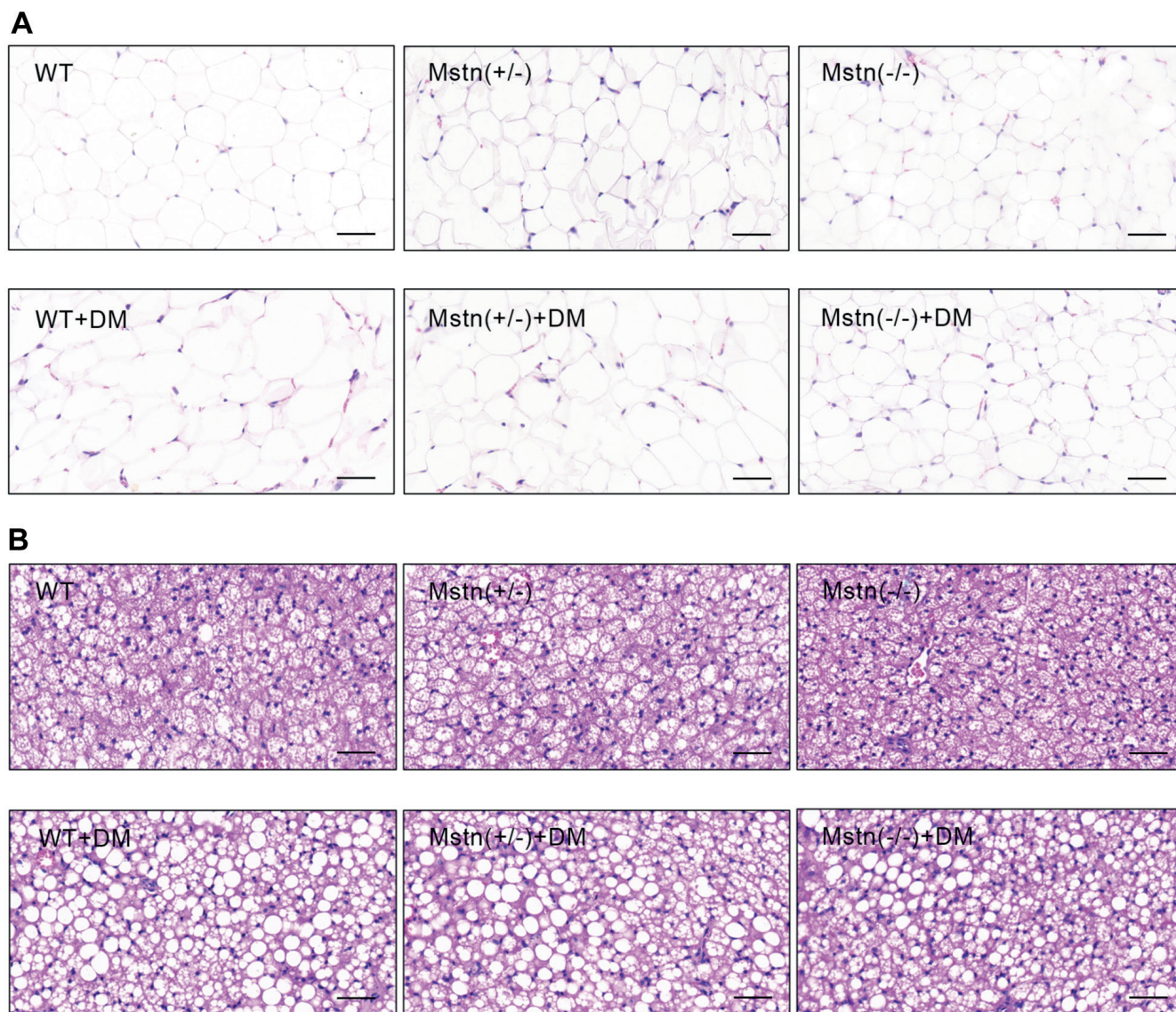


Fig. 3. Hematoxylin and eosin (H&E) staining of white and brown fat (magnification:  $\times 400$ , scale bar: 50  $\mu\text{m}$ ). A. The morphology of white adipocytes; B. The morphology of brown adipocytes

DM – diabetes mellitus; WT – wild-type; Mstn – myostatin.

## Morphology of brown adipocytes

The brown adipocytes in the WT, Mstn(+/-) and Mstn(-/-) groups all showed multilocular morphology, and no single-vesicle adipocytes were observed. When compared to the WT and Mstn(+/-) groups, the Mstn(-/-) group showed a more dense distribution of brown adipocytes. In the WT+DM group, many single-vesicle adipocytes were present among the multilocular brown adipocytes, and there was a circular lipid droplet in the center of each cell. In the Mstn(-/-)+DM group, multilocular brown adipocytes were distributed among the single-vesicle adipocytes, the number of which was significantly reduced, and the volume of lipid droplets was significantly decreased compared with the WT+DM group. As expected, the results for the Mstn(+/-)+DM group were between those of the WT+DM and Mstn(-/-)+DM groups (Fig. 3B).

## Expression levels of PPAR $\gamma$ , PGC-1 $\alpha$ , UCP1, and CD137 protein in white and brown fat

The expression levels of PPAR $\gamma$ , PGC-1 $\alpha$  and CD137 proteins in white and brown fat in the Mstn(-/-) group were higher than those in the WT and Mstn(+/-) groups ( $p < 0.05$ ). The UCP1 protein in white and brown fat demonstrated higher expression in the Mstn(-/-) group compared to the WT group ( $p < 0.05$ ). The PPAR $\gamma$ , PGC-1 $\alpha$ , UCP1, and CD137 protein expression levels in white and brown fat were reduced in the WT+DM group compared to the WT group ( $p < 0.05$ ). Moreover, the expression levels of PPAR $\gamma$ , PGC-1 $\alpha$ , UCP1, and CD137 proteins in white and brown fat were higher in the Mstn(-/-)+DM group than in the WT+DM and Mstn(+/-)+DM groups ( $p < 0.05$ ) (Supplementary Table 3,4 and Fig. 4,5).

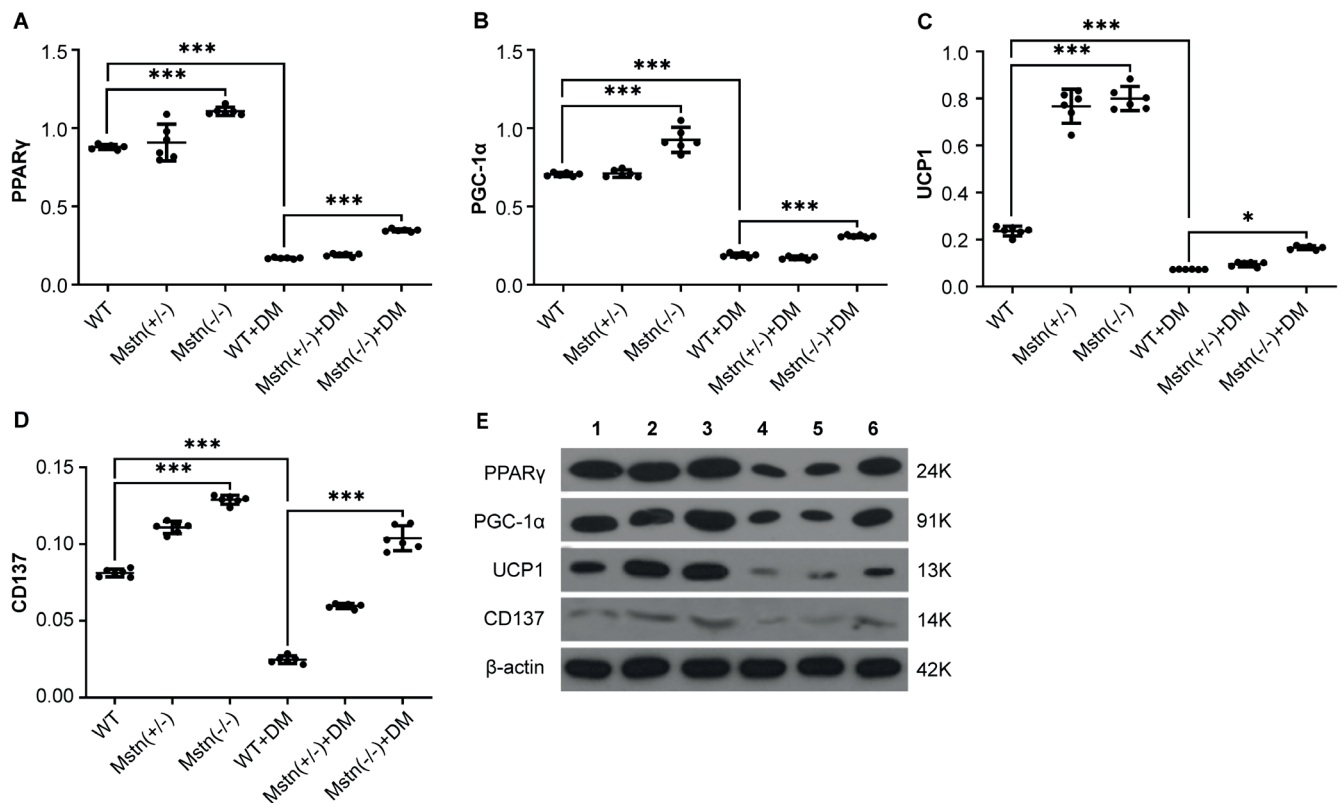


**Fig. 4.** Expression of peroxisome proliferator-activated receptor gamma (PPAR $\gamma$ ) (A), peroxisome proliferator-activated receptor-gamma coactivator-1 alpha (PGC-1 $\alpha$ ) (B), uncoupling protein 1 (UCP1) (C), and cluster of differentiation 137 (CD137) (D) in white fat. Western blot of PPAR $\gamma$ , PGC-1 $\alpha$ , UCP1, and CD137 in white fat (E). Means and 95% confidence intervals (95% CI) are presented. Bootstrap one-way analysis of variance (ANOVA) was used for comparisons between the 6 groups

\* $p < 0.05$ ; \*\*\* $p < 0.001$ ; DM – diabetes mellitus; Mstn – myostatin; WT – wild-type.

## Expression levels of Mstn in the gastrocnemius muscle and serum

The expression levels of Mstn in the gastrocnemius muscle and serum of WT heterozygous and homozygous mice gradually decreased with the decrease of gene abundance. The Mstn was not detected in the Mstn(-/-) and Mstn(-/-)+DM groups, suggesting that protein expression was completely inhibited after *Mstn* knockout. The Mstn expression level was correlated with gene abundance. Compared with the same-genotype non-diabetic group, the expression level of Mstn protein in the gastrocnemius of the WT+DM and Mstn(+/-)+DM groups significantly increased ( $p < 0.05$ ), suggesting that skeletal muscle secretion of Mstn increases in T2DM (Supplementary Table 5 and Fig. 6).

## Discussion

In this study, we examined the effect of Mstn on white fat browning in T2DM mice. Obesity is a global public health problem and a significant cause of T2DM and other metabolic disorders. Recently, the browning of white fat has been a topic of great interest in the treatment

of obesity. Exploring the sensing and regulatory mechanisms of the conversion of white fat to brown fat promoted by an external stimulus will help develop new drugs for the treatment of obesity.

The Mstn is mainly expressed in the skeletal muscle and negatively regulates its growth and development.<sup>2</sup> Moreover, previous studies have shown that Mstn may regulate fat metabolism.<sup>3</sup> For example, the subcutaneous fat content to body weight ratio and the serum TG levels were significantly lower in the Mstn(-/-) Meishan pigs than in the WT pigs.<sup>4</sup> Our research demonstrated several interesting results, namely that Lee's index and the serum HDL-C levels were lower in the WT+DM group than in the WT group, whereas the fat index and the serum TG, TC, LDL-C, and FFA levels were higher in the WT+DM group when compared to the WT group. Lee's index, fat index, and serum TG, TC, LDL-C, and FFA levels were lower in the Mstn(-/-)+DM group than in the WT+DM group, while the serum HDL-C level was higher in the Mstn(-/-)+DM group than in the WT+DM group. These results suggest that *Mstn* knockout significantly antagonizes obesity characteristics, such as fat accumulation and lipid metabolism disorderliness, caused by T2DM. The decrease in fat mass observed in the Mstn(-/-) mice may be associated with Mstn-induced inhibition

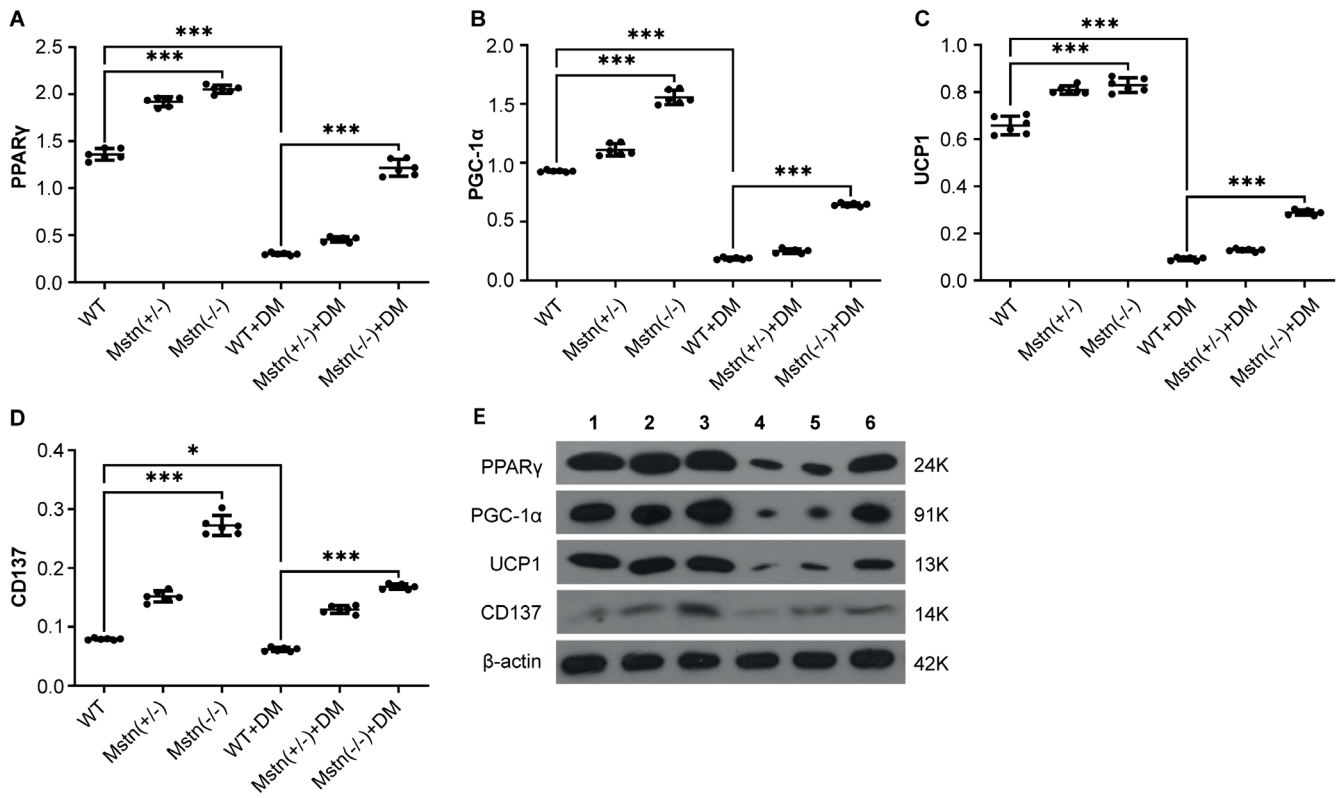


**Fig. 5.** Expression of peroxisome proliferator-activated receptor gamma (PPAR $\gamma$ ) (A), peroxisome proliferator-activated receptor-gamma coactivator-1 alpha (PGC-1 $\alpha$ ) (B), uncoupling protein 1 (UCP1) (C), and cluster of differentiation 137 (CD137) (D) in brown fat. Western blot of PPAR $\gamma$ , PGC-1 $\alpha$ , UCP1, and CD137 in brown fat (E). Means and 95% confidence intervals (95% CIs) are presented. Bootstrap one-way analysis of variance (ANOVA) was used for comparisons between the 6 groups

\*p < 0.05; \*\*\*p < 0.001; DM – diabetes mellitus; Mstn – myostatin; WT – wild-type.

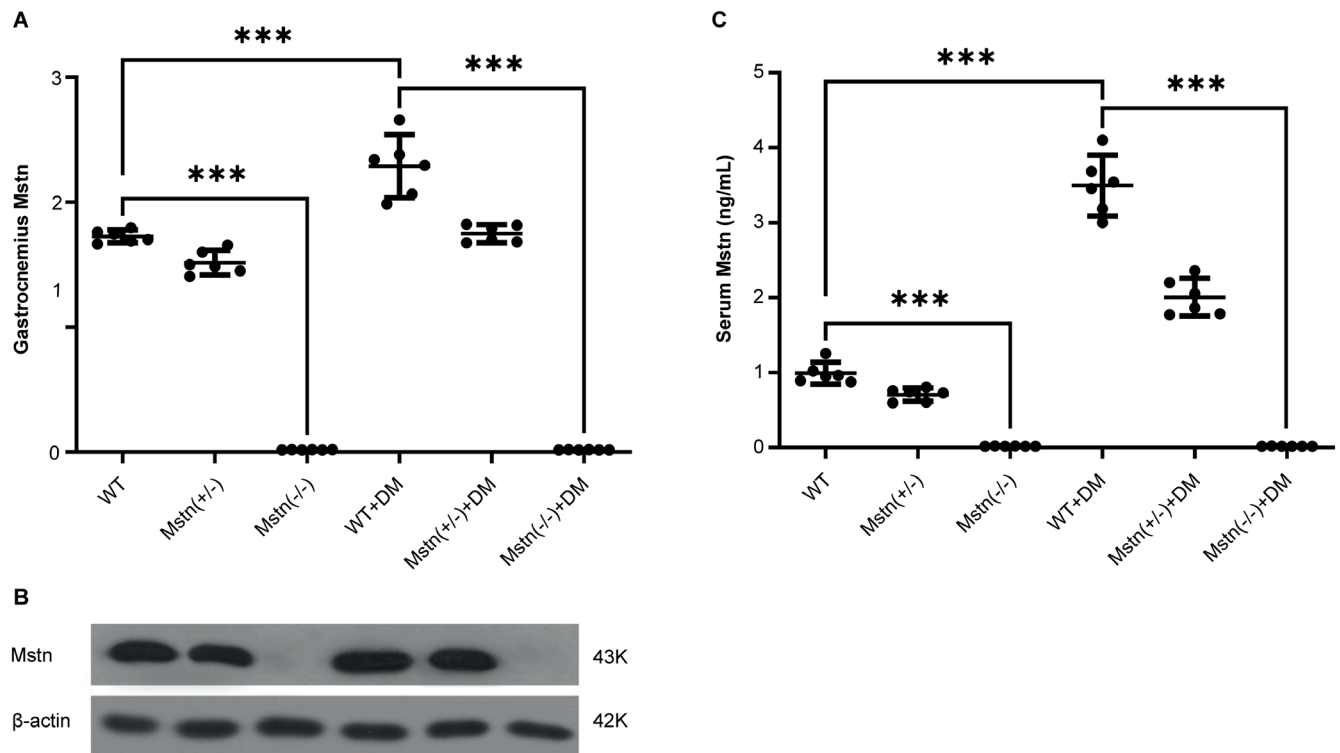


**Fig. 6.** Expression of myostatin (Mstn) in the gastrocnemius muscle and serum. A,B. The expression level of Mstn in the gastrocnemius muscle and western blot; C. Levels of serum Mstn. Means and 95% confidence intervals (95% CIs) are presented. Bootstrap one-way analysis of variance (ANOVA) was used for comparisons between the 6 groups

\*p < 0.05; \*\*\*p < 0.001; DM – diabetes mellitus; WT – wild-type.



of the differentiation of pre-adipocytes into mature adipocytes. This decrease in the number of mature adipocytes leads to a reduction in total fat.<sup>5</sup>

White adipose tissue is mainly distributed in subcutaneous and internal organs, such as mesenteric organs and gonads. White fat cells contain a single large lipid droplet and a high level of TG. The main function of the white adipose tissue is to store excess energy in the body in the form of fat, which then becomes the main factor leading to obesity. Conversely, brown adipose tissue is mainly distributed between the shoulder blades, the back of the neck, the axilla, the mediastinum, and around the kidneys. The body's brown fat gradually decreases with age. Brown adipocytes contain small multilocular lipid droplets and many mitochondria, which consume TG stored in white fat through uncoupled oxidative phosphorylation, generating heat and regulating the body's temperature balance.<sup>6</sup> Beige fat is an intermediate form of white fat in the process of being converted to brown fat. It is activated by cold and other external stimuli, and exerts a heat-generating effect like brown fat, leading to white fat browning.<sup>6</sup> Both brown and beige fat improve body fat metabolism and reduce obesity, and the cells of both fat cells carry highly expressed marker genes. Studies have confirmed that *PPAR $\gamma$* , *PGC-1 $\alpha$* , *UCP1*, PR domain-containing 16 (*PRDM16*), and cell death-inducing DNA fragmentation factor  $\alpha$ -like effector A (*CIDEA*) are highly expressed in brown adipocytes, while *CD137* and transmembrane protein 26 (*TMEM26*) are highly expressed in beige adipocytes. Therefore, these genes are markers of white fat browning.<sup>7–9</sup>

The *Mstn* has also been shown to regulate white fat browning. Studies have reported that *Mstn*( $-/-$ ) mice display increased energy utilization and resistance to genetic or diet-induced obesity. Moreover, subcutaneous white fat demonstrates some of the characteristics of brown fat, in which the expression levels of *PGC-1 $\alpha$* , *UCP1*, *CD137*, and *Tmem26* were increased.<sup>10</sup>

This study shows that the expression levels of *PPAR $\gamma$* , *PGC-1 $\alpha$* , *UCP1*, and *CD137* in the white and brown fat were higher in the *Mstn*( $-/-$ ) group than in the WT group, lower in the WT+DM group than in the WT group, and higher in the *Mstn*( $-/-$ )+DM group compared to the WT+DM group. Combined with the H&E staining of white and brown adipose tissues, these results suggested that T2DM may decrease the expression of brown fat and beige fat marker genes and increase white fat phenotypes and energy storage. Thus, it may be surmised that *Mstn* knockout significantly antagonizes this phenomenon, promotes white fat browning, increases heat production in the body, and promotes the consumption of white fat, thereby reducing obesity. The *Mstn* can inhibit the differentiation of brown adipocytes by activating Smad3 phosphorylation.<sup>11</sup> We found that after *Mstn* treatment of brown adipocytes, the expression of the *PPAR $\gamma$* , *UCP1*, *PGC-1*, and *PRDM16* genes was downregulated. The expression of these genes was further suppressed after

$\beta$ -catenin activator treatment. Furthermore, there are interactions between the Smad3 and Wnt/ $\beta$ -catenin pathways.<sup>11</sup> The *Mstn* can induce phosphorylation of Smad3, further increasing the stability of  $\beta$ -catenin, and the Wnt/ $\beta$ -catenin pathway can inhibit the differentiation of brown adipocytes.<sup>11–13</sup> However, the specific mechanism involved requires further study.

## Limitations

This study was beset by certain limitations, including the small sample size and a lack of an investigation into the underlying molecular mechanisms. The specific mechanism underlying the role of *Mstn* in white fat browning requires further studies. Moreover, female mice have different fat metabolism characteristics compared to male mice. To exclude the effect of estrogen, male mice were chosen for this experiment. We expect similar results in female mice, in which fat deposition and type are strongly dependent on estrogen and its signaling.

## Conclusions

This study suggests that inhibiting *Mstn* expression may antagonize obesity phenotypes, such as white fat accumulation and lipid metabolism derangement caused by T2DM, upregulate the expression of *PPAR $\gamma$* , *PGC-1 $\alpha$* , *UCP1*, and *CD137*, promote white fat browning, and alleviate obesity.

## Supplementary data

The Supplementary materials are available at <https://doi.org/10.5281/zenodo.8392519>. The package contains the following files:

Supplementary Table 1. Growth and obesity indicators.

Supplementary Table 2. Lipid metabolism indicators.

Supplementary Table 3. Expression levels of *PPAR $\gamma$* , *PGC-1 $\alpha$* , *UCP1*, and *CD137* protein in white fat.


Supplementary Table 4. Expression levels of *PPAR $\gamma$* , *PGC-1 $\alpha$* , *UCP1*, and *CD137* protein in brown fat.


Supplementary Table 5. Expression levels of *Mstn* in the gastrocnemius and serum.


Supplementary File 1. Materials and methods description.


## ORCID iDs

Jingwei Cheng  <https://orcid.org/0000-0001-5370-3998>

Jaewoo Lee  <https://orcid.org/0000-0001-7617-9308>

Yangqing Liu  <https://orcid.org/0000-0002-5243-261X>

Yanfang Wang  <https://orcid.org/0009-0002-8223-0469>

Mingtao Duan  <https://orcid.org/0000-0002-4167-375X>

Zhen Zeng  <https://orcid.org/0009-0001-0221-100X>

## References

1. Pedersen BK, Febbraio MA. Muscles, exercise and obesity: Skeletal muscle as a secretory organ. *Nat Rev Endocrinol*. 2012;8(8):457–465. doi:10.1038/nrendo.2012.49

2. Sharma M, McFarlane C, Kambadur R, Kukreti H, Bonala S, Srinivasan S. Myostatin: Expanding horizons. *IUBMB Life*. 2015;67(8):589–600. doi:10.1002/iub.1392
3. Akpan I, Goncalves MD, Dhir R, et al. The effects of a soluble activin type IIB receptor on obesity and insulin sensitivity. *Int J Obes*. 2009;33(11):1265–1273. doi:10.1038/ijo.2009.162
4. Cai C, Qian L, Jiang S, et al. Loss-of-function myostatin mutation increases insulin sensitivity and browning of white fat in Meishan pigs. *Oncotarget*. 2017;8(21):34911–34922. doi:10.18632/oncotarget.16822
5. Sun WX, Dodson MV, Jiang ZH, Yu SG, Chu WW, Chen J. Myostatin inhibits porcine intramuscular preadipocyte differentiation in vitro. *Domest Anim Endocrinol*. 2016;55:25–31. doi:10.1016/j.domaniend.2015.10.005
6. Bartelt A, Heeren J. Adipose tissue browning and metabolic health. *Nat Rev Endocrinol*. 2014;10(1):24–36. doi:10.1038/nrendo.2013.204
7. Tanaka-Yachi R, Takahashi-Muto C, Adachi K, et al. Promoting effect of  $\alpha$ -tocopherol on beige adipocyte differentiation in 3T3-L1 cells and rat white adipose tissue. *J Oleo Sci*. 2017;66(2):171–179. doi:10.5650/jos.ess16137
8. Dinas PC, Valente A, Granzotto M, et al. Browning formation markers of subcutaneous adipose tissue in relation to resting energy expenditure, physical activity and diet in humans. *Horm Mol Biol Clin Investig*. 2017;31(1):j/hmbci.2017.31.issue-1/hmbci-2017-0008/hmbci-2017-0008.xml. doi:10.1515/hmbci-2017-0008
9. Efremova A, Colleluori G, Thomsen M, et al. Biomarkers of browning in cold exposed Siberian adults. *Nutrients*. 2020;12(8):2162. doi:10.3390/nu12082162
10. Shan T, Liang X, Bi P, Kuang S. Myostatin knockout drives browning of white adipose tissue through activating the AMPK-PGC1 $\alpha$ -Fndc5 pathway in muscle. *FASEB J*. 2013;27(5):1981–1989. doi:10.1096/fj.12-225755
11. Kim WK, Choi HR, Park SG, Ko Y, Bae KH, Lee SC. Myostatin inhibits brown adipocyte differentiation via regulation of Smad3-mediated  $\beta$ -catenin stabilization. *Int J Biochem Cell Biol*. 2012;44(2):327–334. doi:10.1016/j.biocel.2011.11.004
12. Ge X, Sathiakumar D, Lua BJG, Kukreti H, Lee M, McFarlane C. Myostatin signals through miR-34a to regulate Fndc5 expression and browning of white adipocytes. *Int J Obes*. 2017;41(1):137–148. doi:10.1038/ijo.2016.110
13. Li HX, Luo X, Liu RX, Yang YJ, Yang GS. Roles of Wnt/ $\beta$ -catenin signaling in adipogenic differentiation potential of adipose-derived mesenchymal stem cells. *Mol Cell Endocrinol*. 2008;291(1–2):116–124. doi:10.1016/j.mce.2008.05.005





# CCN1 inhibition affects the function of endothelial progenitor cells under high-glucose condition

Yanting Dong<sup>1,2,A–E</sup>, Xiaohui Zhou<sup>3,B,C</sup>, Nan Zhang<sup>1,C,F</sup>

<sup>1</sup> Department of Endocrinology, Sir Run Run Shaw Hospital, School of Medicine, Zhejiang University, Hangzhou, China

<sup>2</sup> Department of Endocrinology, Suichang County Hospital of Traditional Chinese Medicine, Lishui, China

<sup>3</sup> Department of Endocrinology, Huzhou Central Hospital, China

A – research concept and design; B – collection and/or assembly of data; C – data analysis and interpretation;

D – writing the article; E – critical revision of the article; F – final approval of the article

Advances in Clinical and Experimental Medicine, ISSN 1899–5276 (print), ISSN 2451–2680 (online)

*Adv Clin Exp Med.* 2024;33(6):619–631

## Address for correspondence

Nan Zhang  
E-mail: 3198047@zju.edu.cn

## Funding sources

This project was supported by the Zhejiang Provincial Natural Science Foundation of China (grant No. Y16H070002).

## Conflict of interest

None declared

## Acknowledgements

The authors would like to thank the staff of the Department of Endocrinology, Sir Run Run Shaw Hospital, School of Medicine, Zhejiang University, China, for their valuable input and support throughout this study.

Received on August 8, 2022

Reviewed on May 8, 2023

Accepted on August 13, 2023

Published online on October 19, 2023

## Cite as

Dong Y, Zhou X, Zhang N. CCN1 inhibition affects the function of endothelial progenitor cells under high-glucose condition.

*Adv Clin Exp Med.* 2024;33(6):619–631.

doi:10.17219/acem/170998

## DOI

10.17219/acem/170998

## Copyright

Copyright by Author(s)

This is an article distributed under the terms of the Creative Commons Attribution 3.0 Unported (CC BY 3.0)

(<https://creativecommons.org/licenses/by/3.0/>)

## Abstract

**Background.** The impact of cysteine-rich angiogenic inducer 61 (Cyr61, also called CCN1) on endothelial progenitor cells (EPCs) from diabetic-rat-derived whole peripheral and bone marrow remains poorly understood. Therefore, the expression levels of CCN1, CCN1-induced C-X-C chemokine receptor type 4 (CXCR4), and stromal-cell-derived factor-1 (SDF-1) were explored under high glucose (HG) conditions.

**Objectives.** The aim of the study was to explore the effects of high CCN1 levels on EPC activity in diabetic rats through mitogen-activated protein kinase kinase (MEK)/extracellular signal-regulated kinase (ERK) pathway modulation.

**Materials and methods.** Primary EPCs were isolated from bone marrow and whole peripheral blood of streptozocin (STZ)-induced diabetic Sprague–Dawley rats and controls. Cell migration, tube formation ability and viability were determined using transwell, Cell Counting Kit-8 (CCK-8), and Matrigel®-based capillary-like tube formation assays. Protein and gene expression levels were measured by western blot and real-time quantitative polymerase chain reaction (RT-qPCR).

**Results.** The study findings showed that EPC migration, viability and tube formation ability were significantly lower under HG conditions. High CCN1 expression levels restored EPC function by inducing SDF-1 and CXCR4 in EPCs under HG conditions. Furthermore, HG suppressed MEK/ERK phosphorylation, while an ERK1/2 agonist rescued EPC CCN1-SDF-1/CXCR4 expression under HG conditions through the activation of the MEK/ERK pathway.

**Conclusions.** This study demonstrates that high CCN1 expression levels restored EPC functions, partly by modulating MEK/ERK signaling. These findings provide a basis for developing novel therapeutic methods for diabetic vascular neogenesis and vascular injury repair.

**Key words:** CXCR4, EPCs, CCN1, high-glucose MEK/ERK signaling pathway, SDF-1

## Introduction

Cysteine-rich angiogenic inducer 61 (Cyr61, also called CCN family member 1 or CCN1) is a 40-kDa signaling protein localized in the extracellular matrix (ECM) and encoded by the *CYR61* gene in humans.<sup>1</sup> The CCN1 mediates inflammation during inflammatory responses, implying that its expression could be modulated to manage acute lung injury.<sup>2</sup> In addition, CCN1 regulates several cellular processes, such as adhesion, apoptosis, proliferation, differentiation, and senescence, by interacting with heparan sulfate proteoglycans and cell surface integrin receptors. The CCN1 also plays a vital role in vascular integrity, blood vessel formation and cardiac septal morphogenesis in the placenta and during embryonic development.<sup>3,4</sup> In adults, CCN1 is involved in tissue repair and inflammation, and is associated with diseases involving persistent inflammation, such as retinopathy, diabetes-related nephropathy, atherosclerosis, rheumatoid arthritis, and various cancers.<sup>5</sup>

Neovascularization is impaired in diabetes mellitus, leading to peripheral artery disease attributed to endothelial progenitor cell (EPC) dysfunction.<sup>6</sup> Endothelial progenitor cells infiltrate injured vessels from the bone marrow, participate in neovascularization, and promote endothelial regeneration, playing a significant role in angiogenesis.<sup>7</sup> The levels of recruited EPCs and their function are significantly lowered under diabetic conditions,<sup>8,9</sup> and EPC dysfunction in diabetes might result in cardiovascular complications and defective angiogenesis. Low EPC levels in the blood and the EPC dysfunction are involved in diabetic vascular conditions. Notably, EPC transplantation restores their function and induces angiogenesis after hind limb ischemia in diabetic mice. Diabetic EPCs are characterized by impaired adhesion and proliferation and have a deformed morphology compared to nondiabetic EPCs,<sup>10</sup> though studies have yet to explore the mechanisms behind diabetes-induced EPC impairment.

The CCN1 is a regulator of angiogenesis, involved in reducing EPC levels and functions under high glucose (HG) conditions.<sup>11</sup> Furthermore, atherosclerotic plaques have high CCN1 expression levels that initiate cerebrovascular, cardiovascular and peripheral arterial diseases.<sup>12</sup> The CCN1 is a significant genetic regulator in coronary artery disease (CAD) and plays a role in protecting the murine heart against ischemia reperfusion injury.<sup>13</sup> The C-X-C chemokine receptor type 4 (CXCR4) and stromal cell-derived factor 1 (SDF-1 or CXCL12) are essential CCN1 targets during the modulation of angiogenesis, cell proliferation and energy metabolism.<sup>14</sup> The SDF-1 is overexpressed in injured tissues, and the SDF-1/CXCR4 pathway modulates hematopoiesis, wound healing, angiogenesis, and progenitor homing.<sup>15</sup> Moreover, the SDF-1/CXCR4 axis is involved in EPC recruitment into ischemic tissue during angiogenesis.<sup>16</sup> Kawakami et al.<sup>17</sup> showed the involvement of the SDF-1/CXCR4 pathway in EPC mobilization and incorporation in fracture healing.

The EPCs isolated from diabetic animals exhibit altered migration in response to CCN1, and the migration ability of EPCs to SDF-1 binding is defective in patients with type 1 or type 2 diabetes.<sup>18</sup> Recently, EPC transplantation has been found to improve limb function in diabetic mice with unilateral hind limb ischemia by restoring local blood flow through the overexpression of CCN1.<sup>11</sup> Yet, it is unknown whether the CCN1 pathway plays a role in the mechanisms of EPC therapy in diabetes.

The mitogen-activated protein kinase kinase (MEK)/extracellular signal-regulated kinase (ERK) pathway (Ras-Raf-MEK-ERK pathway) mediates communications from the cell surface to the nucleus. The EPC-induced activities, such as capillary sprouting, are significantly reduced by the inhibition of MEK/ERK signaling.<sup>19</sup> The CCN1 inhibition using an anti-CCN1 antibody suppressed MEK and ERK phosphorylation in acute myeloid leukemia (AML) cells.<sup>20</sup> A study on type 2 diabetic patients with aberrant EPC number, migration and nitrogen oxide synthase (NOS) activity showed that these phenotypes were associated with low SDF-1/CXCR4 expression levels and downregulation of the MEK/ERK signaling pathway.<sup>21</sup> These findings provide a basis for the potential mechanisms underlying hyperglycemia-impaired EPC migration in type 2 diabetes mellitus.

Herein, the impact of HG on EPC function was explored in diabetic rats. In addition, the role of CCN1 in MEK/ERK signaling-dependent modulation of EPC activity was evaluated.

## Objectives

The study aimed to explore the impact of CCN1 on EPCs using whole peripheral blood and bone marrow samples derived from diabetic rats. The expression levels of CCN1, CXCR4 and SDF-1 were evaluated under HG conditions, and the effects of high CCN1 levels on the MEK/ERK pathway-dependent modulation of EPC activity were assessed in diabetic rats.

## Materials and methods

### Animals

Our animal experiments were in accordance with the guidelines of the Animal Care Committee of Sir Run Run Shaw Hospital (approval No. SYXK 2017-0006). Sprague–Dawley rats (7–8-week old males) were obtained from Shanghai S&P (Shall Kay Laboratory Animal Co., Ltd., Shanghai, China). The rats were housed in a humidity- and temperature-controlled environment, with free access to water and food, and were separated into 2 groups of 3 animals each (Fig. 1). Group 1 was a control group and was administered a standard laboratory diet (SLD).

## Construction of a diabetic rat model (STZ)

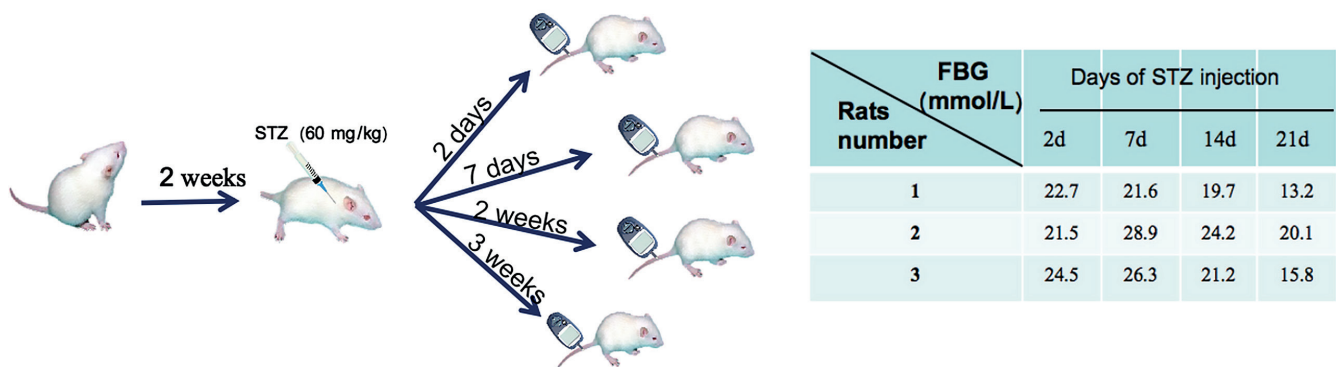


Fig. 1. Construction of the diabetic rat model. Group 1 was a control group and was administered a standard laboratory diet (SLD). Group 2 received an intraperitoneal injection of 45 mg/kg streptozocin (STZ) in 50 mM of sodium citrate buffer, pH 4.5, and was fed a SLD. The rats exhibiting non-fasting blood glucose (non-FBG) levels  $\geq 11.1$  mmol/L were considered diabetic

Group 2 received an intraperitoneal injection of 45 mg/kg streptozocin (STZ) in 50 mM of sodium citrate buffer, pH 4.5, and was fed a SLD. Blood glucose levels were determined 3 weeks after STZ administration using a glucometer. The rats exhibiting non-fasting blood glucose (non-FBG) levels  $\geq 11.1$  mmol/L were considered diabetic.

### Endothelial progenitor cell isolation, culture and identification

All healthy rats were euthanized by cervical dislocation, and the femur and tibia were harvested aseptically for EPC isolation. A 20-mL peripheral blood and bone marrow cell suspension was prepared, and mononuclear cells were isolated using a separation medium (Lonza, Basel, Switzerland). Samples were washed twice with phosphate-buffered saline (PBS) (Josonbio, Shanghai, China), and the cells were resuspended in a complete medium supplemented with 10% fetal bovine serum (FBS) (Gibco, Baltimore, USA). Then, 10 mg/L of basic fibroblast growth factor (FGF) and 10 mg/L of vascular endothelial growth factor (VEGF) (both from TBD Science, Tianjin, China) were added to the cells. The cells were seeded on 25 cm<sup>2</sup> flasks at  $5 \times 10^5$  cells/mL and cultured in a humidified incubator at 37°C with 5% carbon dioxide (CO<sub>2</sub>). The medium was replaced every 4 days to remove non-adherent cells and maintained for 2 weeks. The EPC phenotype was explored using fluorescence microscopy by double-positive staining for fluorescein isothiocyanate-Ulex Europaeus Agglutinin-1 (FITC-UEA-1) binding (green) and Dil acetylated low-density lipoprotein (Dil-ac-LDL) (red). Glucose was added to the EPC cultures at 5 or 22 mM to mimic normal glucose (NG) and HG, respectively.

### Recombinant adenovirus

A first-generation adenovirus was regulated by the cytomegalovirus promoter using an open reading frame (ORF)

shuttling system (Vigene Biosciences, Inc., Rockville, USA). Rat CCN1 complementary deoxyribonucleic acid (cDNA) (NM\_024359) (Vigene Biosciences, Inc.) was harvested from the pENTR vector and transferred to a pAD-ORF transfer vector. Recombinant adenoviral constructs were transfected into 293 cells to obtain a recombinant adenovirus with a high Ad-CCN1 titer ( $1 \times 10^{10}$  plaque-forming unit (pfu)/mL). The Ad-CCN1 was obtained using a customized adenovirus (Vigene Biosciences, Inc.). An empty adenovirus was used as the Ad-control. Infection efficiency was determined by labeling all adenovirus vectors with a flag. The effects of adenovirus infection were explored by western blot analysis to verify whether Ad-CCN1 was highly expressed.

### Cell viability assay

Cell viability was explored using the Cell Counting Kit-8 (CCK-8) assay. The EPCs were seeded to flat-bottomed 96-well microplates at a density of  $1 \times 10^4$  cells/well. Then, the cells were incubated for 24 h in an endothelial basal medium-2 (EBM-2; Lonza, Walkersville, USA) containing 2% FBS (6 wells per group). The culture medium was replaced with EBM-2 medium containing 10% FBS and cultured for 6 h. The cells were then cultured in HG media (22 mM of glucose for 24 h). Control cells were not treated. The CCK-8 (10  $\mu$ L/well) was added to the wells at the end of the experiment. The absorbance was measured on a microplate reader at 450 nm after incubation at 37°C for 48 h, and the proliferation of the treated EPCs was determined relative to the control EPCs.

### Cell migration assay

The EPC migration rate was evaluated using transwell assays with 8-mm pore filters (Corning Inc., Corning, USA). After treating EPCs with HG or overexpressing CCN1,  $5 \times 10^4$  cells in 100  $\mu$ L of non-FBS EBM-2 medium

were seeded into the upper chamber, and 500  $\mu$ L of culture medium with 20% FBS was added to the lower chamber. The EPCs were cultured for 24 h, then the transwell membranes were stained with 0.1% crystal violet for 30 min. The number of migrated cells was determined in 3 random fields of view using an IX51 inverted fluorescence microscope (Olympus, Tokyo, Japan). All experiments were performed in triplicate.

### Matrigel-based capillary-like tube formation assay

The impact of HG on the capillary-like tube formation capacity of EPCs was determined using the capillary tube formation angiogenesis assay kit (ECM625; Merck Millipore, Burlington, USA). A total of  $1 \times 10^4$  cells/well were seeded onto Matrigel-precoated 96-well plates (Corning Inc.) after treatment of EPCs with HG for 24 h. An IX51 inverted light microscope (Olympus) was used to observe tube formation. Three independent fields were measured per well, and the average number of tubes was determined using WimTube quantitative image analysis (Wimasis, Cordoba, Spain).

### Semi-quantitative real-time polymerase chain reaction

Total ribonucleic acid (RNA) was extracted using TRIzol (Invitrogen, Carlsbad, USA), and 0.5  $\mu$ g of RNA was used for reverse transcription using the PrimerScript<sup>TM</sup> RT reagent kit (Takara, Shiga, Japan). Samples were incubated for 1 h at 42°C, and the reaction was terminated at 70°C for 15 min. The CCN1 forward primer (5'-TCA CCC TTC TCC ACT TGA CC-3') and reverse primer (5'-AAT TGC ATT CCA GCC CCT TG-3'), and the  $\beta$ -actin forward primer (5'-CAC GAT GGA GGG GCC GGA CTC ATC-3') and reverse primer (5'-TAA AGA CCT CTA TGC CAA CAC AGT-3') were used for polymerase chain reaction (PCR) amplification. The PCR products were separated and analyzed using agarose gels, and the CCN1 bands were confirmed through sequencing.

### Real-time polymerase chain reaction

Total RNA was extracted using TRIzol (Invitrogen) and retrotranscribed with the PrimeScript 1<sup>st</sup> strand cDNA synthesis kit (D6110A; Takara Bio USA, Inc., San Jose, USA). The real-time (RT) PCR assay used SYBR Green Real-time PCR Master Mix (QPK-201, QPK-201T; Toyobo, Osaka, Japan) under the following conditions: 95°C for 30 s, followed by 40 cycles at 95°C for 5 s and 60°C for 30 s. The analysis was performed in triplicate, and the gene expression levels were determined using the  $2^{-\Delta\Delta CT}$  method. The CCN1 forward primer was 5'-TTG TAG GCA CGG CTG CTA TGC T-3', the CCN1 reverse primer was 5'-GGT GCT CCA TTC TCA GAA CCT G-3', the SDF-1 forward primer was 5'-GGA GGA TAG ATG TGC TCT GGA AC-3',

the SDF-1 reverse primer was 5'-AGT GAG GAT GGA GAC CGT GGT G-3', the CXCR4 forward primer was 5'-GAC TGG CAT AGT CGG CAA TGG A-3', the CXCR4 reverse primer was 5'-CAA AGA GGA GGT CAG CCA CTG A-3', the glyceraldehyde 3-phosphate dehydrogenase (GAPDH) forward primer was 5'-AGA CAG CCG CAT CTT CTT GT-3', and the GAPDH reverse primer was 5'-CTT GCC GTG GGT AGA GTC AT-3'.

### Western blotting

The EPCs were lysed with a lysis buffer containing 100 mM of phenylmethanesulfonyl fluoride, and the proteins were resolved using 10% sodium dodecyl sulfate-polyacrylamide gel electrophoresis (SDS-PAGE). The proteins were transferred onto polyvinylidene difluoride (PVDF) membranes and incubated with primary antibodies against CCN1 (1:1000; Life Technologies, Carlsbad, USA), SDF-1 (1:1000; Life Technologies), CXCR4 (1:1000; Life Technologies), ERK1/2 (1:1000; Santa Cruz Biotechnology Inc., Dallas, USA), p-ERK1/2 (1:1000; Santa Cruz Biotechnology Inc.), ERK (1:1000; Santa Cruz Biotechnology Inc.), p-ERK (1:1000; Santa Cruz Biotechnology Inc.), and GAPDH (1:3000; Santa Cruz Biotechnology Inc.). The western blot signal was developed using an enhanced chemiluminescence detection kit (Merck Millipore).

The first experiment was considered a pre-experiment. Based on the results and their reliability, the second experiment was conducted with the same design and sample selection criteria to ensure stronger credibility of the experimental results. Using successfully isolated, cultured, and identified EPCs in the first experiments, all experiments were repeated twice, including cell migration, tube formation ability and viability. Protein and gene expression levels were measured using western blot and real-time quantitative polymerase chain reaction (RT-qPCR) tests, respectively (detailed experimental procedures were described previously). Finally, data from the 2 experiments were combined for statistical analyses.

### Statistical analyses

Statistical analyses employed SPSS v. 21.0 (IBM Corp., Armonk, USA) software. One-way analysis of variance (ANOVA) and multiple comparison post-hoc tests (Bonferroni) compared means between experimental groups. Due to the small sample size, we used a bootstrap ANOVA. The differences between the 2 groups were determined using Student's t-test, with p-values  $\leq 0.05$  considered statistically significant (\* p < 0.05, statistically significant difference; \*\* p < 0.01, very significant difference; \*\*\* p < 0.001, extremely significant difference). In all figures, the long horizontal line in the middle indicates the sample mean of the group, the range between the short horizontal lines at both ends indicates the 95% confidence intervals, and the points indicate the within-sample distribution.



## Results

### Endothelial progenitor cell isolation, establishment and characterization

Bone marrow EPCs (BM-EPCs) and whole peripheral blood EPCs (PB-EPCs) were isolated from normal and STZ-treated diabetic rats. The cells were passaged and characterized, as described by Brandl et al.<sup>22</sup> Then, they were centrifuged using Percoll density gradient centrifugation and cultured for 2 weeks. The EPC phenotype was confirmed by staining with Dil-ac-LDL (red) and FITC-UEA-1 (green) and observed under fluorescence microscopy (model BX53; Olympus Corp., Tokyo, Japan) (Fig. 2A). After less than 24 h in culture, cells appeared small and round. The EPCs exhibited a spindle-shaped morphology after 4–7 days and developed cord-like structures after 10 days in culture (Fig. 2B). Additionally, after 10 days, significantly more control PB-EPCs were positive for FITC-UEA-1 (72.80 ± 1.92%) compared to diabetic PB-EPCs (56.80.3 ± 4.55%,  $p \leq 0.05$ ). Consistently, significantly more control BM-EPCs (70.00 ± 1.58%) were positive for Dil-ac-LDL and FITC-UEA-1 compared to diabetic BM-EPCs (57.00 ± 2.92%,  $p \leq 0.05$ ). Overall, diabetic rats had significantly fewer EPCs (Fig. 2C and Supplementary Table 1).

### High glucose affected endothelial progenitor cell migration, viability and capillary-like tube formation

Angiogenesis involves EPC activation, proliferation, migration, and capillary-like tube formation. The impact of glucose on EPC activity, viability, tube formation, and migration was explored under NG (5 mM of glucose) and HG (22 mM of glucose) conditions. The CCK-8 assay determined EPC viability, which was significantly lower in diabetic rats compared to normal rats (Fig. 3). In addition, EPC levels were lower in the bone marrow and peripheral blood samples cultured in the HG medium than in the NG medium (all  $p < 0.05$ , Fig. 3A and Supplementary Tables 2,3).

Angiogenesis is influenced by effective migration. Therefore, the impact of HG on EPC migration was explored using transwell assays. High glucose significantly decreased EPC migration in diabetic rats compared to the control rats. The migration rate was markedly lower in the HG medium compared to the NG medium in the bone marrow and peripheral blood samples (Fig. 3B,C and Supplementary Tables 4,5).

The inhibitory effect of HG on EPC tube formation was explored. The HG medium suppressed EPC tube formation, as shown by a marked decrease in segment length, mean tube length and junction numbers (Fig. 3D). These findings indicate that HG inhibits EPC tube formation, implying that it can play a suppressive role in EPC neo-angiogenesis.

### High glucose downregulated CCN1, SDF-1 and CXCR4 mRNA expression by EPCs

The CCN1 messenger RNA (mRNA) and protein expression levels were determined after culturing EPCs in HG medium using western blotting, RT-qPCR and semi-quantitative RT-PCR (sqRT-PCR). Furthermore, the protein levels of EPC targets (SDF-1 and CXCR4) were determined after culture in the HG medium. The sqRT-PCR and RT-qPCR analyses showed that HG significantly suppressed the expression of *CCN1* (Fig. 4A,B and Supplementary Table 6). The CCN1 protein levels in whole peripheral blood and bone marrow were significantly downregulated in EPCs from diabetic rats and HG medium (Fig. 4C,D and Supplementary Table 7). Western blot showed significant decreases in the levels of CCN1 targets (SDF-1 and CXCR4) (Fig. 4E–G and Supplementary Tables 8,9). These findings imply that CCN1 inhibition and its target genes, *SDF-1/CXCR4*, are involved in HG-induced EPC dysfunction.

### CCN1 overexpression ameliorated high-glucose impairment of EPC viability, migration and capillary-like tube formation

The findings outlined above showed that HG correlated with low CCN1, SDF-1 and CXCR4 expression levels, which are known neovascularization inducers in EPCs. Recombinant adenoviral particles containing the *CCN1* ORF controlled by a constitutive CMV promoter explored whether *CCN1* could alleviate the negative impact of HG on EPC functions. Cell migration, viability and tube formation were assessed, as detailed above, for BM-EPCs under NG or HG conditions after adenovirus infection for 48 h. Notably, the inhibition of cell viability and migration in BM-EPCs under HG (Fig. 5A–C and Supplementary Tables 10–13) was reversed by the overexpression of *CCN1*. In addition, BM-EPC tube formation impairment under HG was improved by the upregulation of *CCN1* (Fig. 5D). The RT-qPCR and western blot analysis revealed that the upregulation of *CCN1* rescued the reduced SDF-1 and CXCR4 mRNA and protein levels triggered by HG (Fig. 5E–G and Supplementary Tables 14,15). The CCN1 mRNA (Fig. 5E) and protein (Fig. 5F,G) levels were upregulated after adenoviral infection and normalized by HG medium. These findings show that the overexpression of *CCN1* improved EPC tube formation ability, migration and viability after HG treatment. The results imply that HG-induced *CCN1* downregulation, leading to CCN1-mediated *SDF-1/CXCR4* suppression, could be involved in neovascularization in EPCs of diabetic rats.



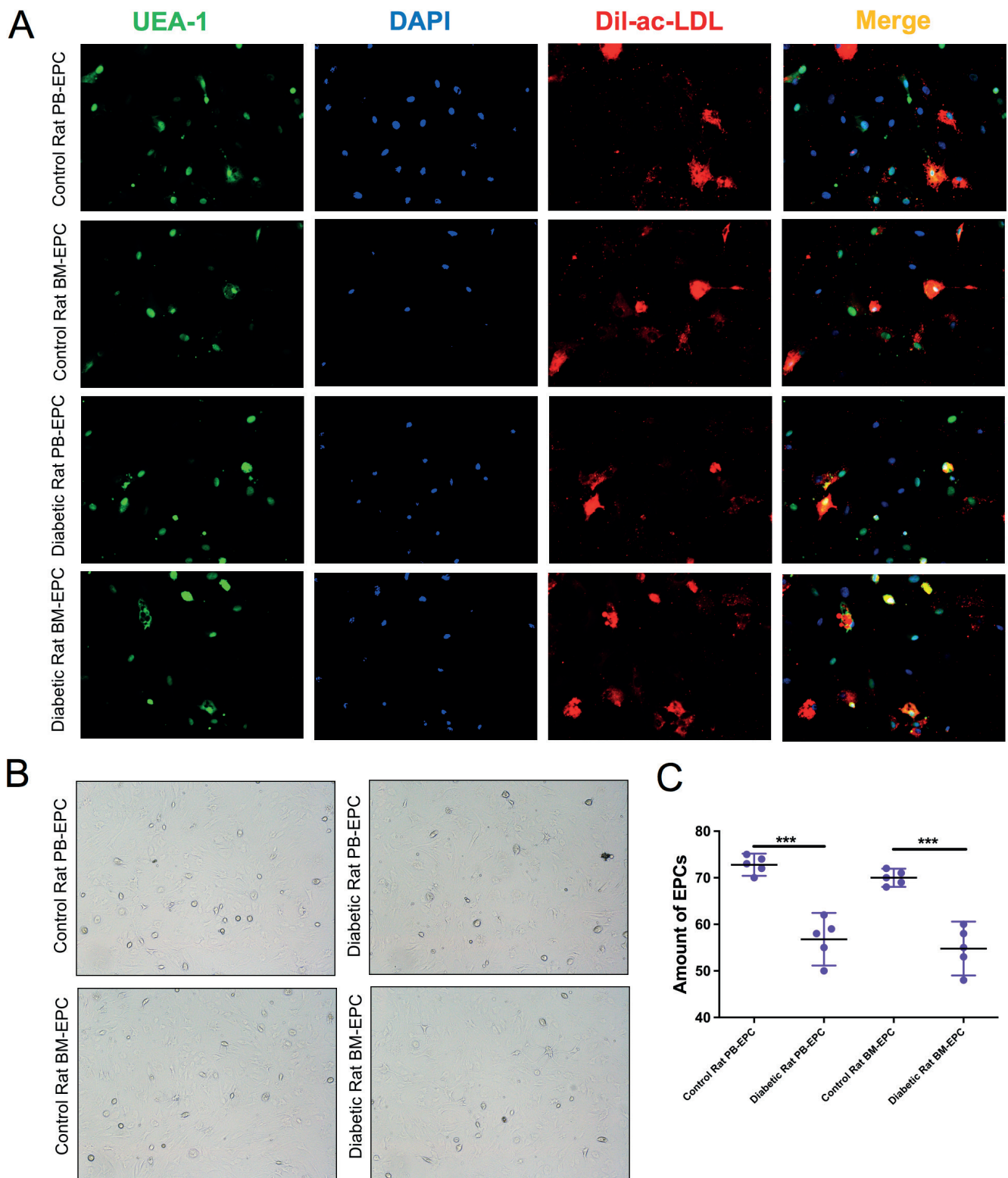


**Fig. 2.** Establishment and phenotypic characterization of cultured endothelial progenitor cells (EPCs). **A.** Diabetic or control rat peripheral blood (PB)-EPCs and bone marrow (BM)-EPCs were double positive for the EPC markers: fluorescein isothiocyanate-Ulex Europaeus Agglutinin-1 (FITC-UEA-1) (green) and Dil acetylated low-density lipoprotein (Dil-ac-LDL) (red). The nuclei were counterstained with 4',6-diamidino-2-phenylindole (DAPI) (blue). Scale bars = 200  $\mu$ m; **B.** EPC morphology after 10 days in culture. After seeding, EPCs from buffy coats formed colonies characterized by cobblestone-like cell morphology on day 10. Scale bars = 200  $\mu$ m; **C.** EPC numbers were determined using ImageJ software, and the number of EPCs per image was expressed as the number of cells per  $\text{cm}^2$  (analysis of variance (ANOVA)). For a detailed statistical analysis of the results, see Supplementary Table 1

\*\*\*  $p < 0.001$ .

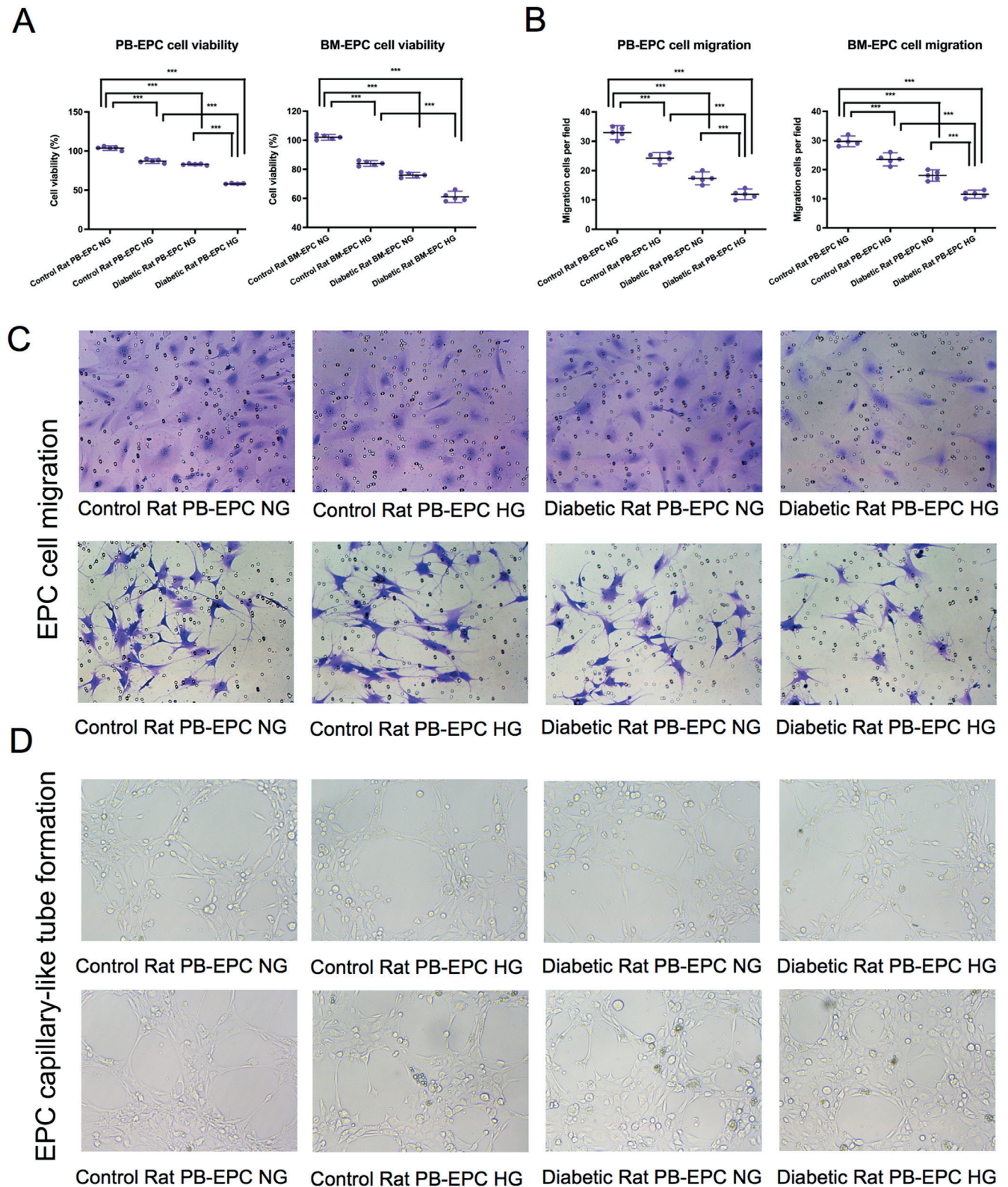


**Fig. 3.** Migration rate, viability and tube formation of endothelial progenitor cells (EPCs). A. EPCs were seeded on 96-well plates and cultured in normal glucose (NG) or high glucose (HG) media. Cell viability was determined after 48 h using the Cell Counting Kit-8 (CCK-8) assay (analysis of variance (ANOVA)). For a detailed statistical analysis of the results, see Supplementary Tables 2,3; B. The migration rate of EPCs after HG treatment. The EPCs were seeded onto the upper chamber and allowed to migrate for 24 h, and migratory cells in the bottom chamber were stained with 0.1% crystal violet for 30 min and observed under an inverted fluorescence microscope (ANOVA). For a detailed statistical analysis of the results, see Supplementary Tables 4,5; C. EPC levels were determined manually using ImageJ software, and the number of EPCs per image was expressed as the number of cells per cm<sup>2</sup>; D. Tube formation capacity of EPCs treated with HG media. EPCs were seeded on Matrigel-coated plates in HG or NG medium. Tube formation was explored after 24 h by light microscopy

\*\*\* p < 0.001; PB – peripheral blood, BM – bone marrow.



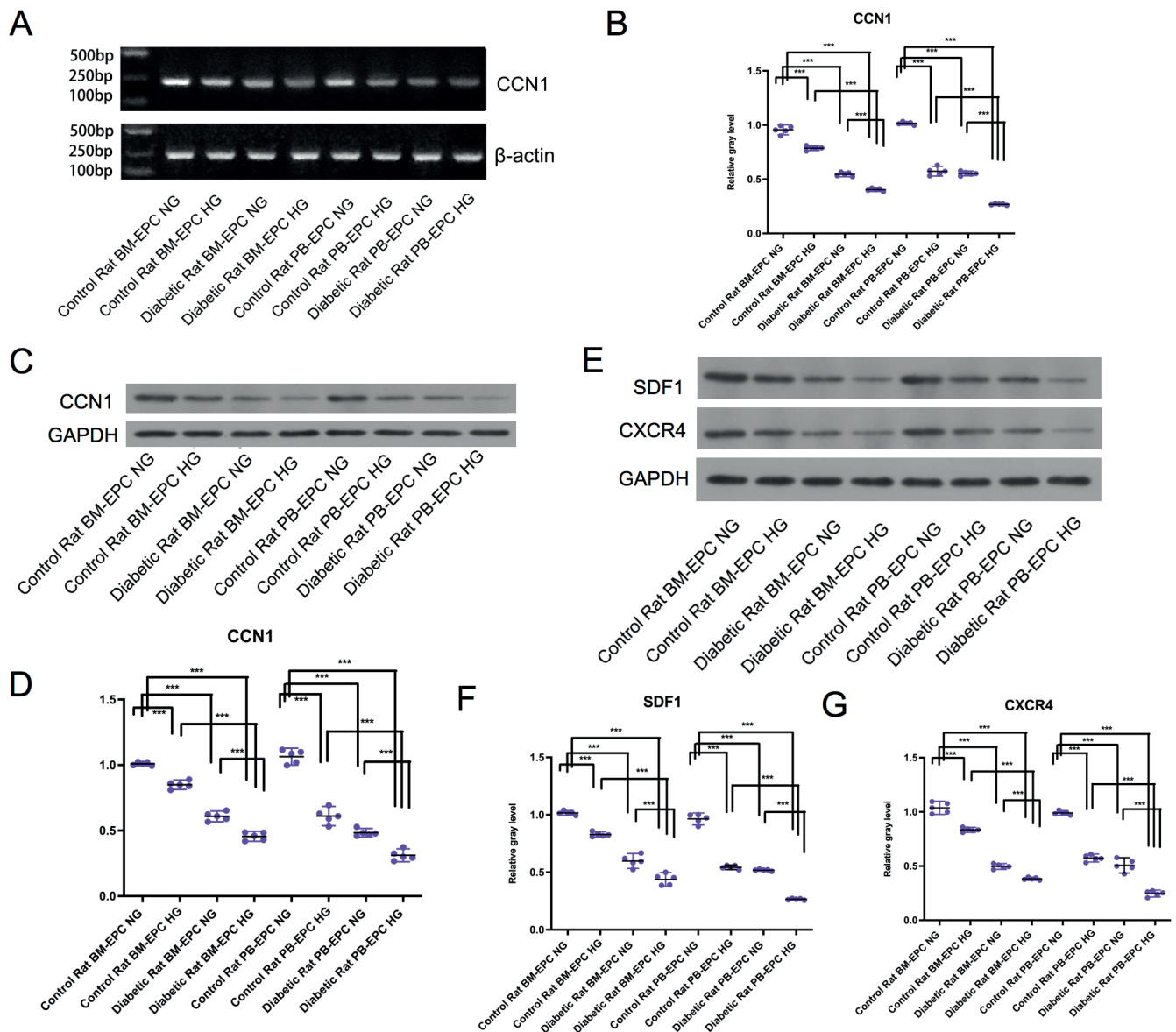


**Fig. 4.** High glucose (HG) significantly decreased messenger ribonucleic acid (mRNA) and protein levels of cysteine-rich angiogenic inducer 61 (CCN1), stromal-cell-derived factor-1 (SDF-1) and C-X-C chemokine receptor type 4 (CXCR4). A. Semi-quantitative real-time polymerase chain reaction (sqRT-PCR) showed that HG reduced *CCN1* mRNA expression levels;  $\beta$ -actin was used as a loading control; B. Real-time (RT)-qPCR analysis showed that HG reduced the expression of *CCN1* mRNA (analysis of variance (ANOVA)). For a detailed statistical analysis of the results, see Supplementary Table 6; C. Representative western blot analysis of CCN1 after treatment with HG or normal glucose (NG) medium. Glyceraldehyde 3-phosphate dehydrogenase (GAPDH) was used as a loading control; D. The stoichiometric relationship of CCN1 in the western blot analysis (ANOVA). For a detailed statistical analysis of the results, see Supplementary Table 7; E. Representative western blot analysis of SDF-1 and CXCR4 after treatment with NG or HG medium. GAPDH was used as a loading control; F,G. The stoichiometric relationship of SDF-1 and CXCR4 in the western blot analysis (ANOVA). For a detailed statistical analysis of the results, see Supplementary Tables 8,9

\*\*\*  $p < 0.001$ ; BM-EPC – bone marrow endothelial progenitor cell; PB-EPC – peripheral blood endothelial progenitor cell.

### High-glucose exposure decreased CCN1 expression levels in EPCs from diabetic rats by suppressing the MEK/ERK pathway

We explored whether CCN1 plays a role in alleviating the negative effects of HG on EPCs through MEK/ERK signaling. The MEK/ERK protein levels and their phosphorylated forms (p-MEK/p-ERK) under HG and NG conditions were evaluated by western blotting. The phosphorylation of MEK and ERK was inhibited by HG (Fig. 6A,B). To evaluate

if the rescue effect of CCN1 on EPC dysfunction is mediated through the MEK/ERK signaling pathway, the CCN1 protein levels were measured in the absence or presence of wortmannin, a MEK agonist, with or without HG. Wortmannin markedly restored the HG-reduced p-MEK and p-ERK protein levels. Moreover, HG suppression of CCN1 was restored by the MEK agonist (Fig. 6C,D and Supplementary Tables 16–18). These findings indicate that CCN1-mediated attenuation of EPC dysfunction caused by HG in diabetic rats requires MEK/ERK signaling activation, at least partially.

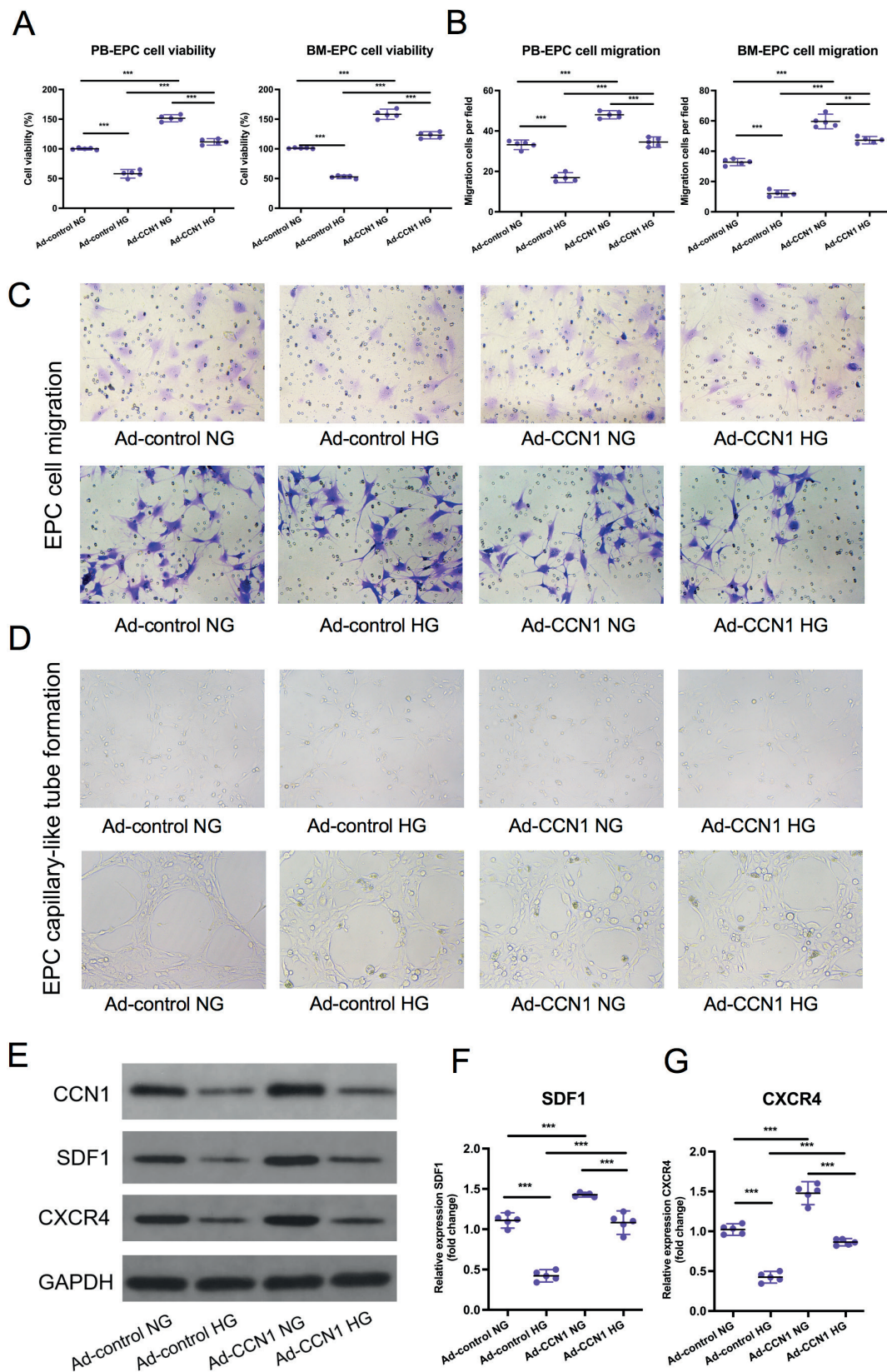


**Fig. 5.** Cysteine-rich angiogenic inducer 61 (CCN1) overexpression restored the function of peripheral blood (PB)-endothelial progenitor cells (EPCs) and bone marrow (BM)-EPCs. **A.** PB-EPCs and BM-EPCs were infected with Ad-CCN1 for 48 h to increase CCN1 expression. PB-EPC and BM-EPC viability was determined using the Cell Counting Kit-8 (CCK-8) assay after Ad-CCN1 infection and culturing in a normal (NG) or high glucose (HG) medium (analysis of variance (ANOVA)). For a detailed statistical analysis of the results, see Supplementary Tables 10,11; **B.** The migration rate of PB-EPCs and BM-EPCs treated with Ad-CCN1 under HG or NG conditions (ANOVA). For a detailed statistical analysis of the results, see Supplementary Tables 12,13; **C.** PB-EPC and BM-EPC levels were determined manually using ImageJ software. Representative migratory cells were observed microscopically over time; **D.** Tube formation capacity of BM-EPCs infected with Ad-CCN1 under HG or NG conditions. PB-EPCs and BM-EPCs were seeded on Matrigel-coated plates and observed under a light microscope; **E.** Representative western blot analysis of stromal-cell-derived factor-1 (SDF-1), CCN1 and C-X-C chemokine receptor type 4 (CXCR4) proteins after Ad-CCN1 infection and culturing in NG or HG media; glyceraldehyde 3-phosphate dehydrogenase (GAPDH) was used as a loading control; **F,G.** Real-time quantitative polymerase chain reaction (RT-qPCR) analysis of SDF-1 and CXCR4 messenger ribonucleic acid (mRNA) levels after Ad-CCN1 infection and culture in NG or HG media (ANOVA). For a detailed statistical analysis of the results, see Supplementary Tables 14,15

\*\*  $p < 0.01$ ; \*\*\*  $p < 0.001$ .

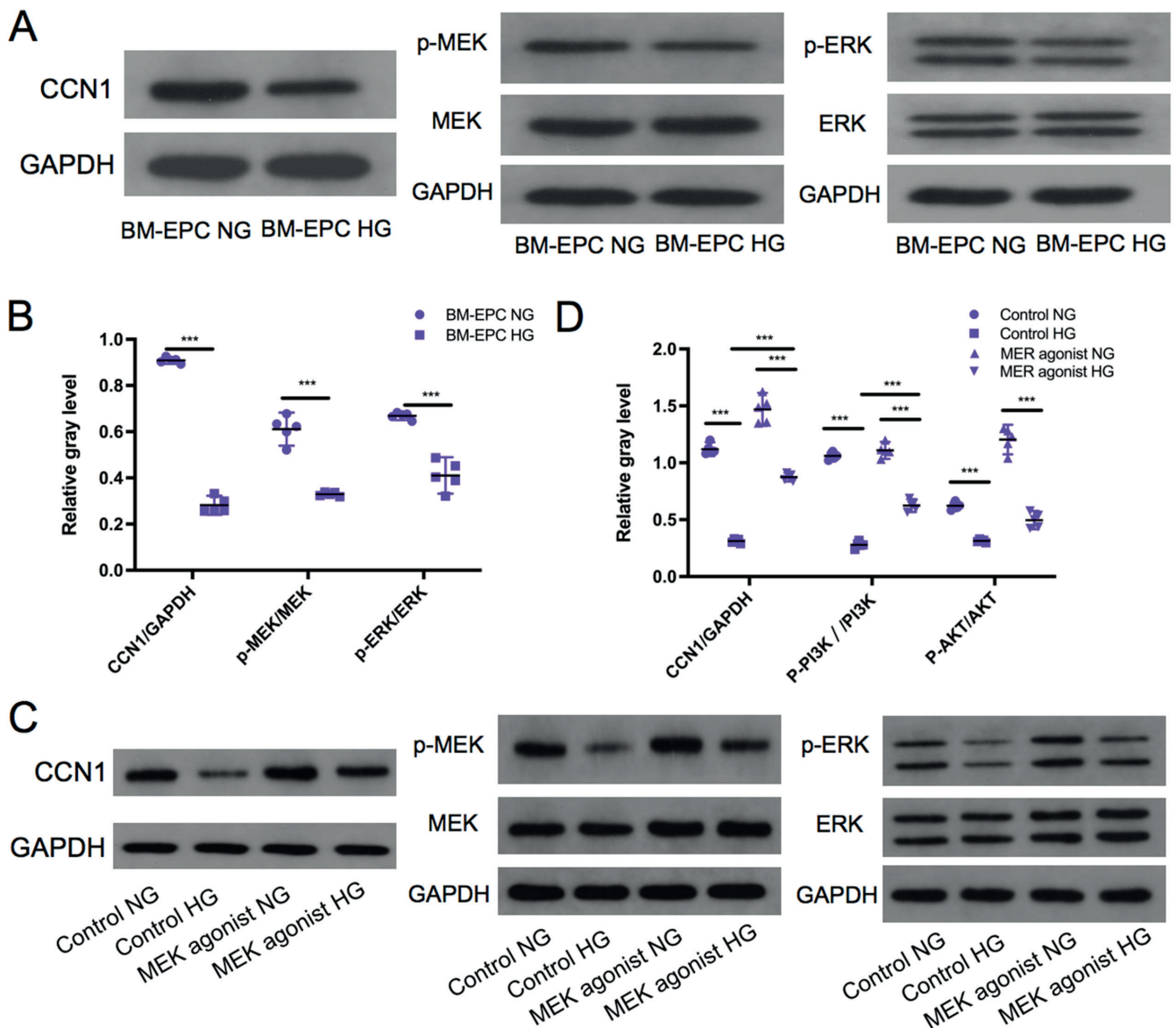


**Fig. 6.** High glucose (HG) decreased cysteine-rich angiogenic inducer 61 (CCN1) expression in bone marrow-endothelial progenitor cells (BM-EPCs) by regulating mitogen-activated protein kinase kinase/extracellular signaling kinase (MEK/ERK) signaling. **A.** Western blot analysis of CCN1, phosphorylated (p)-MEK, MEK, p-ERK, and ERK levels after HG treatment; glyceraldehyde 3-phosphate dehydrogenase (GAPDH) was used as a loading control; **B.** The stoichiometric relationship between CCN1 and GAPDH (CCN1/GAPDH), p-MEK and MEK (p-MEK/MEK), and p-ERK and ERK (p-ERK/ERK) protein levels in BM-EPCs with or without HG (Student's *t*-test); **C.** Representative CCN1, p-MEK, MEK, p-ERK, and ERK western blot analysis after MEK agonist treatment, with or without HG; GAPDH was used as a loading control; **D.** The stoichiometric relationship between CCN1/GAPDH, p-MEK/MEK, and p-ERK/ERK protein levels in BM-EPCs after MEK agonist treatment with or without HG (analysis of variance (ANOVA)). For a detailed statistical analysis of the results, see Supplementary Tables 16–18

\*\*\*  $p < 0.001$ .

## Discussion

Vascular complications are significantly responsible for the morbidity and mortality in diabetes mellitus. Indeed, hyperglycemia is a key factor leading to vascular disorders and results in neovascularization and endothelial dysfunction.<sup>23</sup> Endothelial progenitor cells circulating in the blood modulate neovascularization and vascular repair.<sup>18</sup> The findings of the present study show that the negative impact of HG on EPCs in diabetic rats is mediated through the suppression of *CCN1* expression and its target genes, *SDF-1* and *CXCR4*.<sup>14,24</sup> Furthermore, the overexpression

of *CCN1* alleviated EPC dysfunction by activating MEK/ERK signaling,<sup>25</sup> implying that defective EPCs can be modulated by pharmacological interventions using MEK agonists to restore cell function. In addition, this study showed that *CCN1* modulates MEK/ERK signaling in EPCs, potentially by regulating SDF-1 and CXCR4 activity.<sup>26</sup> These findings indicate that *CCN1* is highly expressed in EPCs and performs its function through the MEK/ERK pathway by modulating SDF-1 and CXCR4 activity.

Currently, the effects of EPCs on vascular dysfunction in diabetes are not well understood. Indeed, there are significant differences in endothelial cell behaviors,



vascularization and impaired microvascular processes in the eye,<sup>27</sup> which can be partly attributed to the variability of circulating EPC subpopulations involved in the regenerative processes of impaired vascular beds. Available data from type 1 and type 2 diabetic rodent models suggests that diabetic EPCs are not involved in vascular injury repair.<sup>28</sup> Notably, endothelial dysfunction precedes atherosclerosis and its clinical manifestations. Thus, approaches aimed at restoring the endothelial cell layer and endothelial functions play crucial roles in maintaining healthy vessels.<sup>29</sup> Neovascularization is driven by the accumulation of EPCs at the endothelial injury site, the migration and proliferation of differentiated endothelial cells, and the incorporation of EPCs into the nascent endothelium.<sup>30</sup> In animal models, EPCs constitute 25% of all endothelial cells in newly formed vessels.<sup>29</sup>

The *CCNI* has low expression levels under normal conditions and high expression levels in pathological states such as atherosclerosis, colitis, diabetic retinopathy, rheumatoid arthritis, and Graves' orbitopathy,<sup>13,31</sup> and has been reported to have a causative role in atherosclerosis,<sup>31</sup> while *CCNI* polymorphisms are associated with the risk of acute coronary syndrome (ACS) in humans.<sup>32</sup> Low *CCNI* expression levels in rats with carotid balloon injury restore vascular smooth muscle cell (VSMC) proliferation, alleviating vascular intimal hyperplasia.<sup>33</sup> In addition, the suppression of *CCNI* signaling results in reduced VSMC senescence in the smooth muscle cell layer of the human coronary artery.<sup>34</sup> Moreover, *CCNI* was reported to affect 30-day mortality in CAD and acute heart failure (AHF) patients, and it could identify myocardial ischemic injury and the clinical progression of ACS.<sup>35</sup> Hence, even though the present study reports that the high expression of *CCNI* is beneficial for EPC functions, it also appears to be involved in CAD. As such, it could be hypothesized that *CCNI* is indeed causative in CAD, but EPCs evolve to respond to increased *CCNI* expression. However, this hypothesis needs to be examined in future studies. Furthermore, the relationship between CAD and circulating *CCNI* in diabetic and non-diabetic patients has not been fully explored.

Endothelial progenitor cells have a direct role in vasculogenesis and pro-angiogenic factor secretion. The SDF-1, and its receptor CXCR4, are involved in the retention and quiescence of EPCs within their niche in the bone marrow.<sup>36</sup> The SDF-1 desensitizes insulin in adipocytes, and its expression is induced in obesity and during fasting. Moreover, SDF-1 plays a role in the chemotactic recruitment of several types of cells, e.g., hematopoietic stem cells and mesenchymal progenitor cells.<sup>37</sup> Studies report that the SDF-1/CXCR4 axis modulates fracture healing by fine-tuning of the recruitment and differentiation of progenitor and stem cells at fracture sites.<sup>15,38</sup> The SDF-1 is also involved in the pathogenesis, progression and diverse pathological effects of type 2 diabetes, including adipose tissue

inflammation, nephropathy and insulinitis.<sup>39</sup> Arakura et al.<sup>40</sup> reported that SDF-1 and CXCR4 expression and localization at fracture sites showed changes in the course of fracture healing in a diabetic model, probably associated with defective fracture healing and the inhibition of angiogenesis. The dysregulation of the interaction between SDF-1 and CXCR4 is a potential approach for EPC mobilization.

Previous studies report that low *SDF-1* expression levels in diabetic wound tissues are involved in impaired diabetic wound healing. The activation of MEK/ERK signaling induces the phosphorylation of the insulin receptor substrate 1 (IRS-1) protein at a serine residue, degradation of IRS-1, glucose uptake, and attenuation of insulin-facilitated protein kinase B (AKT) phosphorylation.<sup>21,41</sup> Furthermore, plasma SDF-1 levels correlate with type 2 diabetes.<sup>24</sup> The present study showed that HG reduced *CCNI* expression, and the overexpression of *CCNI* restored EPC function. The *CCNI* overexpression also rescued HG-induced suppression of SDF-1 and CXCR4 protein levels, enhancing EPC viability, migration and tube formation.

Various studies indicate that HG reduces EPC function by impairing MEK/ERK signaling. Indeed, the impairment of early EPCs induced by HG can be restored by modulating the mitogen-activated protein kinase (MAPK) pathway.<sup>42</sup> Consistent with these findings, the current study showed that HG downregulated MEK/ERK protein levels and phosphorylation. An ERK1/2 agonist rescued EPC dysfunction caused by HG and restored *CCNI*-SDF-1/CXCR4 protein levels.<sup>43</sup> Yan et al.<sup>36</sup> reported that the interaction between SDF-1 and CXCR4 upregulates matrix metalloproteinase 9 (MMP-9) activity and VEGF expression, inducing angiogenesis and tissue regeneration. Furthermore, the binding of SDF-1 to CXCR4 induces the activation of ERK, AKT and mammalian target of rapamycin (mTOR) signaling and promotes cell proliferation and differentiation, resulting in angiogenesis and tissue regeneration and ultimately ordered remodeling. The findings indicate that the *CCNI*-mediated attenuation of EPC dysfunction due to HG partly requires the activation of MEK/ERK signaling.

Impaired EPCs were observed in type 1 and 2 diabetes, prediabetes, metabolic syndrome, and insulin resistance,<sup>44,45</sup> and were also identified as a cause of vascular complications of diabetes.<sup>46</sup> The exact mechanisms of EPC impairment in diabetes remain poorly understood. The reduced numbers of EPCs are thought to be related to decreased mobilization from the bone marrow, decreased proliferation and shorter survival, as observed in the present study. The EPC mobilization is controlled by chemokines such as SDF-1, VEGF, granulocyte-colony stimulating factor (G-CSF), and CXCR4.<sup>47,48</sup> Still, the SDF-1/CXCR4 axis is activated in diabetes,<sup>49,50</sup> indicating that other mechanisms are at play. Insulin resistance is a possible culprit, since the development of insulin resistance and diabetes has been shown to lead to weaker EPCs.<sup>9,51,52</sup> Knocking down nuclear factor kappa-B (NF- $\kappa$ B), a key player in insulin resistance and diabetes, improved EPC

functions.<sup>52</sup> Unfortunately, the biomarkers of insulin resistance and genes/proteins involved in insulin resistance were not assessed in the present study, though they will be explored in future research.

## Limitations

Endothelial progenitor cells were isolated without differentiating between early and late EPCs,<sup>7,8,10,53</sup> which reflects the biological reality more accurately, since both types of cells can be found in animals and humans. Still, future studies could explore possible differences between EPC subtypes. Only a few genes and proteins were examined, preventing the determination of the exact mechanisms involved in EPC functional impairment in diabetes.

## Conclusions

High glucose significantly affected the viability, migration and tube formation ability of EPCs. The study shows that the mechanism underlying impaired EPC function is associated with the CCN1-SDF-1/CXCR4-MEK/ERK signaling. These findings indicate that MEK agonists could be used in patients with diabetes mellitus-associated vascular disorders. However, further studies should explore the effects of *CCN1* overexpression and ERK agonists in vivo.

## Supplementary data

The supplementary materials are available at <https://doi.org/10.5281/zenodo.8219770>. The package contains the following files:

Supplementary Table 1. Number of EPCs in each group of rats.

Supplementary Tables 2–5. High glucose affects EPC migration, viability and capillary-like tube formation.


Supplementary Tables 6–9. High glucose downregulates CCN1, SDF-1 and CXCR4 mRNA expression by EPCs.

Supplementary Tables 10–15. CCN1 overexpression ameliorates EPCs viability, migration and capillary-like tube formation impairment by high glucose.

Supplementary Tables 16–18. High-glucose exposure decreases expression levels of CCN1 in EPCs from rats with diabetes by suppressing MEK/ERK pathway.

## ORCID iDs

Yanting Dong  <https://orcid.org/0009-0006-6379-9915>

Xiaohui Zhou  <https://orcid.org/0009-0005-8327-6444>

Nan Zhang  <https://orcid.org/0009-0000-4151-0478>

## References

- Hirayama M, Ahsan MdN, Mitani H, Watabe S. *CYR61* is a novel gene associated with temperature-dependent changes in fish metabolism as revealed by cDNA microarray analysis on a medaka *Oryzias latipes* cell line. *J Cell Biochem*. 2008;104(4):1297–1310. doi:10.1002/jcb.21708
- Sun Y, Zhang J, Zhou Z, et al. CCN1, a pro-inflammatory factor, aggravates psoriasis skin lesions by promoting keratinocyte activation. *J Invest Dermatol*. 2015;135(11):2666–2675. doi:10.1038/jid.2015.231
- Yang R, Chen Y, Chen D. Biological functions and role of CCN1/Cyr61 in embryogenesis and tumorigenesis in the female reproductive system (review). *Mol Med Rep*. 2017;17(1):3–10. doi:10.3892/mmr.2017.7880
- Espinoza I, Menendez JA, Kvp CM, Lupu R. CCN1 promotes vascular endothelial growth factor secretion through  $\alpha\beta 3$  integrin receptors in breast cancer. *J Cell Commun Signal*. 2014;8(1):23–27. doi:10.1007/s12079-013-0214-6
- Wu P, Xu H, Li N, et al. Hypoxia-induced Cyr61/CCN1 production in infantile hemangioma. *Plast Reconstr Surg*. 2021;147(3):412e–423e. doi:10.1097/PRS.00000000000007672
- Eleftheriadou I, Dimitrakopoulou N, Kafasi N, et al. Endothelial progenitor cells and peripheral neuropathy in subjects with type 2 diabetes mellitus. *J Diabetes Complications*. 2020;34(4):107517. doi:10.1016/j.jdiacomp.2019.107517
- Zahran AM, Mohamed IL, El Asheer OM, et al. Circulating endothelial cells, circulating endothelial progenitor cells, and circulating microparticles in type 1 diabetes mellitus. *Clin Appl Thromb Hemost*. 2019;25:107602961882531. doi:10.1177/1076029618825311
- Pyšná A, Bém R, Němcová A, et al. Endothelial progenitor cells biology in diabetes mellitus and peripheral arterial disease and their therapeutic potential. *Stem Cell Rev Rep*. 2019;15(2):157–165. doi:10.1007/s12015-018-9863-4
- Hu L, Dai SC, Luan X, Chen J, Cannavici A. Dysfunction and therapeutic potential of endothelial progenitor cells in diabetes mellitus. *J Clin Med Res*. 2018;10(10):752–757. doi:10.14740/jocmr3581w
- Berezin AE. Endothelial progenitor cells dysfunction and impaired tissue reparation: The missed link in diabetes mellitus development. *Diabetes Metab Syndr*. 2017;11(3):215–220. doi:10.1016/j.dsx.2016.08.007
- Yu Y, Gao Y, Qin J, et al. CCN1 promotes the differentiation of endothelial progenitor cells and reendothelialization in the early phase after vascular injury. *Basic Res Cardiol*. 2010;105(6):713–724. doi:10.1007/s00395-010-0117-0
- Yu Y, Gao Y, Wang H, et al. The matrix protein CCN1 (CYR61) promotes proliferation, migration and tube formation of endothelial progenitor cells. *Exp Cell Res*. 2008;314(17):3198–3208. doi:10.1016/j.yexcr.2008.08.001
- Grote K, Salguero G, Ballmaier M, Dangers M, Drexler H, Schieffer B. The angiogenic factor CCN1 promotes adhesion and migration of circulating CD34<sup>+</sup> progenitor cells: Potential role in angiogenesis and endothelial regeneration. *Blood*. 2007;110(3):877–885. doi:10.1182/blood-2006-07-036202
- Mayorga ME, Kiedrowski M, McCallinhart P, et al. Role of SDF-1: CXCR4 in impaired post-myocardial infarction cardiac repair in diabetes. *Stem Cell Transl Med*. 2018;7(1):115–124. doi:10.1002/sctm.17-0172
- Yano T, Liu Z, Donovan J, Thomas MK, Habener JF. Stromal cell-derived factor-1 (SDF-1)/CXCL12 attenuates diabetes in mice and promotes pancreatic  $\beta$ -cell survival by activation of the pro-survival kinase Akt. *Diabetes*. 2007;56(12):2946–2957. doi:10.2337/db07-0291
- Holmes D. SDF-1 dysregulation mediates diabetic stem cell mobilopathy. *Nat Rev Endocrinol*. 2015;11(6):318–318. doi:10.1038/nrendo.2015.63
- Kawakami Y, li M, Matsumoto T, et al. SDF-1/CXCR4 axis in Tie2-lineage cells including endothelial progenitor cells contributes to bone fracture healing. *J Bone Miner Res*. 2015;30(1):95–105. doi:10.1002/jbmr.2318
- Wang K, Dai X, He J, et al. Endothelial overexpression of metallothionein prevents diabetes-induced impairment in ischemia angiogenesis through preservation of HIF-1 $\alpha$ /SDF-1/VEGF signaling in endothelial progenitor cells. *Diabetes*. 2020;69(8):1779–1792. doi:10.2337/db19-0829
- Tian C, Chang H, La X, Li JA, Ma L. Wushenziye formula inhibits pancreatic  $\beta$ -cell apoptosis in type 2 diabetes mellitus via MEK-ERK-caspase-3 signaling pathway. *Evid Based Complement Alternat Med*. 2018;2018:4084259. doi:10.1155/2018/4084259
- Niu CC, Zhao C, Yang Z, et al. Inhibiting CCN1 blocks AML cell growth by disrupting the MEK/ERK pathway. *Cancer Cell Int*. 2014;14(1):74. doi:10.1186/s12935-014-0074-z
- Yang P, Wang G, Huo H, Li Q, Zhao Y, Liu Y. SDF-1/CXCR4 signaling up-regulates survivin to regulate human sacral chondrosarcoma cell cycle and epithelial–mesenchymal transition via ERK and PI3K/AKT pathway. *Med Oncol*. 2015;32(1):377. doi:10.1007/s12032-014-0377-x

22. Brandl A, Yuan Q, Boos AM, et al. A novel early precursor cell population from rat bone marrow promotes angiogenesis in vitro. *BMC Cell Biol.* 2014;15(1):12. doi:10.1186/1471-2121-15-12
23. Steele AM, Shields BM, Wensley KJ, Colclough K, Ellard S, Hattersley AT. Prevalence of vascular complications among patients with glucokinase mutations and prolonged, mild hyperglycemia. *JAMA.* 2014;311(3):279. doi:10.1001/jama.2013.283980
24. Gholami Farashah MS, Pasbakhsh P, Omid A, Nekoonam S, Aryanpour R, Regardi Kashani I. Preconditioning with SDF-1 improves therapeutic outcomes of bone marrow-derived mesenchymal stromal cells in a mouse model of STZ-induced diabetes. *Avicenna J Med Biotechnol.* 2019;11(1):35–42. PMID:30800241. PMCID:PMC6359696.
25. Shimizu K, Imai H, Kawashima A, et al. Induction of CCN1 in growing saccular aneurysms: A potential marker predicting unstable lesions. *J Neuropathol Exp Neurol.* 2021;80(7):695–704. doi:10.1093/jnen/nlab037
26. Rother M, Krohn S, Kania G, et al. Matricellular signaling molecule CCN1 attenuates experimental autoimmune myocarditis by acting as a novel immune cell migration modulator. *Circulation.* 2010;122(25):2688–2698. doi:10.1161/CIRCULATIONAHA.110.945261
27. Buemi M, Allegra A, D'Anna R, et al. Concentration of circulating endothelial progenitor cells (EPC) in normal pregnancy and in pregnant women with diabetes and hypertension. *Am J Obstet Gynecol.* 2007;196(1):68.e1–68.e6. doi:10.1016/j.ajog.2006.08.032
28. Georgescu A, Alexandru N, Constantinescu A, Titorencu I, Popov D. The promise of EPC-based therapies on vascular dysfunction in diabetes. *Eur J Pharmacol.* 2011;669(1–3):1–6. doi:10.1016/j.ejphar.2011.07.035
29. Deshpande R, Kanitkar M, Kadam S, et al. Matrix-entrapped cellular secretome rescues diabetes-induced EPC dysfunction and accelerates wound healing in diabetic mice. *PLoS One.* 2018;13(8):e0202510. doi:10.1371/journal.pone.0202510
30. Avci-Adali M, Ziemer G, Wendel HP. Induction of EPC homing on bio-functionalized vascular grafts for rapid in vivo self-endothelialization: A review of current strategies. *Biotechnol Adv.* 2010;28(1):119–129. doi:10.1016/j.biotechadv.2009.10.005
31. Hsu PL, Chen JS, Wang CY, Wu HL, Mo FE. Shear-induced CCN1 promotes atheroprone endothelial phenotypes and atherosclerosis. *Circulation.* 2019;139(25):2877–2891. doi:10.1161/CIRCULATIONAHA.118.033895
32. Li YH, Luo JY, Fang BB, et al. Association between *CCN1* gene polymorphism and acute coronary syndrome in Chinese Han and Uygur populations. *Hereditas.* 2021;158(1):16. doi:10.1186/s41065-021-00180-2
33. Mo FE, Muntean AG, Chen CC, Stolz DB, Watkins SC, Lau LF. Cyr61 (CCN1) is essential for placental development and vascular integrity. *Mol Cell Biol.* 2002;22(24):8709–8720. doi:10.1128/MCB.22.24.8709-8720.2002
34. Grzeszkiewicz TM, Lindner V, Chen N, Lam SCT, Lau LF. The angiogenic factor cysteine-rich 61 (CYR61, CCN1) supports vascular smooth muscle cell adhesion and stimulates chemotaxis through integrin  $\alpha 6 \beta 1$  and cell surface heparan sulfate proteoglycans. *Endocrinology.* 2002;143(4):1441–1450. doi:10.1210/endo.143.4.8731
35. Feng B, Xu G, Sun K, Duan K, Shi B, Zhang N. Association of serum Cyr61 levels with peripheral arterial disease in subjects with type 2 diabetes. *Cardiovasc Diabetol.* 2020;19(1):194. doi:10.1186/s12933-020-01171-9
36. Yan X, Dai X, He L, et al. A novel CXCR4 antagonist enhances angiogenesis via modifying the ischaemic tissue environment. *J Cell Mol Med.* 2017;21(10):2298–2307. doi:10.1111/jcmm.13150
37. Shin J, Fukuhara A, Onodera T, et al. SDF-1 is an autocrine insulin-desensitizing factor in adipocytes. *Diabetes.* 2018;67(6):1068–1078. doi:10.2337/db17-0706
38. Aboumrad E, Madec AM, Thivolet C. The CXCR4/CXCL12 (SDF-1) signalling pathway protects non-obese diabetic mouse from autoimmune diabetes. *Clin Exp Immunol.* 2007;148(3):432–439. doi:10.1111/j.1365-2249.2007.03370.x
39. Humpert PM, Neuwirth R, Battista MJ, et al. SDF-1 genotype influences insulin-dependent mobilization of adult progenitor cells in type 2 diabetes. *Diabetes Care.* 2005;28(4):934–936. doi:10.2337/diacare.28.4.934
40. Arakura M, Lee SY, Takahara S, et al. Altered expression of SDF-1 and CXCR4 during fracture healing in diabetes mellitus. *Int Orthop.* 2017;41(6):1211–1217. doi:10.1007/s00264-017-3472-8
41. Zhang ZJ, Guo MX, Xing Y. ERK activation effects on GABA secretion inhibition induced by SDF-1 in hippocampal neurons of rats [in Chinese]. *Zhongguo Ying Yong Sheng Li Xue Za Zhi.* 2015;31(5):443–447. PMID:26827538.
42. Lu F, Liu L, Yu DH, Li XZ, Zhou Q, Liu SM. Therapeutic effect of *Rhizoma dioscoreae nipponicae* on gouty arthritis based on the SDF-1/CXCR4 and p38 MAPK pathway: An in vivo and in vitro study. *Phytother Res.* 2014;28(2):280–288. doi:10.1002/ptr.4997
43. Arai A, Aoki M, Weihua Y, Jin A, Miura O. Crkl plays a role in SDF-1-induced activation of the Raf-1/MEK/Erk pathway through Ras and Rac to mediate chemotactic signaling in hematopoietic cells. *Cell Signal.* 2006;18(12):2162–2171. doi:10.1016/j.cellsig.2006.05.001
44. Fadini GP, Sartore S, Agostini C, Avogaro A. Significance of endothelial progenitor cells in subjects with diabetes. *Diabetes Care.* 2007;30(5):1305–1313. doi:10.2337/dc06-2305
45. Dhananjayan R, Koundinya KSS, Malati T, Kutala VK. Endothelial dysfunction in type 2 diabetes mellitus. *Ind J Clin Biochem.* 2016;31(4):372–379. doi:10.1007/s12291-015-0516-y
46. Fadini GP. Circulating CD34<sup>+</sup> cells, metabolic syndrome, and cardiovascular risk. *Eur Heart J.* 2006;27(18):2247–2255. doi:10.1093/eurheartj/ehl198
47. Hattori K, Dias S, Heissig B, et al. Vascular endothelial growth factor and angiopoietin-1 stimulate postnatal hematopoiesis by recruitment of vasculogenic and hematopoietic stem cells. *J Exp Med.* 2001;193(9):1005–1014. doi:10.1084/jem.193.9.1005
48. Maeda Y, Miyatake J, Naiki Y, et al. Transient eosinophilia by HIV infection. *Ann Hematol.* 2000;79(2):99–101. doi:10.1007/s002770050019
49. Liu WS, Hua LY, Zhu SX, et al. Association of serum stromal cell-derived factor 1 levels with EZSCAN score and its derived indicators in patients with type 2 diabetes. *Endocr Connect.* 2022;11(4):e210629. doi:10.1530/EC-21-0629
50. Vidaković M, Grdović N, Dinić S, Mihailović M, Uskoković A, Arambašić Jovanović J. The importance of the CXCL12/CXCR4 axis in therapeutic approaches to diabetes mellitus attenuation. *Front Immunol.* 2015;6:403. doi:10.3389/fimmu.2015.00403
51. Makino H, Okada S, Nagumo A, et al. Decreased circulating CD34<sup>+</sup> cells are associated with progression of diabetic nephropathy. *Diabet Med.* 2009;26(2):171–173. doi:10.1111/j.1464-5491.2008.02638.x
52. Desouza CV, Hamel FG, Bidasee K, O'Connell K. Role of inflammation and insulin resistance in endothelial progenitor cell dysfunction. *Diabetes.* 2011;60(4):1286–1294. doi:10.2337/db10-0875
53. Shu C, Li TY, Tsang LL, et al. Differentiation of adult rat bone marrow stem cells into epithelial progenitor cells in culture. *Cell Biol Int.* 2006;30(10):823–828. doi:10.1016/j.cellbi.2006.06.004



# Nerolidol inhibited U-251 human glioblastoma cell proliferation and triggered apoptosis via the upregulation of the p38 MAPK signaling pathway

Zhijin Lu<sup>1,A,B,D,F</sup>, Tao Tang<sup>1,A,C,D</sup>, Juan Huang<sup>2,A,D</sup>, Yongqiang Shi<sup>3,4,A,D,F</sup>

<sup>1</sup> Trauma Surgery Emergency Center, Ganzhou People's Hospital, China

<sup>2</sup> Physical Examination Center, Ganzhou People's Hospital, China

<sup>3</sup> Surgical Intensive Care Unit, Xi'an Children's Hospital, China

<sup>4</sup> Department of Neurosurgery, Xi'an Children's Hospital, China

A – research concept and design; B – collection and/or assembly of data; C – data analysis and interpretation; D – writing the article; E – critical revision of the article; F – final approval of the article

Advances in Clinical and Experimental Medicine, ISSN 1899–5276 (print), ISSN 2451–2680 (online)

*Adv Clin Exp Med.* 2024;33(6):633–640

## Address for correspondence

Yongqiang Shi  
E-mail: zqxj100@sina.com

## Funding sources

None declared

## Conflict of interest

None declared

Received on November 7, 2022

Reviewed on February 22, 2023

Accepted on July 31, 2023

Published online on September 25, 2023

## Cite as

Lu Z, Tang T, Huang J, Shi Y. Nerolidol inhibited U-251 human glioblastoma cell proliferation and triggered apoptosis via the upregulation of the p38 MAPK signaling pathway.

*Adv Clin Exp Med.* 2024;33(6):633–640.

doi:10.17219/acem/170184

## DOI

10.17219/acem/170184

## Copyright

Copyright by Author(s)

This is an article distributed under the terms of the Creative Commons Attribution 3.0 Unported (CC BY 3.0) (<https://creativecommons.org/licenses/by/3.0/>)

## Abstract

**Background.** Glioblastoma multiforme (GBM) is a lethal brain tumor with high mortality and morbidity. Nerolidol (NRD) is a sesquiterpene alcohol sequestered from the essential oils of aromatic flora with potent antioxidant, antiviral, anticancer, cardioprotective, and neuroprotective activity.

**Objectives.** The aim of the study was to investigate the underlying cell-cycle mechanisms of NRD-mediated antiproliferative and apoptosis activities in GBM using human U-251 cells.

**Materials and methods.** The current research investigated the antiproliferative and apoptotic activities of NRD on U-251 cells. The effects of NRD were measured using a Cell Counting Kit-8 (CCK-8) assay, 4',6-diamidino-2-phenylindole (DAPI) staining, messenger ribonucleic acid (mRNA) level assessment, and western blot assay.

**Results.** Nerolidol decreased U-251 viability in a dose-dependent manner, as well as induced apoptotic activity, reduced B-cell lymphoma-2 (BCL-2) levels, and increased mRNA expression of BCL-2-associated X (Bax), caspase-3 and caspase-9. The attenuation of the cyclin-D1, cyclin-dependent kinase 4 (CDK4) and CDK6 mRNA expression confirmed cell cycle regulation. Western blot analysis of CDK1 indicated reductions in cyclin-B1 and p21. Furthermore, NRD prompted apoptosis through p38 amelioration and increased phosphorylated extracellular signal-related kinase 1 (p-ERK1) and phosphorylated c-Jun N-terminal protein kinase 1 (p-JNK1) levels.

**Conclusions.** Nerolidol inhibited GBM cell viability and induced apoptosis through the regulation of cell-cycle proteins via p38 mitogen-activated protein kinase (MAPK) signaling pathways. Thus, NRD could be developed as a potential natural therapeutic agent for GBM.

**Key words:** glioblastoma, p38 MAPK, apoptosis, nerolidol, U-251 cells



## Background

Glioblastoma multiforme (GBM) is a fatal cancer of the central nervous system; this primary brain malignancy has an annual prevalence of 3.19/100,000<sup>1,2</sup> and a high mortality rate, with a survival rate fewer than 12 months.<sup>3</sup> Owing to its rapid progression and infiltrative features, GBM is incurable despite the current treatment modalities of surgery, chemotherapy, c-irradiation, and immunotherapy.<sup>4,5</sup> Clinical research suggests that the quick propagation and high invasiveness of GBM cells make it incurable and cause relapse.<sup>6</sup> Treatment failure and continuous disease progression result in an average lifespan of 1–1.5 years.<sup>7</sup> The malignant glioma appears to proliferate incessantly. Hence, innovative approaches are urgently required to manage these devastating tumors.

Recent research suggests that novel drug development may entail targeting cell signaling pathways, with multiple signaling networks, cell cycle protein regulation, and apoptosis-associated proteins likely critical to cancer prevention.<sup>8</sup> The cell cycle is tightly controlled by regulatory proteins, such as cyclins and cyclin-dependent kinases (CDKs) that facilitate the checkpoint switches between G1/S, S and G2/M phases.<sup>9,10</sup> Anomalies in cell division or apoptosis lead to irregular cell growth, eventually causing tumor development. As such, apoptosis, a form of programmed cell death, is crucial for the growth and maintenance of healthy tissues and is regulated by specific caspases and proteases.<sup>11,12</sup>

Mitogen-activated protein kinases (MAPKs) are involved in intracellular signaling through propagation, disparity and apoptosis.<sup>13</sup> It is thought that glioma cell incursion and metastasis require the triggering of precise signaling cascades, particularly the p38 MAPK pathway.<sup>14,15</sup> Therefore, inhibiting p38 MAPK signaling is a central goal of GBM management.

Numerous natural phytochemicals act as anticancer agents by regulating the proliferation, invasion and metastasis of diverse cancer cells.<sup>16</sup> Nerolidol (NRD) is a sesquiterpene alcohol (3,7,11-trimethyl-1,6,10-dodecatrien-3-ol) extracted as an essential oil from aromatic florae, such as ginger, neroli, lemongrass, tea tree, and lavender.<sup>17</sup> It has anti-inflammatory, antioxidative, anticancer, and apoptotic properties.<sup>18</sup> Recently, NRD was shown to mitigate oxidative stress, apoptosis and inflammation in cardiotoxicity prompted by the chemotherapeutic mediator cyclophosphamide.<sup>19</sup> Furthermore, NRD blocked inflammatory responses in lipopolysaccharide (LPS)-induced acute lung injury (ALI) by modulating antioxidants and the adenosine 5'-monophosphate-activated protein kinase (AMPK)/nuclear factor erythroid 2-related factor 2 (Nrf-2)/heme oxygenase-1 (HO-1) signaling pathway.<sup>20</sup> Moreover, NRD is a beneficial antitumor compound due to its efficacy in targeting cell survival and proliferation molecules<sup>21</sup> that act as chemosensitizers in tumors.<sup>22,23</sup> Nerolidol improves the effectiveness of doxorubicin (DOX) in mammary carcinogenesis<sup>22</sup> and enhances its efficacy in ovarian cancer and lymphoblast cells.<sup>24</sup>

Nerolidol is hydrophobic in nature, with an XlogP3 value of 4.6, and can readily cross the blood–brain barrier,<sup>25</sup> where it exerts neuroprotective effects through its anti-inflammatory and antioxidant properties. Baicalein was determined to be a viable treatment for GBM in studies similar to the current research, because it reduced the viability of GBM cells and caused apoptosis by inhibiting nuclear factor kappa B (NF- $\kappa$ B)-p65 activity.<sup>26</sup> However, the anti-glioma action of NRD through MAPK signaling remains uncertain.

## Objectives

We assessed the protective influence of NRD on U-251 human GBM cells by examining proliferation, cell cycle protein regulation and apoptosis.

## Materials and methods

### Chemicals

Nerolidol, fetal bovine serum (FBS), antibiotics (penicillin-streptomycin), phosphate-buffered saline (PBS), 4',6-diamidino-2-phenylindole (DAPI), dimethyl sulfoxide (DMSO), and sodium dodecyl sulfate (SDS) were purchased from Bio-Rad Laboratories (Hercules, USA). The antibodies were obtained from Roche Diagnostics (Risch, Switzerland).

### Cell lines

The U-251 human GBM cells were purchased from Shanghai Aiyuan Biotechnology Co., Ltd. (Shanghai, China), and grown in a Dulbecco's modified Eagle's medium (DMEM) consisting of FBS (10%), streptomycin (100  $\mu$ g/mL) and penicillin (100 U/mL) under a CO<sub>2</sub> atmosphere (5%) with less than 95% humidified air at 37°C.

### Investigation of cell viability

Cell proliferation was examined using the Cell Counting Kit-8 (CCK-8) assay (Alpha Diagnostics International, San Antonio, USA). The U-251 cells were seeded onto a 96-well plate at  $1 \times 10^5$  cells per well, incubated and supplemented with different NRD dosages (10–70  $\mu$ M). The CCK-8 solution (10  $\mu$ L) was added separately to all wells. After 1 h of incubation, the optical density (OD) was determined at 450 nm using a microplate absorbance reader, model No. 1681130 (Bio-Rad Laboratories).

### Apoptosis exploration by DAPI staining

Human GBM U-251 cells were seeded into 6 wells at  $1 \times 10^5$  cells/well. Each well was then supplemented with

NRD (30  $\mu\text{M}$  and 40  $\mu\text{M}$ ). Treated U-251 cells were stained with DAPI and observed under a fluorescence microscope (Eclipse TS100; Nikon, Tokyo, Japan) with a digital camera (4500 Coolpix; Nikon) to assess cellular apoptotic changes, according to a previously described method.<sup>27</sup>

## Determination of messenger ribonucleic acid expression

Total ribonucleic acid was isolated from human GBM cells U-251 as per the manufacturer's protocol using TRIzol<sup>®</sup> reagent (Abcam, Cambridge, USA). The isolated messenger RNA (mRNA) was reverse-transcribed into complementary DNA (cDNA) using a cDNA reverse transcription kit (Abcam), according to the manufacturer's instructions. Then, SYBR Green Real-Time PCR Master Mixes (Thermo Fisher Scientific, Waltham, USA) examined the cDNAs using the company's protocols. The band intensity was observed after electrophoresis using 1.5% agarose gels. The band intensity was measured using ImageJ v. 1.48 software (National Institutes of Health, Bethesda, USA). Primer sequences used included B-cell lymphoma-2 (BCL-2), BCL-2 associated X (Bax), caspase-3, cyclin-D1, cyclin-dependent kinase 4 (CDK4), CDK6, and glyceraldehyde 3-phosphate dehydrogenase (GAPDH), as outlined below in Table 1:

Table 1. List of designed gene-specific primer pairs

Primer	Sequence
BCL-2	5'-GAGGATTGTGGCCTTCTTTG-3'
	5'-ACAGTTCACAAAGGCATCC-3'
Bax	5'-TTTGCTTCAGGGTTTCATCC-3'
	5'-CAGTTGAAGTTGCCGTCAGA-3'
Caspase-3	5'-TGTGAGGCGGGTTGATAGAAATT-3'
	5'-GCTGCATCGACATCTGTACC-3'
Cyclin-D1	5'-CCGAGGAGCTGCTGCAAATGGAG-3'
	5'-TGAAATCGTGCGGGTCATTGCG-3'
CDK4	5'-CAGAGCTCTTAGCCGAGCGT-3'
	5'-GGCACCGACCAATTCAG-3'
CDK6	5'-AGTCTGATTACCTGCTCCG-3'
	5'-CCTCGAAGCGAAGTCTCAA-3'
GAPDH	5'-GTCTTCACCACCATGGAGAA-3'
	5'-CGTTCAGTCTGGGATGACC-3'

BCL-2 – B-cell lymphoma 2 protein family; Bax – BCL-2-associated X protein; CDK4 – cyclin-dependent kinases 4; CDK6 – cyclin-dependent kinases; GAPDH – glyceraldehyde-3-phosphate dehydrogenase.

## Western blot study

Human U-251 GBM cells were treated with NRD (30  $\mu\text{M}$  and 40  $\mu\text{M}$ ) and cultured for 24 h. Cell lysates were prepared for western blot analysis using an ice-cold lysis buffer containing protease inhibitors. Total protein content was measured using Protein BCA Assay Kit (Pierce Chemical,

Rockford, USA). The proteins were electrophoretically dispersed and transferred to a polyvinylidene difluoride (PVDF) film, which was blocked with a probe for 60 min at room temperature and incubated with primary antibodies (1:1000 dilutions) overnight at 4°C. Thereafter, the secondary antibodies were added and visualized using an enhanced chemiluminescence protein detection kit (Pierce Chemical).

## Statistical analyses

All statistical analyses employed GraphPad Prism v. 8.0.1 (GraphPad Software, San Diego, USA) and IBM Statistical Package for Social Sciences (SPSS) v. 25 (IBM Corp., Armonk, USA) software. The measurement data were reported as medians and quartiles. The normality of the distribution was tested using the Kolmogorov–Smirnov test (Supplementary Table 1), and although all data displayed a normal distribution, a nonparametric test was used due to small sample sizes. Comparisons among groups (control (n = 6), 30  $\mu\text{M}$  (n = 6) and 40  $\mu\text{M}$  (n = 6)) utilized the Kruskal–Wallis test followed by Dunn's test. When the test standard had a value of  $p < 0.05$ , the difference was considered statistically significant.

## Results

All variables had a normal distribution. Table 2 displays the results of comparing variables between groups.

### Effects of nerolidol on U-251 cytotoxicity

The U-251 GBM cell proliferation was assessed using multiple NRD treatments (10, 20, 30, 40, 50, and 60  $\mu\text{M}/\text{mL}$ )

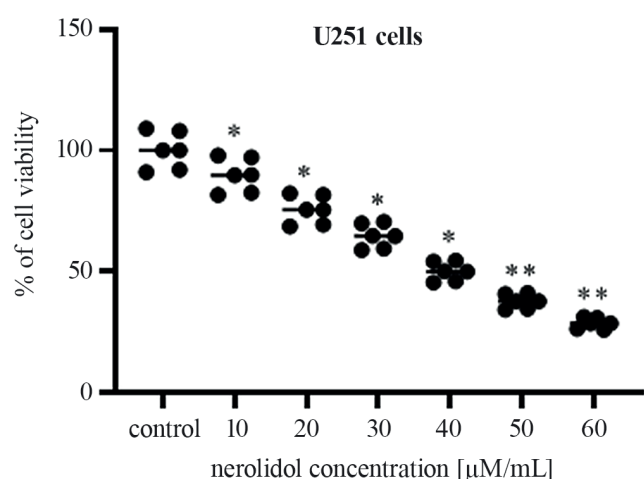


Fig. 1. Nerolidol (NRD) inhibited U-251 human glioblastoma cell viability. Cells were supplemented with various concentrations (10–70  $\mu\text{M}$ ) of NRD and cultured for 1 day. The cell viability was then evaluated using a Cell Counting Kit-8 (CCK-8) assay. The differences between the groups were analyzed using the Kruskal–Wallis test with Dunn's post-hoc analysis. The data are expressed as median and quartiles

n = 3; \* $p < 0.01$ ; \*\* $p < 0.05$ .

**Table 2.** The normality of the distribution (Kolmogorov–Smirnov test)

Variables	Groups			
	Control (n = 6)	30 $\mu$ M (n = 6)	40 $\mu$ M (n = 6)	p-value
Caspase-3	1 (0.91, 1.08)	1.21 (1.10, 1.32)	1.49 (1.36, 1.62)	<0.001
Caspase-9	1 (0.91, 1.08)	1.19 (1.08, 1.30)	1.42 (1.29, 1.55)	<0.001
Bax	1 (0.91, 1.08)	1.29 (1.17, 1.41)	1.67 (1.52, 1.82)	<0.001
BCL-2	1 (0.91, 1.08)	0.75 (0.68, 0.82)	0.50 (0.46, 0.55)	<0.001
Cyclin-D1	1 (0.91, 1.08)	0.79 (0.72, 0.86)	0.61 (0.56, 0.66)	<0.001
CDK4	1 (0.91, 1.08)	0.68 (0.62, 0.74)	0.48 (0.44, 0.52)	<0.001
CDK6	1 (0.91, 1.08)	0.74 (0.67, 0.81)	0.54 (0.49, 0.59)	<0.001
Cyclin-B1	1 (0.91, 1.08)	0.75 (0.68, 0.82)	0.48 (0.44, 0.52)	<0.001
CDK1	1 (0.91, 1.08)	0.63 (0.57, 0.69)	0.39 (0.35, 0.43)	<0.001
p21	1 (0.91, 1.08)	1.20 (1.09, 1.31)	2.1 (1.91, 2.29)	<0.001
p-p38 MAPK/p38 MAPK	1 (0.91, 1.08)	1.36 (1.24, 1.48)	2.60 (2.37, 2.83)	<0.001
p-JNK/JNK	1 (0.91, 1.08)	1.45 (1.32, 1.58)	2.29 (2.08, 2.50)	<0.001
p-ERK/ERK	1 (0.91, 1.08)	1.51 (1.37, 1.65)	2.86 (2.60, 3.12)	<0.001

Data are presented as median (1<sup>st</sup> quartile (Q1) and 3<sup>rd</sup> quartile (Q3)). The p-values were generated using Kruskal–Wallis test. There was a significant difference among all groups in Dunn's test.

for 24 h. Nerolidol significantly ( $p < 0.05$ ) reduced cell proliferation in a concentration-dependent manner. The optimum dosages of 30  $\mu$ M and 40  $\mu$ M, identified as the IC<sub>50</sub> values, were used for further experiments (Fig. 1). Nerolidol treatment at 30  $\mu$ M and 40  $\mu$ M significantly ( $p < 0.05$  and  $p < 0.01$ , respectively) inhibited U-251 growth, indicating that NRD is a potential bioactive remedy for GBM.

### Effects of nerolidol on U-215 apoptosis

The DAPI-stained control U-251 cells remained viable, while NRD-treated cells (30  $\mu$ M and 40  $\mu$ M) showed significant apoptosis induction ( $p < 0.05$ ). The shrinkage of cytoplasm, nuclear membrane loss and nucleus disintegration were observed with NRD usage. The administration of 40  $\mu$ M NRD caused an increased apoptotic effect (Fig. 2).

### Effects of nerolidol on apoptotic mRNA expression

The untreated U-251 GMB cells had decreased caspase-3 and Bax mRNA levels, whereas the levels of BCL-2 were elevated (Fig. 3). Nerolidol (30  $\mu$ M and 40  $\mu$ M) treatment enhanced the levels of Bax and caspase-3, and diminished BCL-2 significantly ( $p < 0.05$ ). These findings indicate that NRD reduced U-251 viability through apoptosis.

### Effects of nerolidol on cell cycle gene expression

The mRNA levels in NRD-treated U-251 GMB cells are shown in Fig. 4. The untreated cells had augmented mRNA levels of cyclin-D1, CDK4 and CDK6. Nerolidol (30  $\mu$ M and

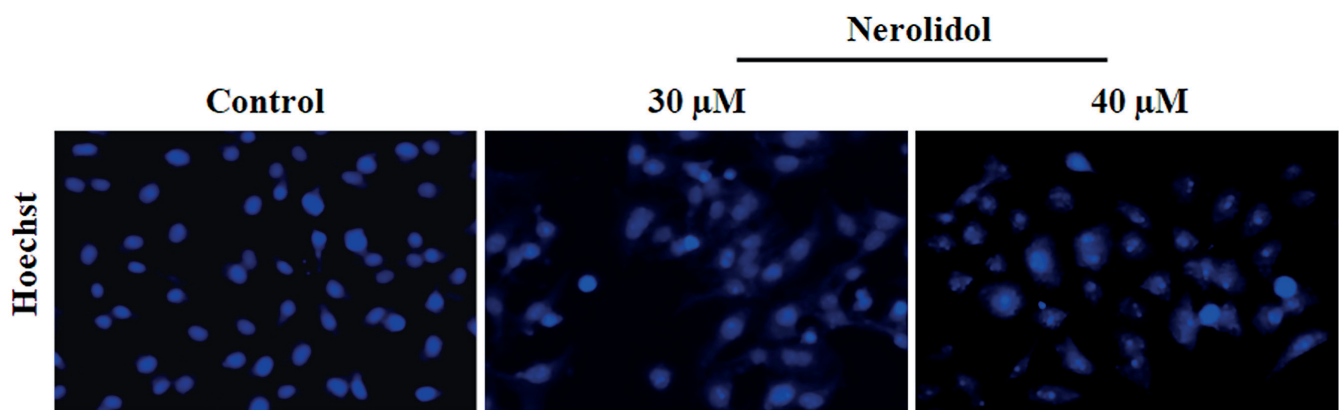


**Fig. 2.** The effects of nerolidol (NRD) on U-251 human glioblastoma cell apoptosis as detected using DAPI staining. The U-251 cells were supplemented with 30  $\mu$ M/mL or 40  $\mu$ M/mL doses of NRD for 1 day; then, cell death was examined with DAPI staining using a fluorescence microscope. The differences between the groups were analyzed using the Kruskal–Wallis test with Dunn's post-hoc analysis. Data are expressed as median and quartiles

$n = 3$ ; \* $p < 0.01$ ; DAPI – 4',6-diamidino-2-phenylindole.

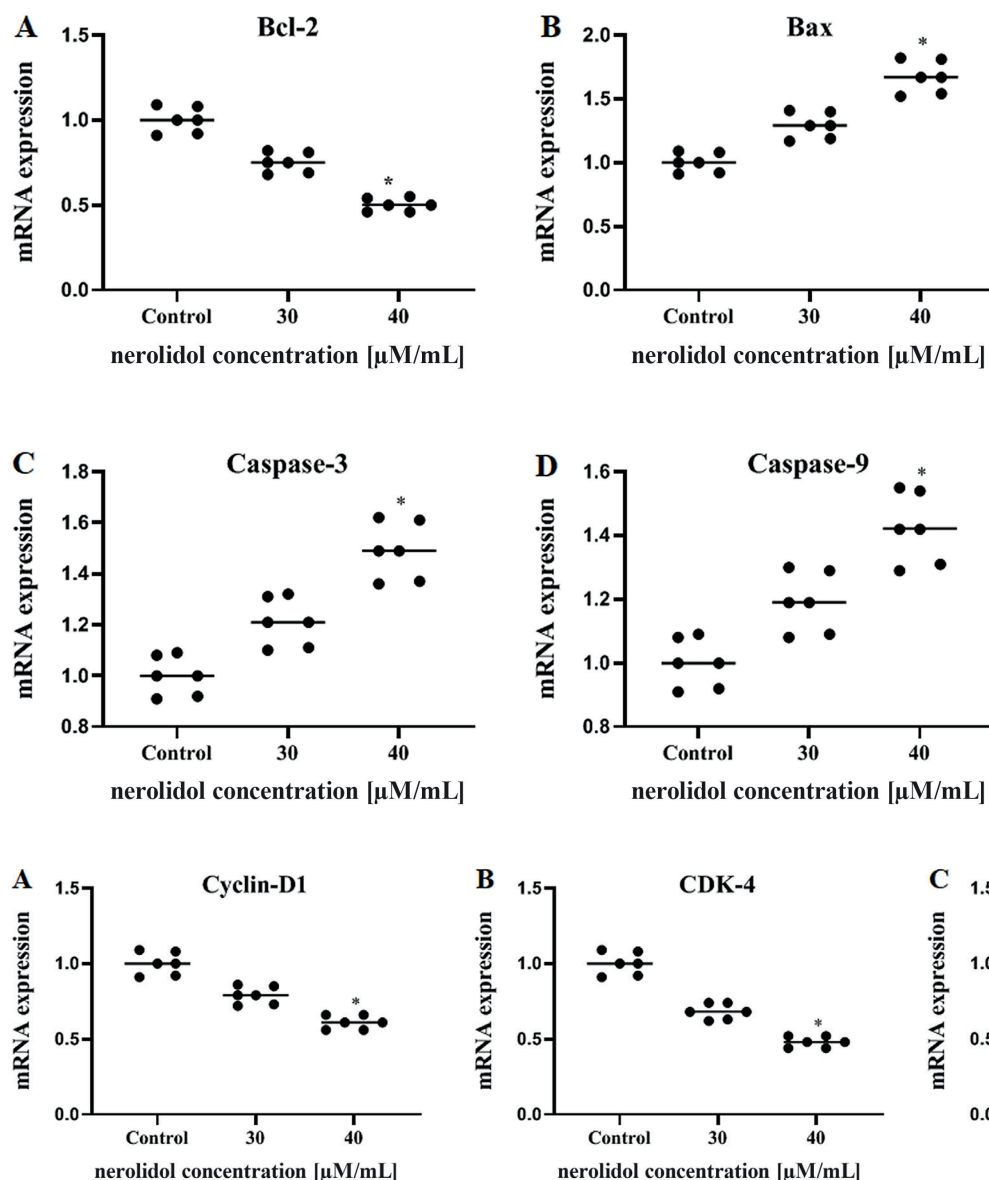


**Fig. 3.** The effects of nerolidol (NRD) on the mRNA levels of BCL-2 (A), Bax (B), caspase-3 (C), and caspase-9 (D). The U-251 cells were supplemented with 30 μM or 40 μM doses of NRD. The mRNA levels of BCL-2, Bax and caspase-3 were assessed using reverse transcription polymerase chain reaction (RT-PCR). The differences between the groups were analyzed using the Kruskal–Wallis test with Dunn’s post-hoc analysis. The data are expressed as median and quartiles

n = 3; \*p < 0.01; BCL-2 – B-cell lymphoma-2; Bax – BCL-2 associated X protein; mRNA – messenger ribonucleic acid.

**Fig. 4.** The effects of nerolidol (NRD) on the mRNA levels of cyclin D1 (A), CDK4 (B) and CDK6 (C) in U-251 human glioblastoma cells supplemented with 30 μM or 40 μM NRD. The cyclin D1, CDK4 and CDK6 mRNA levels were assessed using reverse transcription polymerase chain reaction (RT-PCR). The differences between the groups were analyzed using the Kruskal–Wallis test with Dunn’s post-hoc analysis. Data are expressed as median and quartiles n = 3; \*p < 0.01; CDK4 – cyclin-dependent kinase 4; CDK6 – cyclin-dependent kinase 6; mRNA – messenger ribonucleic acid.

40 μM) significantly (p < 0.05) reduced the mRNA levels, with 40 μM NRD causing greater reductions than 30 μM.

### Effects of nerolidol on cyclin-B1, CDK1 and p21 protein levels

Nerolidol (30 μM and 40 μM) reduced cyclin-B1 and CDK1, whereas it augmented p21 in a dosage-reliant way. The increase in protein expressions indicates that NRD controlled the cell cycle and apoptosis in U-251 cells (Fig. 5).

### Effects of nerolidol on MAPK protein levels

Administration of NRD (30 μM and 40 μM) significantly enhanced phosphorylated p38 MAPK protein levels

(p < 0.05) in U-251 cells. Meanwhile, phosphorylated extracellular signal-related kinase 1 (p-ERK) and phosphorylated c-Jun N-terminal protein kinase 1 (p-JNK) were also slightly increased (Fig. 6). The enhanced MAPK protein expression indicates that NRD-induced apoptosis in U-251 cells is associated with p38 MAPK signaling.

## Discussion

The GBM is the most aggressive primary brain malignancy and has high mortality and morbidity.<sup>1,2</sup> Moreover, GBM patients have a poor prognosis, with a median survival time of 10–12 months.<sup>3,7</sup> Chemopreventive agents treat all phases of tumor evolution and prevent cancer cell



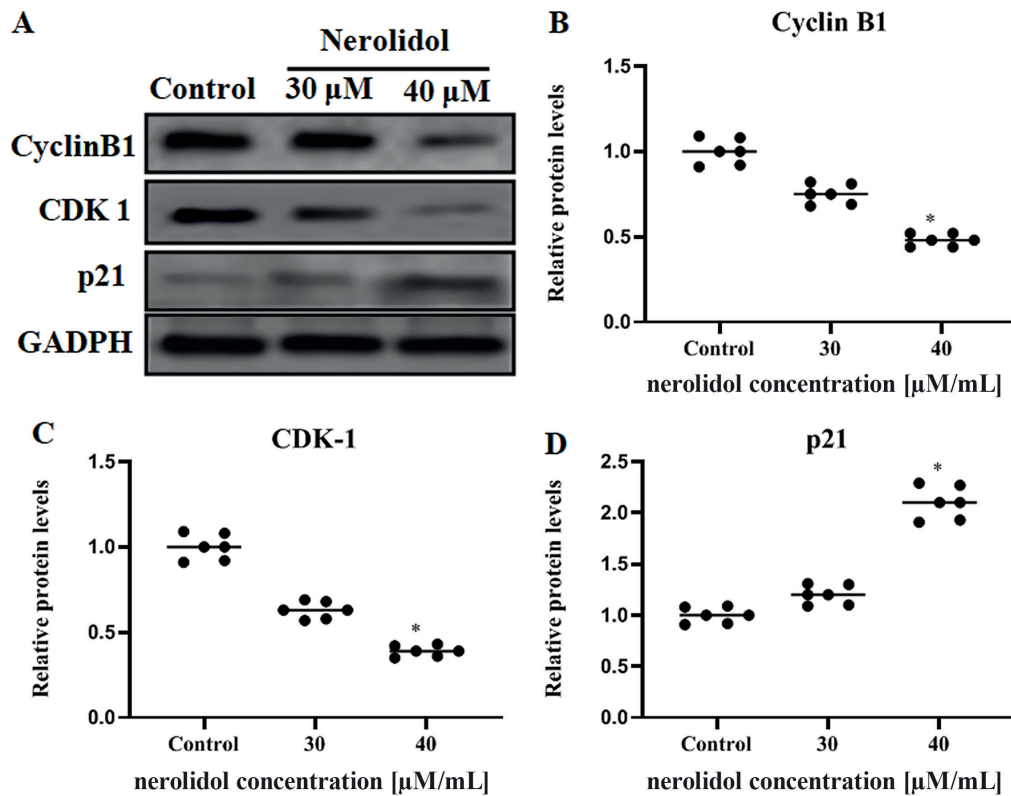


**Fig. 5.** A. Effects of nerolidol (NRD) on CDK1, cyclin-B1 and p21 protein levels. The U-251 human glioblastoma cells supplemented with 30  $\mu\text{M}/\text{mL}$  or 40  $\mu\text{M}/\text{mL}$  NRD were incubated for 1 day before western blot analysis of protein levels; B–D. The differences between the groups were analyzed using the Kruskal–Wallis test with Dunn’s post-hoc analysis. Data are expressed as median and quartiles

$n = 3$ ; \* $p < 0.01$ ; CDK1 – cyclin-dependent kinase 1.

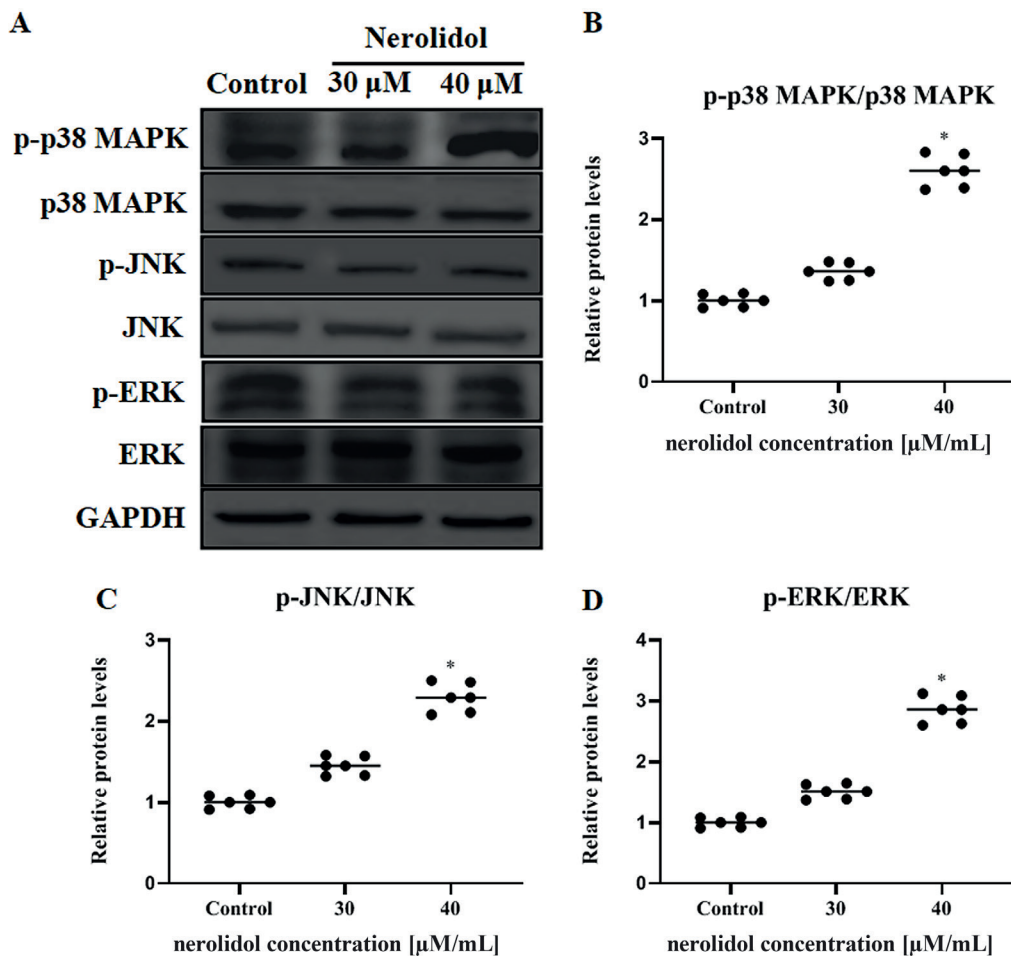


**Fig. 6.** The effects of nerolidol (NRD) on MAPK protein levels. The U-251 human glioblastoma cells were supplemented with 30  $\mu\text{M}/\text{mL}$  or 40  $\mu\text{M}/\text{mL}$  of NRD and cultured for 1 day. A. The protein levels of p38 MAPK, JNK, and ERK were examined using western blot; B–D. The differences between the groups were analyzed using the Kruskal–Wallis test with Dunn’s post-hoc analysis. Data are expressed as median and quartiles

$n = 3$ ; \* $p < 0.01$ ; MAPK – mitogen-activated protein kinase; JNK – c-Jun N-terminal kinase; ERK – extracellular signal-regulated kinase.



propagation, incursion and metastasis,<sup>16</sup> and several phytochemicals act by inhibiting proliferation, invasion, metastasis, angiogenesis, and stimulating apoptosis.<sup>14,15</sup> The anticancer effects of NRD have been extensively explored in numerous cancers, including breast cancer,<sup>22</sup> hepatocellular carcinomas,<sup>28</sup> osteosarcomas,<sup>29</sup> oral cancer,<sup>30</sup> and ovarian cancer.<sup>24</sup> The current research evaluated the anti-GBM effects of NRD by assessing its anti-proliferative, cell-cycle protein regulation and apoptotic properties. Our results showed that NRD inhibited U-251 cell multiplication and cell cycle proteins and induced apoptosis in a dose-dependent manner.

Apoptosis is a well-recognized cell death program triggered by various stimuli.<sup>11,12</sup> Certain natural bioactive anticancer agents were shown to eliminate malignant cells by restoring defective apoptosis.<sup>31</sup> The CCK-8 assay demonstrated that NRD could dramatically inhibit GBM cell viability, indicating that NRD displayed a robust anti-proliferative action on U-251 cells. Furthermore, DAPI staining showed that NRD treatment improved programmed cell death in GBM cells. Likewise, reverse transcription polymerase chain reaction (RT-PCR) results showed reduced BCL-2 and elevated Bax and caspase-3 mRNA levels after NRD treatment. These are well-known as apoptosis-associated proteins, and the ratio of BCL-2 to Bax was markedly reduced by NRD. Similar anti-proliferative and apoptotic properties of NRD were reported in hepatocellular carcinoma<sup>27</sup> and osteosarcoma.<sup>28</sup> Our findings demonstrate that NRD inhibited proliferation and stimulated apoptosis in U-251 cells.

Cell-cycle checkpoints play a vital role in cellular development and apoptosis,<sup>9,10</sup> and NRD is described as an anti-proliferative mediator in leiomyoma cells by diminishing the cyclin-D1 and CDK4/6 G1-S checkpoint proteins. Matus et al. reported that NRD (cis- and trans-) stimulated G1 cell cycle arrest in ELT3 cells.<sup>32</sup> Satomi et al. confirmed that NRD triggered G1 cell cycle arrest in human hepatocellular carcinoma cells by increasing cytochrome-P450 enzymes.<sup>33</sup> As such, the underlying anticancer mechanisms of NRD are thought to involve cell cycle arrest,<sup>27</sup> oxidative phosphorylation reduction<sup>32</sup> and apoptosis.<sup>34</sup> In the current research, NRD treatment reduced the mRNA expression of cyclin-D1, CDK4 and CDK6, while it increased p21 expression and reduced CDK1 and cyclin-B1 protein levels. The cell-cycle transition from the S phase to the G2/M phase is largely determined by the CDK1 and cyclin-B1 complexes.<sup>9,10</sup> Collectively, these findings suggest that NRD employed anti-proliferative effects in GBM cells by stimulating cell death through cell-cycle arrest.

The MAPKs play a central role in cell development, proliferation and death. Highly conserved MAPKs in mammalian cells consist of p38, ERK and JNK, which are stimulated via a phosphorylation cascade.<sup>13</sup> The ERK stimulates cellular proliferation, while p38 and JNK induce apoptosis.<sup>13,14</sup> This study established that NRD can successfully suppress p38 MAPK phosphorylation via

JNK- and ERK-regulated signalling pathway. Previous research showed that NRD essential oil isolated from *Lindera erythrocarpa* inhibited I $\kappa$ B degradation and NF- $\kappa$ B phosphorylation through MAPK phosphorylation in LPS-stimulated macrophages.<sup>35</sup> This study demonstrated that NRD showed anti-proliferative and apoptotic activity on U-251 cells via MAPK signaling.

## Limitations

Our study highlights NRD as a pharmacological inhibitor of the p38 signaling pathway in GBM cells; additional details of its underlying anticancer actions need to be examined in the future studies.

## Conclusions

Our study revealed that NRD inhibited proliferation and induced apoptosis in U-251 cells. Nerolidol also induced apoptosis by stimulating pro-apoptotic proteins and inhibiting anti-apoptotic proteins. Indeed, NRD triggered apoptosis and cell cycle arrest via p38-MAPK stimulation. This pathway could be intricately linked with the antitumor action of NRD in U-251 cells. Hence, NRD is a promising natural anticancer and chemopreventive agent for GBM. However, in vivo studies are needed to understand the apoptosis mechanism and cell-cycle regulation induced by NRD in GBM cells.

## Supplementary data

The supplementary materials are available at <https://doi.org/10.5281/zenodo.8202031>. The package contains the following files:

Supplementary Table 1. Results of normality tests as presented in Fig. 3.


Supplementary Table 2. Results of normality tests as presented in Fig. 4.


Supplementary Table 3. Results of normality tests as presented in Fig. 5.

Supplementary Table 4. Results of normality tests as presented in Fig. 6.

## ORCID iDs

Zhijin Lu  <https://orcid.org/0000-0003-2334-7720>

Tao Tang  <https://orcid.org/0000-0002-1649-7694>

Juan Huang  <https://orcid.org/0000-0002-1551-2821>

Yongqiang Shi  <https://orcid.org/0000-0003-3276-813X>

## References

- Lapointe S, Perry A, Butowski NA. Primary brain tumours in adults. *Lancet*. 2018;392(10145):432–446. doi:10.1016/S0140-6736(18)30990-5
- Senders JT, Harary M, Stopa BM, et al. Information-based medicine in glioma patients: A clinical perspective. *Comput Math Methods Med*. 2018;2018:8572058. doi:10.1155/2018/8572058
- Wen PY, Kesari S. Malignant gliomas in adults. *N Engl J Med*. 2008;359(5):492–507. doi:10.1056/NEJMra0708126

4. Hagemann C. A complete compilation of matrix metalloproteinase expression in human malignant gliomas. *World J Clin Oncol*. 2012; 3(5):67. doi:10.5306/wjco.v3.i5.67
5. Onishi M, Ichikawa T, Kurozumi K, Date I. Angiogenesis and invasion in glioma. *Brain Tumor Pathol*. 2011;28(1):13–24. doi:10.1007/s10014-010-0007-z
6. Xiao W, Gao Z, Duan Y, Yuan W, Ke Y. Notch signaling plays a crucial role in cancer stem-like cells maintaining stemness and mediating chemotaxis in renal cell carcinoma. *J Exp Clin Cancer Res*. 2017;36(1):41. doi:10.1186/s13046-017-0507-3
7. Stupp R, Mason WP, Van Den Bent MJ, et al. Radiotherapy plus concomitant and adjuvant temozolomide for glioblastoma. *N Engl J Med*. 2005;352(10):987–996. doi:10.1056/NEJMoa043330
8. Ouyang L, Luo Y, Tian M, et al. Plant natural products: From traditional compounds to new emerging drugs in cancer therapy. *Cell Prolif*. 2014;47(6):506–515. doi:10.1111/cpr.12143
9. Donzelli M, Draetta GF. Regulating mammalian checkpoints through Cdc25 inactivation. *EMBO Rep*. 2003;4(7):671–677. doi:10.1038/sj.embor.embor887
10. Peters JM. The anaphase-promoting complex. *Molecular Cell*. 2002; 9(5):931–943. doi:10.1016/S1097-2765(02)00540-3
11. Hajra KM, Liu JR. Apoptosome dysfunction in human cancer. *Apoptosis*. 2004;9(6):691–704. doi:10.1023/B:APPT.0000045786.98031.1d
12. Strasser A, O'Connor L, Dixit VM. Apoptosis signaling. *Annu Rev Biochem*. 2000;69(1):217–245. doi:10.1146/annurev.biochem.69.1.217
13. Chang L, Karin M. Mammalian MAP kinase signalling cascades. *Nature*. 2001;410(6824):37–40. doi:10.1038/35065000
14. Woo JS, Kim SM, Jeong CH, Ryu CH, Jeun SS. Lipoxigenase inhibitor MK886 potentiates TRAIL-induced apoptosis through CHOP- and p38 MAPK-mediated up-regulation of death receptor 5 in malignant glioma. *Biochem Biophys Res Commun*. 2013;431(2):354–359. doi:10.1016/j.bbrc.2012.11.134
15. Kim SM, Park JG, Baek WK, et al. Cadmium specifically induces MKP-1 expression via the glutathione depletion-mediated p38 MAPK activation in C6 glioma cells. *Neurosci Lett*. 2008;440(3):289–293. doi:10.1016/j.neulet.2008.05.064
16. Kumar M, Kaur V, Kumar S, Kaur S. Phytoconstituents as apoptosis inducing agents: Strategy to combat cancer. *Cytotechnology*. 2016; 68(4):531–563. doi:10.1007/s10616-015-9897-2
17. Azzi J, Auezova L, Danjou PE, Fourmentin S, Greige-Gerges H. First evaluation of drug-in-cyclodextrin-in-liposomes as an encapsulating system for nerolidol. *Food Chem*. 2018;255:399–404. doi:10.1016/j.foodchem.2018.02.055
18. Chan WK, Tan L, Chan KG, Lee LH, Goh BH. Nerolidol: A sesquiterpene alcohol with multi-faceted pharmacological and biological activities. *Molecules*. 2016;21(5):529. doi:10.3390/molecules21050529
19. Iqbal A, Sharma S, Ansari MA, et al. Nerolidol attenuates cyclophosphamide-induced cardiac inflammation, apoptosis and fibrosis in Swiss Albino mice. *Eur J Pharmacol*. 2019;863:172666. doi:10.1016/j.ejphar.2019.172666
20. Ni YL, Shen HT, Su CH, et al. Nerolidol suppresses the inflammatory response during lipopolysaccharide-induced acute lung injury via the modulation of antioxidant enzymes and the AMPK/Nrf-2/HO-1 pathway. *Oxid Med Cell Longev*. 2019;2019:9605980. doi:10.1155/2019/9605980
21. Biazzi BI, Zanetti TA, Baranoski A, Corveloni AC, Mantovani MS. Cis-nerolidol induces endoplasmic reticulum stress and cell death in human hepatocellular carcinoma cells through extensive CYP2C19 and CYP1A2 oxidation. *Basic Clin Pharmacol Toxicol*. 2017;121(4): 334–341. doi:10.1111/bcpt.12772
22. Hanušová V, Caltová K, Svobodová H, et al. The effects of  $\beta$ -caryophyllene oxide and trans-nerolidol on the efficacy of doxorubicin in breast cancer cells and breast tumor-bearing mice. *Biomed Pharmacother*. 2017;95:828–836. doi:10.1016/j.biopha.2017.09.008
23. Ambrož M, Boušová I, Skarka A, et al. The influence of sesquiterpenes from *Myrica rubra* on the antiproliferative and pro-oxidative effects of doxorubicin and its accumulation in cancer cells. *Molecules*. 2015;20(8):15343–15358. doi:10.3390/molecules200815343
24. Ambrož M, Matoušková P, Skarka A, Zajdlová M, Žáková K, Skálová L. The effects of selected sesquiterpenes from *Myrica rubra* essential oil on the efficacy of doxorubicin in sensitive and resistant cancer cell lines. *Molecules*. 2017;22(6):1021. doi:10.3390/molecules22061021
25. Javed H, Azimullah S, Abul Khair SB, Ojha S, Haque ME. Neuroprotective effect of nerolidol against neuroinflammation and oxidative stress induced by rotenone. *BMC Neurosci*. 2016;17(1):58. doi:10.1186/s12868-016-0293-4
26. Grimm D, Bauer J, Kossmehl P, et al. Simulated microgravity alters differentiation and increases apoptosis in human follicular thyroid carcinoma cells. *FASEB J*. 2002;16(6):604–606. doi:10.1096/fj.01-0673fje
27. Glumac M, Čikeš Čulić V, Marinović-Terzić I, Radan M. Mechanism of cis-nerolidol-induced bladder carcinoma cell death. *Cancers (Basel)*. 2023;15(3):981. doi:10.3390/cancers15030981
28. Yu Y, Velu P, Ma Y, Vijayalakshmi A. Nerolidol induced apoptosis via PI3K/JNK regulation through cell cycle arrest in MG-63 osteosarcoma cells. *Environ Toxicol*. 2022;37(7):1750–1758. doi:10.1002/tox.23522
29. Balakrishnan V, Ganapathy S, Veerasamy V, et al. Anticancer and antioxidant profiling effects of nerolidol against DMBA induced oral experimental carcinogenesis. *J Biochem Mol Toxicol*. 2022;36(6):e23029. doi:10.1002/jbt.23029
30. Brown JM, Attardi LD. The role of apoptosis in cancer development and treatment response. *Nat Rev Cancer*. 2005;5(3):231–237. doi:10.1038/nrc1560
31. Dong JR, Chang WW, Chen SM. Nerolidol inhibits proliferation of leiomyoma cells via reactive oxygen species-induced DNA damage and downregulation of the ATM/Akt pathway. *Phytochemistry*. 2021;191: 112901. doi:10.1016/j.phytochem.2021.112901
32. Matus DQ, Lohmer LL, Kelley LC, et al. Invasive cell fate requires G1 cell-cycle arrest and histone deacetylase-mediated changes in gene expression. *Dev Cell*. 2015;35(2):162–174. doi:10.1016/j.devcel.2015.10.002
33. Satomi Y, Nishino H, Shibata S. Glycyrrhetic acid and related compounds induce G1 arrest and apoptosis in human hepatocellular carcinoma HepG2. *Anticancer Res*. 2005;25(6B):4043–4047. PMID:16309197.
34. Ko YJ, Ahn G, Ham YM, et al. Anti-inflammatory effect and mechanism of action of *Lindera erythrocarpa* essential oil in lipopolysaccharide-stimulated RAW264.7 cells. *EXCLI J*. 2017;16:1103–1113. doi:10.17179/EXCLI2017-596
35. Jiang G, Zhang L, Wang J, Zhou H. Baicalein induces the apoptosis of U251 glioblastoma cell lines via the NF- $\kappa$ B-p65-mediated mechanism. *Animal Cells Systems*. 2016;20(5):296–302. doi:10.1080/19768354.2016.1229216

# Lysyl oxidase-mediated elastin upregulation promotes the proliferation and migration of human retinal endothelial cells

Yu Zhang<sup>A,D</sup>, Yurong Zhang<sup>B,C</sup>, Siyu He<sup>C,E</sup>, Weixing Wang<sup>E,F</sup>

Department of Ophthalmology, Nantong Haimen People's Hospital, China

A – research concept and design; B – collection and/or assembly of data; C – data analysis and interpretation; D – writing the article; E – critical revision of the article; F – final approval of the article

Advances in Clinical and Experimental Medicine, ISSN 1899–5276 (print), ISSN 2451–2680 (online)

Adv Clin Exp Med. 2024;33(6):641–651

## Address for correspondence

Yu Zhang

E-mail: drzhangyu006@163.com

## Funding sources

None declared

## Conflict of interest

None declared

Received on February 9, 2023

Reviewed on May 15, 2023

Accepted on August 13, 2023

Published online on February 14, 2024

## Abstract

**Background.** Proliferative diabetic retinopathy (PDR) is a major cause of irreversible blindness in the working age population. The dysfunction of retinal vascular endothelial cells (RVECs) is the primary cause of PDR. Extracellular matrix (ECM) accumulation promotes intracellular signaling required for RVEC proliferation, migration, survival, and tube morphogenesis.

**Objectives.** This study aimed to investigate the role of lysyl oxidase (*LOX*) in the cellular function of RVECs and PDR pathogenesis and to identify the underlying mechanisms.

**Materials and methods.** Protein expression was determined with western blot. The interaction between *LOX* and elastin (*ELN*) was detected using a co-immunoprecipitation (Co-IP) assay, and the Cell Counting Kit-8 (CCK-8) assay evaluated cell viability. A colony formation assay was employed to assess the proliferation of human RVECs (hRVECs), and a transwell assay to determine their migration ability. Streptozotocin was used to establish PDR in mice *in vivo*. A histological analysis was conducted using hematoxylin and eosin (H&E) staining.

**Results.** The results showed that *LOX* was overexpressed in PDR patients. The *LOX* knockdown suppressed ECM formation and hRVEC proliferation and migration. Additionally, *LOX* upregulated *ELN* expression. However, overexpressed *ELN* promoted hRVEC proliferation and migration. *In vivo* experiments showed that curcumin-mediated *LOX* deficiency restored retinal tissue structure.

**Conclusions.** The *LOX*-knockdown suppressed ECM formation and hRVEC proliferation and migration by inactivating *ELN*. Therefore, *LOX/ELN* signaling may be a potential PDR biomarker.

**Key words:** extracellular matrix, proliferative diabetic retinopathy, *LOX*, *ELN*

## Cite as

Zhang Y, Zhang Y, He S, Wang W. Lysyl oxidase-mediated elastin upregulation promotes the proliferation and migration of human retinal endothelial cells.

Adv Clin Exp Med. 2024;33(6):641–651.

doi:10.17219/acem/170999

## DOI

10.17219/acem/170999

## Copyright

Copyright by Author(s)

This is an article distributed under the terms of the Creative Commons Attribution 3.0 Unported (CC BY 3.0) (<https://creativecommons.org/licenses/by/3.0/>)

## Background

Diabetic retinopathy (DR) is a common complication inducing ophthalmic diseases.<sup>1</sup> It can be divided into non-proliferative DR (NPDR) and proliferative DR (PDR) based on the neovascularization status.<sup>2</sup> The dysfunction of retinal vascular endothelial cells (RVECs) is the primary cause of PDR.<sup>3</sup> Recent evidence reveals that metabolic imbalance induced by high glucose levels promotes RVEC degradation and PDR pathogenesis.<sup>4–6</sup> In recent years, great advances have been made in PDR treatment, such as anti-vascular endothelial growth factor (anti-VEGF) strategies.<sup>7–9</sup> However, the mechanisms of the disease are still unclear. Therefore, unveiling the underlying molecular mechanisms may help uncover the Achilles' heel of PDR.

Lysyl oxidase (*LOX*) is a copper-dependent amine oxidase that catalyzes lysine-derived cross-links in collagen and elastin (*ELN*), resulting in extracellular matrix (ECM) reprogramming.<sup>10</sup> The *LOX* plays an important role in vascular diseases. For instance, *LOX* deficiency is closely associated with cardiovascular dysfunction.<sup>11</sup> However, aberrantly high levels of *LOX* promote angiogenesis and tumor metastasis.<sup>12</sup>

In ophthalmic diseases, *LOX* is frequently downregulated in keratoconus patients.<sup>13</sup> However, *LOX* is overexpressed in PDR patients and the retinas of diabetic mice.<sup>14</sup> Interestingly, increasing evidence reports that *LOX* inhibition may be a promising strategy for PDR treatment. For instance, *LOX* knockdown protects against the development of vascular lesions characteristic of DR by suppressing retinal vascular permeability.<sup>15</sup> Meanwhile,  $\beta$ -aminopropionitrile-mediated *LOX* deficiency inhibits the angiogenesis and migration of human umbilical vein endothelial cells.<sup>16</sup> However, the underlying mechanisms are still unclear.

The ECM is rich in *ELN* glycoprotein,<sup>17</sup> and abnormal *ELN* expression is closely associated with vascular endothelial cell (VEC) functions. For instance, idiopathic portal hypertension-induced overexpression of *ELN* in VECs induces the pathogenesis of hepatoportal sclerosis.<sup>18</sup> In eye disorders, *ELN*-mediated choroidal endothelial cell migration contributes to age-related macular degeneration.<sup>19</sup> Also, *ELN*-derived peptides (EDPs) promote the migration and tubulogenesis of human corneal endothelial cells.<sup>20</sup> However, the role of *ELN* in PDR has not been elucidated.

## Objectives

This study aimed to investigate the role of *LOX* in PDR and uncover its underlying mechanisms. Gene levels and expression were determined using enzyme-linked immunosorbent assay (ELISA) and western blot. The interaction between *LOX* and *ELN* was investigated using a co-immunoprecipitation (Co-IP) assay. We hypothesized that *LOX*-mediated *ELN* upregulation promoted the development of PDR.

## Materials and methods

### Ethical approval

The Ethical Committee of Nantong Haimen People's Hospital, China, approved the study (approval No. 2021[07]). All patients provided informed consent.

### Cell culture

Primary human RVECs (hRVECs) were purchased from American Type Culture Collection (ATCC; Manassas, USA) and cultured in Dulbecco's modified Eagles's medium (DMEM) (Gibco, Waltham, USA) containing 10% fetal bovine serum (FBS) at 37°C in 5% carbon dioxide (CO<sub>2</sub>). Cells were exposed to high glucose (HG; 30 mmol/L of d-glucose) or normal glucose (NG; 5.55 mmol/L of d-glucose) conditions.

### Cell transfection

The negative control (NC) and short hairpin *LOX* (*shLOX*) (GenePharma, Shanghai, China) were transfected using a Lipofectamine™ 2000 kit (Thermo Fisher Scientific, Waltham, USA), according to the manufacturer's protocol. After 48 h, cells were used in the experiments outlined below. The sequences of sh ribonucleic acids (shRNAs) and their NCs are listed in Supplementary Table 1.

### Real-time quantitative polymerase chain reaction

Total RNA was extracted from cells or tissues using RNA isolation reagents and then quantified using a NanoDrop™ 2000 spectrophotometer (Thermo Fisher Scientific). Afterward, complementary deoxyribonucleic acid (cDNA) was synthesized using a PrimeScript® RT Reagent Kit (Takara, Shiga, Japan), according to the manufacturer's protocols. Polymerase chain reaction (PCR) was performed using a PrimeScript real-time (RT)-PCR kit (Takara) on an ABI 7500 Real-Time PCR system (Thermo Fisher Scientific). Glyceraldehyde-3-phosphate dehydrogenase (*GAPDH*) served as the loading control. Relative messenger RNA (mRNA) levels were determined with the 2<sup>- $\Delta\Delta C_q$</sup>  method.<sup>21</sup> The primers used are listed in Supplementary Table 2.

### Immunofluorescence (IF)

Cells were fixed with 4% paraformaldehyde and permeabilized with 0.2% Triton X-100. Afterward, cells were blocked with 5% FBS and incubated with primary antibodies against *LOX* (ab174316), collagen I alpha-1 (*Col1A1*) (ab138492) and *Col4A1* (ab308360) (all from Abcam, Cambridge, USA). Then, the cells were counterstained with 4',6-diamidino-2-phenylindole (DAPI) and visualized with



the use of an immunofluorescence microscope (Axio Imager 5; Carl Zeiss, Oberkochen, Germany).

## Western blot

Cells were collected and lysed with radioimmunoprecipitation assay (RIPA) lysis buffer. Then, the protein was collected and concentrated using a bicinchoninic acid assay (BCA) kit (Abcam, Cambridge, UK) according to the manufacturer's protocols. After isolation using 12% sodium dodecyl-sulfate polyacrylamide gel electrophoresis (SDS-PAGE), the protein was transferred onto a polyvinylidene fluoride (PVDF) membrane (Thermo Fisher Scientific). The membranes were blocked with 5% skimmed milk and then incubated with primary antibodies against *LOX* (ab221936; 1:1,000), *ELN* (ab307150; 1:1,000) or *GAPDH* (ab9485; 1:2,500), and goat-anti-rabbit secondary antibodies (ab6721; 1:10,000) (all from Abcam). Finally, the bands were captured using an enhanced chemiluminescence (ECL) kit (Abcam).

## Co-immunoprecipitation

The Co-IP was performed using the Pierce™ Classic Magnetic Co-IP Kit (Thermo Fisher Scientific) according to the manufacturer's protocols.<sup>22</sup> Briefly, the cells were lysed with IP lysis buffer and homogenized. Afterward, they were centrifuged at 12,000 × g, and the supernatants were collected. The protein was incubated with antibodies against immunoglobulin G (*IgG*) (ab174316) or *LOX* (ab174316) (both from Abcam) and immobilized on protein A/G beads. The beads were then washed and microcentrifuged. Finally, the bands were analyzed using western blot.

## Bioinformatics analysis

The genes interacting with *LOX* were predicted using Search Tool for the Retrieval of Interacting Genes/Proteins (STRING) database (<https://cn.string-db.org>).

## Colony formation assay

Following transfection, the cells were transferred into a 96-well plate and cultured for 2 weeks. After being washed with phosphate-buffered saline (PBS), the cells were fixed in 95% ethanol and stained with 0.1% crystal violet. Finally, the colonies were counted under a microscope (Primovert; Carl Zeiss AG).

## Transwell assay

The migration assays used transwell chambers without a Matrigel mix coating (BD Biosciences, Franklin Lakes, USA). Homogeneous serum-free single-cell suspensions ( $1 \times 10^5$  cells/well) were added to the upper chambers, and the medium containing 10% FBS was added into the lower

chambers and incubated for 24 h. The migratory and invasive cells were fixed, stained and counted.

## Propidium iodide staining

After transfection, the cells were plated onto a 24-well plate and treated with a propidium iodide (PI) solution (2 µg/mL). Finally, PI-positive cells were captured using a fluorescence microscope (Leica DFC9000 sCMOS; Leica Camera AG, Wetzlar, Germany).

## Flow cytometry

After transfection, the cells were collected and cultured at 37°C. Then, following trypsinization, the cells were cultured with Annexin-V-FITC/PI for 15 min at 37°C. Finally, the apoptotic cells were determined using a FACSCalibur flow cytometer (BD Biosciences) with FlowJo software 7.6 (FlowJo, LLC, Ashland, USA).

## Gene set enrichment database analysis

The *LOX* expression was analyzed using the GSE60436 online microarray database, and the differentially expressed genes were used for Gene Ontology (GO; <https://geneontology.org/>) and Kyoto Encyclopedia of Genes and Genome (KEGG) analysis (<https://www.kegg.jp/kegg/mapper/>).

## In vivo assay

Male C57BL/6J mice (n = 18, 6–8 weeks, 18–22 g) were purchased from the Experimental Animal Center of Nanjing Medical University (Nanjing, China) and used to establish a previously described diabetic model.<sup>23</sup> Mice were housed in pathogen-free cages under a 12-hour light/dark cycle with free access to food and water. The animals were randomly divided into 3 groups: sham group (n = 6), streptozocin (STZ) group (n = 6) and STZ + curcumin group (n = 6). Mice in the sham group were intraperitoneally injected with 10% dimethyl sulfoxide (DMSO), while those in the STZ or STZ+GA groups were injected intraperitoneally with STZ (60 mg/kg) once a day for 5 consecutive days. After 4 weeks, mice were injected intraperitoneally with 100 mg/kg/day curcumin for 4 weeks. Afterward, the animals were euthanized by sodium pentobarbital injection, and retinal samples were collected and stained with hematoxylin and eosin (H&E) for histological analysis.

## Statistical analyses

Data were analyzed using GraphPad Prism 9.0 (GraphPad Software, San Diego, USA). Each experiment was performed in triplicate. The Mann–Whitney U test was employed to compare differences between 2 groups, while the Kruskal–Wallis test followed by Dunn's post hoc test



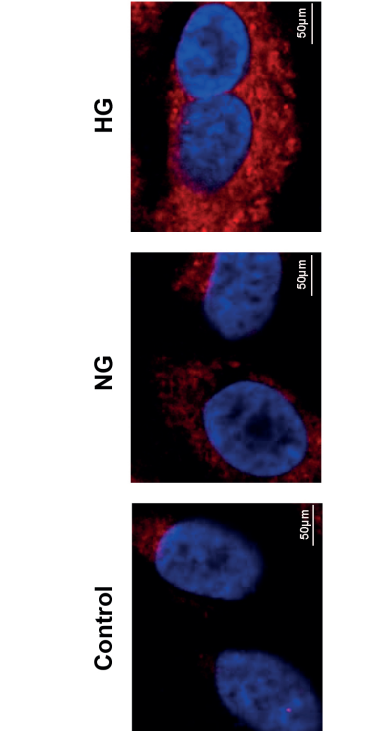
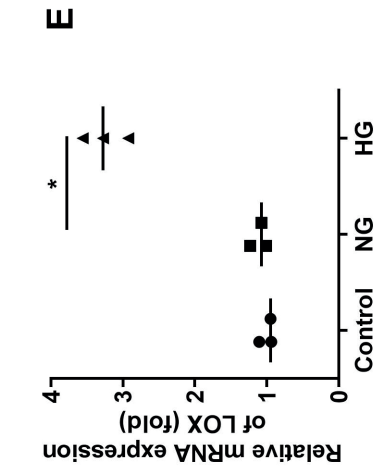
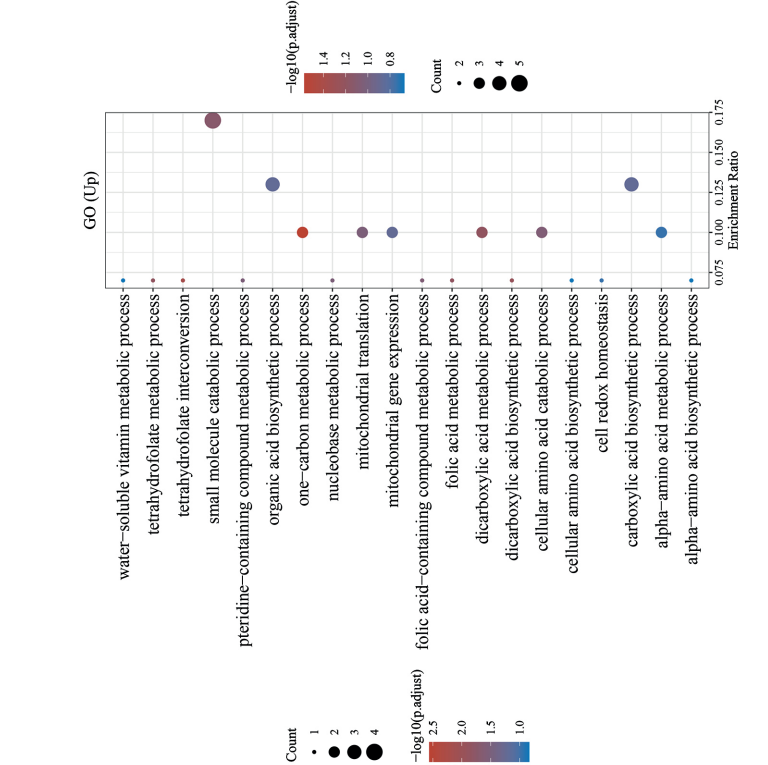
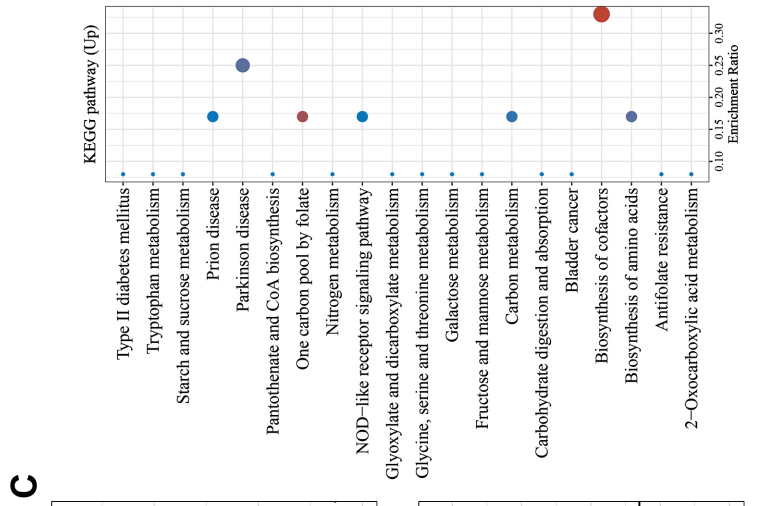
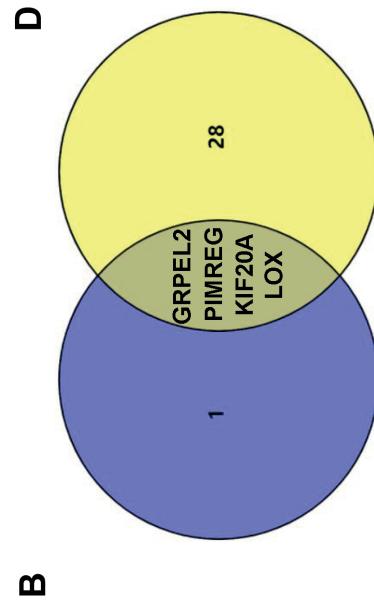
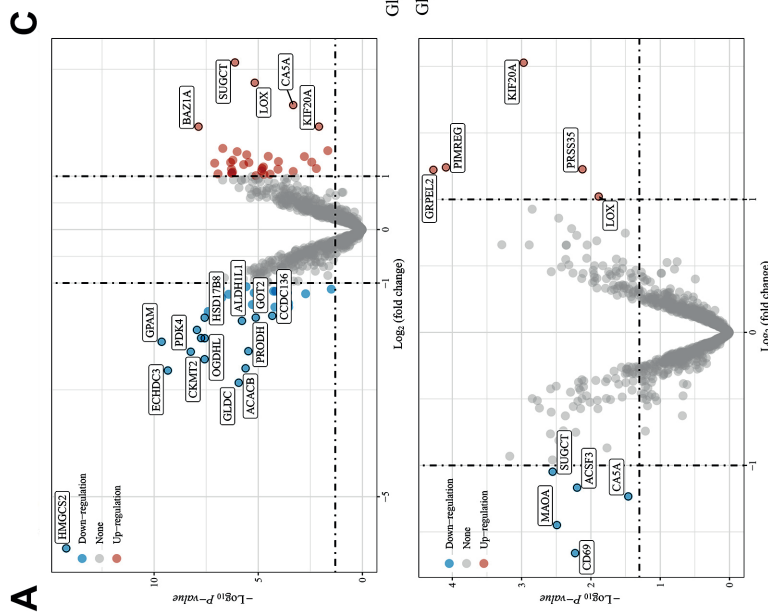


**Fig. 1.** Lysyl oxidase (LOX) is overexpressed in proliferative diabetic retinopathy (PDR). A. Differentially expressed genes in diabetic retinopathy (DR) patients were analyzed using GSE60436; B. Differentially expressed genes in PDR compared to non-proliferative PDR (NPDR) patients; C. Kyoto Encyclopedia of Genes and Genome (KEGG) and Gene Ontology (GO) analysis of the differentially expressed genes; D. LOX messenger ribonucleic acid (mRNA) expression in human retinal vascular endothelial cells (hrVECs) was detected using real-time quantitative polymerase chain reaction (qPCR); E. LOX expression in hrVECs was detected using immunofluorescence (IF). Results were statistically analyzed using the Kruskal–Wallis test followed by Dunn’s post hoc test. Data were expressed as data points. The horizontal lines represent the median value. NG – normal glucose; HG – high glucose; \*\* $p < 0.05$  compared to short hairpin negative control (shNC).

were used to analyze the differences between multiple groups (Supplementary Table 3). Statistical significance was set at  $p < 0.05$ .

## Results

### Lysyl oxidase was upregulated in diabetic retinopathy

The GSE60436 database was applied to analyze the differentially expressed genes in DR patients. As shown in Fig. 1A, 32 genes were significantly upregulated and 39 were downregulated in DR patients. Moreover, GO and KEGG analysis showed that the upregulated genes were enriched in amino acid metabolism (Fig. 1B). To further analyze the role of these genes in DR, we divided DR patients into 2 subtype groups: NPDR and PDR. We found that,

among the 35 upregulated genes, the expression of GrpE protein homolog 2 (*GRPEL2*), phosphatidylinositol binding clathrin assembly protein interacting mitotic regulator (*PIMREG*), kinesin family member 20A (*KIF20A*), and *LOX* increased significantly in PDR patients compared to NPDR patients (Fig. 1C). Among the upregulated genes in PDR, high levels of *LOX* promote the pathogenesis of PDR.<sup>14,24</sup> Therefore, we selected *LOX* for further study. Cells were exposed to HG conditions to further confirm the roles of *LOX* in PDR. The results showed that *LOX* mRNA expression increased markedly in the HG group (Fig. 1D), consistent with the Co-immunofluorescence assay results (Fig. 1E).

### Lysyl oxidase was required for extracellular matrix production

The *LOX*, a crucial ECM remodeler, is a potential therapeutic target for fibrosis and cardiovascular disease.

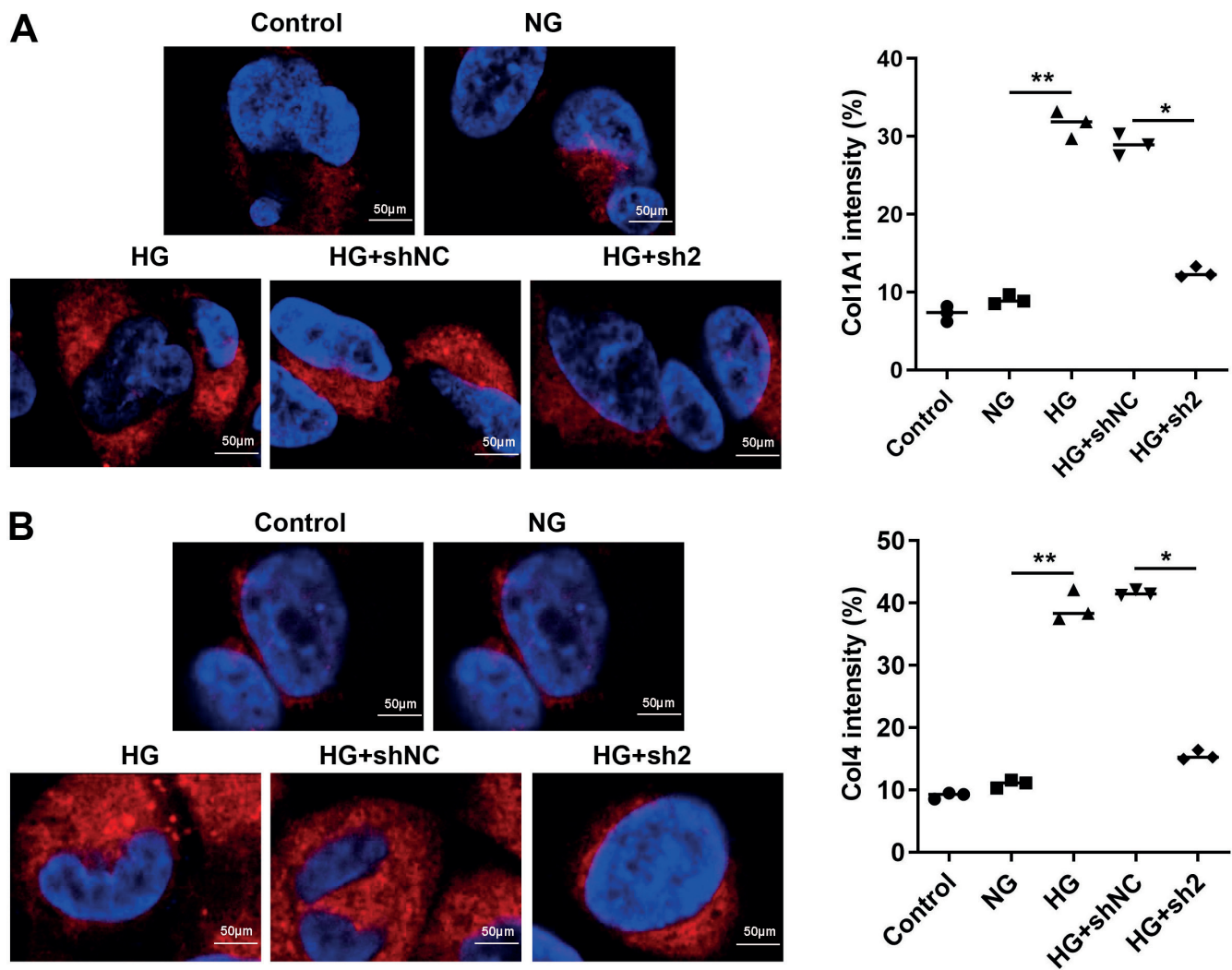
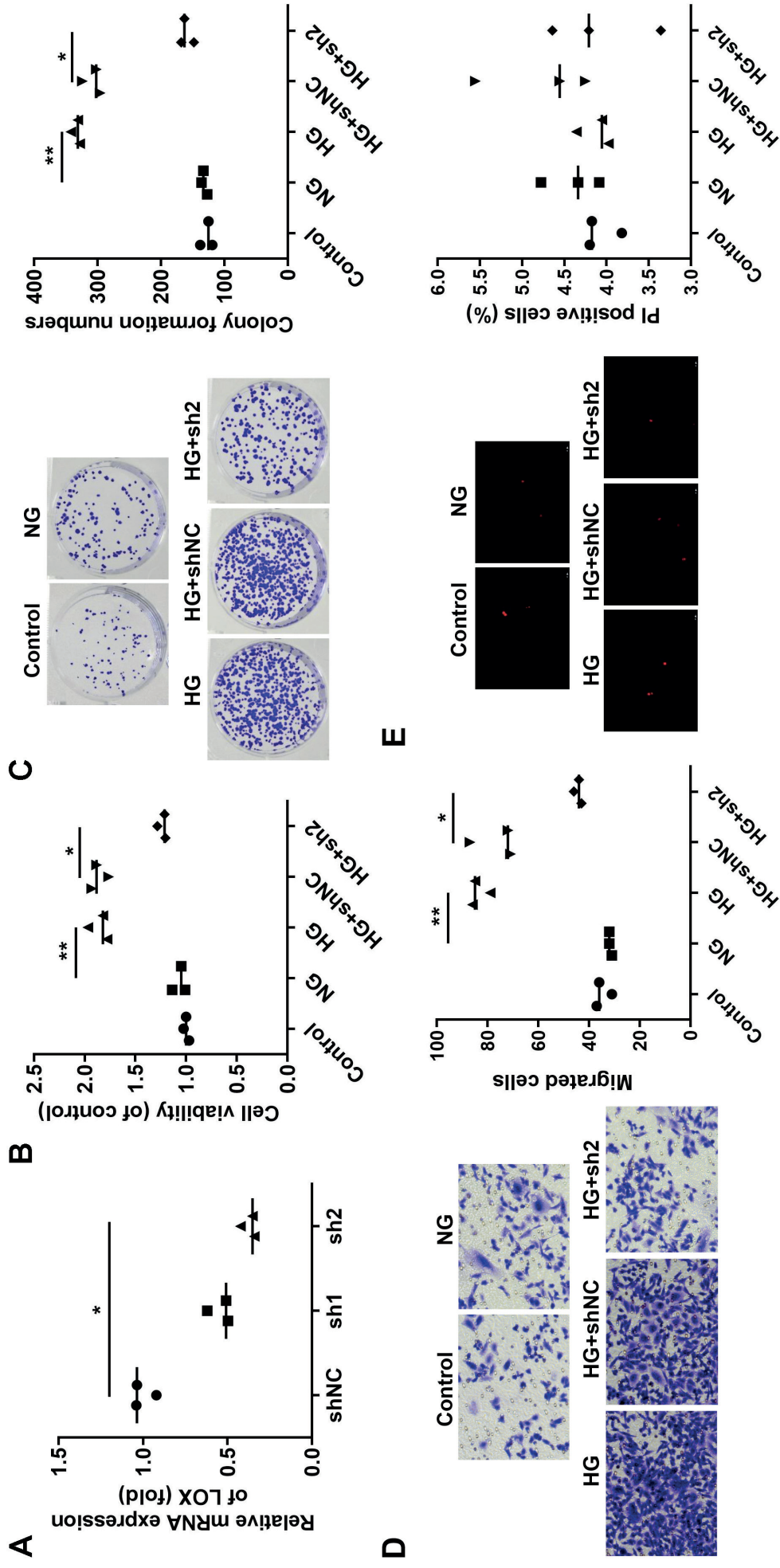


Fig. 2. Lysyl oxidase (LOX) is required for extracellular matrix (ECM) production. A. Collagen 1 alpha-1 (*Col1A1*) expression in human retinal vascular endothelial cells (hRVECs) was detected with immunofluorescence (IF); B. *Col4A1* expression in hRVECs was detected using IF. Results were statistically analyzed using the Kruskal–Wallis test followed by Dunn’s post hoc test. Data were expressed as data points. The horizontal lines represent the median value

NG – normal glucose; HG – high glucose; \*\* $p < 0.01$  compared to short hairpin negative control (shNC); \* $p < 0.05$  compared to HG+shNC.



**Fig. 3.** Lysyl oxidase (LOX) promotes human retinal vascular endothelial cell (hrVEC) proliferation and migration. **A.** LOX messenger ribonucleic acid (mRNA) expression in hrVECs was detected using real-time quantitative polymerase chain reaction (qPCR); **B.** Cell viability was detected using the Cell Counting Kit-8 (CCK-8) assay; **C.** Cell proliferation determined with colony formation assay (CFA;  $\times 40$  magnification); **D.** Cell migration detected using transwell assay ( $\times 100$  magnification); **E.** Cell death detected with propidium iodide (PI) staining ( $\times 100$  magnification). Results were statistically analyzed using the Kruskal–Wallis test followed by Dunn’s post hoc test. Data were expressed as data points. The horizontal lines represent the median value

NG – normal glucose; HG – high glucose; \*\* $p < 0.01$  compared to short hairpin negative control (shNC); \* $p < 0.05$  compared to HG+shNC.



Therefore, we determined the roles of *LOX* in the ECM and found that the fluorescence intensity of *Col1A1* was significantly increased after HG exposure (Fig. 2A). However, *LOX* knockdown markedly inhibited the increase in HG-induced *Col1A1* expression, and markedly reduced *Col4A1* expression (Fig. 2B). These findings suggested that *LOX* promoted ECM formation.

### Lysyl oxidase promoted human retinal vascular endothelial cell proliferation and migration

Figure 3A shows the transfection efficiency of *shLOX*. The sh2 had remarkable effects and was used in the following experiment. The *LOX* knockdown markedly suppressed the increased cell viability induced by HG (Fig. 3B). Moreover, the *LOX* knockdown significantly inhibited hRVEC colony formation (Fig. 3C). Transwell assays showed that HG-induced hRVEC migration was dampened by *LOX* knockdown (Fig. 3D). Whether it could induce hRVEC death required further verification, with cellular functions determined using PI and flow cytometry. The results showed that HG and/or *LOX* knockdown had no significant impact on hRVEC death (Fig. 3E and Supplementary Fig. 1), suggesting that *LOX* is required for promoting hRVEC morbidity.

### Lysyl oxidase upregulated elastin

The STRING database was used to analyze the genes interacting with *LOX* (Fig. 4A). We found that *LOX* interacted with fibronectin 1 (*FN1*), matrix metalloproteinase 2 (*MMP2*) and *ELN*. The *ELN* encodes proteins enriched in hydrophobic amino acids such as glycine and

proline. Therefore, we speculated that *LOX* may participate in amino acid metabolism via *ELN* upregulation. The Co-IP assay confirmed the interaction between *LOX* and *ELN* (Fig. 4B). Moreover, *LOX* knockdown decreased *ELN* protein expression, which was reversed by *ELN* overexpression (Fig. 4C).

### Overexpressed elastin promoted human retinal endothelial cell proliferation and migration

Rescue assays were performed to verify the role of *ELN* in PDR. The experiments were conducted using cells exposed to HG conditions. The *ELN* mRNA expression was significantly increased by *ELN* overexpression plasmids (Fig. 5A), suggesting that the cells were successfully transfected. Overexpressed *ELN* markedly increased hRVEC viability (Fig. 5B). Moreover, overexpressed *ELN* significantly increased hRVEC colony formation (Fig. 5C). Additionally, *ELN* overexpression remarkably increased hRVEC migration ability (Fig. 5D).

### Curcumin alleviated proliferative diabetic retinopathy in vivo

The GeneCards online database (<https://www.genecards.org>) was used to choose drugs approved for *LOX*. Among the approved drugs, acetylsalicylic acid (aspirin) increases cardiovascular vitality, and bleomycin and cisplatin are used for cancer therapy, with outstanding side effects, such as vascular malformation. Therefore, we chose curcumin to induce *LOX* deficiency in vivo. As shown in Fig. 6A, the layers of retinal tissues were loose and irregular in the STZ group. Moreover, the number of ganglion cells

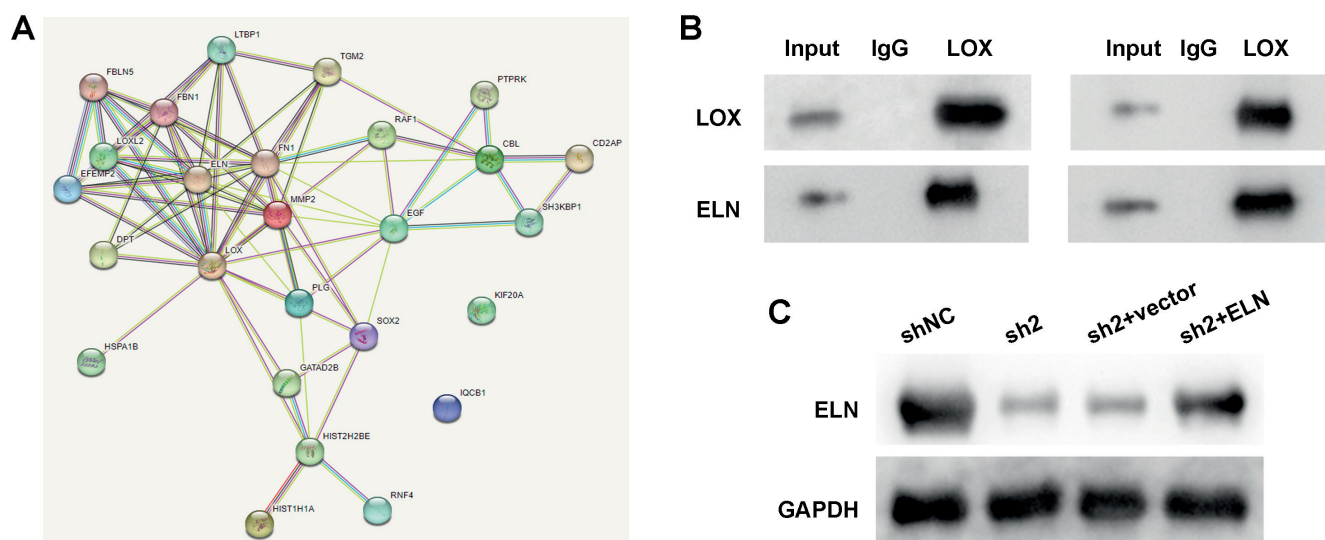


**Fig. 4.** Lysyl oxidase (*LOX*) upregulates elastin (*ELN*). **A.** The genes interacting with *LOX* were predicted using Search Tool for the Retrieval of Interacting Genes/Proteins (STRING) database; **B.** The interaction between *ELN* and *LOX* was verified with co-immunoprecipitation (Co-IP) assay; **C.** *ELN* protein expression was determined with western blot (n = 3)

IgG – immunoglobulin G; GAPDH – glyceraldehyde-3-phosphate dehydrogenase; shNC – short hairpin negative control.

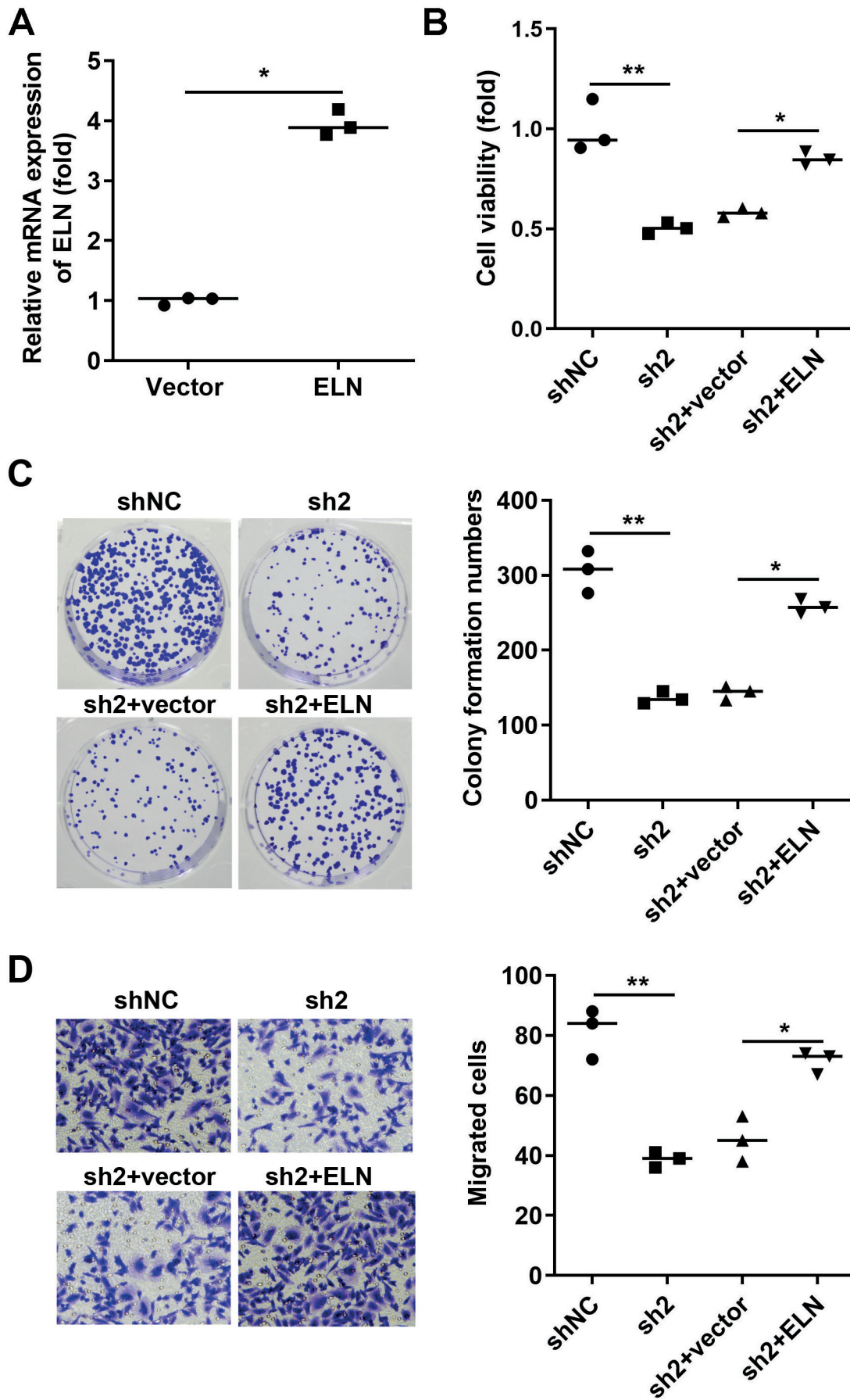


Fig. 5. Overexpressed elastin (ELN) promoted human retinal vascular endothelial cell (hRVEC) proliferation and migration.

A. ELN messenger ribonucleic acid (mRNA) expression in hRVECs was detected using real-time quantitative polymerase chain reaction (qPCR); B. Cell viability was detected using Cell Counting Kit-8 (CCK-8) assay; C. Cell proliferation determined with colony formation assay (CFA;  $\times 40$  magnification); D. Cell migration detected using transwell assay ( $\times 100$  magnification) ( $n = 3$ ). Results were statistically analyzed using the Kruskal–Wallis test followed by Dunn's post hoc test or a Mann–Whitney U test. Data were expressed as data points. The horizontal lines represent the median value

\*\* $p < 0.01$  compared to short hairpin negative control (shNC) or vector; \* $p < 0.05$  compared to sh2+vector.



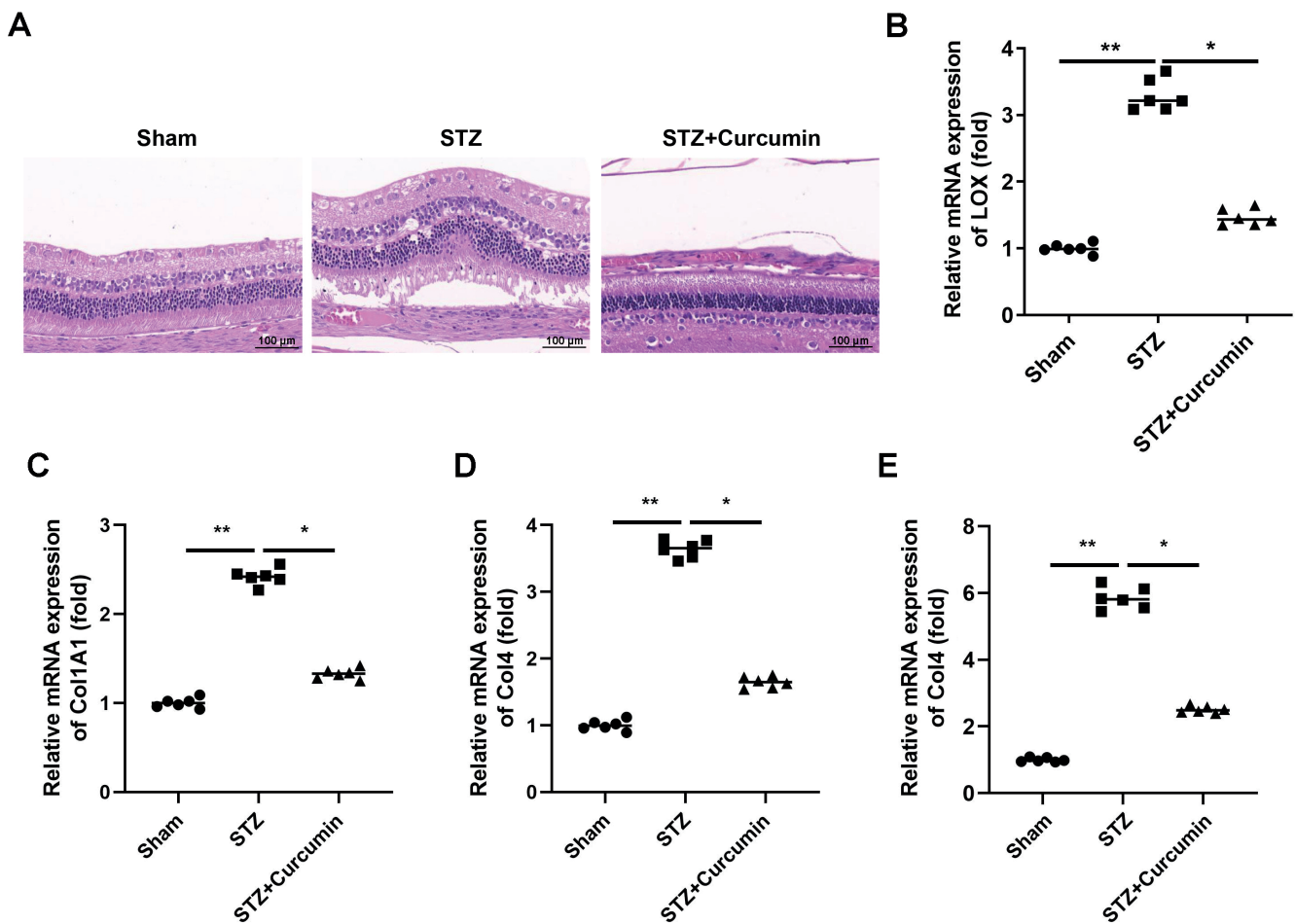


Fig. 6. Curcumin alleviated proliferative diabetic retinopathy (PDR) in vivo. A. Histological analysis was performed using hematoxylin and eosin (H&E) staining; B. Lysyl oxidase (*LOX*) expression in mice determined with real-time quantitative polymerase chain reaction (qPCR); C. *Col1A1* expression in mice determined with qPCR; D. *Col4* expression in mice determined with qPCR; E. *ELN* expression in mice determined with qPCR. Results were statistically analyzed using the Kruskal–Wallis test followed by Dunn’s post hoc test. Data were expressed as data points. The horizontal lines represent the median value

\*\* $p < 0.01$  compared to sham; \* $p < 0.05$  compared to streptozocin (STZ).

was reduced, and the ganglion cell layer displayed obvious vacuolar degeneration. Additionally, *LOX*, *Col1A1*, *Col4A1*, and *ELN* expression significantly decreased after curcumin injection (Fig. 6B–E).

## Discussion

In this study, *LOX* was overexpressed in PDR patients. The *LOX* deficiency markedly suppressed ECM formation and hRVEC proliferation and migration, and alleviated PDR in vivo. Furthermore, *LOX* upregulated *ELN*, thereby promoting hRVEC proliferation and migration.

The *LOX* is often abnormally expressed in ophthalmic diseases.<sup>12–14</sup> For instance, HG-induced upregulation of *LOX* promotes monolayer permeability and compromises barrier functional integrity.<sup>25</sup> Moreover, the overexpression of *LOX* is associated with PDR and rhegmatogenous retinal detachment.<sup>14</sup> Therefore, *LOX* may promote the pathogenesis of ophthalmic diseases.

Increasing evidence demonstrates that *LOX* inhibition using specific shRNAs or *LOX* inhibitors may be a promising PDR treatment strategy.<sup>14,15</sup> In this study, the expression of *LOX* was increased in PDR patients, suggesting that *LOX* may play a positive role in PDR development. However, *LOX* knockdown markedly suppressed ECM formation and hRVEC proliferation and migration, suggesting that *LOX* deficiency mediated hRVEC morbidity inhibition and may be a promising strategy for PDR therapy.

The pathogenesis of DR is influenced by ECM capillary basement membrane alterations,<sup>26</sup> which may induce changes in the characteristics of the endothelium.<sup>27</sup> The ECM accumulation promotes intracellular signaling required for cell proliferation, migration, survival, and tube morphogenesis.<sup>28,29</sup> As an ECM constituent, *ELN* is a key gene modulating endothelial cell functions via stiff substrate and stenotic phenotype regulation.<sup>30</sup> However, *ELN* mutation or abnormal expression contributes to polypoidal choroidal vasculopathy.<sup>31</sup> In this study, *LOX*-mediated *ELN* upregulation promoted ECM synthesis and enhanced

hRVEC proliferation and migration. Therefore, *LOX/ELN* signaling may be a therapeutic target for PDR.

Curcumin is a natural compound widely used in the treatment of retinal diseases.<sup>32</sup> For instance, curcumin suppresses the release of pro-inflammatory cytokines and alleviates DR.<sup>33</sup> Moreover, it inhibits the development of PDR by inactivating vascular endothelial growth factor (*VEGF*).<sup>34</sup> These findings suggest that curcumin, with anti-inflammatory, anti-oxidant and anti-angiogenic effects, has beneficial effects in DR treatment. Moreover, curcumin suppresses the accumulation of pro-inflammatory cytokines and alleviates retinal inflammatory injury, contributing to decreased endothelial cell permeability and pathological angiogenesis, which is frequently found in the late stages of DR and PDR.<sup>35,36</sup> Furthermore, curcumin represses ECM-receptor interactions in the diabetic retina.<sup>37</sup> In this study, curcumin treatment improved the retinal structure and suppressed endothelial cell permeability, suggesting that curcumin-mediated *LOX* deficiency may be a promising strategy for PDR treatment.

## Limitations

Due to the limitations of the experimental conditions, future studies should assess the role of *LOX* in PDR patients. As a collagen cross-linking enzyme, *LOX* regulates cellular functions by inducing metabolic reprogramming, such as glycolysis and amino acid metabolism; whether *LOX*-mediated collagen formation and cell proliferation and migration by inducing metabolic reprogramming requires further study.

## Conclusions

In conclusion, the overexpression of *LOX* was associated with PDR development. The *LOX* deficiency suppressed ECM formation and hRVEC proliferation and migration by inactivating *ELN* (see the graphical abstract). Therefore, *LOX/ELN* may be a novel therapeutic target for PDR.

## Supplementary data

The supplementary materials are available at <https://doi.org/10.5281/zenodo.8202183>. The package includes the following files:

- Supplementary Fig. 1. The apoptosis rates of hRVECs.
- Supplementary Table 1. The sequences of shRNAs used in transfection.
- Supplementary Table 2. The sequences of the primers used in PCR.
- Supplementary Table 3. Statistical significance of the differences presented in figures.

## Data availability

The datasets generated and/or analyzed during the current study are available from the corresponding author on reasonable request.

## Consent for publication

Not applicable.

## ORCID iDs

Yu Zhang  <https://orcid.org/0000-0002-6360-646X>  
 Yurong Zhang  <https://orcid.org/0009-0000-5082-9616>  
 Siyu He  <https://orcid.org/0009-0008-8604-1503>  
 Weixing Wang  <https://orcid.org/0009-0002-7890-1581>

## References

1. Cheung N, Mitchell P, Wong TY. Diabetic retinopathy. *Lancet*. 2010; 376(9735):124–136. doi:10.1016/S0140-6736(09)62124-3
2. Kashim R, Newton P, Ojo O. Diabetic retinopathy screening: A systematic review on patients' non-attendance. *Int J Environ Res Public Health*. 2018;15(1):157. doi:10.3390/ijerph15010157
3. Thomas AA, Biswas S, Feng B, Chen S, Gonder J, Chakrabarti S. lncRNA H19 prevents endothelial–mesenchymal transition in diabetic retinopathy. *Diabetologia*. 2019;62(3):517–530. doi:10.1007/s00125-018-4797-6
4. Yang Y, Liu Y, Li Y, et al. MicroRNA-15b targets VEGF and inhibits angiogenesis in proliferative diabetic retinopathy. *J Clin Endocrinol Metab*. 2020;105(11):3404–3415. doi:10.1210/clinem/dgaa538
5. Cao J, Zhao C, Gong L, et al. MiR-181 enhances proliferative and migratory potentials of retinal endothelial cells in diabetic retinopathy by targeting KLF6. *Curr Eye Res*. 2022;47(6):882–888. doi:10.1080/02713683.2022.2039206
6. Wang X, Chen W, Lao W, Chen Y. Upregulation of PCED1B-AS1 in proliferative diabetic retinopathy and its involvement in retinal vascular endothelial cell proliferation. *BMC Ophthalmol*. 2022;22(1):450. doi:10.1186/s12886-022-02683-6
7. Gross JG, Glassman AR, Jampol LM, et al; Writing Committee for the Diabetic Retinopathy Clinical Research Network. Panretinal photocoagulation vs intravitreal ranibizumab for proliferative diabetic retinopathy: A randomized clinical trial. *JAMA*. 2015;314(20):2137. doi:10.1001/jama.2015.15217
8. Martinez-Zapata MJ, Salvador I, Martí-Carvajal AJ, et al. Anti-vascular endothelial growth factor for proliferative diabetic retinopathy. *Cochrane Database Syst Rev*. 2023;2023(3):CD008721. doi:10.1002/14651858.CD008721.pub3
9. Liu Y, Wu N. Progress of nanotechnology in diabetic retinopathy treatment. *Int J Nanomed*. 2021;16:1391–1403. doi:10.2147/IJN.S294807
10. Chen W, Yang A, Jia J, Popov YV, Schuppan D, You H. Lysyl oxidase (LOX) family members: Rationale and their potential as therapeutic targets for liver fibrosis. *Hepatology*. 2020;72(2):729–741. doi:10.1002/hep.31236
11. Rodriguez C, Martinez-Gonzalez J, Raposo B, Alcudia JF, Guadall A, Badimon L. Regulation of lysyl oxidase in vascular cells: Lysyl oxidase as a new player in cardiovascular diseases. *Cardiovasc Res*. 2008; 79(1):7–13. doi:10.1093/cvr/cvn102
12. Liburkin-Dan T, Toledano S, Neufeld G. Lysyl oxidase family enzymes and their role in tumor progression. *Int J Mol Sci*. 2022;23(11):6249. doi:10.3390/ijms23116249
13. Dudakova L, Jirsova K. The impairment of lysyl oxidase in keratoconus and in keratoconus-associated disorders. *J Neural Transm*. 2013; 120(6):977–982. doi:10.1007/s00702-013-0993-1
14. Coral K, Angayarkanni N, Madhavan J, et al. Lysyl oxidase activity in the ocular tissues and the role of LOX in proliferative diabetic retinopathy and rhegmatogenous retinal detachment. *Invest Ophthalmol Vis Sci*. 2008;49(11):4746. doi:10.1167/iovs.07-1550

15. Song B, Kim D, Nguyen NH, Roy S. Inhibition of diabetes-induced lysyl oxidase overexpression prevents retinal vascular lesions associated with diabetic retinopathy. *Invest Ophthalmol Vis Sci.* 2018;59(15):5965. doi:10.1167/iovs.18-25543
16. Shi L, Zhang N, Liu H, et al. Lysyl oxidase inhibition via  $\beta$ -aminopropionitrile hampers human umbilical vein endothelial cell angiogenesis and migration in vitro. *Mol Med Rep.* 2018;17(4):5029–5036. doi:10.3892/mmr.2018.8508
17. Wang Y, Song EC, Resnick MB. Elastin in the tumor microenvironment. *Adv Exp Med Biol.* 2020;1272:1–16. doi:10.1007/978-3-030-48457-6\_1
18. Sato Y, Ren XS, Harada K, et al. Induction of elastin expression in vascular endothelial cells relates to hepatoportal sclerosis in idiopathic portal hypertension: Possible link to serum anti-endothelial cell antibodies. *Clin Exp Immunol.* 2012;167(3):532–542. doi:10.1111/j.1365-2249.2011.04530.x
19. Navneet S, Rohrer B. Elastin turnover in ocular diseases: A special focus on age-related macular degeneration. *Exp Eye Res.* 2022;222:109164. doi:10.1016/j.exer.2022.109164
20. Xuan M, Wang S, Liu X, He Y, Li Y, Zhang Y. Proteins of the corneal stroma: Importance in visual function. *Cell Tissue Res.* 2016;364(1):9–16. doi:10.1007/s00441-016-2372-3
21. Livak KJ, Schmittgen TD. Analysis of relative gene expression data using real-time quantitative PCR and the  $2^{-\Delta\Delta CT}$  method. *Methods.* 2001;25(4):402–408. doi:10.1006/meth.2001.1262
22. Yuan K, Lan J, Xu L, et al. Long noncoding RNA TLNC1 promotes the growth and metastasis of liver cancer via inhibition of p53 signaling. *Mol Cancer.* 2022;21(1):105. doi:10.1186/s12943-022-01578-w
23. Xia JP, Liu SQ, Wang S. Intravitreal conbercept improves outcome of proliferative diabetic retinopathy through inhibiting inflammation and oxidative stress. *Life Sci.* 2021;265:118795. doi:10.1016/j.lfs.2020.118795
24. Subramanian ML, Stein TD, Siegel N, et al. Upregulation of lysyl oxidase expression in vitreous of diabetic subjects: Implications for diabetic retinopathy. *Cells.* 2019;8(10):1122. doi:10.3390/cells8101122
25. Chronopoulos A, Tang A, Beglova E, Trackman PC, Roy S. High glucose increases lysyl oxidase expression and activity in retinal endothelial cells: Mechanism for compromised extracellular matrix barrier function. *Diabetes.* 2010;59(12):3159–3166. doi:10.2337/db10-0365
26. Miller CG, Budoff G, Prenner JL, Schwarzbauer JE. Minireview: Fibronectin in retinal disease. *Exp Biol Med (Maywood).* 2017;242(1):1–7. doi:10.1177/1535370216675245
27. Yang R, Liu H, Williams I, Chaqour B. Matrix metalloproteinase-2 expression and apoptogenic activity in retinal pericytes: Implications in diabetic retinopathy. *Ann N Y Acad Sci.* 2007;1103(1):196–201. doi:10.1196/annals.1394.000
28. Chaqour B, Karrasch C. Eyeing the extracellular matrix in vascular development and microvascular diseases and bridging the divide between vascular mechanics and function. *Int J Mol Sci.* 2020;21(10):3487. doi:10.3390/ijms21103487
29. Giblin MJ, Ontko CD, Penn JS. Effect of cytokine-induced alterations in extracellular matrix composition on diabetic retinopathy-relevant endothelial cell behaviors. *Sci Rep.* 2022;12(1):12955. doi:10.1038/s41598-022-12683-7
30. Wang A, Cao S, Stowe JC, Valdez-Jasso D. Substrate stiffness and stretch regulate profibrotic mechanosignaling in pulmonary arterial adventitial fibroblasts. *Cells.* 2021;10(5):1000. doi:10.3390/cells10051000
31. Yanagisawa S, Sakurada Y, Miki A, Matsumiya W, Imoto I, Honda S. The association of elastin gene variants with two angiographic subtypes of polypoidal choroidal vasculopathy. *PLoS One.* 2015;10(3):e0120643. doi:10.1371/journal.pone.0120643
32. Chandrasekaran PR, Madanagopalan VG. Role of curcumin in retinal diseases: A review. *Graefes Arch Clin Exp Ophthalmol.* 2022;260(5):1457–1473. doi:10.1007/s00417-021-05542-0
33. Kowluru RA, Kanwar M. Effects of curcumin on retinal oxidative stress and inflammation in diabetes. *Nutr Metab (Lond).* 2007;4(1):8. doi:10.1186/1743-7075-4-8
34. Mrudula T, Suryanarayana P, Srinivas PNBS, Reddy GB. Effect of curcumin on hyperglycemia-induced vascular endothelial growth factor expression in streptozotocin-induced diabetic rat retina. *Biochem Biophys Res Commun.* 2007;361(2):528–532. doi:10.1016/j.bbrc.2007.07.059
35. Filippelli M, Campagna G, Vito P, et al. Anti-inflammatory effect of curcumin, homotaurine and vitamin D3 on human vitreous in patients with diabetic retinopathy. *Front Neurol.* 2021;11:592274. doi:10.3389/fneur.2020.592274
36. Stitt AW, Curtis TM, Chen M, et al. The progress in understanding and treatment of diabetic retinopathy. *Prog Retin Eye Res.* 2016;51:156–186. doi:10.1016/j.preteyeres.2015.08.001
37. Xie T, Chen X, Chen W, et al. Curcumin is a potential adjuvant to alleviate diabetic retinal injury via reducing oxidative stress and maintaining Nrf2 pathway homeostasis. *Front Pharmacol.* 2021;12:796565. doi:10.3389/fphar.2021.796565



# Full operating parameter recording as an essential component of the reproducibility of laser-tissue interaction and treatments

Steven Parker<sup>1,A–F</sup>, Kinga Grzech-Leśniak<sup>2,3,A,C–F</sup>, Mark Cronshaw<sup>1,A–F</sup>,  
Jacek Matys<sup>2,3,D,F</sup>, Aldo Brugnera Jr<sup>4,B,C,E,F</sup>, Samir Nammour<sup>5,A–F</sup>

<sup>1</sup> Faculty of Health and Life Sciences, De Montfort University, Leicester, UK

<sup>2</sup> Laser Laboratory, Department of Dental Surgery, Wrocław Medical University, Poland

<sup>3</sup> Polish Society of Laser Society (PTSL), Cracow, Poland

<sup>4</sup> Visiting Professor and Research Collaborator at the IFSC-University of São Paulo, Brazil

<sup>5</sup> Department of Dentistry, Faculty of Medicine, University of Liège, Belgium

A – research concept and design; B – collection and/or assembly of data; C – data analysis and interpretation;  
D – writing the article; E – critical revision of the article; F – final approval of the article

Advances in Clinical and Experimental Medicine, ISSN 1899–5276 (print), ISSN 2451–2680 (online)

*Adv Clin Exp Med.* 2024;33(6):653–656

## Address for correspondence

Kinga Grzech-Leśniak

E-mail: kinga.grzech-lesniak@umw.edu.pl

## Funding sources

None declared

## Conflict of interest

None declared

Received on January 30, 2024

Reviewed on May 31, 2024

Accepted on June 7, 2024

Published online on June 25, 2024

## Cite as

Parker S, Grzech-Leśniak K, Cronshaw M, Matys J, Brugnera A, Nammour S. Full operating parameter recording as an essential component of the reproducibility of laser-tissue interaction and treatments.

*Adv Clin Exp Med.* 2024;33(6):653–656.

doi:10.17219/acem/189795

## DOI

10.17219/acem/189795

## Copyright

Copyright by Author(s)

This is an article distributed under the terms of the Creative Commons Attribution 3.0 Unported (CC BY 3.0) (<https://creativecommons.org/licenses/by/3.0/>)

## Abstract

**Background.** The number and diversity of published peer-reviewed studies in the discipline of laser dentistry have grown considerably during the past 10 years.

**Objectives.** Within primary research, the development of protocols to guide and formulate clinical practice demands precision and ease of reproducibility. Errors in data acquisition and management may become amplified as the applied randomized clinical trials (RCTs) forge new levels of clinical diversity and predictability in the use of laser photonic energy in both ablative (surgical) and sub-ablative (photobiomodulation (PBM) or photodynamic therapy (PDT)) applications.

**Materials and methods.** A comprehensive range of empirical and computational operating parameters must be included in published studies to facilitate the uniformity of power- and time-related values of laser irradiation.

**Results.** Choosing the correct “tissue irradiation parameters” is difficult and depends on the pathology and symptoms, the surface area to be treated, laser wavelength, the thermal relaxation time of each targeted tissue, and controlling penetration depth of the light into tissues. Therefore, to allow the reproducibility of the results, it is recommended that authors mention with the greatest care and clarity the irradiation parameters used in their study.

**Conclusions.** This paper outlines the concerns felt regarding the general shortfalls and proposes a minimum range of laser operating parameters that should be represented in future peer-reviewed publications.

**Key words:** dentistry, laser, operating parameter, photobiomodulation, surgery



## Background

Laser use in the disciplines of clinical dentistry, oral surgery and oral medicine has developed over a period of more than 30 years. During this time, from a rudimentary base of non-awareness of the scientific processes involved and the scope of possible applications, the knowledge and understanding of lasers have grown and benefitted from structured research, postgraduate courses and qualifications. Both the sophistication and scope of using laser photonic energy have increased significantly, to the extent that lasers can be incorporated to benefit almost all areas of patient-centered clinical dentistry.

Research into laser-assisted therapies has reinforced the importance of “tissue irradiation parameters” to maximize the benefits of applied coherent, monochromatic light energy to a given procedure while minimizing the risk of conversion of excessive energy into heat and consequent collateral thermal damage.

However, broad scrutiny of peer-reviewed published studies and reviews has highlighted the range of disparity when examining the combination of applied laser techniques and the amount of photonic energy delivered. The latter may be viewed as either photon density delivered to complete the chosen clinical procedure or the energy applied over a chosen timeframe as part of the tissue healing phase. Collectively, this may be considered as the “light dose”, representing energy density (also known as fluence or radiant exposure) or power density (also known as irradiation).

Collectively, it may be argued that this disparity has contributed to confusion as to the effectiveness and benefits of adjunctive laser therapy. Additionally, the inconsistent nature of outcomes has resulted in the leading opinions of representative bodies as to the unsuitability of laser-assisted clinical therapy, which has been further compounded by the lack of clarity regarding the optimal dosage and frequency of laser therapy. It is notable that 2 periodontal and endodontic representative organizations have issued a series of position papers on the subject.<sup>1,2</sup>

An example of the uncertainty as to the success of lasers in dentistry was published in the 1991 paper by Zakariasen and Dederich,<sup>3</sup> who summarized in the article abstract as follows:

“Laser dentistry must be developed through extensive scientific inquiry – as all of our treatment modalities should be. We, as a profession, must insist that such laser development is done properly, not foisted upon us based on anecdotal reports and incomplete research.”

Central to the overall progress of evidence-based research should be clear and disciplined adherence to the principles of probity and reproducibility of the published studies. A common failing is amplified through the predominance of incomplete systematic reviews wherein so often, the concluding statement is “more studies are needed”.

The use of lasers in clinical dentistry represents a highly complex form of irradiation, with anisotropic hard and

soft oral and dental structures in close proximity to non-target sites. The key to successful and efficient laser use, whether surgical or non-surgical, is to achieve optimal target absorption with an adequate “light dose” to support the treatment objective. Therefore, the fundamental issue in the safe delivery of laser photonics remains the adoption of the acronym MIMO – minimum input to achieve maximum outcome.

## Objectives

Laser therapies are effective, and their benefits are based on the principle of inducing a biological response through energy transfer.<sup>4,5</sup> This applies to both surgical (ablative) therapy and sub-ablative photobiomodulation (PBM) or antimicrobial photodynamic therapy (aPDT).

Selecting the optimal “tissue irradiation parameters” is a challenging task. The choice is influenced by several factors, including the pathology and symptoms, the surface area to be treated, the laser wavelength, the thermal relaxation time of each targeted tissue, and the depth of light penetration into the tissues.<sup>6,7</sup>

Additional factors related to irradiation parameters may be viewed as:

- “Single, instantaneous” dose;
- “Cumulative” dose – repetition of single dose events over time/gated – continuous wave (CW) or free-running pulsed (FRP) emission mode [Hz];
- 2-dimensional dose: fluence/energy density/radiant exposure [ $\text{J}/\text{cm}^2$ ];
- 2-dimensional dose: Power density – irradiance [ $\text{W}/\text{cm}^2$ ];
- 3-dimension (volume) dose: fluence/energy density/radiant exposure [ $\text{J}/\text{cm}^3$ ];
- 3-dimensional dose: power density – irradiation [ $\text{W}/\text{cm}^3$ ];
- Total energy delivered [J].

The consequence of such appreciation is to enable the chosen laser parameters to be employed, and to avoid the disadvantage of excessive and possibly deleterious thermal increases and resultant collateral tissue damage.

Whether the intended use of a laser is diagnostics, sub-ablative PBM/aPDT or supra-ablative target tissue manipulation, 3 essential elements require careful consideration:

- (1) the correct or appropriate laser wavelength;
- (2) the correct or appropriate light delivery parameters, and
- (3) the appropriate thermal relaxation process management.

However, the parameters selected will represent the mainstay of competency on the part of clinicians.<sup>8</sup> Failure to observe such parameters may result in unwanted and damaging collateral thermal rises, but also a change in the optical properties of the target tissue that may indeed alter the optimal desired laser–tissue interaction.

A common characteristic of many studies to research further the phenomenon of laser-assisted uneventful healing has highlighted the lack of availability of full laser operating parameters. Additional errors amounting to significant power losses along optic delivery fibers may compromise study validity.<sup>9</sup> This contributes to imprecise replication of the treatment modality and protocol, with an attendant risk of patient harm or limitation of the effectiveness of the applied treatment. Thus, the use of a power meter to calibrate the delivered laser beam seems essential for future research study publications.

## Discussion

A further consideration is the delivery of PBM therapy to pathology located below the surface. Fortunately, within the confines of the oral and maxillofacial regions, the maximum depth from any surface – skin or intraoral mucosa – is in the region of 10 mm (1.0 cm). The applied surface dose must be computed to account for 2 basic variables, the applied wavelength and the optical properties of the overlying tissue. In addition, the nature of the therapy required (biostimulation/analgesia/bio-inhibition) must be taken into account.<sup>5,10</sup> This is summarized in Table 1.

Incomplete materials and methods and the specific lack of a record of using a power meter to confirm the delivered laser photonic dose (relative to the control panel values) are very important considerations. A series of recent systematic reviews have highlighted the absence of comprehensive operating parameters and laser-tissue interaction data. It is proposed that these deficiencies have contributed to a distorted evaluation of lasers as an evidence-based adjunctive instrument. Therefore, to allow the reproducibility of the results, it is recommended that the authors mention with the greatest care and clarity the irradiation parameters used in the study: effective output power delivered [W], energy [J], beam diameter at the target tissue [cm], energy density [J/cm<sup>2</sup>], pulse duration [s], repetitive rate of pulses per second [Hz], the total irradiation time [s], contact or non-contact mode, distance from the tip to the target, the angle of beam divergence when using a fiber [°], the beam diameter at the focal point in cases using beam focalization from an articulated delivery system, and the treated surface area [cm<sup>2</sup>]. In case of repetition of the same procedure, clear enumeration of the number of sessions per week and the total number of sessions is essential. This is summarized in Table 2. The recording of full operating parameters relative to the anatomical location will seek to readdress the challenge of study reproducibility and assist in the harmonization of the laser–tissue interaction.

**Table 1.** Basic laser emission and interactive parameters applied within submission guidelines for peer-reviewed publication. There are greater influences of extended light dose errors with PBM compared to similar errors with surgical laser operating power values<sup>4</sup>

Laser emission and interactive parameters		
Type of study: RCT	Sample size/groups/control/randomization	Blinding (single/double blinding)
Laser used, emission wavelength [nm]	Delivery system fiber, waveguide, articulated arm	Gaussian/flat top beam x-section
Emission mode (CW, gated-CW, FRP)	Power meter used and output calibrated	Mean, median, max/min power [W]
Target tissue/lesion dimensions [mm]/target tissue depth [mm]	Tip to tissue distance [mm] Beam divergence angle [°]	Irradiated spot size [cm <sup>2</sup> ]
Energy density (fluence/radiant exposure) [J/cm <sup>2</sup> ]	Irradiation/power density/irradiance [W/cm <sup>2</sup> ]	Total energy delivered [J]
Irradiation PBM therapy time [s]	Irradiation frequency (n × days)	Tip movement/area covered (mm/area)

PBM – photobiomodulation; RCT – randomized controlled trial; CW – continuous wave; FRP – free-running pulse.

**Table 2.** World Federation of Laser Dentistry (WFLD) guidelines: Operative laser emission and interactive parameters applied within submission guidelines for peer-reviewed publication. Full parameter disclosure may differ according to laser type, delivery and emission mode

WFLD guidelines on laser operating parameters for submission of peer-reviewed publications			
Laser make/model and laser wavelength (λ) [nm]	Technique employed: (contact/non-contact; static/scanning)	Energy density [J/cm <sup>2</sup> ] (fluence) at surface	Repetitive rate of pulses per second [Hz]
Coaxial adjuncts water (%/mL/min) air (%/mL/min)	Estimated target size and approximate depth	Estimated energy density [J/cm <sup>2</sup> ] (fluence) at depth	Total number of treatment sessions
Emission mode (CW, gated-CW, FRP)	Diameter of optic delivery probe/spot size Gaussian/flat top	Estimated power density (irradiation) [W/cm <sup>2</sup> ] at surface	Treatment frequency/repetition
Fiber initiation (as required)	Optical spot size at target [cm]	Estimated power density (irradiation) [W/cm <sup>2</sup> ] at depth	Total energy delivered [J]
Beam divergence angle (fiber in non-contact use)	Approximate treatment time [s]	Effective output power [W]: Verified and calibrated using power meter	Laser safety – controlled area, eyewear, test fire

CW – continuous wave; FRP – free-running pulse.

## Limitations

In summary of the above, there are 3 categories of laser parameters:

- “Fixed” parameters relate to the machine being used and are set by the laser manufacturer;
- “Adjustable” parameters relate to the capacity of the operator to adjust power output, frequency, time, etc.; and
- “Calculated” parameters relate to the product of 2 or more parameters, to confer specificity of the actual photonic “light” dose.

It is of little importance to report fixed parameters, other than laser make, wavelength and emission mode. Conversely, the recording of both adjustable and computed values, consistent with entries in Table 2, will develop a context for the evaluation of outcomes and the reproducibility of the study by later workers.

## Conclusions

The impact and extent of incompletely recording laser operating parameters have been investigated. Recommendations have been made as to the adoption of full disclosure as part of submission guidelines for research presented through the World Federation of Laser Dentistry (WFLD). It is difficult to fully estimate the delay in the progress of laser dentistry due to the consequences of the (possibly inadvertent) lack of standardization in operational data and techniques. Equally, it is of relevance to acknowledge the contagion effect of poorly designed or incomplete data studies that are referenced in successive studies, often by the same group of researchers. There must be a responsibility on the part of peer-reviewed scientific journals to ensure full reproduction of the techniques and operating parameters. This may be achievable through the completion of a “tick box” declaration on the part of the authors. Additionally, it is worthy of consideration, when human in vivo studies are proposed, for full parameter disclosure to be included in the ethical approval application. Through a concerted effort to maintain the highest standards of representation of evidence-based laser dentistry, it is hoped that the extensive range of laser-adjunctive therapies may be confidently explored.

## Data availability

The datasets generated and/or analyzed during the current study are available from the corresponding author on reasonable request.

## Consent for publication

Not applicable.

## ORCID iDs

Steven Parker  <https://orcid.org/0000-0003-2317-8381>  
 Kinga Grzech-Leśniak  <https://orcid.org/0000-0002-5700-4577>  
 Mark Cronshaw  <https://orcid.org/0009-0009-3911-4842>  
 Jacek Matys  <https://orcid.org/0000-0002-3801-0218>  
 Aldo Jr Brugnera  <https://orcid.org/0000-0002-8634-743X>  
 Samir Nammour  <https://orcid.org/0000-0003-0321-9764>

## References

1. Mills MP, Rosen PS, Chambrone L, et al. American Academy of Periodontology best evidence consensus statement on the efficacy of laser therapy used alone or as an adjunct to non-surgical and surgical treatment of periodontitis and peri-implant diseases. *J Periodontol*. 2018;89(7):737–742. doi:10.1002/JPER.17-0356
2. Duncan HF, Kirkevang L, Peters OA, et al. Treatment of pulpal and apical disease: The European Society of Endodontology (ESE) S3-level clinical practice guideline. *Int Endodontic J*. 2023;56(Suppl 3):238–295. doi:10.1111/iej.13974
3. Zakariasen KL, Dederich DN. Dental lasers and science. *J Can Dent Assoc*. 1991;57(7):570–573. PMID:1873743.
4. Parker S. Laser photonic energy delivery in clinical dentistry: Scrutiny of parameter variables [doctoral thesis]. Leicester, UK: De Montfort University; 2023. <https://dora.dmu.ac.uk/items/5a60b157-6d26-46ad-ab2a-657aebbef704>.
5. Hadis MA, Zainal SA, Holder MJ, et al. The dark art of light measurement: Accurate radiometry for low-level light therapy. *Lasers Med Sci*. 2016;31(4):789–809. doi:10.1007/s10103-016-1914-y
6. Cronshaw M, Parker S, Anagnostaki E, Mylona V, Lynch E, Grootveld M. Photobiomodulation dose parameters in dentistry: A systematic review and meta-analysis. *Dent J*. 2020;8(4):114. doi:10.3390/dj8040114
7. Dederich DN. Laser/tissue interaction: What happens to laser light when it strikes tissue? *J Am Dent Assoc*. 1993;124(2):57–61. doi:10.14219/jada.archive.1993.0036
8. Parker S, Cronshaw M, Anagnostaki E, Bordin-Aykroyd SR, Lynch E. Systematic review of delivery parameters used in dental photobiomodulation therapy. *Photobiomodul Photomed Laser Surg*. 2019;37(12):784–797. doi:10.1089/photob.2019.4694
9. Parker S, Cronshaw M, Grootveld M, et al. The influence of delivery power losses and full operating parametry on the effectiveness of diode visible–near infra-red (445–1064 nm) laser therapy in dentistry: A multi-centre investigation. *Lasers Med Sci*. 2022;37(4):2249–2257. doi:10.1007/s10103-021-03491-y
10. Melnik IS, Steiner RW, Kienle A. Light penetration in human skin: In-vivo measurements using isotropic detector. Presented at: OE/LASE'93: Optics, Electro-Optics, & Laser Applications in Science & Engineering. Los Angeles, USA: OE/LASE; 1993:222–230. doi:10.1117/12.146313